

**IMPROVING THE PROPERTIES OF RECLAIMED WASTE TIRE
RUBBER BY BLENDING WITH POLY(ETHYLENE-*co*-VINYL
ACETATE) AND ELECTRON BEAM IRRADIATION**

SUGANTI RAMARAD

**Thesis submitted to the University of Nottingham
for the degree of Doctor of Philosophy**

FEBRUARY 2016

Dedications

To my parents,

Ramarad Sannasy & Fydamah Applanaidu

(for your relentless effort and care that made me an obnoxious knowledge craving person)

To my husband,

Ramesh Yanki Naidu

(for your presence, patience and never saying “NO”)

To my son,

Shiveesh Ramesh

(for inspiring me to push the limits and always strive for the best)

Abstract

Non-degradable waste tire generation around the world is growing at an alarming rate. Diversifying the recycling route of these waste tires is essential to solve the problem. One way is to incorporate them into polymers and convert them into new products. However, incorporation of ground tire rubber into thermoplastics has been hampered due to lack of toughness and adhesion between phases. To address the issue, this study utilized reclaimed waste tire rubber (RTR) instead; and evaluated the properties of RTR and poly(ethylene-co-vinyl acetate) (EVA) blends. The properties of the RTR/EVA blends were further enhanced by compatibilization and electron beam irradiation.

Processing, mechanical, thermal and dynamic mechanical properties of RTR were tremendously improved by blending with EVA. However, the interfacial adhesion was found to lack in the blends. Compatibilization by reactive, physical and combination strategies were explored utilizing (3-Aminopropyl)triethoxy silane (APS), liquid styrene butadiene rubber (LR) and maleated EVA (MAEVA), respectively. APS and MAEVA were found to be the most and least favourable compatibilizer, respectively. Apart from functioning as reactive compatibilizer, APS also reclaimed the RTR phase further. These lead to improved dispersion of smaller RTR phase in EVA matrix and enhanced the interfacial adhesion.

Electron beam irradiation revealed the presence of radical stabilizing and scavenging additives within RTR which retards the crosslinking process in RTR and RTR/EVA blends. Though chain scissions were predominant; study showed the replacement of S-S and S-C bonds with stronger and stiffer C-C bonds ensures the retention of RTR and RTR/EVA blends properties upon irradiation. Compatibilization of RTR/EVA blend by APS (50RTR/5APS) also improved the crosslinking efficiency. However, the blend still suffered from oxidative degradation from irradiation in air. Radiation sensitizers, trimethylol propane triacrylate (TMPTA), tripropylene glycol diacrylate (TPGDA) and N,N-1,3 Phenylene Bismaleimide (HVA2), were used to accelerate the irradiation induced crosslinking in RTR and 50RTR/5APS blends. Presence of radiation sensitizers leads to simultaneous improvement in toughness and tensile strength of RTR and 50RTR/5APS blends. Elastic capacity of RTR phase was restored and interfacial adhesion enhanced in the presence of radiation sensitizers.

List of publications

RAMARAD, S., RATNAM, C. T., KHALID, M., CHUAH, L. A., HANSON, S. Effect of reactive compatibilization and electron beam irradiation on enhancing the properties of reclaimed waste tire rubber/EVA blend. *Journal of Materials Science*, Submitted, 2016

RAMARAD, S., RATNAM, C. T., KHALID, M., CHUAH, L. A. Improved dynamic mechanical properties of reclaimed waste tire rubber/EVA blends under the influence of electron beam irradiation. *Iranian Polymer Journal*, Under review, 2015

RAMARAD, S., KHALID, M., RATNAM, C. T., CHUAH, L. A., RASHMI, W. 2015 Waste tire rubber in polymer blends: A review on the evolution, properties and future. *Progress in Material Science*, 72, 100 – 140.

RAMARAD, S., RATNAM, C. T., KHALID, M., CHUAH, L. A. 2015 Improving the properties of reclaimed waste tire rubber by blending with poly(ethylene-co-vinyl acetate) and electron beam irradiation. *Journal of Applied Polymer Science*, 132, DOI: 10.1002/app.41649

RATNAM, C. T., **RAMARAD, S.**, SIDDIQUI, M. K., ZAINAL ABIDIN, A. S. & CHUAH, L. T. 2014. Irradiation cross-linking of ethylene vinyl acetate/waste tire dust: Effect of multifunctional acrylates. *Journal of Thermoplastic Composite Materials*. DOI: 10.1177/0892705713518814.

Acknowledgements

OM SAI RAM. GOD BLESSES.

Growing up in the middle of rubber plantation, smelling the freshness of rubber tree, running around every morning collecting liquid and coagulated rubber and learning to count with the rubber seeds is how I spent my childhood. Hence, the passion to work with reviving the rubber waste problem came naturally. However passionate I was, I could never have completed this PhD without the help of some wonderful people, where the least I could do is acknowledging them here, in my masterpiece.

First and foremost, my ultimate gratitude to my parents, for encouraging, accommodating and allowing me to be the continuous knowledge seeking person. Their presence, guidance and faith have been my best motivator to be who I am today. Finishing my PhD is my form of gift of honor to my parent, to make them happy and proud.

Everyone would agree on how tough it is to run a family while doing a PhD. I feel so lucky to have a supportive family who understood my role as a PhD student. My husband told me to put a break to cooking while I wrote my thesis. My sister fetched my son home whenever I ran late from lab work. My son quietly sat and worked on his scribbling and drawing while I decoded my reaction mechanism. My mother and mother in law tirelessly cooked for us and lovingly cared for my son. I could not have asked for more. They were perfectly in sync with my needs.

The most important mention will go to my set of supervisory, Dr. Mohammad Khalid Siddiqui, Dr. Chantara Theyv Ratnam and Prof. Luqman Chuah. Dr. Khalid has been the best motivator and supporter in ensuring the papers gets published. He struggled with the bewitching “which” that frequently repeats itself throughout the thesis to bring more coherence to my writing style. Dr. Chantara was instrumental in guiding the laboratory analysis and data analysis step by step despite her busy schedules. She ensured all the facts has been detailed and discussed adequately in the thesis. Prof. Luqman Chuah was always willing to help and guide the progress of my study. They have collectively helped in making sure I had a clear path towards finishing my PhD. Each chapter and published paper profited from their expert input. Special thanks for their

immediate attention in funding some of the required testing. I'd also like to thank Dr. Svenja Hanson for her availability and kindness.

I'd like to thank Government of Malaysia for providing the financial assistance through "MyBrain-MyPhd" scholarship and to University of Nottingham Malaysia Campus (UNMC) for the fee waiver. I'd also like to convey my humbled gratitude to Malaysia Nuclear Institute (Nuclear M'sia) for allowing me the access to their laboratory and radiation facilities.

Support from another sort came from the laboratory coordinators, who were instrumental in helping me to run the relevant testing. It was a joy to work with Mr. Wan Ali (physical lab – Nuclear M'sia), Mr. Azmi, Mr. Shaari (Electron beam irradiation – Nuclear M'sia), Mr. Hasnul Nizam (DSC – Nuclear M'sia), Mr. Mohd. Nurfalah (Tensile and TEM – Nuclear M'sia), Mr. Hafiz (TEM – Nuclear M'sia), Mr. Asyraf (DMA – Universiti Kebangsaan Malaysia), Mr. Mohd. Faizal (analytical lab – UNMC), Ms. Filzah (SEM lab – UNMC) and Ms. Noor Fatihah (TGA – UNMC). It would have taken me ages to complete the lab work without their support and goodwill. Not to forget Mrs. Siti Zaharatul Asyiqin and Ms. Yogeswary of Engineering Research office that made sure the PhD progression and examination went smoothly.

Last but not least, a special mention to all my friends and PhD cohorts, who made the journey a memorable and joyful one. I was fortunate enough to have your listening ears, advices and boosters. My special thank you to Priyanka Jagadish, Feven Mathews Micheal, Anand Anush and Tissa Chandesa for their peer review help.

TABLE OF CONTENTS

Dedications	i
Abstract	ii
List of publications	iii
Acknowledgements	iv
List of Tables	xi
List of Figures & Schemes	xiii
Abbreviations	xviii
Symbols	xx
CHAPTER 1. INTRODUCTION	1
1.1. Problem statement.....	3
1.2. Scope of study.....	4
1.3. Aims and objectives.....	4
1.4. Research methodology and limitations	5
1.5. Organization of thesis.....	5
CHAPTER 2. LITERATURE REVIEW	6
2.1. Introduction	6
2.2. Tires.....	6
2.3. Waste tires	7
2.4. Legislations.....	8
2.5. Waste tires utilization	11
2.6. Recycling waste tires	13
2.6.1. Downsizing waste tires.....	13
2.6.2. Reclaiming and devulcanization	14
2.7. GTR and RTR in polymer blends.....	18
2.7.1. Compatibilization	19

2.7.2.	Crosslinking	20
2.8.	Thermoplastics – waste tire rubber blends	22
2.8.1.	Mechanical properties	22
2.8.2.	Thermal properties.....	32
2.8.3.	Dynamic mechanical analysis.....	35
2.9.	Summary.....	36
CHAPTER 3. METHODOLOGY.....		37
3.1.	Introduction	37
3.2.	Materials	37
3.3.	Melt compounding.....	38
3.4.	Compression moulding.....	39
3.5.	Electron beam irradiation	41
3.6.	Molar mass distribution	41
3.7.	Gel content.....	42
3.8.	Tensile properties.....	42
3.9.	Tear properties	43
3.10.	Hardness test	43
3.11.	Scanning electron microscopy.....	43
3.12.	Transmission electron microscopy	44
3.13.	Thermal degradation and stability	44
3.14.	Crystallinity.....	44
3.15.	Dynamic mechanical analysis	45
3.16.	Equilibrium swelling.....	46
3.17.	Fourier Transform Infrared analysis	47
CHAPTER 4. EFFECT OF BLEND RATIO ON THE PROPERTIES OF RTR/EVA BLENDS.....		48
4.1.	Introduction	48

4.2.	Processing characteristics	48
4.3.	Gel content analysis.....	50
4.4.	Mechanical properties.....	53
4.4.1.	Tensile properties	53
4.4.2.	Tear and hardness.....	55
4.5.	Morphological study	57
4.5.1.	SEM.....	57
4.5.2.	TEM	60
4.6.	Thermal properties	62
4.6.1.	TGA analysis	62
4.6.1.	DSC analysis.....	65
4.7.	Dynamic mechanical analysis	69
4.7.1.	Storage modulus	69
4.7.2.	Loss modulus.....	72
4.7.3.	Tan delta.....	73
4.8.	Equilibrium swelling.....	75
4.8.1.	Empirical analysis	78
4.9.	Summary.....	79
CHAPTER 5. EFFECT OF DIFFERENT COMPATIBILIZATION STRATEGIES ON THE PROPERTIES OF RTR/EVA BLEND		80
5.1.	Introduction	80
5.2.	Processing characteristics	80
5.3.	Gel content	84
5.4.	Mechanical properties.....	88
5.4.1.	Tensile properties	88
5.4.2.	Tear and hardness.....	94
5.5.	Compatibilization mechanism	96
5.5.1.	APS.....	97

5.5.2.	Liquid rubber (LR)	101
5.5.3.	Maleic anhydride grafted EVA (MAEVA)	102
5.6.	Morphological study	103
5.6.1.	SEM.....	103
5.6.2.	TEM	105
5.7.	Thermal properties	107
5.7.1.	TGA analysis	107
5.7.1.	DSC analysis.....	109
5.8.	Dynamic mechanical analysis	113
5.8.1.	Storage modulus	113
5.8.2.	Loss modulus.....	115
5.8.3.	Tan delta.....	117
5.9.	Equilibrium swelling.....	119
5.9.1.	Empirical analysis	119
5.10.	Summary.....	123
CHAPTER 6. EFFECT OF DIFFERENT RADIATION SENSITIZERS ON THE PROPERTIES OF RTR/EVA BLEND.....		124
6.1.	Introduction	124
6.2.	Processing characteristics	125
6.3.	Gel content	127
6.4.	Mechanical properties.....	131
6.4.1.	Tensile strength	131
6.4.2.	Elongation at break.....	134
6.4.3.	Tensile modulus.....	136
6.4.4.	Tear strength.....	139
6.4.5.	Hardness	139
6.5.	Morphological study	142
6.6.	Thermal properties	147

6.6.1.	TGA analysis	148
6.6.2.	DSC analysis.....	152
6.7.	Dynamic mechanical properties	157
6.7.1.	Storage modulus	157
6.7.2.	Loss modulus.....	158
6.7.3.	Tan delta.....	161
6.8.	Equilibrium swelling.....	162
6.8.1.	Empirical analysis	164
6.9.	Summary.....	166
CHAPTER 7. CONCLUSION.....		167
7.1.	Introduction	167
7.2.	Principal findings	167
7.3.	Limitations.....	169
7.4.	Recommendation for future studies	170
BIBLIOGRAPHY		172
APPENDIX		192

List of Tables

Table 2.1 Composition of materials used in tire manufacturing	7
Table 2.2 General methods of waste tire downsizing	15
Table 2.3 Energy required for cleaving sulphur or carbon bonds	17
Table 2.4 Physical, chemical and microbial processes of tire rubber reclaiming/devulcanization	18
Table 3.1 Properties and supplier information of the additives used	37
Table 3.2 Designation of the blends	39
Table 4.1 p_0/q_0 values of RTR, EVA and RTR/EVA blends	52
Table 4.2 Degradation temperatures and residual weight of RTR, EVA and blends	63
Table 4.3 Different parameters of sorption behavior of RTR, EVA and RTR/EVA blends before and after irradiation. (n , $\log \text{min}^{1/2}$; k , unitless; D , $\times 10^5 \text{ cm}^2\text{min}^{-1}$; S , unitless; P , $\times 10^4 \text{ cm}^2\text{min}^{-1}$)	78
Table 5.1 Total mixing energy (kNm) of 50RTR and compatibilized blends	84
Table 5.2 Weight average molecular weight (M_w), number average molecular weight (M_n) and polydispersity index (PDI) of RTR and RTR with 3wt% APS (RTR/3APS)	86
Table 5.3 Values of p_0/q_0 of compatibilized blends	87
Table 5.4 Percentage of changes in tensile properties of blends at 200 kGy irradiation compared to non-irradiated blends	92
Table 5.5 Degradation temperatures and residual weights of 50RTR and compatibilized blends before irradiation	108
Table 5.6 Storage modulus (MPa) of control and compatibilized blends at different temperatures, before and after irradiation	114
Table 5.7 Values corresponding to peak of loss modulus and tan delta curve of 50RTR and compatibilized blends	116
Table 5.8 Effect of compatibilizers and irradiation on different parameters of sorption behavior of 50RTR blends	122
Table 6.1 Values p_0/q_0 of RTR, EVA and 50RTR/5APS blends in the presence of radiation sensitizers	130
Table 6.2 Degradation temperatures and residual weight of RTR, RTR/TMPTA and RTR/TPGDA at different irradiation doses	149
Table 6.3 Degradation temperatures and residual weight of EVA/TMPTA and EVA/TPGDA and EVA/HVA2 at different irradiation doses	150

Table 6.4 Degradation temperatures and residual weight of 50RTR/5APS/ TMPTA and 50RTR/5APS/TPGDA and 50RTR/5APS/HVA2 at different irradiation doses	152
Table 6.5 Storage modulus of 50RTR/5APS, 50RTR/5APS/TMPTA, 50RTR/ 5APS/TPGDA and 50RTR/5APS/HVA2 at different temperature, before and after irradiation	160
Table 6.6 Values corresponding to peak of loss modulus and tan delta curve of 50RTR/5APS, 50RTR/5APS/TMPTA, 50RTR/5APS/TPGDA and 50RTR/5APS/HVA2	160
Table 6.7 Different sorption parameters of 50RTR/5APS, 50RTR/5APS/ TMPTA, 50RTR/5APS/TPGDA and 50RTR/5APS/HVA2 compositions before and after irradiation	164

List of Figures & Schemes

Figure 2.1 Three main models governing the management of waste tire	10
Figure 2.2 Models of waste tire management in EU, showing largest recovery/recycling organization in EPR model governing countries	10
Figure 2.3 Flow of waste tire utilization	11
Figure 2.4 Breakdown of waste tire utilization in EU from 1994 to 2012	12
Figure 2.5 Hierarchy of waste tire utilization	12
Figure 2.6 The surface of GTR produced from the different downsizing processes. (a) ambient – mechanical; (b) water jet; (c) cryogenic – pin mill; (d) ambient – rotary mill; (e) cryogenic – rotary mill	16
Figure 2.7 Schematic representation of devulcanization and reclaiming	16
Figure 2.8 Influence of the particle size of GTR on mechanical properties of thermoplastic blends	24
Figure 2.9 SEM micrographs of increasing GTR loading in EVA matrix a) 10wt%, b) 20wt%, c) 50wt% and d) 70wt% GTR	24
Figure 2.10 Influence of tire rubber loading on the mechanical properties of thermoplastic blends	26
Figure 2.11 Morphological changes in a) GTR/PP, b) GTR/PP/MAgSEBS, c) amine treated GTR/PP and d) amine treated GTR/PP/MAgSEBS	27
Figure 2.12 Schematic diagram showing the difference in microstructure of polymer blends with GTR and RTR	30
Figure 3.1 Schematic representation of the compression molding process: a) the mould arrangement with mould cavity filled with pieces of blended material; b) the mould is transferred to the press and the pressure cycles are applied; c) the mould is cooled and removed from the press to release the molded slabs from the cavity	40
Figure 4.1 Torque – time curve of RTR, EVA and RTR/EVA blends	49
Figure 4.2 Mixing torque values of RTR, EVA and RTR/EVA blend	49
Figure 4.3 Gel content of RTR, EVA and RTR/EVA blends as a function of irradiation dose	50
Figure 4.4 Tensile properties of RTR, EVA and RTR/EVA blends as a function of irradiation dose a) Tensile strength, b) Modulus 100, c) Elongation at break	54
Figure 4.5 a) Tear strength and b) Hardness of RTR, EVA and RTR/EVA blends as a function of irradiation dose	56

Figure 4.6 Tensile fracture surface of RTR at a) 0kGy, b) 50kGy, c) 100kGy and d) 200kGy	58
Figure 4.7 Tensile fracture surface of 50RTR at a) 0kGy, b) 50kGy, c) 100kGy and d) 200kGy	59
Figure 4.8 Tensile fracture surface of EVA at a) 0kGy, b) 50kGy, c) 100kGy and d) 200kGy	60
Figure 4.9 TEM micrographs of 50RTR blends before irradiation a) 5000X, b) 50000X and after irradiation c) 5000X and d) 50000X magnification	61
Figure 4.10 Typical TGA curve for RTR, EVA and RTR/EVA blends, a) Mass loss curve, b) Derivative curve	63
Figure 4.11 Typical heat flow curve of a) EVA and RTR/EVA blends, b) irradiated EVA and c) irradiated 50RTR blend	66
Figure 4.12 Effect of irradiation dose on a) crystallization temperature, b) melting temperature, c) heat of fusion and d) crystallinity of EVA and RTR/EVA blends	67
Figure 4.13 Dynamic mechanical properties; a) Storage modulus, b) Loss modulus and c) $\tan \delta$ of RTR, EVA and 50RTR blend before and after irradiation	70
Figure 4.14 Mol percent toluene uptake of a) EVA and RTR/EVA blends at 0 kGy, b) EVA at 0, 50 and 200 kGy, c) 50RTR blend at 0, 50 and 200 kGy; and d) RTR at 50 and 200 kGy irradiation doses	77
Figure 5.1 Illustration of reactive (chemical bond) and non-reactive (wetting) compatibilization strategy	81
Figure 5.2 Torque vs time profile of a) APS, b) LR and c) MAEVA compatibilized blends at different compatibilizer loading	82
Figure 5.3 Mixing torque values of APS, LR and MAEVA compatibilized 50RTR blends	84
Figure 5.4 Gel content of 50RTR blend as a function of compatibilizer type, compatibilizer loading and irradiation dose	85
Figure 5.5 Stress vs strain plot of 50RTR and compatibilized blends at different loading before irradiation	88
Figure 5.6 Representation of a) tensile strength, b) elongation at break and c) modulus 100 of compatibilized blends before and after irradiation	91
Figure 5.7 Influence of irradiation dose, compatibilizer type and loading on a) tear strength and b) hardness of compatibilized 50RTR blends	95

Figure 5.8 FTIR representation of EVA and EVA/3APS indicating a) bending of —CH ₃ group (1350 – 1360 cm ⁻¹), b) Silane group (2100 – 2360 cm ⁻¹), c) bending of primary amine group (1550 – 1650 cm ⁻¹) and d) stretching of primary amine (3400 – 3500 cm ⁻¹)	100
Figure 5.9 Schematic representation of RTR/EVA blend compatibilization by LR	101
Figure 5.10 FTIR spectra representation of RTR, a) full spectrum and b) enlargement of wavenumber 3000 to 4000 cm ⁻¹ which shows a broad peak indicating stretching of —OH group	102
Figure 5.11 SEM micrographs of (a,b)3APS, (c,d)3LR, (e,f)3MAEVA compatibilized 50RTR blends before irradiation (0 kGy) showing overview at (a,c,e) 1000x magnification; as well as focused RTR particle at (d,f) 2000x and (b)5000x magnification	104
Figure 5.12 TEM micrographs of APS compatibilized blend before (a,b) and after 200 kGy irradiation (c,d) at 5000x (a,c) and 40000x (b,d) magnification	106
Figure 5.13 TEM micrographs of LR compatibilized blend before (a,b) and after 200 kGy irradiation (c,d) at 5000x (a,c) and 40000x (b,d) magnification	106
Figure 5.14 Typical TGA curves of 50RTR, 50RTR/5APS, 50RTR/5LR and 50RTR/5MAEVA samples, a) Mass loss curve, b) Derivative curve	108
Figure 5.15 TGA curves of 50RTR/5LR blends before and after 200 kGy irradiation	110
Figure 5.16 Heating and cooling DSC thermograms of 50RTR and compatibilized 50RTR blends before irradiation	110
Figure 5.17 Effect of irradiation dose on a) crystallization temperature, b) melting temperature, c) heat of fusion and d) crystallinity of 50RTR and compatibilized 50RTR blends	112
Figure 5.18 Storage modulus of 50RTR, 50RTR/3APS, 50RTR/3LR and 50RTR/3MAEVA a) before and b) after irradiation	114
Figure 5.19 Loss modulus of 50RTR, 50RTR/3APS, 50RTR/3LR and 50RTR/3MAEVA blends a) before and b) after irradiation (200 kGy)	116
Figure 5.20 Tan delta of 50RTR, 50RTR/3APS, 50RTR/3LR and 50RTR/3MAEVA blends a) before and b) after irradiation (200 kGy)	118

Figure 5.21 Sorption behavior of a) 50RTR and compatibilized blends before irradiation, b) APS compatibilized blends, c) LR compatibilized blends and d) MAEVA compatibilized blends with irradiation	121
Figure 6.1 Chemical structure of a) TMPTA, b) TPGDA and c) HVA2	124
Figure 6.2 Torque-time curve of a) RTR, b) EVA and c) 50RTR/5APS blend; in the presence of radiation sensitizers	126
Figure 6.3 Gel content values of a) RTR, b) EVA and c) 50RTR/5APS blends as a function of radiation sensitizers and radiation dose	128
Figure 6.4 Effect of radiation sensitizers on tensile strength of a) RTR, b) EVA and c) 50RTR/5APS blends at various radiation doses	132
Figure 6.5 Effect of radiation sensitizers on elongation at break of a) RTR, b) EVA and c) 50RTR/5APS blends at various radiation doses	135
Figure 6.6 Effect of radiation sensitizers on modulus at 100% elongation of a) RTR, b) EVA and c) 50RTR/5APS blends at various radiation doses	138
Figure 6.7 Effect of radiation sensitizer on tear strength of a) RTR, b) EVA and c) 50RTR/5APS blends at various radiation doses	140
Figure 6.8 Effect of radiation sensitizers on hardness of a) RTR, b) EVA and c) 50RTR/5APS blends at various radiation doses	141
Figure 6.9 SEM micrographs of RTR composition with TMPTA (a,b) and TPGDA (c,d) at 50 kGy (a,c) and 200 kGy (b,d) irradiation doses	143
Figure 6.10 SEM micrographs of EVA composition with TMPTA (a,b), TPGDA (c,d) and HVA2 (e,f) at 50 kGy (a,c,e) and 200 kGy (b,d,f) irradiation doses	145
Figure 6.11 SEM micrographs of 50RTR/5APS composition with TMPTA (a,b), TPGDA (c,d) and HVA2 (e,f) at 50 kGy (a,c,e) and 200 kGy (b,d,f) irradiation doses	146
Figure 6.12 Typical TGA curve of a) RTR/TMPTA and b) RTR/TPGDA at different irradiation doses	149
Figure 6.13 Typical TGA curve of a) EVA/TPMTA, b) EVA/TPGDA and c) EVA/HVA2 compositions at different irradiation doses	150
Figure 6.14 Typical TGA curve of a) 50RTR/5APS/TMPTA, b) 50RTR/5APS/TPGDA and c) 50RTR/5APS/HVA2 compositions at different irradiation doses	151

Figure 6.15 Effect of irradiation dose on a) crystallization temperature, b) melting temperature, c) heat of fusion and d) crystallinity of EVA in the presence of TMPTA, TPGDA and HVA2	154
Figure 6.16 Effect of irradiation dose on a) crystallization temperature, b) melting temperature, c) heat of fusion and d) crystallinity of 50RTR/5APS blends in the presence of TMPTA, TPGDA and HVA2	156
Figure 6.17 Dynamic mechanical properties; a) storage modulus, b) loss modulus and c) $\tan \delta$ of 50RTR/5APS in the presence of radiation sensitizer	159
Figure 6.18 Sorption behaviour of a) RTR, b) EVA and c) 50RTR/5APS under the influence of TMPTA, TPGDA and HVA2 at 100 kGy irradiation dose	163
Scheme 5.1 Hydrolysis and self-condensation reaction in APS	97
Scheme 5.2 Interaction between APS and RTR	98
Scheme 5.3 Interaction between APS and EVA	99
Scheme 5.4 Interaction between MAEVA and RTR through a) covalent bond, b) intermolecular dipole-dipole interaction, as well as representation of EVA chain of MAEVA wetting into EVA matrix	103

Abbreviations

3R	Reduce, reuse and recycle
Aam	Acrylamide
APS	(3-Aminopropyl)triethoxy silane
ASTM	American society for testing and materials
BR	Butadiene rubber
CB	Carbon black
DCP	Dicumyl peroxide
DMA	Dynamic mechanical analysis
DSC	Differential scanning calorimetry
EB	Electron beam
Eb	Elongation at break
EPDM	Ethylene propylene diene monomer rubber
EPR	Ethylene propylene rubber
EU	European Union
EVA	Poly(ethylene-co-vinyl acetate)
GPC	Gel permeation chromatography
GTR	Ground tire rubber
HDPE	High density PE
HVA2	N,N-1,3 Phenylene Bismaleimide
IPN	Interpenetrating network
LDPE	Low density PE
LLDPE	Linear LDPE
LR	Liquid styrene butadiene rubber
MA	Maleic anhydride
MAEVA	Maleic anhydride grafted EVA
MAGPE	MA grafted PE
MAGPP	MA grafted PP
MAGSEBS	MA grafted SEBS

MFA	Multi-functional acrylates
MFI	Melt flow index
NR	Natural rubber
PE	Polyethylene
php	Part per hundred polymer
phr	Part per hundred rubber
p_0/q_0	Ratio of main chain rupture to main chain crosslinks
PP	Polypropylene
PVC	Polyvinyl chloride
rpm	Rotation per minute
RTR	Reclaimed tire rubber
SBR	Styrene butadiene rubber
SBS	Styrene butylene styrene block copolymer
SEBS	Styrene-ethylene-butylene-styrene block copolymer
SEM	Scanning electron microscopy
TEM	Transmission electron microscopy
T_g	Glass transition temperature
TGA	Thermogravimetric analysis
THF	Tetrahydrofuran
T_m	Melting temperature
TM	Tensile modulus
T_{max}	Temperature at maximum weight loss
TMPTA	Trimethylol propane triacrylate
TOR	<i>Trans</i> -polyoctylene rubber
TPGDA	Tripropylene glycol diacrylate
TS	Tensile strength
$T_{X\%}$	Degradation temperature at X% weight loss
US	United States
UV	Ultra-violet
wt	Weight

Symbols

Symbol	Definition	Unit(s)
D	Irradiation dose	Gray (Gy)
F	Force	Newton (N)
H _f	Heat of fusion	Joule (J)
l	Length	meter (m)
M	Mass	gram (g)
Q	Solvent uptake	mol
T	Temperature	degree Celsius (°C)
t	Time	second (s), minute (min), hour
V	Volume	Liter (L), cubic meter (m ³)
w	Weight	gram (g)
X _c	Crystallinity	percentage (%)
ε	Strain	percentage (%)
σ	Stress	Pascal (Pa)

CHAPTER 1. INTRODUCTION

The evolution of tires is a marvel to engineering world, having evolved from simple wheel into today's pneumatic tires (Rodgers and Waddell, 2011). Scientists, technologists and engineers have played their part in making tires such a complex and durable product. However, with growing demands for automobile, the disposal of tires has turned into an environmental threat, as it is non-degradable and painstaking to recycle. A tire is generally made up of 40 to 50% rubber and 20 to 30% carbon black fillers, two main materials which are very commonly used in polymeric products (Shulman, 2011, Sienkiewicz et al., 2012). At the point of wear, a tire would have only lost about one third of its original weight (van Beukering and Janssen, 2001), leaving behind about 67% of useable, recyclable material behind. This information highlights the need to reuse and recycle the waste tires.

One could call this era as polymeric/plastic age, as the population is greatly dependent on polymeric products. It is no surprise; polymeric materials have replaced many conventionally used materials such as wood and metal in vast areas of application. Waste tires, which consist of rubber and carbon black filler, a common face to polymeric world, could be blended with polymers as a mean to recycle the waste tire as well as producing cheaper products. In order to incorporate waste tire into polymeric products, it has to be shredded and granulated to smaller size. This shredding and granulating process is a technologically difficult process, as the waste tires possess a complex structure with high mechanical properties (Amari et al., 1999). The product of this process is commonly described as ground tire rubber which has different structure and size depending on the type of machinery and process equipped to shred and granulate the waste tire (Karger-Kocsis et al., 2013).

Ground tire rubber (GTR) has been commonly used in polymeric matrices as fillers (Karger-Kocsis et al., 2013). However, the mechanical properties of the polymeric matrices, be it rubber, thermoplastic or thermoplastic elastomer; was found to deteriorate with the incorporation of GTR (da Costa and Ramos, 2008, De et al., 2007, Hong and Isayev, 2001, Ismail et al., 2006). The vulcanized structure of GTR renders the polymeric blend/composite stiff, hence, fails to enhance the properties. This has hampered the use of GTR in polymeric

matrices. To overcome this problem, reclaimed tire rubber (RTR) which has regained some extent of plasticity from breaking down the vulcanized structure of the rubber through a reclaiming process could be used instead (Li et al., 2012a, Li et al., 2012b). However, the properties of RTR were found to be very inferior from all the wear and tear and recycling process of waste tire. In this study, poly(ethylene-co-vinyl acetate) (EVA) was utilized to enhance the inferior properties of RTR. The effect of EVA incorporation on RTR and vice versa has been studied.

One of the factors contributing to the failure of polymer matrix reinforcement by GTR has been due to weak interfacial adhesion between the polymer and GTR (Karger-Kocsis, 2013). Vast number of different methods in improving the interfacial properties has been studied with only a few showing positive results (Awang et al., 2007, Awang et al., 2008, Colom et al., 2009, Grigoryeva et al., 2008, Ismail et al., 2006). RTR on the other hand, believed to display better interfacial properties compared to GTR, due to the devulcanized surface which permits better interaction between host matrix and RTR. Nevertheless, a compatibilizing strategy is seriously needed even in RTR, in order to enhance the properties of the blends/composites. In this study, three different compatibilization strategy was employed; namely, reactive, physical and a combination; on RTR/EVA blends. The effectiveness of each compatibilization strategy of the blends has been thoroughly studied.

Radiation processing of polymeric materials involves treatment of polymeric material with ionizing radiation to modify their physical and chemical properties. Properties of polymeric materials can be modified by irradiation as it is bound to crosslink, degrade, grafted or cured when subjected to ionizing radiation (Makuuchi and Cheng, 2012b). Use of ionizing radiation in developing a sustainable management of polymeric waste by manipulating the crosslinking and chain scission yield is a new and emerging field of application. In this study, electron beam (EB) irradiation was used onto RTR, EVA and RTR/EVA blends to enhance the properties. The efficiency of EB irradiation in improving the properties of RTR/EVA blends has been reported.

1.1. Problem statement

Tires are known as rubber composite which have been crosslinked. The crosslinked rubber structure gives the rubber stability, durability and strength for the application as tires. However, the complexity of the rubber composite has hampered the recycling of the waste tires while the structure and durability rendered the tires non-biodegradable. Thus, the generation of waste tires is growing at an alarming rate around the globe causing numerous problems.

Furthermore, researchers have yet to find a suitable biodegradable compound that could replace the rubbers used in tire making. Ironic is the fact that the major composition of a tire rubber is natural rubber, a natural polymer capable of biodegradation. The crosslinking process during tire making transforms the natural rubber into three dimensional network structure which is incapable of biodegradation. Even if biodegradation is possible, it takes a very long time, implying recycling is the only way to address the management of crosslinked rubber. In fact, finding an efficient and effective way to recycle waste tire rubber could possibly result in a sustainable way of managing waste tires.

These bulky waste tires need to be physically down sized into smaller shreds and powder in order to be recycled. These shreds and powder are known as ground tire rubber (GTR). Another form of waste tire derivatives commonly used along with polymers is reclaimed tire rubber (RTR), which is a chemically treated GTR to breakdown the three-dimensional structure. Having gone through a lifetime on the road as well as physical and chemical treatments, GTR and RTR have very poor properties. Blending these GTR and RTR with polymeric matrices such as thermoplastic would improve the inferior properties.

However, literature survey also showed the lack of adhesion between GTR/RTR and thermoplastic matrices. Compatibilization of the blends is necessary to ensure retention of toughness and elongation at break properties. Apart from this, more radical but feasible methods such as ionizing radiation could also effectively enhance the inferior properties of waste tire rubber compounds.

1.2. Scope of study

The main focus of this study is to improve the inferior properties of waste tire rubber by blending with EVA, compatibilization and EB irradiation. Reclaimed rubber has very poor mechanical, thermal and chemical resistance properties while displaying acceptable dynamic mechanical properties. Blending of RTR with EVA, compatibilization of the blends and treatment with EB irradiation are expected to improve these properties to a nominal level.

RTR was adopted as an elastomer in RTR/EVA blend compound and not as reinforcing filler as the way it has been adopted in the past literature. This is important to ensure the feasibility of recycling the RTR with inferior properties. Improvement of properties was compared to RTR instead of EVA, as this study focuses on the improvement of the RTR properties.

1.3. Aims and objectives

This study aims to improve the properties of RTR by: (1) blending with EVA at different weight ratio; (2) compatibilizing RTR/EVA blends with compatibilizers such as (3-Aminopropyl)triethoxy silane (APS), liquid styrene butadiene rubber (LR) and maleated EVA (MAEVA); and (3) electron beam irradiation with and without the presence of radiation sensitizers such as trimethylol propane triacrylate (TMPTA), tripropylene glycol diacrylate (TPGDA) and N,N-1,3 phenylene bismaleimide (HVA2).

Therefore, the objectives of this study are:

- I. To study the different blend ratio of RTR/EVA; to verify the optimum blend ratio.
- II. To assess the physical and mechanical properties of RTR/EVA blends.
- III. To evaluate the thermal stability and the dynamic mechanical properties of RTR/EVA blends.
- IV. To determine the chemical stability of RTR/EVA blends using equilibrium swelling test.
- V. To study the effect of irradiation induced cross linking with and without the presence of radiation sensitizers on the compatibility and properties of RTR/EVA blends.

1.4. Research methodology and limitations

To evaluate the feasibility of improving the inferior RTR properties, RTR was blended with EVA in an internal mixer and compression molded. The molded specimens were subjected to electron beam irradiation to further evaluate the influence of ionizing radiation on the properties enhancement.

The properties mentioned here have been limited to physical, mechanical, thermal, dynamic mechanical and equilibrium swelling properties only.

1.5. Organization of thesis

This thesis contains 7 chapters and an appendix. The **second chapter** presents an extensive review on literatures related to thermoplastic blends utilizing waste tire compounds.

Chapter 3 details the materials and methodology employed in executing the experimental work of this study. Methods of mixing and molding along with the characterization have been detailed. Particular attention has been focused on mechanical, thermal, dynamic mechanical and equilibrium swelling methods.

Chapter 4 addresses the first aims of this study, whereby, the influence of EVA loading on RTR properties was discussed. The changes in the properties with respect to electron beam irradiation were also verified.

Chapter 5 reports the influence of different compatibilization strategies on the properties of RTR/EVA blends. The influence of different types and loadings of compatibilizers were focused. Here again, influence of electron beam irradiation in enhancing the properties of compatibilized blends was conferred.

Chapter 6 was focused solely on role of electron beam irradiation on enhancing the properties of RTR/EVA blends in the presence of radiation sensitizers. The crosslinking efficiency of different types of radiation sensitizers was compared and contrasted to determine the role of crosslink network formation on the properties of RTR/EVA blends. Originality and novelty of the study has been claimed in this section.

Chapter 7 articulates the main findings from this study and recommendations for future studies.

CHAPTER 2. LITERATURE REVIEW

2.1. Introduction

This chapter presents a review of the literature on waste tire rubber containing thermoplastic blends. An overview on the waste tire governing law and recovery is discussed in section 2.4 and 2.5 respectively. The recycling process of waste tires through downsizing to ground tire rubber and reclaiming/devulcanizing ground tire rubber is detailed in section 2.6. Finally the properties of waste tire rubber blends with thermoplastic were given in section 2.8. This chapter has been included as a part of a thorough review on waste tire rubber recycling by blending with polymers (Ramarad et al., 2015a).

2.2. Tires

Today's tire is a complex engineering structure having evolved from the old age's simple wheel into current pneumatic tire. Tires are highly engineered and complex assemblage of components that possess a wide range of properties. They are constructed from many dissimilar materials, to form a highly complex engineering structure that is required to operate in a wide range of environment. Automobile tires contain about twelve components and truck tires about twenty (Rodgers and Waddell, 2011). Rubber makes up for the biggest components used to construct a tire. Table 2.1 shows the typical composition of materials used in passenger and truck tire manufacturing. Examples of rubbers used in tire manufacturing are natural rubber (NR), styrene butadiene rubber (SBR), butadiene rubber (BR) and ethylene-propylene-diene-monomer rubber (EPDM) (Fukumori et al., 2002). It is no surprise that the tire industry is the biggest consumer of natural and synthetic rubbers (Shulman, 2011, Karger-Kocsis et al., 2013, Fukumori et al., 2002, van Beukering and Janssen, 2001).

Individual rubber, blends of rubbers, reinforcing materials, curatives and plasticizer contribute individually and collectively to the compound properties. These components are vulcanized together to impart specific properties to a tire composite. Vulcanization is defined as the process of rubber crosslinking utilizing sulphur or sulphur containing compound, an irreversible process discovered by Charles Goodyear in 1839 (Rajan et al., 2006, Akiba and Hashim,

1997). As a result, transverse bonds connect the rubber chains to form cross-linked structure of rubber. That is why tires are elastic, insoluble and infusible thermoset material that cannot be re-melted and processed, as is the case with thermoplastic materials. The use of a wide range of additives such as stabilizers, antioxidants and antiozonants are also one of the prime reasons why tires are extremely resistant to biodegradation, photochemical decomposition, chemical reagents and high temperatures (Adhikari et al., 2000, Ferrão et al., 2008, Roche et al., 2011). It is for these reasons that the management of used tires has become such a serious technological, economic and ecological challenge.

Table 2.1 Composition of materials used in tire manufacturing (Shulman, 2011, Karger-Kocsis et al., 2013, Sienkiewicz et al., 2012, Fang et al., 2001)

Type of tire	Car/Passenger (%)	Truck (%)
Rubber/Elastomer	41 – 48	41 – 45
Carbon black	22 – 28	20 – 28
Metal/Steel	13 – 16	20 – 27
Textile	4 – 6	0 – 10
Additives	10 – 12	7 – 10

2.3. Waste tires

Dramatic growth in the number of used tires around the globe was recorded due to increasing number of vehicles. According to van Beukering and Janssen (2001); approximately 800 million tires are discarded around the globe annually. This figure is estimated to increase by 2% every year. Similarly, Sienkiewicz et al. (2012) reported the annual global production of tires is about 1.4 billion unit, which corresponds to an estimated 17 million tonnes of used tires each year.

Land filling and tire mono filling were among the earliest ways of tire disposal around the world. Land filling is one of the most undesirable methods of disposing the used tires as it causes severe environmental problems and holds no promising future. Shape and impermeability of discarded tires allow it to hold water for a long period of time, providing sites for mosquito larva breeding's that are vectors of deadly diseases such as dengue and malaria. Discarded tires

could also present breeding ground to other animals such as rodents and snakes (Fiksel et al., 2011, Adhikari et al., 2000).

Moreover, discarded tires pose fire threat, especially during summers and it is difficult to be extinguished. Jang et al. (1998) mentioned a whole discarded tire presents a void space of 75% which makes it difficult to either quench the fire with water or cut off the oxygen supply. Water on fires often increases the production of pyrolytic oil, provides a mode of transportation to carry oils off site, and aggravates contamination of soils and water. Tire fire by-products may cause contamination of surface and subsurface water and soils. Air pollutants from tire fires include dense black smoke, which impairs visibility, and toxic gas emissions. A fire that took place at Tire King Recycling, Hagersville, Ontario, Canada in February 1990, lasted for 17 days before it was put out (Yang, 1993). This incident serves as a reminder of the danger of land filling discarded tires. The danger of tire fire is increased in discarded tire mono-fills compared to landfills.

Eco-toxicity of landfills are also affected due to discarded tires as leaching of metals and additives such as stabilizers, flame retardants, colorants and plasticizers could occur from the tire. Leaching of these materials from the bulk of the tires to the soil is not eco-friendly as these materials could possibly retard or kill the advantageous bacterial colony in the soil (Adhikari et al., 2000, Ferrão et al., 2008).

2.4. Legislations

Legislations were one of the driving forces behind the development of sustainable waste tire management. In United States (US), most of the states imposed legislations that require tires to be processed (cut, sliced or shredded) prior to land filling. Whole tires are discouraged from landfills (in almost all cases) either by law or high disposal fees. In 1990, 12 states passed or finalized waste tire laws, regulations or amendments. Later in 2000, about 36 states have waste tire legislations while about 9 states have bills proposed or in draft form to regulate waste tires (EPA, 1993, Jang et al., 1998).

European Union (EU) waste tire management was fueled by three different legislatives. The first was bound in 1999 named "Directive on Landfill of the

Waste 1000/31/EC” which prohibited the stockpiling of whole tires in landfills from July 2003, and ground tires from July 2006. Second legislation involved was the “End of Life Vehicle Directive 2000/53/EC”, passed in the year 2000, which regulates the removal of the tires from vehicle prior to demolition to ensure that the tire are recycled instead. The third was the legislation on “Incineration of Waste” directive aimed at reducing dioxins emissions to 90% by 2005 resulted in the use of tires for energy recovery and material recycling (Shulman, 2011, Sienkiewicz et al., 2012).

In Taiwan, Regulation for Recovery and Disposal of Discarded Tires was introduced in 1989, subjecting the manufacturers and/or importers responsible for the collection, recycling and disposal of waste tires (Yang, 1993). Korea and Japan also have their specified directives and legislatives to manage storage, processing, hauling and landfilling of waste tires (Jang et al., 1998).

Mainly three different models can be culminated from the literatures on the management of waste tire (Ferrão et al., 2008, EPA, 1993, Sienkiewicz et al., 2012). These models and their functions are illustrated in Figure 2.1. The EPR model popularly adopted in EU was found to be very successful with almost 100% recovery of waste tires. Figure 2.2 shows the model used in the management of waste tires in EU. Collectively, EU’s estimated recovery of waste tires achieved 95%, as compared with 69% for papers and 58% for plastics in 2011 (ETRMA, 2013). Comparatively, EU success rate at waste tire recovery is better than Japan (free market system) and US (mixed system) where the recovery was 91% and 89% waste tires respectively.

It is important to analyze the recovery rates of waste tires as it indicates the possibility of waste tire utilization. Higher recovery rates ensure the ‘rich’ waste tires do not actually go to ‘waste’, more importantly it eliminates the environmental threat imposed to humankind.

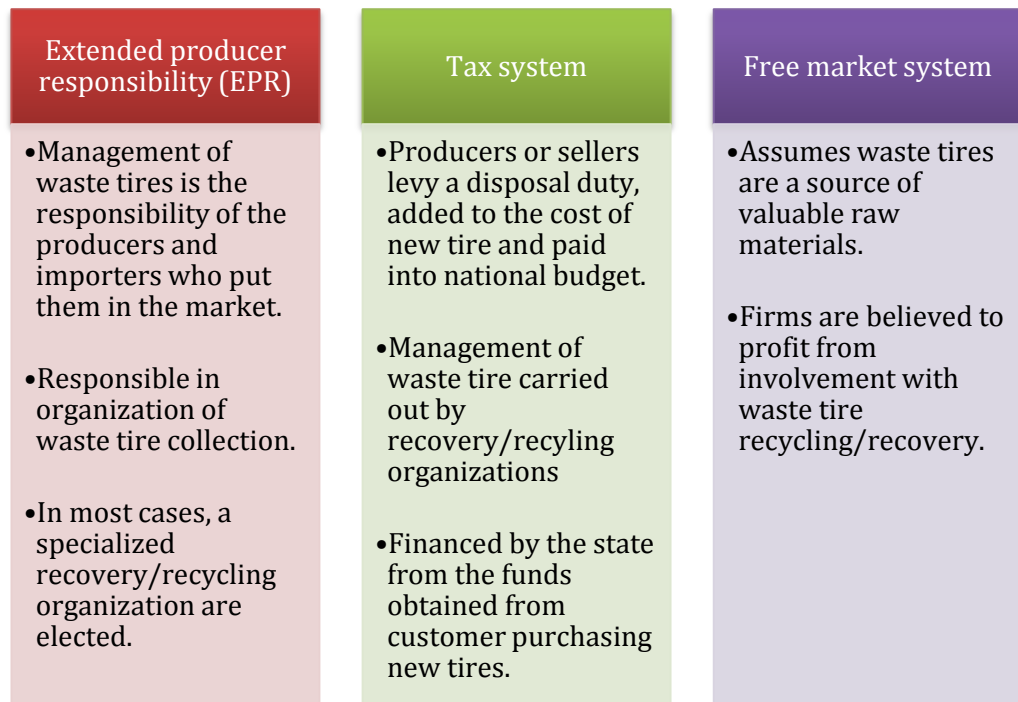


Figure 2.1 Three main models governing the management of waste tire (Ferrão et al., 2008, EPA, 1993, Sienkiewicz et al., 2012)

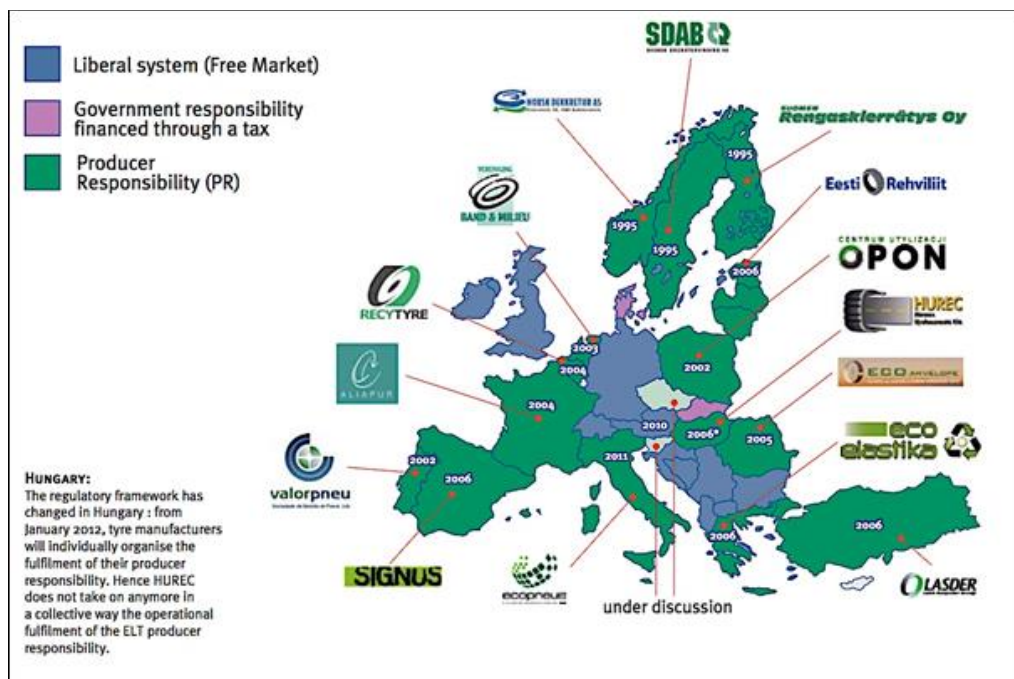


Figure 2.2 Models of waste tire management in EU, showing largest recovery/recycling organization in EPR model governing countries (Sienkiewicz et al., 2012)

2.5. Waste tires utilization

Recovered waste tires are considered to be 'rich' material because of their composition and properties and thus the sources of valuable raw materials. The efficiency of waste tire recovery models has led to the effective conversion of waste tires to energy or material. These 'rich' waste tires can be used to produce new goods of practical or utilitarian significance. Figure 2.3 illustrates the flow of waste tire utilization.

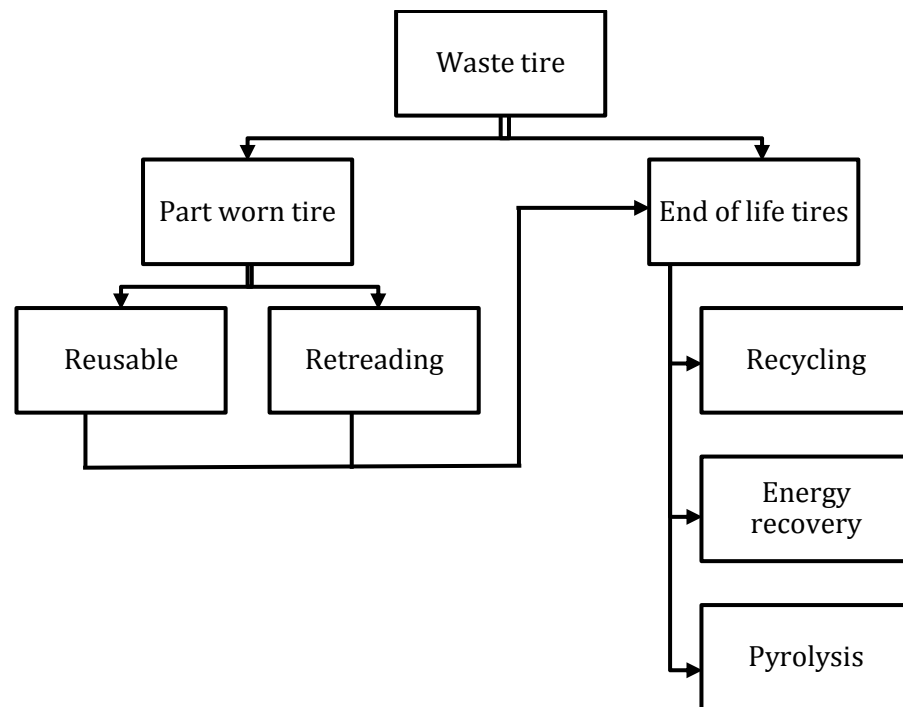


Figure 2.3 Flow of waste tire utilization

Figure 2.4 shows the breakdown of waste tire utilization from year 1994 to 2012 in EU. This trend is expected to be similar around the world. Energy recovery and recycling methods are the largest consumer of waste tire. Extracting from literature, the best waste tire utilization hierarchy is as shown in Figure 2.5. First and foremost, waste tire generation should be prevented. In an article, van Beukering and Janssen (2001) emphasized the properly inflated, rotated and cared for tires would last 50 to 90% longer on the road. Awareness among consumers should be created to cultivate good driving behavior and tire care in order to increase the tire life on the road. This will ensure proper usage of tires and delay the waste tire generation as it is impossible to prevent the generation of waste tire. A proper tire care would also result in waste tire with good casing

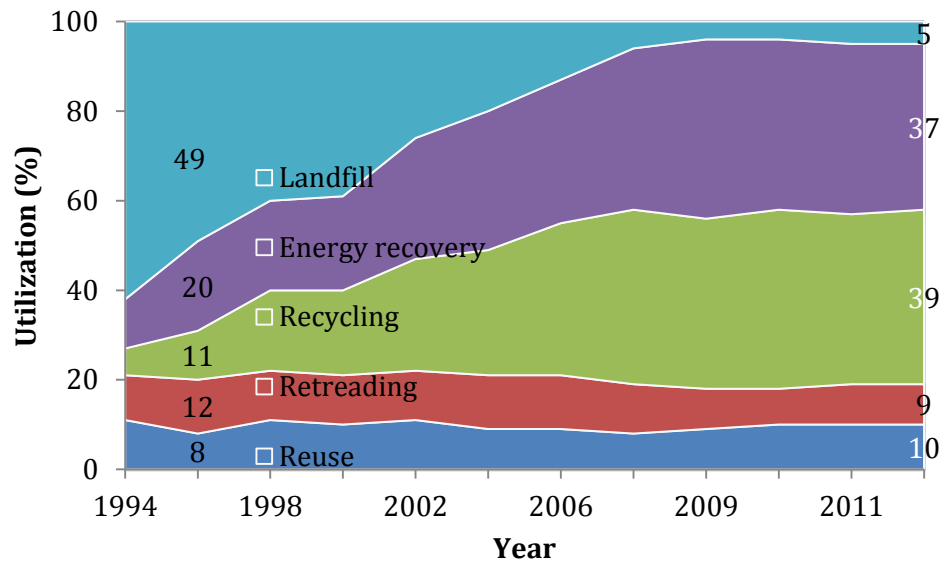


Figure 2.4 Breakdown of waste tire utilization in EU from 1994 to 2012 (ETRMA, 2013)

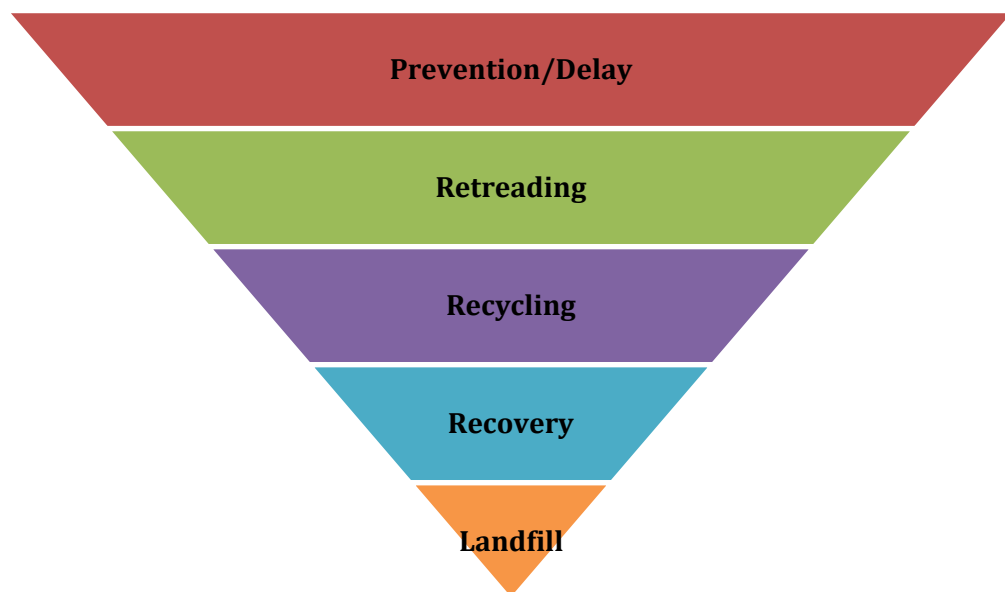


Figure 2.5 Hierarchy of waste tire utilization

which would boost the supply of retreading industry. When a retreaded tire enters the market, it reduces the manufacturing of one new tire, literally reducing the amount of waste being generated (Ferrer, 1997, Purcell, 1978). Retreading is the most economically viable method of waste tire utilization as it requires only 30% of energy and 25% of raw materials used to manufacture a new tire (van Beukering and Janssen, 2001). However, at current market,

retreaded tires are scarce (Wang et al., 2009a). Efforts should be taken to boost the market for retreaded tire. Third solution to waste tire utilization is recycling, followed by recovery. Currently, recycling and recovery are the most used methods of utilization. Recycling should be preferred to recovery as recovery method is only capable of recovering 30 to 38% of energy embedded in new tires (Ferrão et al., 2008, Fukumori et al., 2002). Finally, the least preferred method would be to landfill; even then it should be residual waste from all the above mentioned waste tire utilization methods not the whole tire by itself. In this chapter, detailed overview is given to recycling method where waste tires are used in polymeric blends.

2.6. Recycling waste tires

Nowadays, the world is heavily in touch and dependent on polymeric products. Polymeric materials have replaced a large number of conventional materials such as wood and metal in vast areas of applications. Waste tire, having almost 50% rubber is also a polymeric material commonly referred to as waste tire rubber. Blending waste tire rubber with polymers would permit for lowering the cost of the products created. Finding a market sector for these blends is not a tough job as the opportunities are enormous. Incorporating waste tire rubber into polymeric blends also supports the world's 3R (reduce, reuse and recycle) notion, whereby one would reduce the amount of virgin polymer used, reusing the tire rubber and this serves as a mean for recycling the waste tires. These factors have encouraged scientists and researchers around the world to create and evaluate waste tire rubber containing polymer blends and composites.

2.6.1. Downsizing waste tires

In order for waste tires to be incorporated in to polymeric blends, it has to be shredded to smaller sized particles (Amari et al., 1999). This process can be regarded as downsizing or down-cycling (Karger-Kocsis et al., 2013). Downsizing waste tires is a technologically complicated process, whereby; it requires special machinery and equipment capable of shredding and granulating waste tires; which possesses complex structure and high mechanical properties (Sunthonpagasit and Duffey, 2004).

Table 2.2 lists the main methods of waste tire downsizing with their advantages and disadvantages. In line with the granulation processes, the textiles and steels from waste tires will be removed by pneumatic separators and electromagnets respectively (Sunthonpagasit and Duffey, 2004). Figure 2.6 reveals the surface characteristics of ground tire rubber (GTR) obtained from different downsizing processes. The figure apparently shows different type of surfaces and sizes of GTR from different downsizing processes. Ambient processing tends to produce GTR particles with rough and irregular surfaces while cryogenic process provides smooth and edgy surfaces.

2.6.2. Reclaiming and devulcanization

Reclaiming or devulcanization is the oldest method used to modify GTR (Adhikari et al., 2000, Rajan et al., 2006). After GTR, reclaimed or devulcanized rubber is the most used form of waste tire rubber in the polymer blends. By definition, these two processes are very different. Reclaiming is defined as scission of carbon – carbon bond on the rubber back bone aiming to reduce the molecular weight to attain plasticity (Tao et al., 2013). Devulcanization is the cleavage of sulphur – sulphur and carbon – sulphur bond to breakdown the three dimensional structure formed during vulcanization process to attain plasticity (Amari et al., 1999, Myhre et al., 2012). Even though both processes aims to obtain a rubber compound which can be processed and vulcanized similar to fresh/virgin rubber, it is impossible to specifically target the cleavage of the bonds as per the definition. At any given time, both reclaiming and devulcanization would be taking place simultaneously as illustrated in Figure 2.7 (Li et al., 2005). At present, methods of breaking down a vulcanized rubber structure target the cleavage of mono, di and poly-sulphidic bonds while trying to minimize the carbon – carbon bond cleavage (which would still happen to a certain extent) (Rooj et al., 2011). This is possible as the energy needed to break the sulphur bonds is lesser compared to breaking a carbon – carbon bond as presented in Table 2.3. Hence, the term ‘reclaimed’ or ‘devulcanized’ rubber can be used interchangeably.

Table 2.2 General methods of waste tire downsizing (Karger-Kocsis et al., 2013, Sienkiewicz et al., 2012)

Methods	Description	Advantages	Disadvantages
Ambient 0.3 mm Rough, irregular	Repeated grinding following shredder, mills, knife, granulators and rolling mills.	High surface area and volume ratio.	Temperature could rise up to 130 °C. Oxidation on the surface of granulates. Cooling needed to prevent combustion.
Wet ambient 100 µm Rough, irregular	Grinding suspension of shredded rubber using grindstone. Water cools granulates and grindstone.	Lower level of degradation on granulates. High surface area and volume.	Requires drying step and shredding of tires before grinding.
Water jet	Used for large size tires (trucks and tractors) Water jet of >2000 bar pressure and high velocity used to strip rubber.	Environmentally safe, energy saving, low level of noise and no pollutants.	Requires high pressure and trained personnel.
Berstoff's method	Combines a rolling mill with specially designed twin screw extruder in a line.	Small grain size, large specific area and low humidity.	Not disclosed.
Cryogenic 75 µm Sharp edge flat/smooth	Rubber cooled in liquid Nitrogen and shattered using impact type mill	No surface oxidation of granulates and cleaner granulates.	High cost of liquid Nitrogen. High humidity of granulates.

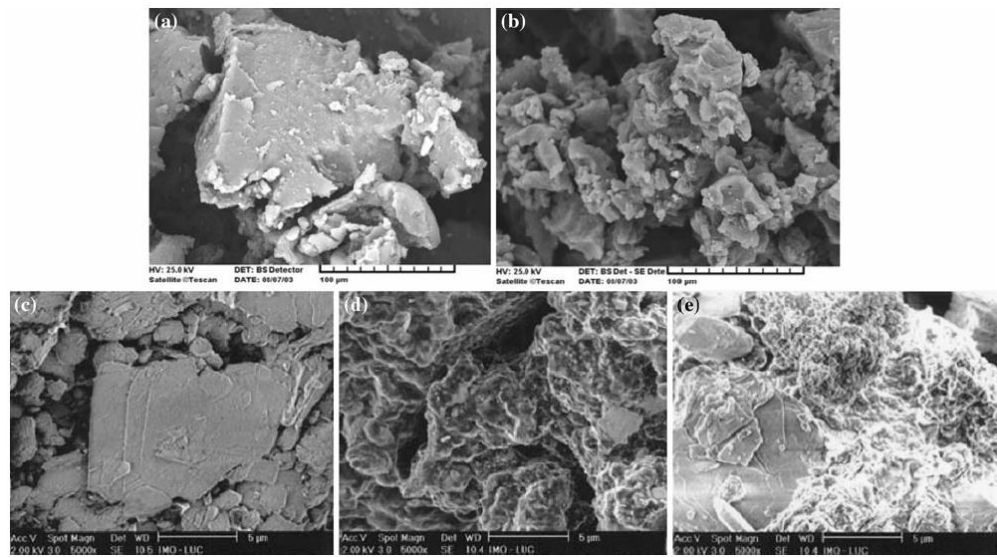


Figure 2.6 The surface of GTR produced from the different downsizing processes. (a) ambient – mechanical; (b) water jet; (c) cryogenic – pin mill; (d) ambient – rotary mill; (e) cryogenic – rotary mill (Karger-Kocsis et al., 2013)

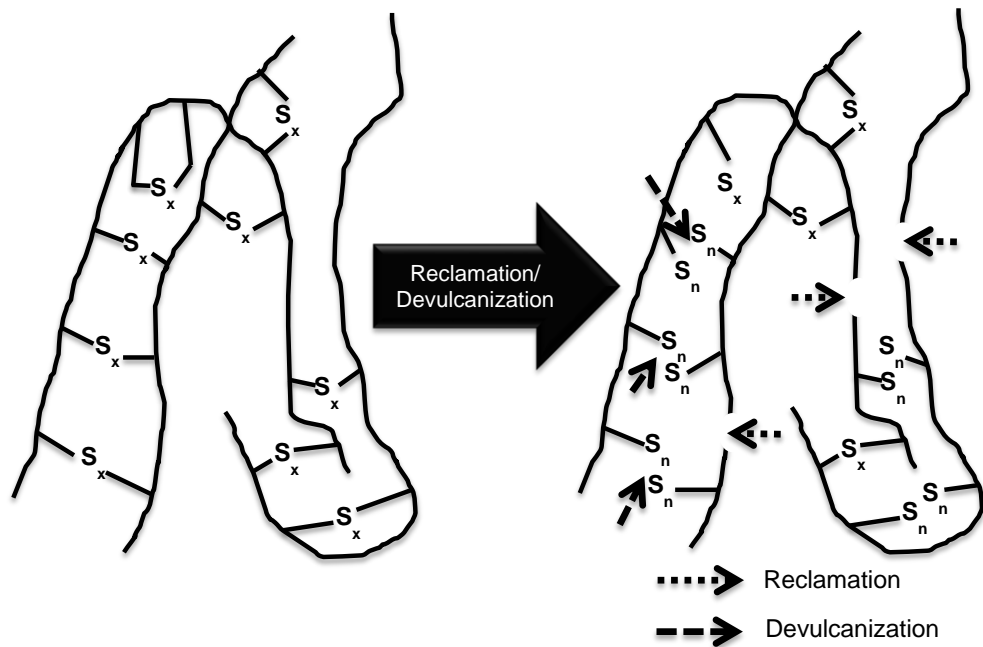


Figure 2.7 Schematic representation of devulcanization and reclaiming

Table 2.3 Energy required for cleaving sulphur or carbon bonds (Karger-Kocsis et al., 2013, Rooj et al., 2011)

Type of bond	Energy required for cleavage (kJ/mol)
C - C	348
C - S - C	273
C - S - S - C	227
C - S _x - C	251

In this thesis, both reclaimed and devulcanized rubber will be termed as reclaimed tire rubber (RTR). Obtained RTR needs to have a soluble fraction with acceptable molecular weight, as the soluble fraction will be responsible for the interaction or bonding with the continuous polymer matrix in the polymer blends later (Adhikari et al., 2000). Soluble fraction with high molecular weight ensures formation of strong adhesion between GTR and continuous polymer matrix. Shi et al. (2013) studied the structure and performance of the reclaimed rubber produced from four different reclaiming methods involving reclaiming factors such as temperature, shear force and atmosphere. They found that all reclaimed samples were mixtures of soluble part, a loosely crosslinked gel part and low molecular substances. Ideally, sol fraction and its molecular weight should be as high as possible to have both good processability and mechanical properties. However, it is difficult to reach high sol fraction and molecular weight due to the nonselective scission of the main chain and crosslink bonds. Thus, the presence of some amount of gel fraction is essential to have a high quality of RTR.

Reclaiming and devulcanization can be carried out using physical, chemical and microbial processes. Table 2.4 gives an overview of rubber reclaiming and devulcanization processes. The complete details of different reclaiming and devulcanization processes have been heavily reviewed in the literature (Adhikari et al., 2000, Isayev, 2011, Myhre et al., 2012). It is noteworthy that the scission of main chain and crosslink bonds happens only on the surface, leaving the core to retain in three dimensional structure. RTR is readily available in the market as the reclaiming and devulcanization process have been in practice for a very long time. RTR is also favored when blending with rubber as the miscibility

of the RTR/rubber blends are reported to be better compared GTR/rubber blends (Li et al., 2005, Balasubramanian, 2009, Rooj et al., 2011, Kumnuantip and Sombatsompop, 2003).

Table 2.4 Physical, chemical and microbial processes of tire rubber reclaiming/devulcanization (Myhre et al., 2012, Vukanti et al., 2009, Shah et al., 2013, Shi et al., 2014)

Physical	Chemical	Microbial
Mechanical	Radical scavengers	Aerobic reactions
Thermo-mechanical	Nucleophilic additives	Anaerobic reactions
Microwave	Catalyst systems	Bacterial
Ultrasonic	Chemical probes	Fungi

2.7. GTR and RTR in polymer blends

GTR and RTR are reused by incorporating them into polymers. Polymers can be grouped into three; thermosets, thermoplastics and rubbers. GTR and RTR can be mixed with all three groups to obtain blends. The market share of polymers are enormously big, incorporating as little as 10 wt% of GTR into polymers, especially thermoplastic, would mean a big consumption of waste tires (Karger-Kocsis et al., 2013). Specific reason fuels the use of GTR in each of the polymer groups. Thermoset industry was interested in improving toughness; thermoplastic industry wanted to attain thermoplastic elastomers while rubber sought for cheap filler.

GTR and RTR contain fillers like carbon black, whereby, their mixture with polymer should yield a composite. Here, for simplicity of discussion, it would be referred as blends.

Generally, for all the three groups of polymer blend, the interface is one of the main issues which govern the final properties of the material. GTR or RTR is incompatible with the polymer matrix and the former exists as dispersed phase in the later. This produces a weak interphase, which needs to be addressed in order to have optimal balanced properties. Two common practices are compatibilization or crosslinking the GTR or RTR with the polymer matrix. Both

compatibilization and crosslinking techniques will be listed hereafter, followed by the general discussion on the properties of GTR or RTR thermoplastic blends in section 2.8.

2.7.1. Compatibilization

In general, the properties of GTR/RTR containing polymer decrease with increasing GTR/RTR content (Ismail et al., 2006, Sakinah et al., 2009, Sonnier et al., 2007) caused by poor interfacial adhesion between the blend components. These blends are simply a physical mixture of two incompatible polymers, in which the continuous matrix phase is largely responsible for the mechanical properties. Therefore, the key to success in producing desirable properties of GTR/RTR containing polymer blends is to compatibilize the blend components. Dynamic reaction of polymer and GTR/RTR in the presence of compatibilizer which acts as a bridge is believed to improve mechanical properties of the blend. In general, compatibilization is essential for GTR/RTR containing polymer blends in order to: 1) Improve adhesion between faces by reducing interfacial tension; 2) Achieve finer dispersion of GTR/RTR in the matrix during blending/mixing; and 3) Morphology stabilization during processing and service life (Mangaraj, 2005).

Compatibilization makes the interfaces of the phases similar to each other or provides specific interaction sites between the phases. One can compatibilize by physio-mechanical, chemical or the combination of the two. Chemical modification is desired as it forms a good adherence between GTR/RTR and the matrix polymer. In this process, interfacial tension is reduced by the enhanced wetting thereby forming a good interphase for stress transfer. Chemical compatibilization can be achieved by reactive and non-reactive methods.

In the non-reactive method, compatibilizers are incorporated into the GTR/RTR containing polymer blends in order to improve the blend compatibility. Compatibilizers which are specially prepared prior to blending as well as commercially available block and graft co-polymers such as Surlyn 1652™ of DuPont and Polybond™ of Uniroyal are often used for compatibilization. Various attempts of non-reactive compatibilization of GTR/RTR with different types of polymer matrices can be found in the literature (Mészáros et al., 2012, Qin et al., 2008, Zhang et al., 2009). However, the block and graft co-polymers are costly.

Whereas, in the reactive method additives are added during blending to bind the GTR/RTR with the polymer matrix, thereby forming chemically linked interphase. The blend component or a reactive third component may participate in the compatibilization. High performance thermoplastic elastomer based on PE, EPDM and GTR with improved mechanical properties has been developed by reactive compatibilization. In this study, the PE component was functionalized with maleic anhydride (MA) while the GTR component was modified via functionalization with MA or acrylamide (AAM) using grafting techniques (Grigoryeva et al., 2008). Reactive compatibilization can also be done with the addition of reactive monomers and initiators, forming a graft copolymer with one or both phases' insitu. Zhang et al. (2010) used bitumen and MA-grafted-styrene-ethylene-butylene-styrene (MAGSEBS) in compatibilization of PP/GTR blends. Reactive compatibilization is preferred over non-reactive compatibilization because it is of lower cost and more efficient. However, the correct selection of the reactive component in order to ensure that it is fully reacted during blending and does not produce by products which are difficult to remove.

At times, combination of both reactive and non-reactive compatibilization yields good properties of the blends. For example, GTR surface might be modified and a suitable additive might be added to form a chemical bond with modified GTR, while the additive is compatible with the matrix. This method is more frequently used in thermoplastics and thermoplastic elastomer blends. Shanmugaraj et al. (2005) compatibilized PP/GTR blends by using allylamine grafted GTR along with MAGPP as compatibilizer and found improvement in the mechanical properties compared to neat blend. Similarly, Kim et al. (2000) compatibilized acrylamide modified GTR and HDPE blends with MAGPE which improved tensile and impact properties of the blend. Even though compatibilization by surface modification is cost effective, it is not as efficient as reactive compatibilization.

2.7.2. Crosslinking

Another common process carried out to obtain a good interphase is crosslinking of GTR and RTR in the blends. This crosslinking process is a must with rubber blends and preferred in thermoplastic elastomer blends, while having a fine share in the thermoplastic blends. Three types of crosslinking process can be

carried out; namely, sulphur crosslinking, peroxide crosslinking and ionizing radiation crosslinking. During the crosslinking process, polymer chains are linked to one another through chemical bonds. The aim here is to form the chemical bonds (or crosslinks) between the GTR/RTR and the polymers used. These chemical bonds will result in enhanced interfacial adhesion between the incompatible GTR/RTR and the polymer matrix.

Sulphur crosslinking is more commonly known as vulcanization. In this process, sulphur will act as the vulcanizing agent in the presence of other additives such as activators (zinc oxide and stearic acid) and accelerators (thiuram and thiazole). This crosslinking system, however, can only be used in unsaturated substance such as natural rubber and styrene butadiene rubber. Sulphur will be mediating a crosslink between two polymeric chains (C-S_x-C) (Akiba and Hashim, 1997). This method of crosslinking is heavily used in the rubber blends.

Peroxide crosslinking is commonly used in saturated polymers such as PE, ethylene-propylene rubber (EPR) and silicone rubber. Common peroxides used are dicumyl peroxide and benzoyl peroxide. The reaction employs decomposition of peroxide which forms radicals that extracts hydrogen atom from the polymer chain creating macromolecular radical. Combinations of the macromolecular radicals forms crosslinking between chains (C-C) (Akiba and Hashim, 1997). Thermoplastic blends comprising GTR or RTR employs peroxide crosslinking to bind the rubber and plastic phases to form an appreciable interphase.

Ionizing radiation such as gamma ray, electron beam and X-ray irradiation are also capable of crosslinking polymeric substances. However, it is less researched due to limited availability of the sources (Makuuchi and Cheng, 2012b). Exposure to ionizing irradiation creates polymer macro molecular radicals which could recombine causing crosslinking of macromolecular chain. Nevertheless, irradiation in the air atmosphere could cause oxidative degradation (Makuuchi and Cheng, 2012a). To overcome this, radiation sensitizers such as multifunctional acrylates, methacrylate esters and bismaleimide can be used to accelerate irradiation induced crosslinking. The sensitizers form very reactive radicals that can graft onto polymeric chains through recombination of sensitizer radicals and polymer macro radicals upon exposure to ionizing irradiation. The sensitizer's efficiency on crosslink

formation is dependent on the functionality and reactivity (Mittal, 2012). However, ionizing irradiation could also cause the detrimental effect of chain scission in polymers, which could be minimized through the use of radiation sensitizers (Mittal, 2012).

Sonnier et al. (2008) achieved in situ compatibilization between GTR particles and HDPE matrix by using a peroxide as a catalyst of dynamic co-crosslinking at the interphase. Various example of compatibilization of GTR/RTR with polymer matrices by co-crosslinking can be found in the literature (Tantayanon and Juikham, 2004, Awang and Ismail, 2008, Awang et al., 2007, Punnarak et al., 2006). The co-crosslinked system can be described as interpenetrating network (IPN).

2.8. Thermoplastics – waste tire rubber blends

Thermoplastics such as polyethylene (PE), polypropylene (PP) and polyvinyl chloride (PVC) are widely used commodity plastics due to their low cost and ease of processing. Blending of thermoplastics and rubber are commonly done to obtain thermoplastic elastomer exhibiting excellent combination of thermoplastic and elastomeric properties along with the ease of processing similar to thermoplastics. These superior thermoplastic elastomer markets are expanding greatly, but are very expensive nevertheless. Combining GTR/RTR in the thermoplastic might offer a solution on utilization of waster rubber while decreasing the current high cost of thermoplastic elastomer. These reasons fueled the potential of GTR/RTR blend with thermoplastics.

2.8.1. Mechanical properties

Mechanical properties of blends comprising GTR/RTR and thermoplastics have been extensively studied. Factors influencing the changes in mechanical properties of thermoplastic-GTR/RTR blends have been detailed here.

2.8.1.1. Influence of particle size

Particle size of dispersed phase plays an important role in mechanical properties of blends. Particle size of GTR was found to influence the mechanical properties,

where the smaller particles rendered better properties compared to bigger particle. Larger particle size has higher probability of failure cracks whereas smaller particle tends to develop smaller micro cracks below the critical length dimension. However, the influence of particle size at higher loadings (above 50 wt%) of GTR are insignificant due to poor interphase factor playing a more dominant role. Ismail et al. (2006) in their work reported particle size $<500\ \mu\text{m}$ rendered better mechanical properties compared to bigger particle size. Colom et al. (2009) observed the drop in tensile strength of 20 wt% GTR containing HDPE blend with $<200\ \mu\text{m}$ particle size was only 25% whereas when bigger particle size ($>500\ \mu\text{m}$) was used the drop observed was 51%. Similar observation was also noted by Mujal-Rosas et al. (2011) in their work with EVA/GTR where they used three different particle sizes (<200 , $200 - 500$, $>500\ \mu\text{m}$). Sonnier et al. (2007) used three different GTR particle sizes which were all $>500\ \mu\text{m}$ and did not observe significant influence of particle size on the mechanical properties of 50 wt% GTR loaded LDPE blend. Tantayanon and Juikham (2004) studied the impact strength of PP/GTR blend comprising $420\ \mu\text{m}$, 1.2mm and $2.4\ \text{mm}$ sized particles and found only the smallest particle size gave an appreciable improvement in impact strength (20%) whereas the other two bigger particle size blends showed only marginal improvement. These observations might send a message that particle size below $500\ \mu\text{m}$ is the most suitable to be used in thermoplastic blends. Figure 2.8 shows the general relationship between the particle sizes of GTR on the mechanical properties of thermoplastic blends. The $500\ \mu\text{m}$ value has been indicated on the figure to emphasize the minimal requirement of particle size to obtain thermoplastic blends with good properties.

2.8.1.2. GTR/RTR loading

Tensile and impact properties generally deteriorated with addition of GTR/RTR. This behavior was associated with poor adhesion between GTR/RTR and plastic matrix interphase. Poor interphase leads to high interfacial tension, forcing the GTR particles to cluster/agglomerate and promotes the formation of voids around GTR. Figure 2.9 indicates the increasing faults, defects and cracks in the matrix with increasing GTR content. Clear indication of lack of interfacial adhesion can be deduced from the clean and easy removal of GTR particle off the matrix.

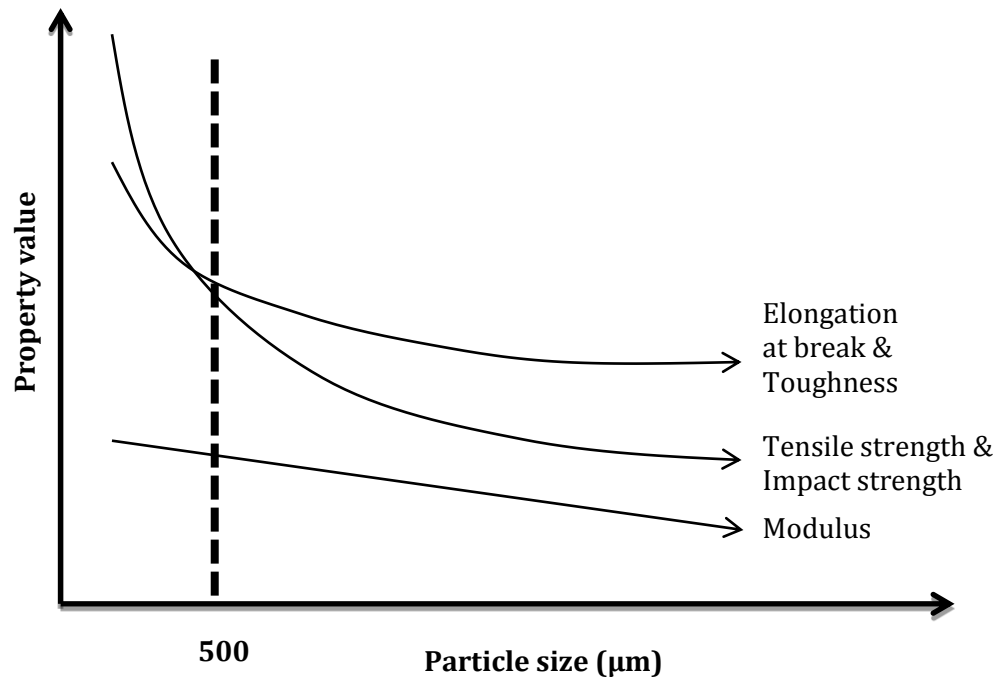


Figure 2.8 Influence of the particle size of GTR on mechanical properties of thermoplastic blends

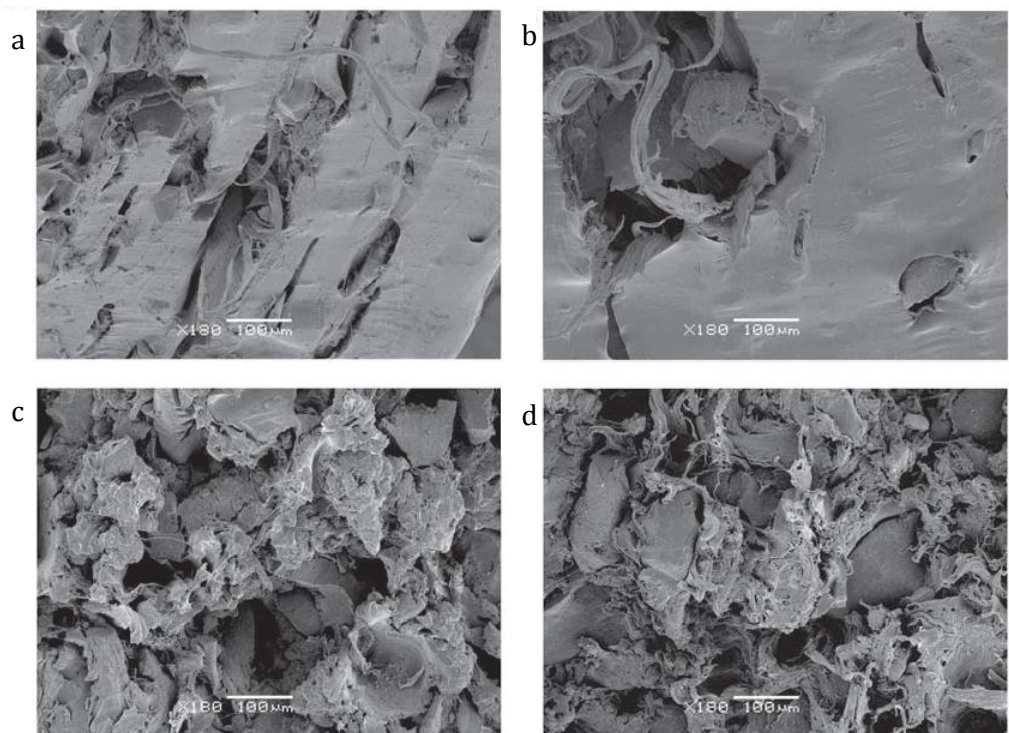


Figure 2.9 SEM micrographs of increasing GTR loading in EVA matrix a) 10wt%, b) 20wt%, c) 50wt% and d) 70wt% GTR (Mujal-Rosas et al., 2011)

Colom et al. (2009) found deterioration in tensile strength (TS), tensile modulus (TM) and elongation at break (Eb) approximately by 25%, 33% and 93% respectively when only 20 wt% GTR was added to HDPE. Recycled HDPE/GTR blends properties were studied by Sonnier et al. (2006) and they found all tensile and impact properties deteriorate considerably with increasing GTR content. At 50 wt% GTR content, tensile properties showed diminution of 40 to 80% while impact strength dropped by 80%. Study using PP/GTR also showed similar pattern where the TS, TM and Eb deteriorated approximately by 20%, 25% and >90% respectively at 30 wt% GTR loading (Ismail et al., 2006). Mujal-Rosas et al. (2011) in their work with EVA/GTR blend showed TS deterioration (by 67% at 70 wt% GTR), TM improved up to 20 wt% GTR followed by deterioration while Eb and tensile toughness diminished significantly (>90%). Another work utilizing EVA and GTR also reported the tensile properties of the blends decreased with increasing GTR loading (TS and Eb drop by \approx 60% while TM drop by \approx 25% at 40 wt% GTR) as per volume rate of additivity where the higher strength EVA molecules are gradually replaced by the lower strength of GTR phase (Sakinah et al., 2009).

Li et al. (2003a) incorporated cryogenically ground GTR into HDPE matrix and found the Eb and impact strength deteriorated by more than 90% and 80% respectively. TS and hardness also reduced in a less remarkable manner. In another study, impact strength was reported to increase by \approx 21% up to 50 wt% RTR loading in HDPE matrix but the tensile strength was found deteriorating continuously up to 70 wt% RTR. Improvement in impact strength up to 50% RTR was due to capability of RTR to absorb the impact energy and reduction upon further increase in RTR was due to increasing CB content in the blends causing defect points which induces a split in the layer structure of the blend providing a shorter path for fracture propagation. However, the tensile properties of the blends continued to decrease with increasing RTR content similar to the other observation reported earlier (Punnarak et al., 2006).

One of the common requirements of thermoplastic elastomer is to have an Eb of at least 100%. However, Eb and toughness were severely reduced with the introduction of GTR/RTR onto the thermoplastic matrix. Figure 2.10 shows the general relationship between mechanical properties of thermoplastic blends with increasing GTR/RTR loading; highlighting the lack of Eb and toughness in blends at higher loading of GTR/RTR.

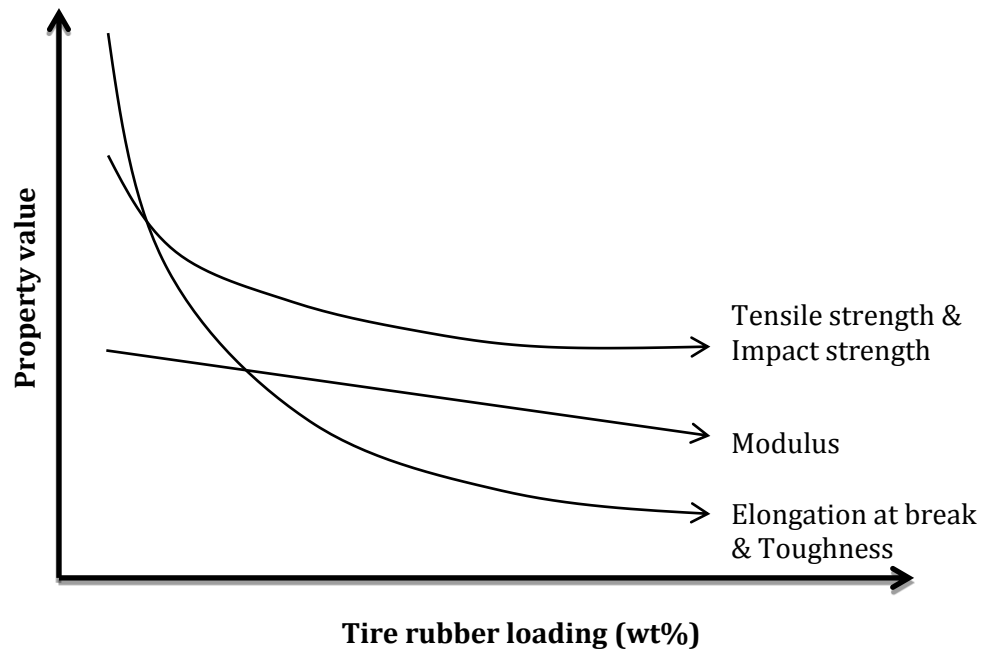


Figure 2.10 Influence of tire rubber loading on the mechanical properties of thermoplastic blends

2.8.1.3. Modified GTR blends

Modifications of GTR are capable of reducing interfacial tension, thus enhancing the properties of the blends. However, different types of modification result in variation of blend properties. Colom et al. (2009) used acidic treatments on GTR to improve the interfacial adhesion with HDPE matrix and successfully improved the TM slightly and almost retained the TS at 20 wt% GTR loading. However, acidic treatment resulted in stiffer GTR due to loss of plasticizer and low molecular weight substance during treatment resulting in drastic drop in Eb. Potassium permanganate treated and gamma irradiated GTR did not show any changes in the tensile properties of HDPE/GTR blend, however, gamma irradiated GTR blend did show slight improvement in the impact strength (Sonnier et al., 2007). Allyamine modified GTR via UV treatment improved the TS and Eb by 9 % and 7 % respectively in PP/GTR blend. However, substituting PP with MAgPP matrix yield significant improvement in Eb while slightly decreasing the TS. Modification of GTR with allyamine also improved the dispersion of GTR in the matrix. Figure 2.11 shows the morphological changes in amine treated GTR with and without compatibilizer. Though amine treated GTR/PP surface appeared more ductile compared to GTR/PP surface; there was still an appreciable presence of vacuole indicating GTR particle pull out. Surface

morphology of amine treated GTR/PP with MAgSEBS as compatibilizer was more homogeneous and it was difficult to distinguish the presence of GTR particle as it was covered completely (Lee et al., 2009). Acrylamide modified GTR was blended with HDPE in the presence of MAgPE and found the tensile and impact properties improved due to enhanced interface from interaction between acrylamide and MAgPE (Kim et al., 2000). Awang et al. (2008) modified GTR with latex and found the properties of modified GTR blends were far better than unmodified GTR blends throughout the blend ratio as the latex modification improved the dispersion of GTR in PP matrix more evenly. Even though in all cases, the surface modification was successful, not many of them provided balanced mechanical properties.

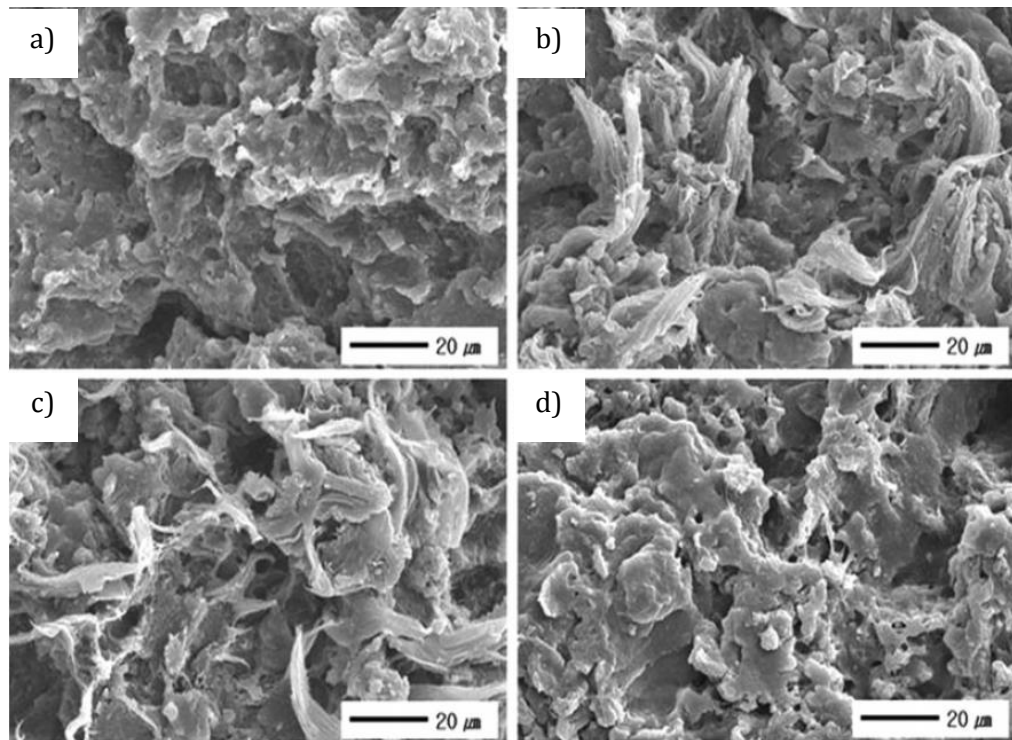


Figure 2.11 Morphological changes in a) GTR/PP, b) GTR/PP/MAgSEBS, c) amine treated GTR/PP and d) amine treated GTR/PP/MAgSEBS (Lee et al., 2009)

2.8.1.4. Influence of compatibilizer

Compatibilizers are commonly used to improve the interfacial adhesion between incompatible blends. Mészáros et al. (2012) used EVA as partial replacement of the LDPE matrix to improve the interfacial adhesion and showed the E_b increased by 50% while TS and TM decreased about 1.4 and 1.7 times respectively due to the nature of EVA (low TM, TS and high E_b). In another

study, three different compatibilizers were used in LLDPE/GTR blend where SBS and EVA were found to be the best and worst compatibilizer respectively. 6 wt% SBS addition improved the Eb by 112.5%, TS by 26.2% and tear strength by 62% compared to uncompatibilized blends (Qin et al., 2008). Zhu and Tzoganakis (2010) synthesized compatibilizer, PP-hydrosilylated-SBR, through reactive method and used it for PP/GTR blends. Improvement in tensile properties was observed (TS 4 – 32%, TM 8 – 32% and Eb 27 – 73%) and inferred the improvement to be due to good wetting between the GTR and SBR group of the compatibilizer. Zhang et al. (2009) evaluated the presence of bitumen as compatibilizer for PP/RTR which improved the Eb ($\approx 160\%$) of blend but slightly decreased the TS ($\approx 3\%$).

Punnarak et al. (2006) used MAgPE in HDPE/RTR blends and found impact strength of 50 wt% RTR blend was 71% higher than un-compatibilized HDPE/RTR blend. Tensile properties were also reported to improve by at least 1x than the un-compatibilized blends. Interestingly, blends compatibilized with MAgPE showed better impact strength compared to the sulphur or peroxide cured blends in this study. Shanmugaraj et al. (2005) used MAgPP to compatibilize allyamine grafted GTR blends and found the TS improved by 10 to 20% while Eb improved by 20 to 50% compared to uncompatibilized blends. Improved interphase was obtained due to interaction of MAgPP with allyamine of modified GTR. Lee et al. (2009) in their work blended GTR with PP and MAgPP matrix in the presence of MAgSEBS compatibilizer and found TS and Eb to increase significantly due to SEBS forming a good wetting with GTR as well as being compatible with the PP matrix (Figure 2.11). Lee et al. (2007) studied the properties of 65 wt% GTR containing PP and MAgPP blends and found MAgPP matrix yield better tensile properties as opposed to PP matrix. In an attempt to compatibilize the blends, SEBS and MAgSEBS were employed. Both SEBS and MAgSEBS improved the properties further believed to be due to compatibility of SEBS with both PP and GTR whereby reactive dynamic compatibilization was taking place.

Li et al. (2003a) incorporated EPDM (10 wt%), silicone oil (4 wt%) and DCP (0.2 wt%) into 40 wt% GTR containing HDPE blends and found the impact strength and Eb improved by a whopping 150% compared to uncompatibilized blends. EPDM and silicone oil was expected to encapsulate the GTR particles reducing the stress concentration around the particles and inhibiting fracture

phenomena. Zhang et al. (2009) subjected GTR to reclamation in the presence of bitumen and incorporated the resulting RTR (50/50 composition of tire rubber/bitumen) into PP matrix. The Eb of PP/RTR blend improved by 160% with negligible drop in TS compared to equivalent PP/GTR. They included 20 wt% compatibilizer replacing the RTR component in the PP/RTR blend of 40/60 composition. SEBS and MAgSEBS showed the best Eb improvement followed by EPDM. SEBS and MAgSEBS recorded an improvement of 149% and 128%, respectively, showing a value of Eb more than 300%. However, the presence of actual tire rubber in the composition is only 20 wt% of total blend composition.

Use of compatibilizers has shed some light on improving the Eb of the blends, which is the key loss factor with incorporating GTR/RTR in thermoplastic matrix. The improvement in impact strength, TS and TM along with Eb is an added advantage. Most of the compatibilized blends, though, showed improvement compared to uncompatibilized counterpart, their properties were still lower as compared to the neat matrix. Though one would argue that the blends properties are still lower than the neat matrix, it is not quite possible for the blends to attain higher values than the matrix as the properties of GTR/RTR by itself is lacking due to being severed during life and recycling processes. Furthermore, GTR/RTR containing CB and other fillers might hinder the improvement of the properties.

2.8.1.5. Effect of crosslinking

Crosslinking the blends by any of the methods discussed in section 2.7.2 should help to improve their interphase and indirectly their properties. Different crosslinking methods yield different observations. Tantayanon and Juikham (2004) in their work compared the impact properties of sulphur cross-linked PP/GTR with PP/RTR blends and found the PP/RTR blends showed an appreciable improvement by 60 to 80% compared to PP. However, PP/GTR only showed marginal improvement indicating RTR has more free chains (from the devulcanization process) to participate in the crosslinking process as opposed to vulcanized GTR rubber. Figure 2.12 shows the schematic diagram illustrating the difference in microstructure of polymer blends with GTR and RTR. The presence of free chains on the surface of RTR allows for co-crosslinking to take place between RTR and polymer matrix. This allows for improved adhesion between

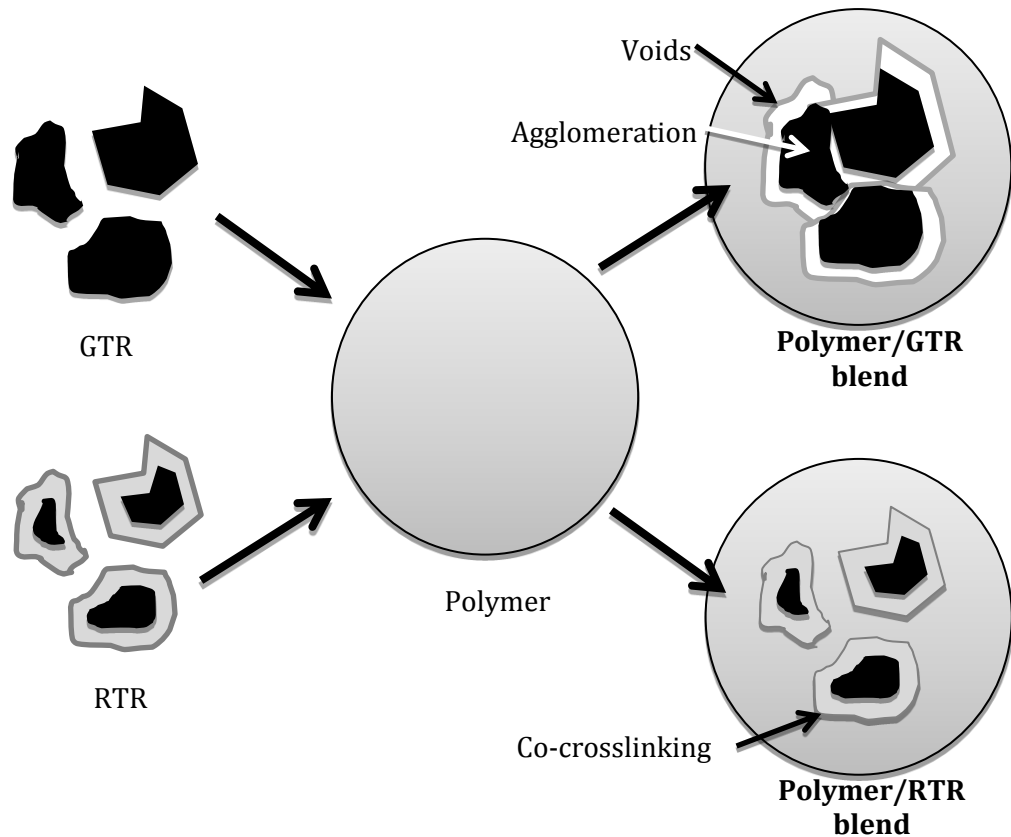


Figure 2.12 Schematic diagram showing the difference in microstructure of polymer blends with GTR and RTR (modified and re-formulated based on Li et al., 2003a, Lee et al., 2007).

RTR and continuous matrix resulting in improved interfacial properties. Further test was done employing MA and DCP to crosslink PP/RTR blend and found the impact strength was even better than sulphur cross-linked system (160% higher than PP). MA was believed to be grafted onto both PP and GTR inducing compatibilization through the dipolar interaction among the MA grafted PP and MA grafted RTR. This causes a reduction in interfacial tension and an increase in interfacial adhesion.

In another study, PP/GTR blends were dynamically vulcanized in the presence of *trans*-polyoctylene rubber (TOR). Eb improved by 20 to 40% while TS and TM showed slight improvement which was due to co-crosslinking of GTR and PP through TOR which locates at the interfacial area (Awang et al., 2007). Punnarak et al. (2006) studied the influence of sulphur, peroxide and mixed crosslinking system on the properties HDPE/RTR blends and found sulphur crosslinking system rendered the best enhancement in the properties throughout the studied

blend ratio. Impact strength and tensile properties improved around 25 to 60% and 10 to 100% respectively in sulphur cured blends. Whereas, peroxide cured blends were showing inferior impact strength compared to non-cured blends.

Sonnier et al. (2008) reported treatment of recycled HDPE/GTR blends with peroxide improved tensile and impact properties. They attributed the improvement to co-crosslinking of HDPE and GTR phase that creates an interfacial adhesion between HDPE and GTR. Incorporation of DCP and HVA2 in PP/GTR blends substantially improved the tensile properties (TS $\approx 1.5x$, Eb $\approx 2.5x$), where DCP facilitates the formation of macromolecular radical in PP and GTR which is scavenged by HVA2 forming a copolymer in the interphase. This built a strong interfacial adhesion between PP and GTR which is reciprocated in the improvement of properties (Awang and Ismail, 2008).

Hassan et al. (2013a) employed gamma irradiation to crosslink RTR and HDPE phase and found that the tensile properties of the blends improved by almost 20 to 50% compared to non-irradiated blends up to 50 wt% RTR at 150 kGy irradiation. On the other hand, gamma irradiated 50 wt% GTR containing recycled HDPE blends showed improvement in TS and Eb approximately by 10% and 20% respectively while TM reducing by about 10%. Impact strength was also improved by 50% at 50 kGy irradiation dose (Sonnier et al., 2006).

Mészáros et al. (2012), irradiated LDPE/EVA/GTR (30 wt% GTR) samples and also noticed substantial improvement in TS ($\approx 1x$) and Eb ($\approx >2x$). Attempt to crosslink EVA and 10 wt% GTR in the presence of multifunctional acrylates (MFA) using electron beam irradiation successfully showed improvement in tensile ($>1x$ for TS and TM) and hardness ($\approx 1x$) properties with small decrease in Eb ($\approx 1x$) (Sakinah et al., 2011).

Crosslinking was found to be also favorable in improving the Eb along with the other properties in most cases. Peroxide crosslinking seems to render mixed results. Though it has not been discussed in any of the literature, this could be due to presence of additives such as stabilizers and antioxidant in the GTR/RTR which stabilizes and/or scavenges the radical formed using peroxides. This is also supported by the observation in ionizing radiation cross-linked blends where the improvements recorded are rather low. Al-Malaika and Amir (1989) discussed the influence of residual additives in GTR when the PP/GTR blend in their work had showed better properties retention upon UV degradation.

Moving forward, influence of crosslinking with blends that have been compatibilized should also be looked into.

As suggested by Sonnier et al. (2008) which they deduced from finite element analysis, it is apparent that interfacial adhesion could not lead to a thermoplastic elastomer in thermoplastic/GTR or RTR blends. However, this should not hamper the movement to incorporate GTR/RTR in thermoplastics as these blends could still find use in many different fields that does not need such high Eb.

RTR blends are expected to offer better mechanical properties compared to GTR blends, especially the Eb, however, not many work was done to highlight this with thermoplastic blends in the literature. Studies should also engage in comparing and contrasting the GTR and RTR blends to address the lack in Eb of GTR blends.

2.8.2. Thermal properties

Thermogravimetry can be employed to study the thermal stability of the blends. It should be an integral part of the study as GTR/RTR is a degraded mass from the use and the recycling processes. Calorimetric analysis can be conducted to verify the influence of GTR/RTR blend on crystallinity or microstructure of the matrix. Melting temperatures and crystallinity index are used as a bench mark for this evaluation.

2.8.2.1. Thermogravimetry analysis

Thermogravimetry analysis is an essential tool to characterize thermal stability of a blend. It is even more important in studies utilizing GTR and RTR as they are degraded material and will be influencing the resulting blends thermal stability significantly. Addition of GTR/RTR to thermoplastic blends was reported to decrease the onset of thermal degradation due to presence of volatile material in GTR/RTR. However, the degradation temperature for 50% ($T_{50\%}$) and 70% ($T_{70\%}$) weight loss increased substantially with increasing GTR/RTR content. Work on RTR/HDPE blends showed the $T_{50\%}$ and $T_{70\%}$ improved by 5% and 22% respectively at 70 wt% RTR (Hassan et al., 2013a).

PP with latex modified GTR did not show any difference in thermal stability compared to unmodified GTR blend even though the mechanical properties of these blends improved indicating the interfacial interaction was only improved by enhanced physical wetting between the phases (Awang et al., 2008).

65 wt% GTR containing MAgPP matrix showed better thermal stability compared to PP matrix. Addition of compatibilizers, SEBS and MAgSEBS, improved the thermal stability further with MAgSEBS showing the highest thermal stability of all. Good compatibility of SEBS with both PP and GTR was suggested to be the reason behind the observation. EB midblock of SEBS was compatible with PP while the MA group could react with GTR enhancing the interfacial bonding though improving the thermal stability of the blends (Lee et al., 2007).

Dynamically vulcanized PP/GTR blends in the presence of TOR showed better thermal stability compared to uncompatibilized blends attributed to improved interfacial adhesion between GTR and PP (Awang et al., 2007). PP/GTR blends cross-linked by DCP and HVA2 showed an improvement in thermal stability by at least 2 °C throughout the temperature range. This was attributed to better interfacial properties of PP/GTR from formation of copolymer in the interphase. The degradation temperature associated with PP also remained unchanged suggesting PP did not undergo structural changes during the peroxide crosslinking process (Awang and Ismail, 2008).

Although some amount of work has been done but it is inadequate in determining the effect of using degraded GTR or RTR in thermoplastics. Again, some amount of attention should be given to thermal stability of the blends, not just paying attention to improving the mechanical properties as it has been reported in the literature.

2.8.2.2. Calorimetric analysis

In general, the incorporation and particle size of GTR/RTR did not significantly influence the melting temperatures, enthalpy of melting and crystallinity of the thermoplastic matrix. Slight decrease in melting temperature is related to slight decrease in the thickness of lamella caused by restriction of crystallite formation imposed by GTR. Enthalpy of melting was also decreased with increasing GTR

content; however this is due to reducing content of crystallisable material (plastic phase) in the blends. These infer the crystallinity index of the matrix is not changed, disturbed or enhanced by the presence of GTR. Sonnier et al. (2007) reported loading and particle size of GTR had no significance on melting temperature and crystallinity index of the LDPE/GTR blends. Mujal-Rosas et al. (2011) in their work with different particle size of GTR dispersed in EVA phase concluded the GTR particle size or loading has no significant influence on the matrix in terms of crystallinity due to little interaction between GTR and EVA. The crystallinity of blends with <200 μm particle size was equivalent to blend with > 500 μm particle size has further enhanced the claim. They also went on to claim the resulting properties of the blend should not attribute to changes in the EVA matrix but to changes in the particles and in the matrix/GTR interphase. Tantayanon and Juikham (2004) worked on PP/RTR blend and also observed no significant effect in the enthalpy of melting and crystallinity with increasing RTR content of the blends.

Incorporation of SBS as compatibilizer in LLDPE/GTR blends depressed the melting temperature and narrowed the melting region due to either formation of imperfect crystal or smaller lamella size, which is indicative of improved compatibility between GTR and LLDPE (Qin et al., 2008).

Tantayanon and Juikham (2004) showed the enthalpy of melting and blend crystallinity decreases upon sulphur crosslinking of PP/RTR blends which was due to sulphur crosslinks acting as local defects, not allowing for the close packing of PP chains. In another study, blends of PP/GTR compatibilized by dynamic vulcanization in the presence of TOR showed slight difference in melting temperature, could be due to presence of co-vulcanized TOR at the interphase slightly decreasing the lamella thickness (Awang et al., 2007). Crystallinity of recycled HDPE/GTR blend did not change up to 0.01 DCP/HDPE ratio in the blend subjected to free radical crosslinking to improve the interfacial adhesion. This is deduced to be due to most of the free radical formed to be concentrated at the interphase co-crosslinking GTR and HDPE phase (Sonnier et al., 2008). Work carried out employing DCP and HVA2 to crosslink PP and GTR showed the structure of PP was not disturbed as the melting temperature of the blends before and after treatment remained unchanged. Presence of HVA2 limited the crosslinking reaction of PP and promoted the formation of copolymer in the interphase between PP and GTR (Awang and Ismail, 2008). Ratnam et al.

(2014) reported decrease in crystallinity of EVA/GTR blend upon electron beam irradiation due to formation of imperfect/defective crystal. They also found the crystallinity of the blend to be improved with the addition of MFA such as trimethylol propane triacrylate (TMPTA) and tripropylene glycol diacrylate (TPGDA). This observation was reported to be due to effective nucleation for the crystallization with the incorporation of MFA.

Apart from the influence of GTR loading and particle size in the thermoplastic blends, other areas remain neglected for calorimetric studies. It could have been due to little significance of GTR loading and particle size hampering the venture into the influence of GTR modification, compatibilization and crosslinking on the blends. However, it is important to look into these areas as the mechanical properties of the blends are highly dependent of the continuous matrix phase and the crystallinity of thermoplastic material.

2.8.3. Dynamic mechanical analysis

Dynamic mechanical analysis will shed some light on the stiffness and damping characteristic of GTR and RTR thermoplastic blends over a range of temperature, as well as informing the changes in glass transition temperature (T_g) of the blends. Addition of GTR/RTR into thermoplastic matrix shows a tan delta peak appearing around -60 to -40 °C, which corresponds to glass transition temperature of the rubber component in GTR/RTR.

Kim et al. (2000) worked on acrylamide modified GTR/HDPE blends and found the storage modulus of modified blends were higher than un-modified blends throughout the studied temperature range due to enhanced interfacial interaction. Both the blend's tan delta curve showed a peak around -55 °C (indicating the T_g of rubber), whereby the peak height was reduced in the modified blends indicating reduction in the damping of rubber phase due to improved adhesion in the HDPE/GTR interphase. In another work, addition of EVA into LDPE/GTR blend shifted the T_g of rubber and plastic phase closer indicating improved interaction between the two components (Mészáros et al., 2012). Li et al. (2003a) found the storage modulus of 40 wt% GTR containing HDPE blends was lower compared to HDPE throughout the studied temperature range. Addition of EPDM and silicone oil in the presence of DCP into the blends further reduced the storage modulus. Tan delta peak of uncompatibilized blends

at -44 °C shifted to -53 °C with the addition of the compatibilizers. The peak of tan delta also decreased with the compatibilization due to reduced damping facilitated by enhanced wetting of HDPE and GTR phases in the presence of rubber and oil.

Electron beam irradiation of LDPE/EVA/30 wt% GTR blend shows increased Tg of both rubber and plastic phase with decreased peak height due to reduced chain flexibility from radiation induced crosslinking in both the phases (Mészáros et al., 2012). Interestingly, in the work carried out by Sakinah et al. (2011) the peak corresponding to the Tg of rubber phase disappeared in EVA/10 wt% GTR blend utilizing MFA coupled with electron beam irradiation suggesting enhanced compatibility.

Dynamic mechanical properties of GTR/RTR thermoplastic blends are rarely studied, hence, only a few studies were extracted from the literature. Moreover, no clear inference could be made on the influence of GTR or RTR thermoplastic blends on the dynamic mechanical properties.

2.9. Summary

Clearly the multitudes of research utilizing the RTR in thermoplastic matrix are limited. Targeting thermoplastic matrix with high toughness such as EVA and thermoplastic polyurethane could help in addressing the low Eb of RTR filled thermoplastics. Characterization of this resulting RTR blends should be thoroughly conducted to identify and emulate ways to empower the waste tire recycling by blending with polymers. Further enhancement of the resulting RTR blends through the use of advancing technologies should also be ventured to diversify the recycling efforts. Hence, in this study; the use of EVA as thermoplastic matrix and role of electron beam irradiation in reflecting the efforts of waste tire recycling has been ventured.

CHAPTER 3. METHODOLOGY

3.1. Introduction

This chapter details the materials and methods used in this study. The details of methodologies adopted have been clearly documented here.

3.2. Materials

Poly(ethylene-co-vinyl acetate) (Grade EVA N8045), EVA, having 18% vinyl acetate content with melt flow index, MFI, value of 2.3 g/10 min and a density of 0.947 g/cm³ was purchased from the TPI POLENA Public Limited Company, Thailand. Reclaimed tire rubber (RECLAIM Rubberplas C), RTR, from waste, heavy duty tires used in this study was supplied by Rubplast Sdn. Bhd., Malaysia. General properties of the RTR are 48% rubber hydrocarbon, 5% ash content, 15% acetone extract, 25% carbon black fillers and density of 1.3 g/cm³. Maleated EVA (MAEVA), (3-Aminopropyl)triethoxy silane (APS) and liquid styrene butadiene rubber (LR) were used as compatibilizers in RTR/EVA blends. Multifunctional acrylates (MFA); trimethylol propane triacrylate (TMPTA) and tripropylene glycol diacrylate (TPGDA) were used as irradiation sensitized crosslinking agents. Whereas N,N-1,3 Phenylene Bismaleimide (HVA2) was used as a conventional irradiation sensitized crosslinking agent. Table 3.1 shows the properties and suppliers of the compatibilizer and crosslinking agents used.

Table 3.1 Properties and supplier information of the additives used

Type	Properties	Supplier
APS	Density, 0.95 g/cm ³ ; Boiling Point, 217 °C; FW, 221.37.	Sigma Aldrich
LR	Density, 0.95 g/cm ³ ; Mw, 8500; Tg, -14 °C.	Kuraray Co. Ltd., Japan
MAEVA	Density, 0.95 g/cm ³ ; MFI, 16 g/10 min; T _m , 71 °C.	DuPont, China (Fusabond C190)
HVA2	Yellow powder; T _m , 196 °C, Functionality, 2.	Sigma Aldrich
TMPTA	Clear liquid; Density, 1.06 g/cm ³ ; Functionality, 3.	Sigma Aldrich
TPGDA	Clear liquid; Density, 1.03 g/cm ³ ; Functionality, 2.	Sigma Aldrich

3.3. Melt compounding

RTR and EVA were melt blended in an internal mixer (Brabender Plasticoder PL2000-6 equipped with co-rotating blades and a mixing head with a volumetric capacity of 69 cm³). The rotor speed was set at 50 rpm while blending temperature was set at 120 °C. The processing parameters were determined from a preliminary work.

Melt compounding was done according to three categories as per the aims of the study. At first, physical mixing of RTR/EVA blends with varied RTR content was prepared. The second category was compatibilization of RTR/EVA blends using different types and loadings of compatibilizers. Finally, RTR/EVA blends were prepared with the different types of crosslinking agents. The loadings of compatibilizers and radiation sensitizers were determined based on previous studies. Designation of the prepared blends is shown in Table 3.2.

EVA was fed into the internal mixer chamber and allowed to melt for two minutes, followed by the addition of RTR. Both EVA and RTR were allowed to mix for 8 minutes before collecting the blends from the internal mixer. The melt-mixing torque readings were detected by a pressure transducer and recorded using built-in software (Brabender Mixer Program, version 3.2.31). Analysis was conducted using fusion behavior evaluation to obtain melt-mixing torque-time curves and data. Compatibilizer (when used) was added simultaneously with RTR at the second minute. Multifunctional acrylates and bismaleimide crosslinking agents (when used) were added at third and seventh minute respectively. Bismaleimide crosslinking agent was added later as it induces crosslinking process in polymers beyond 70 °C; unlike multifunctional acrylates which would only crosslink with exposure to irradiation energy. This ensures the compounded materials can still be processed (or flowing) during subsequent compression molding step. Total mixing time was kept constant to 10 minutes for EVA, RTR and all the blends to ensure similar thermal history. The collected materials were immediately cut into smaller pieces and kept in sealed plastic bags for compression molding process.

Table 3.2 Designation of the blends

Designation	RTR (wt%)	EVA (wt%)	Compatibilizer^a (wt%)	Radiation sensitizers^b (wt%)
RTR	100	0	-	-
70RTR	70	30	-	-
50RTR	50	50	-	-
30RTR	30	70	-	-
EVA	0	100	-	-
50RTR/XAPS^c	50	50	1, 3, 5 & 10	-
50RTR/XLR^c	50	50	1, 3, 5, & 10	-
50RTR/XMAEVA^c	50	50	1, 3 & 5	-
RTR/TMPTA	100	0	-	4
RTR/TPGDA	100	0	-	4
50RTR/5APS/HVA2	50	50	5	4
50RTR/5APS/TMPTA	50	50	5	4
50RTR/5APS/TPGDA	50	50	5	4
EVA/HVA2	0	100	-	4
EVA/TMPTA	0	100	-	4
EVA/TPGDA	0	100	-	4

a wt% of compatibilizer was added based on total RTR weight

b wt% of crosslinking agent was added based on total blend weight

c X denotes the wt% (1, 3, 5 or 10) of compatibilizer loaded

3.4. Compression moulding

Materials collected from internal mixer were compression molded to obtain rectangular slabs. The compounded materials were placed with a slight excess into a steel frame flash mould (200mm x 200mm) covered by disposable polypropylene (PP) sheets (200mm x 200mm x 0.1mm) and aluminium plates (200mm x 200mm x 2mm) on both sides as illustrated in Figure 3.1a. The test specimens thickness and shape determines the thickness and cavity size of the flash mould. Disposable PP sheets were used to ease the release of slabs from the flash mould, by avoiding the slabs from adhering to the aluminium plates.

The filled mould was positioned in between the platens of an automated hydraulic heated press (LP-S-50 Scientific Hot and Cold Press) as shown in

Figure 3.1b. The platens were pre-heated to 130 °C (determined from mean highest temperature recorded during melt compounding). The heat reaches the mould and compounded materials via conduction. The molding cycles involve 3 minutes of preheating without pressure to melt the materials; followed by 20 seconds of pressure cycling (also known as venting) between 0 to 10 MPa to distribute the melted material in the cavity and dislodge any air bubbles; and 3 minutes of holding pressure at 10 MPa.

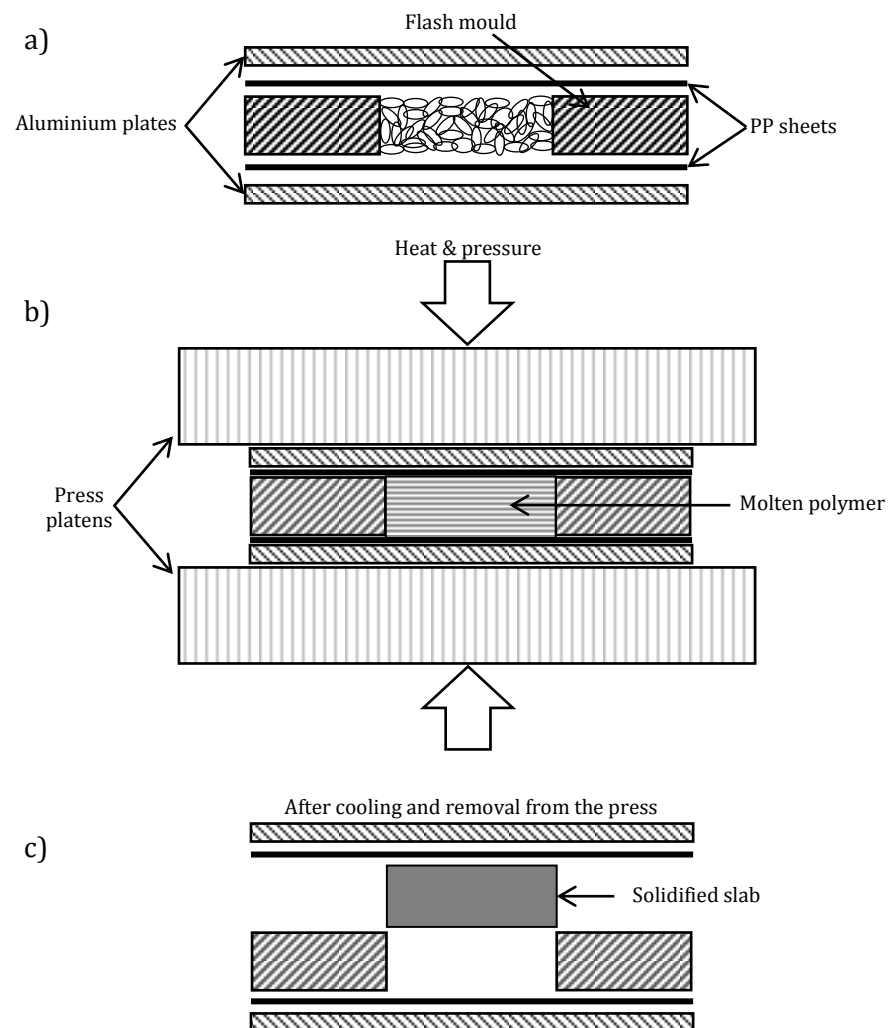


Figure 3.1 Schematic representation of the compression molding process: a) the mould arrangement with mould cavity filled with pieces of blended material; b) the mould is transferred to the press and the pressure cycles are applied; c) the mould is cooled and removed from the press to release the molded slabs from the cavity

Following the holding time, cooling procedure was imposed by carefully removing the mould from the heated press to the adjacent cooling press equipped with water circulating channels pumped with chilled (20 °C) water. Cooling procedure was done for 2 minutes under 10 MPa holding pressure to eliminate non-uniform cooling and warping of the slabs. The cooling rate of the mould was estimated to be between 40 to 50 °C/min. The slabs are then carefully removed from the mould cavity and excess/flash on the slabs was trimmed with a sharp knife.

3.5. Electron beam irradiation

The molded slabs were irradiated using 3 MeV electron beam accelerator (model NHV-EPS-3000) at doses 50, 100, 150 and 200 kGy. The acceleration energy, beam current and dose rate were 2 MeV, 5 mA, and 50 kGy per pass, respectively.

3.6. Molar mass distribution

A couple of RTR samples were subjected to gel permeation chromatography (GPC) characterization to determine the molar mass distribution of the soluble rubber fraction. RTR samples were first extracted in boiling acetone for 24 hours to remove the low molecular weight moieties/additives. Acetone extracted RTR samples were thoroughly washed with toluene; followed by extraction in boiling toluene for 24 hours to dissolve the soluble fraction of the RTR. All extraction was conducted in a Soxhlet apparatus. The RTR samples and toluene were separated using filter paper. Toluene was allowed to evaporate to obtain the soluble rubber fraction of RTR which was later dried in the oven at 50 °C for 6 hours. The dried soluble rubber was used for GPC evaluation. Soluble rubber dissolved in tetrahydrofuran (THF) was passed through a column packed with porous material (where the pore sizes are similar to the macromolecules) that separates polymer chains based on molecule size. Measurements were done according to polystyrene standard using GPC.

3.7. Gel content

The gel content of the samples was determined according to ASTM D2765. Approximately 3 mg weighed samples were placed in a stainless steel wire of 120 mesh size. Three replicates were prepared for each sample. The samples placed in wire mesh were then extracted in boiling Toluene using a Soxhlet apparatus for 24 hours to dissolve the soluble content. Samples were then collected and dried in an oven at 70 °C until a constant weight is obtained. Gel content was calculated as per Equation 3.1 below.

$$\text{Gel content (\%)} = \frac{w_1}{w_0} \times 100 \quad \text{Equation 3.1}$$

w_0 and w_1 are the dried weight of the sample before and after extraction, respectively. Later, Charlesby-Pinner equation (Equation 3.2) was used to quantitate the yield of crosslinking and chain scissions in the blends due to irradiation.

$$S + S^{1/2} = \frac{p_0}{q_0} + \frac{10}{q_0 D u_1} \quad \text{Equation 3.2}$$

Where S is the soluble fraction, u_1 the number averaged degree of polymerization, D is radiation dose (in kGy), p_0 and q_0 are fraction of ruptured and cross linked main-chain units per unit dose respectively. By regression analysis, plots of $S+S^{1/2}$ vs $1/D$ were drawn to determine the p_0/q_0 value which is the intercept of the plot's Y-axis (Refer to Appendix A1). It is to be noted that the soluble fraction used in this evaluation was derived from the absolute yield of gel fraction upon irradiation (gel content before irradiation subtracted by gel content after irradiation) as RTR contained a substantial amount of gel before irradiation.

3.8. Tensile properties

Tensile test specimens were punched out using Wallace die cutter from compression molded slabs. The specimens had a gauge length of 25 mm, width of 6 mm and thickness of 1 mm. Tensile properties measurements were performed at ambient temperature according to ASTM D412 using a computerized tensile tester (Toyoseiki, Japan) with a load cell of 10kN. The

crosshead speed was set at 50mm/min for all samples. Data for tensile strength, modulus at 100% elongation and elongation at break were recorded. At least 7 specimens were used for each set of blend and average results were taken as the resultant value. Standard deviation of the results was less than 10%.

3.9. Tear properties

Tear test specimens were punched out using Wallace die cutter from compression molded sheets. The specimens were cut out according to ASTM D624 Type C (right angle) test piece type. The test pieces had a length of 102 mm, width of 10 mm and thickness of 1.5 mm. Testing was conducted at ambient temperature using a computerized tensile tester (Toyoseiki, Japan) with load cell of 10kN. The crosshead speed was set at 50mm/min for all samples. The maximum force required to cause a rupture in the test piece was determined and divided by the thickness of the test piece to obtain the tear strength. At least 6 specimens were used for each set of blend and average results were taken as the resultant value. Standard deviation of the results was less than 10%.

3.10. Hardness test

Hardness test specimens were compression molded according to ASTM D2240 (Type Shore A) samples. The test pieces had a length of 100 mm, width of 100 mm and thickness of 5mm. Testing was conducted at ambient temperature using hardness tester with the blunt indenture (Durometer Hardness model Zwick 7206). A minimum of 9 hardness readings was recorded for each sample and average results were taken as the resultant value. Standard deviation of the results was less than 10%.

3.11. Scanning electron microscopy

Examination of the fractured surfaces was performed using field emission scanning electron microscope (FESEM, FEI Quanta 400). The surface of the fractured samples was sputter coated with gold before examination to avoid electrostatic charging and poor image resolution.

3.12. Transmission electron microscopy

Morphology of the blends was studied using transmission electron microscope (Jeol-JEM-2100 TEM) on carbon coated copper grid. Ultrathin sections with approximate thickness of 80nm were cut with ultra-microtome (LEICA Ultracut UCT) and placed on a copper grid. Samples were cooled to -100 °C using liquid nitrogen to aid cutting process. Later, the samples were observed under TEM using a voltage of 200 kV. Domain sizes of RTR were measured using the built-in software (Jeol-JEM-2100 TEM).

3.13. Thermal degradation and stability

Thermal degradation and stability of the samples were measured using computerized thermo gravimetric analyzer (Mettler Toledo TGA/DSC 1 equipped with STARe System). Thermal stability was assessed by dynamic thermogravimetry analysis (TGA) experiments. The test was done by heating the sample from room temperature to 600 °C to obtain weight loss vs. temperature thermogram. All analysis was carried out using 5 to 10 mg of samples in Nitrogen atmosphere (flow rate 50 ml/min) and a heating rate of 10 °C/ min. The results were analyzed using STARe System software. The normalized weight loss vs temperature curve was smoothed using a least-squares averaging technique before analysis. $T_{5\%}$, $T_{10\%}$, $T_{25\%}$ and $T_{50\%}$ are defined as the temperature at 5%, 10%, 25% and 50% weight loss respectively. T_{max} is defined as temperature at the maximum rate of weight loss that is identified by the peak of derivative (dW/dT) curve. These temperatures are used to indicate thermal degradation and stability of the samples.

3.14. Crystallinity

Crystallization study was done for blends using computerized differential scanning calorimeter (Mettler Toledo DSC 1/32 equipped with STARe System) to determine crystallization and melting temperature, heat of fusion and degree of crystallinity of the samples. Analysis was carried out using 5 to 10 milligrams of samples in Nitrogen atmosphere (50 ml/min). All samples were subjected to a standard heat/cool/heat cycle in a covered aluminium pan. The test was started

by heating samples from room temperature to 140 °C at 50 °C/min followed by cooling to 0 °C at a cooling rate of 10 °C/min. Second heating was done at a rate of 10 °C/min up to 140 °C to obtain heat flow vs. temperature curve. The initial heat cycle erases thermal history and the controlled cooling state allows polymeric material to reach repeatable enthalpic state associated with the crystallization. The subsequent heat cycle with a defined thermal history is then used to determine crystallization behavior. First heating scan was omitted from data analysis. The results were analyzed using STARE System software. The normalized heat flow vs temperature curve was smoothed using a least-squares averaging technique before analysis. T_c and T_m were defined as crystallization and melting temperature obtained from peak of crystallization and melting curve respectively. ΔH_f is the heat of fusion of the sample determined from the area under the peak of the melting curve. The percentage of crystallinity, X_c , of EVA in the blends was calculated as per Equation 3.3.

$$X_c = \frac{\Delta H_f}{\Delta H_f^\circ \times w_{EVA}} \times 100 \quad \text{Equation 3.3}$$

Where ΔH_f is the heat of fusion of the sample, ΔH_f° is the heat of fusion of a 100% crystalline polyethylene which is 295 J/g and w_{EVA} is the weight fraction of EVA in the blends.

3.15. Dynamic mechanical analysis

DMA was performed in dual cantilever mode using a dynamic mechanical analyzer (TA Instrument TA01 DMA 2980). The temperature interval was - 80 to 100 °C with a heating rate of 5 °C/min, using a frequency of 1 Hz. The samples were cut out to the dimension of 60 x 12 x 3 mm from compression molded slabs. The sample dimensions were kept as similar as possible in order to obtain an accurate comparison. Variation of storage modulus, loss modulus and $\tan \delta$ values with temperature were recorded. E' and E'' are defined as storage and loss modulus respectively. Peak of $\tan \delta$ is taken as the glass transition temperature (T_g) of the sample.

3.16. Equilibrium swelling

Rectangular samples with the dimension of 20 x 20 x 2 mm were cut out of the slabs and immersed in toluene (30 – 40 ml); kept in sealed beaker at ambient temperature. The samples were withdrawn periodically from toluene; any solvent adhering to the sample surface was rubbed off. The samples were immediately weighed on a highly sensitive electronic balance (Mettler Toledo, AB240-S) with an accuracy of 0.0001g and immediately placed into the beaker. This process was continued until equilibrium was reached. The mol uptake (Q_t) of the toluene by 100 g of sample (Equation 3.4) was plotted against square root of time. Q_t was taken as Q_∞ at equilibrium toluene uptake and defined as mol uptake at infinite time.

$$Q_t = \frac{\text{mass of toluene/molar mass of toluene}}{\text{mass of sample}} \times 100 \quad \text{Equation 3.4}$$

The mechanism of sorption was analyzed by two different empirical methods. The first empirical method uses Equation 3.5 while the second empirical method uses Equations 3.6, 3.7 and 3.8 as listed below.

$$\log \frac{Q_t}{Q_\infty} = \log k + n \log t \quad \text{Equation 3.5}$$

Where Q_t is the mol sorption at time t and Q_∞ is the mol sorption at equilibrium. The value k depends on the structural features of polymer in addition to its interaction with the solvent. The value n indicates the mechanism of sorption. Values of n and k were obtained from slope and intercept of regression analysis respectively.

In the second method, diffusion, sorption and permeation coefficient were determined to analyze the mechanism of sorption.

$$D = \pi \left(\frac{hm}{4Q_\infty} \right)^2 \quad \text{Equation 3.6}$$

Where D is diffusion coefficient, h is the initial thickness of the sample, m is the slope of sorption curve before attainment of 50% equilibrium and Q_∞ is the mol sorption at equilibrium.

$$S = \frac{M_\infty}{M_0} \quad \text{Equation 3.7}$$

Where S is the sorption coefficient, M_{∞} is the mass of solvent taken up at equilibrium and M_0 is the initial mass of the polymer.

$$P = DS \quad \text{Equation 3.8}$$

Where P , D and S are the permeability, diffusion and sorption coefficient respectively.

3.17. Fourier Transform Infrared analysis

FTIR test was done using Perkin Elmer Spectrum 2000 via diamond attenuated total reflectance (ATR) technique. The spectrometer was operated with 16 scans at 4 cm^{-1} resolution and within the range of $4000 - 500 \text{ cm}^{-1}$ for each sample. All FTIR spectra were recorded in absorbance unit. The test was conducted directly on approximately 0.1 mm thin film surface.

CHAPTER 4. EFFECT OF BLEND RATIO ON THE PROPERTIES OF RTR/EVA BLENDS

4.1. Introduction

This chapter addresses the first aim of this study which is to improve the inferior properties of RTR by blending with EVA. The content of RTR in RTR/EVA blends were varied at 30, 50 and 70 wt%. Neat RTR and EVA were also prepared as the control sample. Electron beam irradiation was employed to further improve the properties of RTR/EVA blends. The changes in processing, mechanical, thermal, dynamic mechanical and swelling properties of RTR/EVA blends with different RTR content were discussed. This chapter has been published in two separate journals (Ramarad et al., 2015b, Ratnam et al., 2014).

4.2. Processing characteristics

Figure 4.1 compares the evolution of torque during mixing of RTR, EVA and RTR/EVA blends in the internal mixer as a function of blend ratio. This torque–time behavior was used to study the processing characteristics of RTR/EVA blends. A sharp increase in mixing torque was observed at the beginning, owing to the introduction of EVA pellets into the mixing chamber. With the melting of the pellets, the torque was seen to decrease and later reaches a stabilization torque as the pellets completely melt. At about the second minute, an increase in the torque value was observed in all the blends due to the introduction of RTR into the mixing chamber. Stabilization torque was achieved at about the fourth minute; and remained so until the end of the mixing process. The stabilization torque indicates the blends homogeneity has been achieved. Torque reading showed lower values with increasing RTR content indicating easier processability of the blends as compared to EVA. Moreover, after the addition of RTR almost similar mixing trends were exhibited by 70RTR and 50RTR blends. Loading, maximum, minimum and ending torque values of RTR, EVA and RTR/EVA blends have been charted in Figure 4.2. EVA recorded the highest torque values while RTR recorded the lowest torque values. The blend showed an intermediate torque values between RTR and EVA. The loading torque which corresponds to introduction of EVA into the mixing chamber decreases with

increasing RTR content due to decreasing amount of EVA in the blends. Similar reason fuels the observation with minimum torque which corresponds to the complete EVA melting torque. Maximum torque and ending torque which corresponds to introduction of RTR into the mixing chamber and end of mixing process respectively; decreased with increasing RTR content as result of net effect of EVA and RTR torque values whereby RTR records lower torque value. These findings simply indicate the feasibility to process the RTR/EVA blends using conventional techniques at ease.

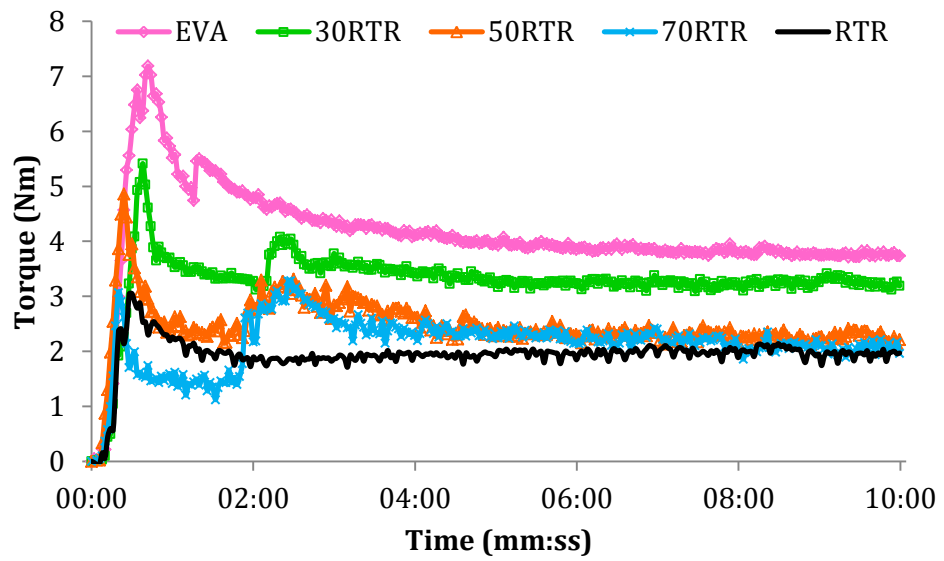


Figure 4.1 Torque - time curve of RTR, EVA and RTR/EVA blends

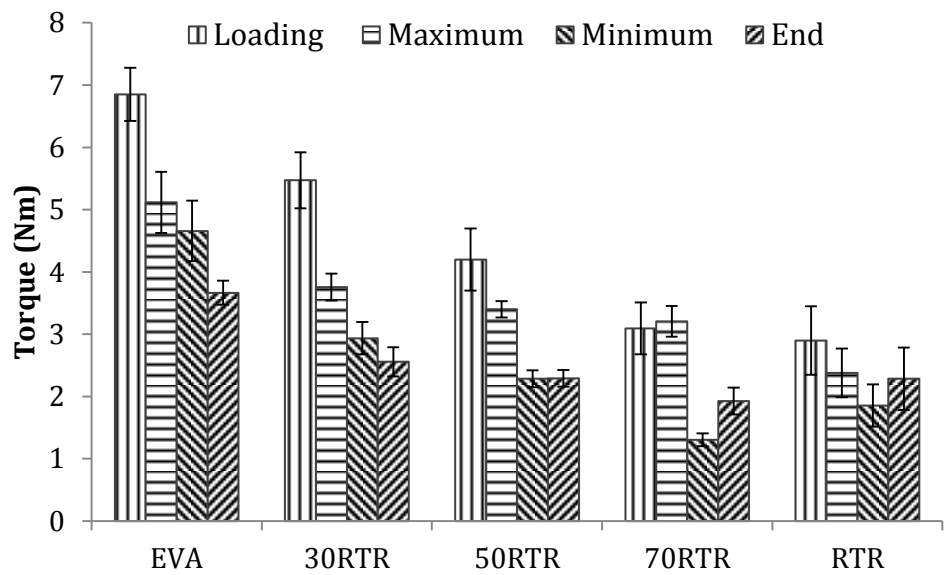


Figure 4.2 Mixing torque values of RTR, EVA and RTR/EVA blend

4.3. Gel content analysis

Figure 4.3 shows the changes in the gel content of RTR/EVA blends with increasing irradiation dose. Generally, the gel content is an estimation of yield of irradiation induced crosslinking. RTR shows 68% of the gel content prior to irradiation (0kGy), affirming the presence of readily existing crosslinks within its matrix. During the reclaiming process, both crosslinks and macromolecular chain breakdown will take place. The breakdown of crosslinks is favorable as it increases the plasticity of the rubber. However, the breakdown of macromolecular chains should be kept minimal to ensure the optimal properties of the resulting RTR. Tao et al. (2013) showed the importance of keeping both crosslinks and macromolecular chains breakdown balanced for the resulting reclaimed rubber to have the optimum plasticity and properties. Therefore, it is common for the reclaimed rubber to have a gel content ranging from 50 to 80% (Tao et al., 2013).

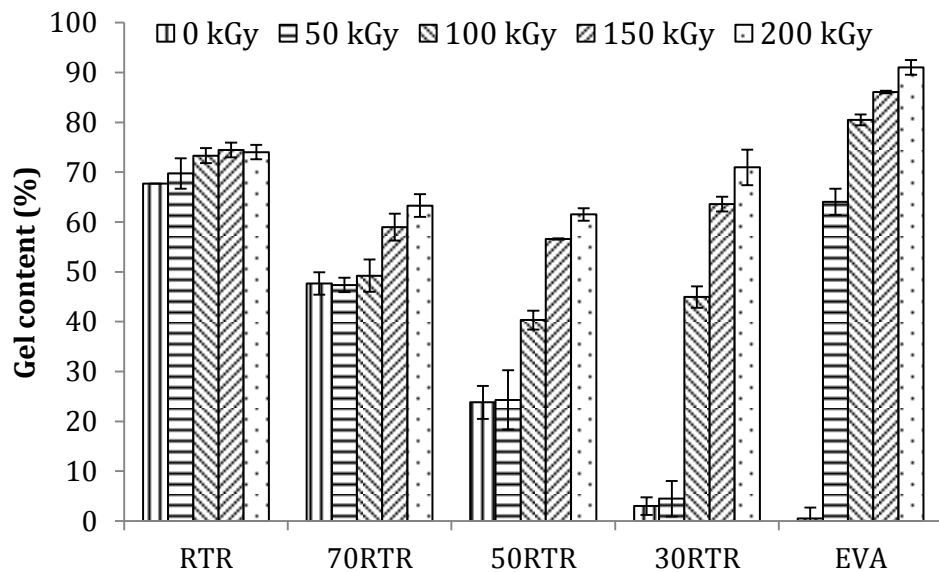


Figure 4.3 Gel content of RTR, EVA and RTR/EVA blends as a function of irradiation dose

The gel content of RTR increased only marginally with the increase in irradiation dose. Similar findings by Ratnam et al. (2000) explained the stabilization of the rubber and the radical scavenging effects by the additives causing a marginal increment in the gel content upon irradiation. Similarly, Hassan et al. (2014a)

found insignificant increment in the gel content of gamma irradiated GTR/PP/EPDM based thermoplastic vulcanizate in the presence of antioxidant, dicumyl peroxide. Tires have many different additives; among them are stabilizers, antioxidants and antiozonants used to prevent tire degradation due to sunlight and ozone attacks. The presence of these additives in the reclaimed rubber is responsible in stabilizing and scavenging the radicals formed within the matrix through the electron beam irradiation, hence retarding the cross-linking process in the RTR and RTR/EVA blends (Ratnam and Zaman, 1999a). Work on chlorosulfonated polyethylene rubber/chlorinated natural rubber/waste rubber powder blends found that incorporating the waste rubber powder enhanced the irradiation resistance of the blends due to the presence of active additives in waste rubber powder (Marković et al., 2013). Al-Malaika and Amir (1989), found the properties retention of the PP/NR/RTR thermoplastic elastomer blends on ageing was far better than the blends of PP/NR and PP/EPDM due to the presence of antioxidants and stabilizers in the RTR. The finding of current study agrees well with the finding of studies discussed above. Another possible inference is the presence of residual reclaiming agent in RTR which could also stabilize and scavenge the radicals formed by electron beam irradiation.

The existing crosslinks within the RTR matrix are also noticeable in the gel content of the non-irradiated blends which are proportionate to the content of RTR in the blend. The non-irradiated EVA and 30RTR samples were dissolved easily in boiling toluene. However, these EVA and 30RTR samples which were irradiated above 50kGy and 100kGy respectively, were insoluble due to the formation of crosslinking in the sample (3-dimensional network) (Dubey et al., 2006).

Additionally, it is observed that the blends require an irradiation dose above 50kGy in order to achieve a significant increase in the gel content. This could be due to the presence of additives in the RTR retarding the crosslinking process in these blends as discussed earlier. At above 100kGy irradiation dose, the gel content of the blends increases slowly and exhibits a marginal difference. A smaller increment in gel content with increasing irradiation dose was observed in blends with higher content of RTR. These also suggest that at or above certain irradiation dose, the formation of free radicals induced by electron beam irradiation exceeds the ability of the additives in RTR to stabilize and scavenge

the radicals, permitting more crosslinking to happen in the blends. However, a marginal increment in the gel content with increasing irradiation dose and RTR loading reflects that, the RTR phase undergoes irradiation induced crosslinking at a lower extent compared to EVA. This finding will be further elaborated along with the discussion on the mechanical, thermal, dynamic mechanical and swelling properties in section 4.4, 4.6, 4.7 and 4.8 respectively.

Ionizing radiation of polymeric materials is known to lead to crosslinking and chain scission. To quantitatively evaluate the crosslinking and chain scission tendency of the blends upon irradiation, Charlesby-Pinner equation was used to obtain p_0/q_0 values as described in section 3.7 and Appendix A1. The p_0/q_0 value is known as the ratio of chain scissions to crosslinking. Table 4.1 lists the experimental and theoretical p_0/q_0 values of RTR, EVA and RTR/EVA blends obtained from regression analysis and Rule of Mixture, respectively.

Table 4.1 p_0/q_0 values of RTR, EVA and RTR/EVA blends

Compound	p_0/q_0 values	
	Experimental	Theoretical
RTR	1.8724	-
70RTR	1.7403	1.3849
50RTR	1.2669	1.0599
30RTR	0.5561	0.7348
EVA	0.2473	-

RTR showed the highest p_0/q_0 ratio of 1.8724, while EVA showed the lowest value of 0.2473 and the blends showing an intermediate value. The p_0/q_0 ratio reduces with increasing EVA content indicating increased efficiency of crosslinking over chain scissioning with the addition of EVA. RTR and RTR/EVA blends containing more than 30% RTR showed p_0/q_0 values larger than one, which leads to the assumption of chain scissions domination over crosslinking in RTR rich blends (Sengupta et al., 2005). This further corroborates the findings of gel content which increased very marginally with increasing RTR content. Moreover, macroradicals formed through irradiations are stabilized or scavenged by additives present in RTR resulting in scission of the polymeric chain. This also reduces the possibility of macroradicals overlapping to form

crosslinking (Ratnam and Zaman, 1999a). It was expected for the p_0/q_0 values of the blends to be in-between RTR and EVA depending on their compositions; however, it was interesting to note the theoretical values showed positive deviation for 70RTR and 50RTR blends while 30RTR blend showed a negative deviation compared to experimental values. This observation could be due to morphological variation and poor RTR-EVA interaction which suggest that the presence of RTR decreases the interaction probability between close lying macroradicals (Dubey et al., 2006). These factors address the importance of improving the RTR-EVA interaction by compatibilization.

4.4. Mechanical properties

4.4.1. Tensile properties

Figure 4.4 shows the tensile properties of RTR/EVA blends as a function of irradiation dose. Tensile strength, modulus 100 and elongation at break increased with increasing EVA content. Prior to irradiation, addition of 70 wt% EVA to RTR, improved tensile strength, modulus and elongation at break of RTR by 2018%, 1934% and 1637%, respectively. This agrees well with the aim of this study, to improve the inferior properties of RTR by blending with EVA. The improvement in tensile properties with the incorporation of EVA can be attributed to EVA's higher tensile strength, modulus 100 and elongation at break compared to RTR (Kim et al., 2013, Zulkepli et al., 2009). Tensile properties of RTR/EVA blends approximately followed the rule of mixture over the whole composition range.

Tensile strength and modulus of RTR and RTR/EVA blends showed a slight increment with increasing irradiation dose. High energy radiation of polymers creates free radicals by the scission of the weakest bonds. This new entities react with each other forming crosslinks within the matrix (Hassan et al., 2007). Increasing the irradiation dose intensifies the crosslinks formation as reflected in the improvement of tensile strength and modulus. It is also worth noting that the marginal increments in the tensile strength (<50% at 200kGy) and modulus (<20% at 200kGy) are in relation to the gel content analysis of RTR and RTR/EVA blends.

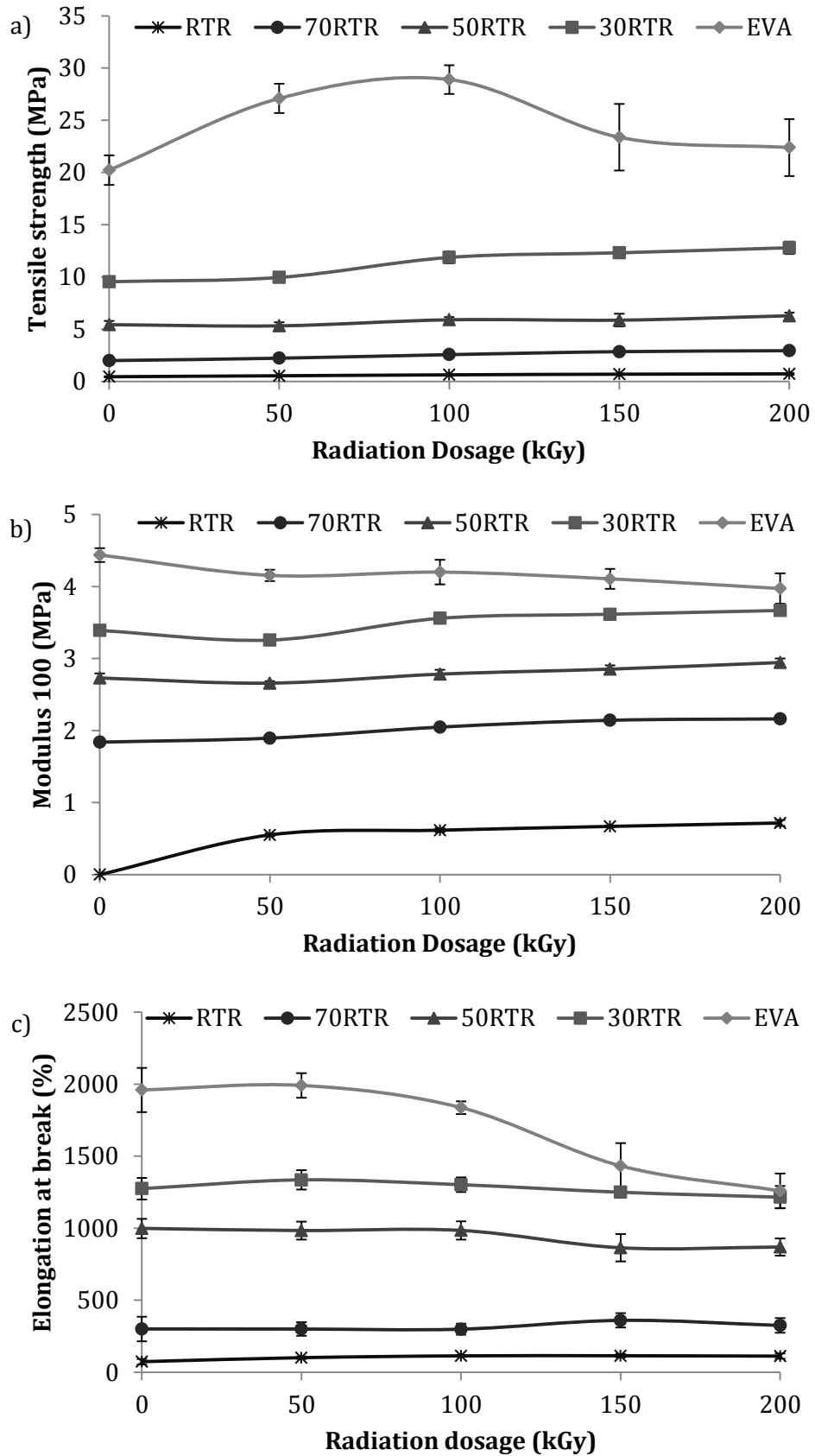


Figure 4.4 Tensile properties of RTR, EVA and RTR/EVA blends as a function of irradiation dose a) Tensile strength, b) Modulus 100, c) Elongation at break

EVA shows a different trend where the tensile strength increases (43%) up to 100kGy irradiation dose followed by a drop. This drop could be associated with the embrittlement of EVA caused by excessive formation of crosslinks above 100kGy irradiation dose. A similar observation was reported by Ratnam et al. (2001d); while working on radiation induced crosslinking of polyvinyl chloride/epoxidised natural rubber blends. In the initial state of irradiation, larger network structure is formed through radiation induced crosslinking resulting in an increase of the strength. However, later at higher irradiation doses, crosslinking are formed between the already crosslinked polymer chains breaking the larger network structure into smaller networks (microgel) resulting in the embrittlement of the polymer matrix (Sharif et al., 2000, Sujit et al., 1996, Dutta et al., 1996).

Elongation at break of RTR was relatively low compared to most NR, BR or SBR rubber compounds. This is due to the breakdown of sulphur crosslinks as well as the rubber macromolecules in RTR during the process of reclaiming. The presence of additives, such as carbon black, might act as stress concentration points and contribute to such low elongation at break of RTR. Interestingly, the elongation at break of RTR was not influenced by the irradiation dose. This trend might again be associated to the marginal increments in the gel content of RTR with irradiation dose and also suggests that no prominent degradation occurred due to the electron beam irradiation of RTR. EVA and RTR/EVA blends containing 30% and 50% of RTR on the other hand, showed a drop after 50kGy irradiation dose. The drop is associated with the decreased ductility of EVA due to the formation of radiation induced crosslinks (Ismail and Suryadiansyah, 2002, Noriman et al., 2010). This could also be observed in the SEM micrographs, discussed later in the section 4.5. Another salient point to note is that the RTR/EVA blend containing 70% of RTR shows a slight upward trend at above 100kGy irradiation. Such increase in elongation at break is believed to be associated with the increase in the compatibility of the blend upon irradiation.

4.4.2. Tear and hardness

Figure 4.5a shows the tear strength of the samples as a function of irradiation dose. Similar to tensile strength, tear strength increases with the addition of EVA (2600%, 30RTR). Similar observation has also been reported for silicone rubber/EVA blends (Ganesh and Unnikrishnan, 2006). However, there was only a marginal improvement (<10% at 200kGy) in the tear strength of RTR/EVA

blends with increasing irradiation dose. On the contrary, EVA showed a distinct increase (18%) in tear strength up to 100kGy irradiation followed by a decrease beyond 100kGy irradiation dose. Such a drop in the tear strength at above 100kGy is in agreement with the observation on tensile strength in which EVA is believed to undergo embrittlement due to the occurrence of excessive radiation induced crosslinking at higher irradiation doses (Ratnam et al., 2001d, Sharif et al., 2000, Sujit et al., 1996, Dutta et al., 1996).

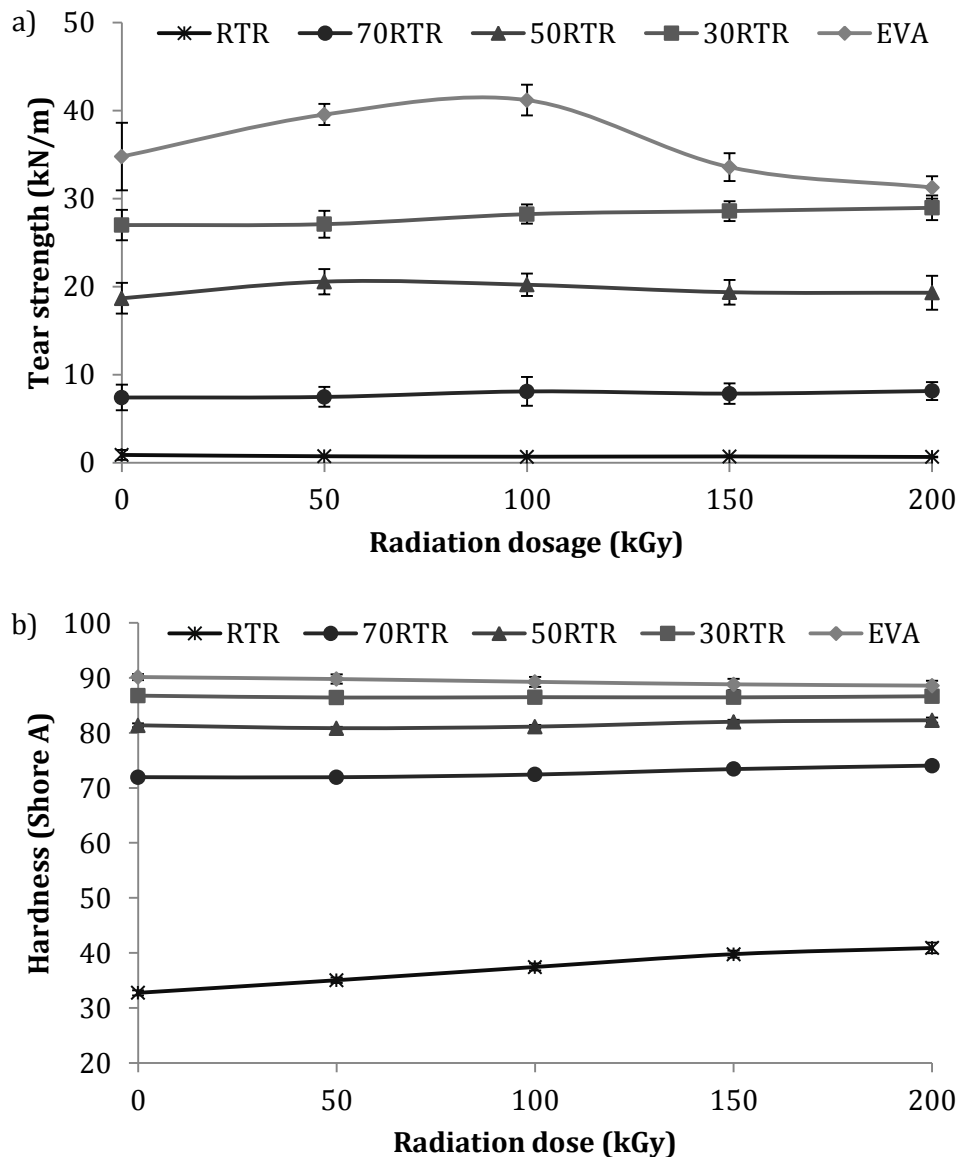


Figure 4.5 a) Tear strength and b) Hardness of RTR, EVA and RTR/EVA blends as a function of irradiation dose

Figure 4.5b shows the hardness of samples as a function of irradiation dose. As observed for the tensile properties, hardness (Shore A) increases with the addition of EVA, reflecting the effect of EVA addition, whereby EVA records a higher hardness value compared to the RTR. The hardness of EVA, RTR and RTR/EVA blends shows an upward trend upon irradiation. Similar to the tensile strength, tear strength and modulus 100; the improvement in hardness of the samples upon irradiation is attributed to the occurrence of irradiation induced crosslinking of EVA and RTR. By definition, hardness is referred to as the resistance of material to the local deformation, (Dubey et al., 2006) and the results proved that even at a low irradiation dose, the crosslinked RTR and RTR/EVA blends were more resistant toward the local deformation consequently leading to the increase in hardness values. The hardness of RTR improved by 25% at 200kGy irradiation dose compared to non-irradiated RTR, although RTR did not exhibit a remarkable increase in the gel fraction upon EB irradiation. This observation indicates that RTR had achieved a better resistance towards the local deformation although the radiation induced crosslinking in RTR occurred at a relatively lower extent compared to EVA.

Several authors have studied the effects of ionizing radiation (gamma or electron beam) on waste tire dust blends (Sonnier et al., 2006, Sonnier et al., 2008, Sonnier et al., 2007, Mészáros et al., 2012). All of them used a single blend with smaller content (either 30 or 50 wt%) of waste tire dust to study the effects of irradiation on the blend properties. This has ensured that the influence of waste tire dust on the resistance towards ionizing radiation goes unnoticed in the literature. The existing report on gamma irradiation of HDPE/RTR blends (Hassan et al., 2013a) (0 to 100 wt% RTR) failed to discuss the reasons behind the poor enhancement of the blend properties with the increasing RTR content. The prospect of waste tire rubber properties enhancement, employing ionizing radiation has neither been fully understood nor fully exploited.

4.5. Morphological study

4.5.1. SEM

Figures 4.6, 4.7 and 4.8 depict the SEM micrographs of the tensile fracture surface of RTR, 50RTR and EVA respectively. RTR shows a brittle fracture surface whereby the matrix phase failed to elongate or prematurely ruptured.

The fracture shows an irregular crack path in different direction, which makes RTR susceptible to low elongation at break. The presence of filler (such as carbon black) with voids around (indicated by arrows) is also evident on the surface of RTR fracture surface. This observation agrees well with low tensile strength and elongation at break discussed in the section 4.4. Also, it is to be noted that there is no significant change in the morphology of RTR with the increasing irradiation dose.

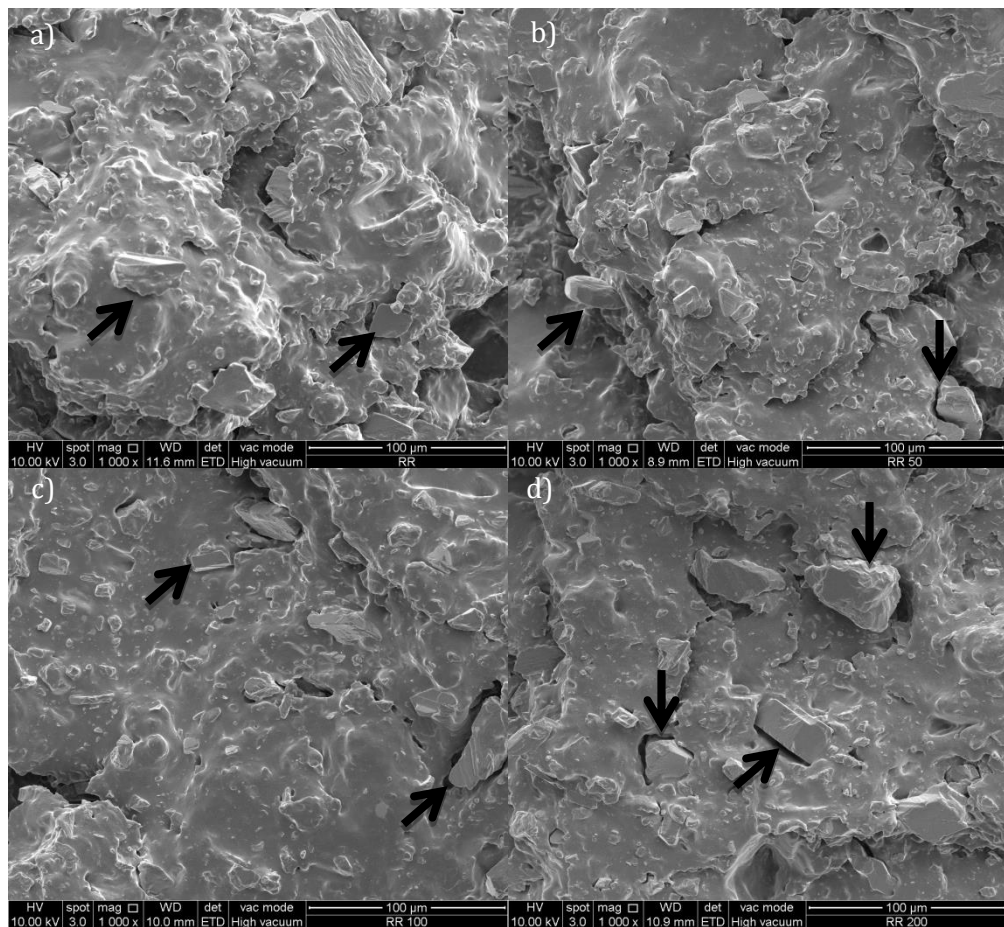


Figure 4.6 Tensile fracture surface of RTR at a) 0kGy, b) 50kGy, c) 100kGy and d) 200kGy

It is observed that with the addition of EVA, the brittle nature of RTR (Figure 4.6a) changes to a fibrillated ductile fracture in the 50RTR blend (Figure 4.7a). This finding is in agreement with tensile studies where the tensile properties of RTR improved tremendously with the addition of EVA. The presence of filler and rubber particle was also visible in 50RTR blends (indicated by arrows). Particle pull out leaving empty voids can be observed due to lack of adhesion between

the RTR particle and EVA matrix. Unlike RTR, 50RTR did show a slight difference between the fracture surface before and after irradiation. The fibril ends/edges of 50RTR fracture surface before irradiation was thinner and longer compared to fibril ends/edges after irradiation. This could be due to the decrease in ductility of the 50RTR sample upon irradiation. These observations are also in line with the gel content analysis where the gel content of RTR and blends were increasing very marginally as compared to EVA due to the stabilization and radical scavenging effect of the additives within the RTR matrix. Lack of adhesion between RTR and EVA was still apparent in the irradiated blends.

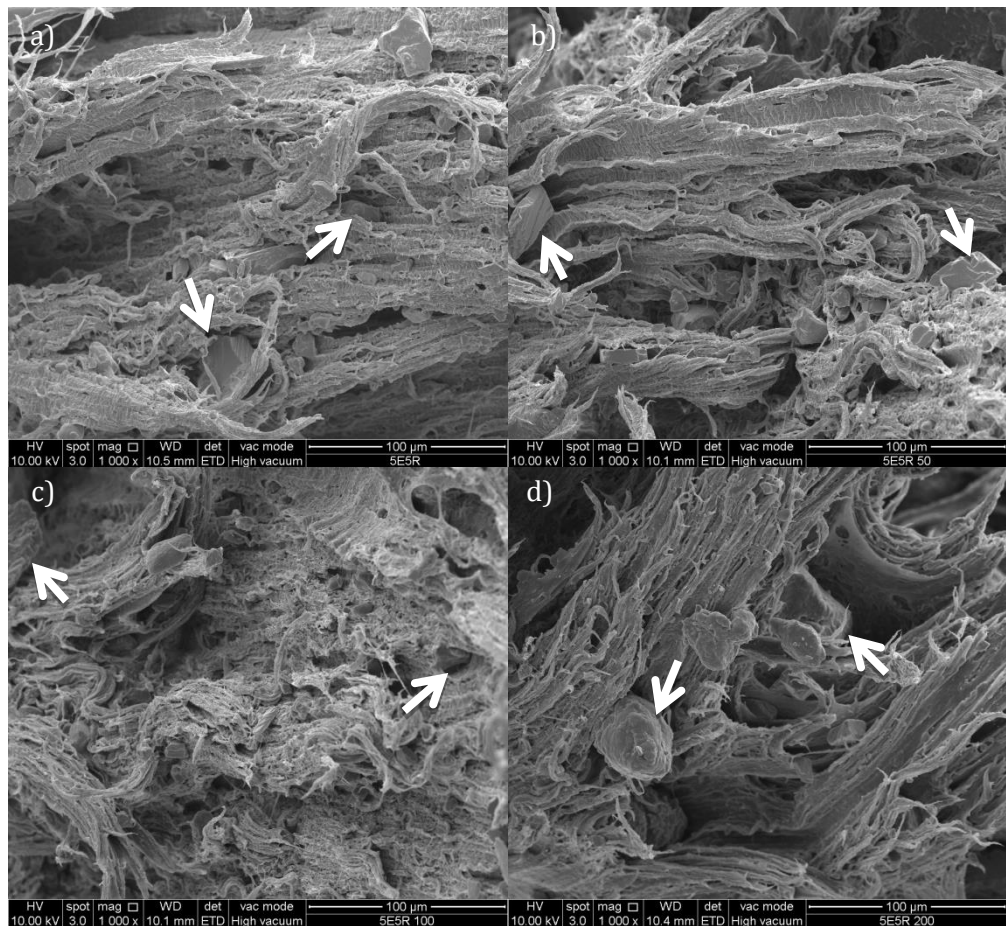


Figure 4.7 Tensile fracture surface of 50RTR at a) 0kGy, b) 50kGy, c) 100kGy and d) 200kGy

The fracture surface of EVA evolved from wavy structure before irradiation to fibrillated waves at 50 and 100kGy irradiation dose. Upon further irradiation (200kGy), smoother fracture surface was observed. Fibril like structure (indicated by arrows) in non-irradiated EVA was tiny and showed only a slight

elongation (Figure 4.8a). However, upon radiation (50 and 100kGy) the fibrils elongated enormously (Figure 4.8(b,c)). Further irradiation (200kGy) (Figure 4.8d) resulted in the diminishing fibril structures (indicated by arrows). Embrittlement of EVA was also evident from Figure 4.8d where the surface resembling multiple coalesced globular surface, clearly set apart from the surface of 0, 50 and 100kGy irradiation. These observations confirm the findings of the tensile properties where the tensile properties of EVA were improved due to the occurrence of irradiation induced crosslinking until 100kGy irradiation and declined upon further irradiation as a consequence of embrittlement caused by excessive crosslinking.

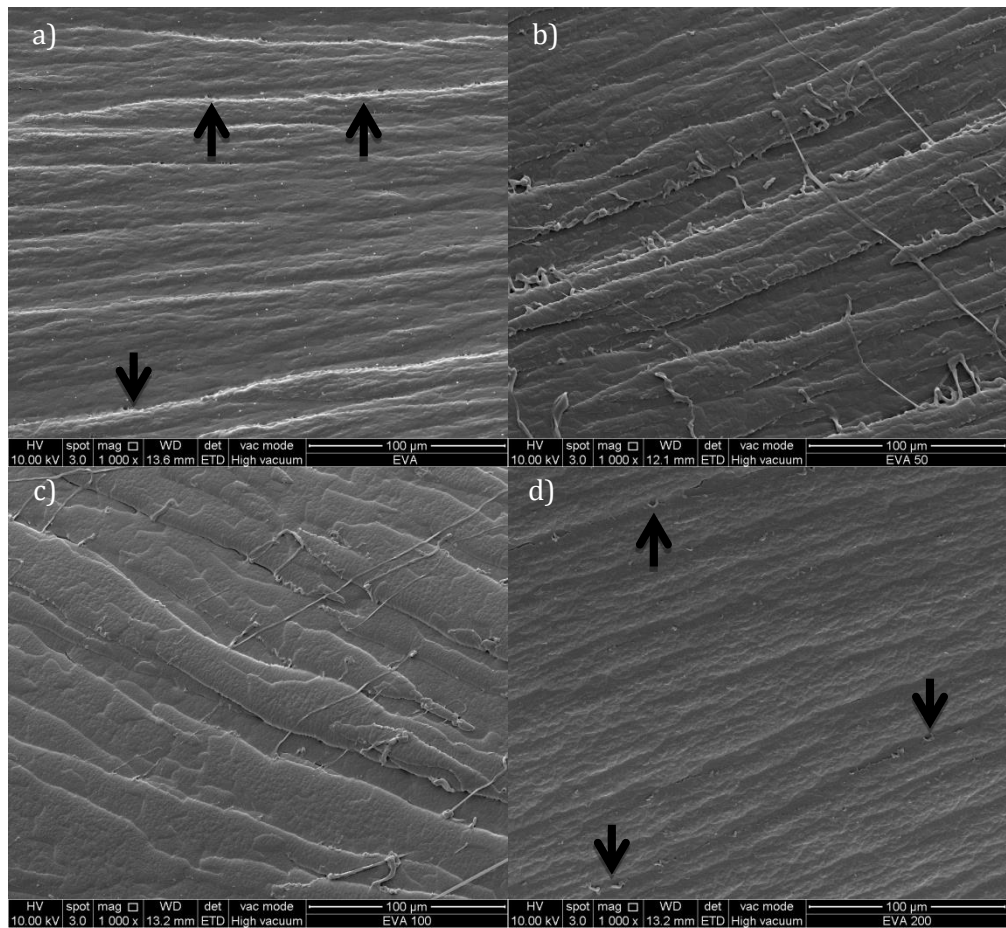


Figure 4.8 Tensile fracture surface of EVA at a) 0kGy, b) 50kGy, c) 100kGy and d) 200kGy

4.5.2. TEM

Figure 4.9 shows the TEM micrographs of 50RTR blend before (a,b) and after irradiation (c,d). At lower magnification (a,c), domains of RTR (in darker grey

shades) were distributed in EVA matrix (lighter grey shades). RTR domains before irradiation were measured to be around 0.5 to 2 μm . However, upon irradiation the RTR domains have lesser contrast compared to EVA phase, more difficult to distinguish and scattered around in EVA matrix. The size of the RTR domains in irradiated 50RTR blend measured to be around 0.1 to 1 μm . Increased molecular movement due bombardment of high energy electron onto sample, allows for rearrangement and re-shuffling to happen in RTR/EVA blends. Furthermore, irradiation on air also causes oxidative degradation on both RTR and EVA phases. These two phenomena, allows for decrease in RTR domain sizes and increased interaction between the phases. This indicates that irradiation improved the dispersion and compatibility of RTR in EVA matrix (Yamauchi et al., 2005). Decreased domain size of RTR with irradiation will effectively increase the surface area of RTR in contact with EVA (l'Abée et al., 2010). Similar observation of decreasing size of rubber phase upon irradiation was also observed in immiscible polymer blends of nylon1010 and high impact polystyrene (Dong et al., 2001).

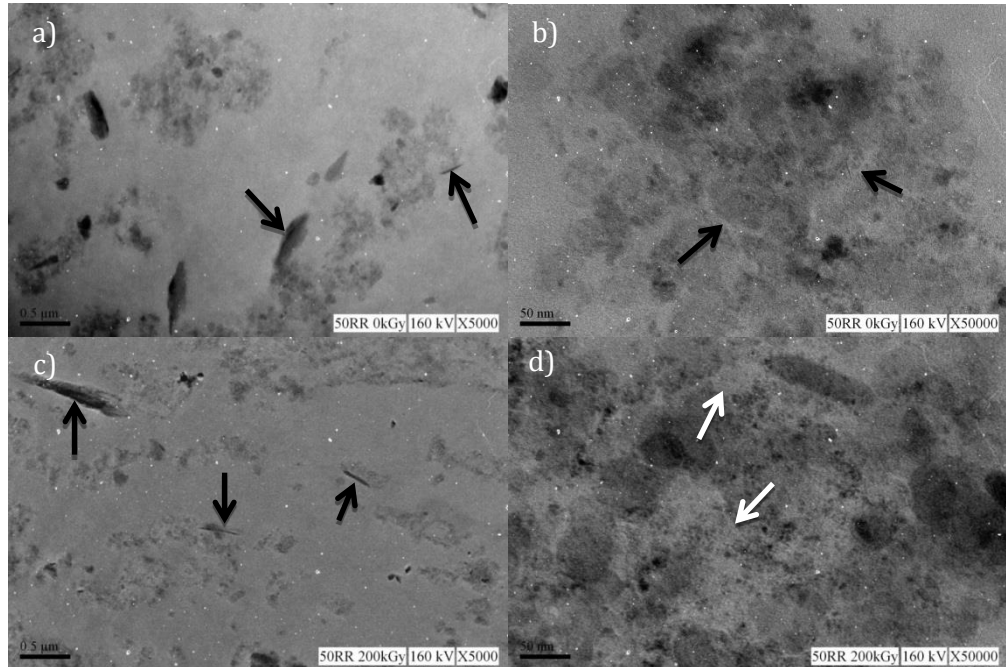


Figure 4.9 TEM micrographs of 50RTR blends before irradiation a) 5000X, b) 50000X and after irradiation c) 5000X and d) 50000X magnification

At lower magnification, in both before (Figure 4.9a) and after irradiation (Figure 4.9c), presence of nano sized fillers or substances (indicated by arrows)

migrated out from RTR into EVA phase were observed. These nano sized fillers or substances could increase the stiffness of EVA matrix resulting in decreased ductility of the blends (Tadiello et al., 2015). Furthermore, nano fillers such as nanoclay (Munusamy et al., 2012, Munusamy et al., 2009) and carbon nanotubes (Li et al., 2013, Jung et al., 2013) have been proved to reduce crosslink network formation in irradiated samples, particularly at lower irradiation doses. At higher magnification (Figure 4.9 b,d), entrapment of EVA phase within RTR phase could be observed (indicated by arrows). Entrapped EVA might intermingle with free chains on the surface of RTR forming an amorphous state (l'Abee et al., 2010). These will be further discussed in sections 4.6 and 4.7 later.

4.6. Thermal properties

4.6.1. TGA analysis

Figure 4.10 shows the mass loss and derivative TGA curves for RTR, EVA, and RTR/EVA blends. In general, two-step degradation process was observed for all the samples. Table 4.2 lists the data obtained from the mass loss and derivative TGA curves. RTR undergoes two step degradation which starts rather early. At first, a continuous mass loss was observed up to 319 °C (refer to inset of Figure 4.10b). This is associated with the evaporation of volatile content such as processing oil, plasticizer and low molecular weight substances. The volatile content in RTR corresponds to 8.25%.

The following degradation process observed is associated with the intensive thermal depolymerization of the rubber backbone (De et al., 2000). The first degradation peak (T_{max1}) was observed at 390 °C whereas the second degradation peak (T_{max2}) was observed at 444 °C in derivative TGA curve which corresponds to two types of rubber in the RTR. The degradation temperature of 390 °C is associated with the degradation of natural rubber (NR) (Chen and Qian, 2003), while the degradation temperature of 444 °C is associated with the degradation of either styrene butadiene rubber (SBR) (Sombatsompop and Kumnuantip, 2003) or butadiene rubber (BR) (Chen and Qian, 2003). All NR, SBR and BR are the common rubber compounds used in the manufacture of tires. Since the source of this study was heavy duty tires, the presence of BR could be more plausible as it is more commonly used in heavy duty tire formulations (Shulman, 2011). The mass loss associated with NR and BR (or

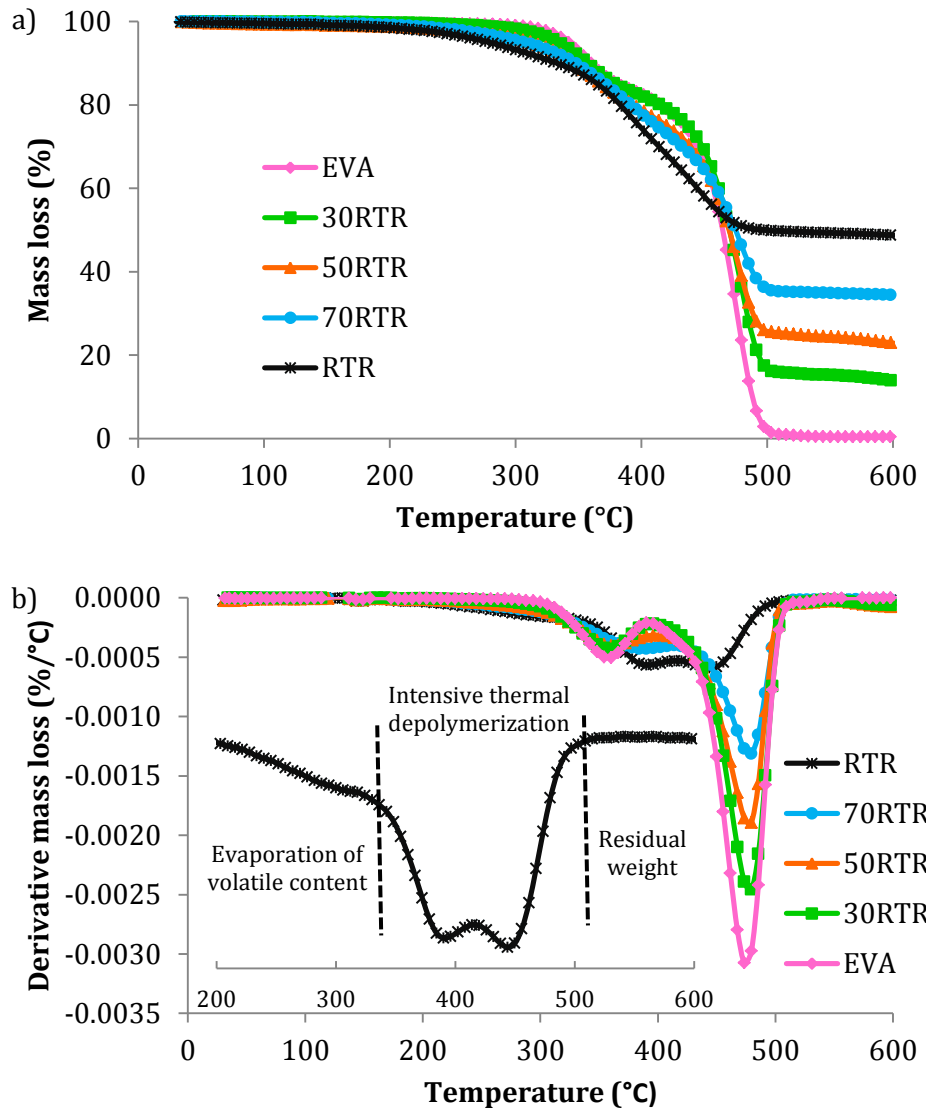


Figure 4.10 Typical TGA curve for RTR, EVA and RTR/EVA blends, a) Mass loss curve, b) Derivative curve

Table 4.2 Degradation temperatures and residual weight of RTR, EVA and blends

Sample designation	Volatile content wt (%)	Degradation temperature (°C)						Residual wt (%)
		T _{5%}	T _{10%}	T _{25%}	T _{50%}	T _{max1}	T _{max2}	
RTR	8.25	282.0	333.3	399.2	497.2	390.3	443.9	48.8
70RTR	5.40	306.0	348.0	413.9	474.2	384.1	479.4	34.3
50RTR	4.06	312.0	348.2	419.9	471.5	360.3	479.4	23.0
30RTR	2.13	333.2	355.3	437.9	470.6	360.2	479.6	13.9
EVA	0.00	342.1	360.1	431.0	465.0	360.0	473.6	0.4

SBR) was 21.75% and 20% respectively. This might indicate that NR and BR (or SBR) are present in approximately 50:50 blend ratio of the total rubber compound in the RTR.

The total rubber content according to the TGA curve is 41.75%. The residual weight of RTR was 50% at about 500 °C which is char of filler, additives and impurities from waste tire such as carbon black. EVA also undergoes a two-step degradation process, where the first step is associated with loss of acetic acid group ($\approx 17\%$) and the second one corresponds to the degradation of the main chain, polyethylene backbone (Mohamad et al., 2006, Boguski et al., 2014).

The blends also displayed similar two-step degradation as shown by EVA and RTR. However, they appear to have an intermediate thermal stability. The amount of volatile content and residual weight was proportionally lowered with the decreasing amount of RTR in the blends. The first and second degradation processes of RTR were merged with the first and second degradation processes of EVA respectively. The merging of degradation process pushes the $T_{\max 1}$ to a lower temperature and the $T_{\max 2}$ to a higher temperature as compared to the RTR with the increasing EVA content. As expected, $T_{\max 1}$ decreased with the increasing EVA content as EVA records a lower $T_{\max 1}$ value compared to RTR. However, all the blends showed a higher $T_{\max 2}$ value compared to both EVA and RTR. This is an indication of molecular level miscibility in RTR/EVA blends. Similar to $T_{\max 1}$, the temperature at mass losses of 5% ($T_{5\%}$), 10% ($T_{10\%}$), 25% ($T_{25\%}$) and 50% ($T_{50\%}$) of the blends showed intermediate values between RTR and EVA. Clearly, all three blends showed a higher thermal stability compared to the RTR up to ≈ 450 °C.

TGA studies on irradiated RTR and RTR/EVA blends showed exactly similar thermal stabilities, similar to samples before irradiation (Figures shown in Appendix A2). This again suggests no prominent degradation has taken place in these samples. Thermal stability of a compound is strongly related to the network structure in the compound (Ghosh et al., 1996, Basfar and Ali, 2011). In irradiated RTR/EVA blends, some extent of chain scissions and crosslinking were occurring concurrently, leaving the net volume of the network almost similar to non-irradiated blends. Hence, no distinct changes were observed in TGA thermograms of irradiated RTR and RTR/EVA blends.

4.6.1. DSC analysis

The heating and cooling DSC thermograms of EVA and EVA/RTR blends at different blend ratio and irradiation dose are shown in Figure 4.11(a-c). Increasing the RTR content in the blends results in shifting of crystallization and melting peak to a lower temperature and an obvious decrease in the peak height (Figure 4.11a). Figure 4.11b shows the shifting in crystallization and melting peak towards lower temperature as well as reduction in peak height with a slight narrowing tendency for EVA samples with increasing irradiation dose. A similar trend was also observed for 50RTR blend (Figure 4.11c) with increasing irradiation dose, however at a smaller extent of changes.

The findings from DSC thermograms have been charted in Figure 4.12 for clearer understanding. Figure 4.12(a-d) shows the changes in crystallization temperature, melting temperature, heat of fusion and crystallinity of EVA and EVA/RTR blend with increasing irradiation dose. Crystallization temperature of EVA was found to decrease from 67 °C to 64 °C at 70% RTR content (increasing RTR content at 0 kGy) due to the delayed nucleation effect rendered by RTR in the blend (da Costa and Ramos, 2008). More flexible RTR can be placed in the inter and intra spherulitic region of EVA crystallite, hence disrupting the packing of EVA macromolecular chain (da Costa et al., 2006). This was observed from TEM micrographs of 50RTR blend (Figure 4.9). EVA phase seen in lighter grey shade was entrapped (indicated by arrows) in and around RTR phase, which has a darker grey shade.

An obvious 8 °C decrease in crystallization temperature with increasing irradiation dose was noted for EVA (67 °C at 0 kGy to 59 °C at 200 kGy). Rearrangement of EVA chains from melt state becomes limited due to irradiation induced crosslinks, hence more imperfect crystallite with smaller size and lesser amount are formed (Khonakdar et al., 2006a, Khonakdar et al., 2006b). These require lesser energy, hence, a decrease in the crystallization temperature of EVA with increasing irradiation dose was observed. Whereas, with increasing irradiation dose, decrease in crystallization temperature was less prominent in the RTR rich blend compared to EVA. As discussed earlier, crosslinking efficiency is reduced in the RTR/EVA blends with increasing RTR content due to the presence of radical scavenging additives, retarding the overall crosslinking process. Hence, limited number of crosslinks is formed in the blends containing RTR which allows for packing of EVA chains.

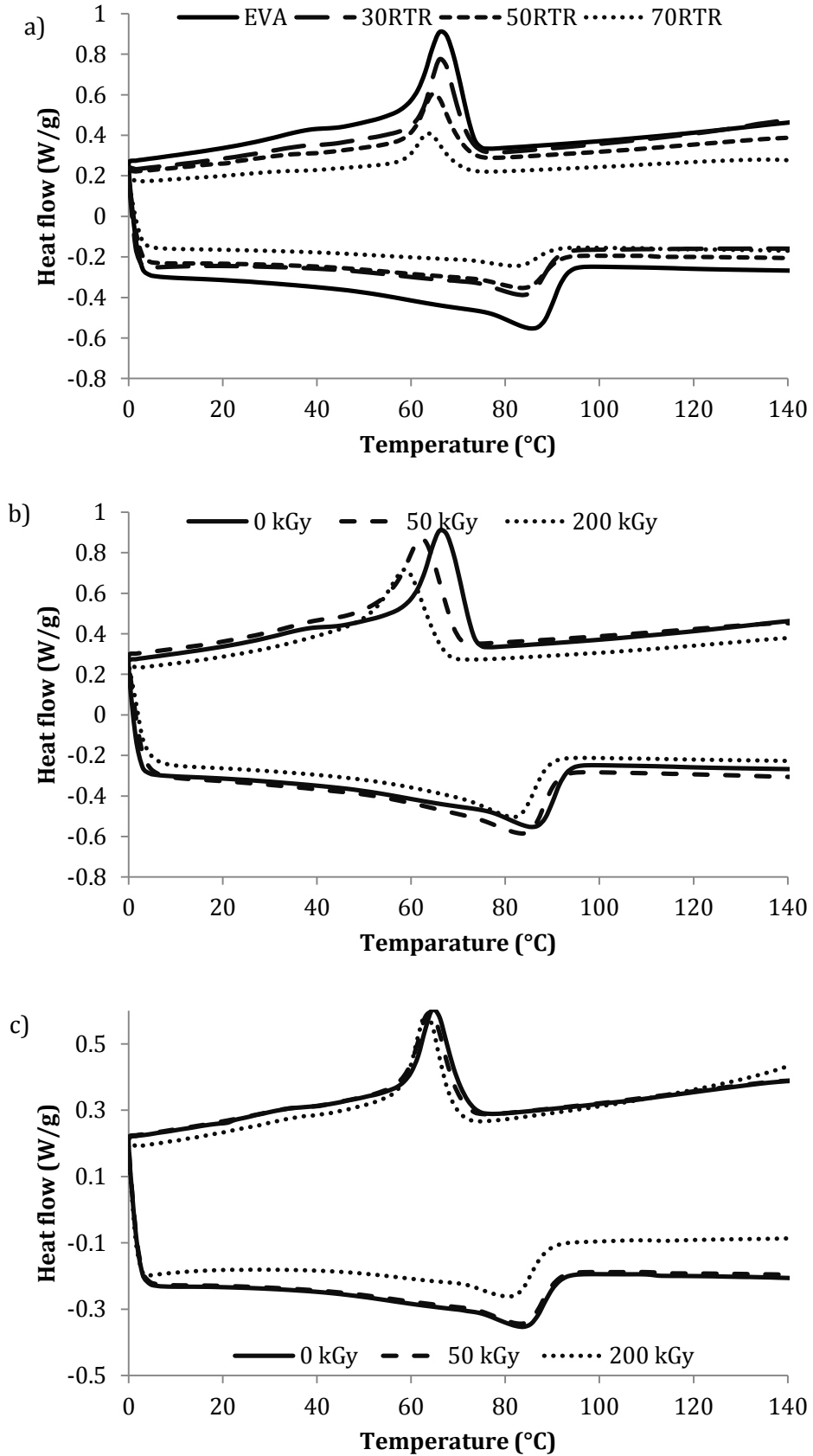


Figure 4.11 Typical heat flow curve of a) EVA and RTR/EVA blends, b) irradiated EVA and c) irradiated 50RTR blend

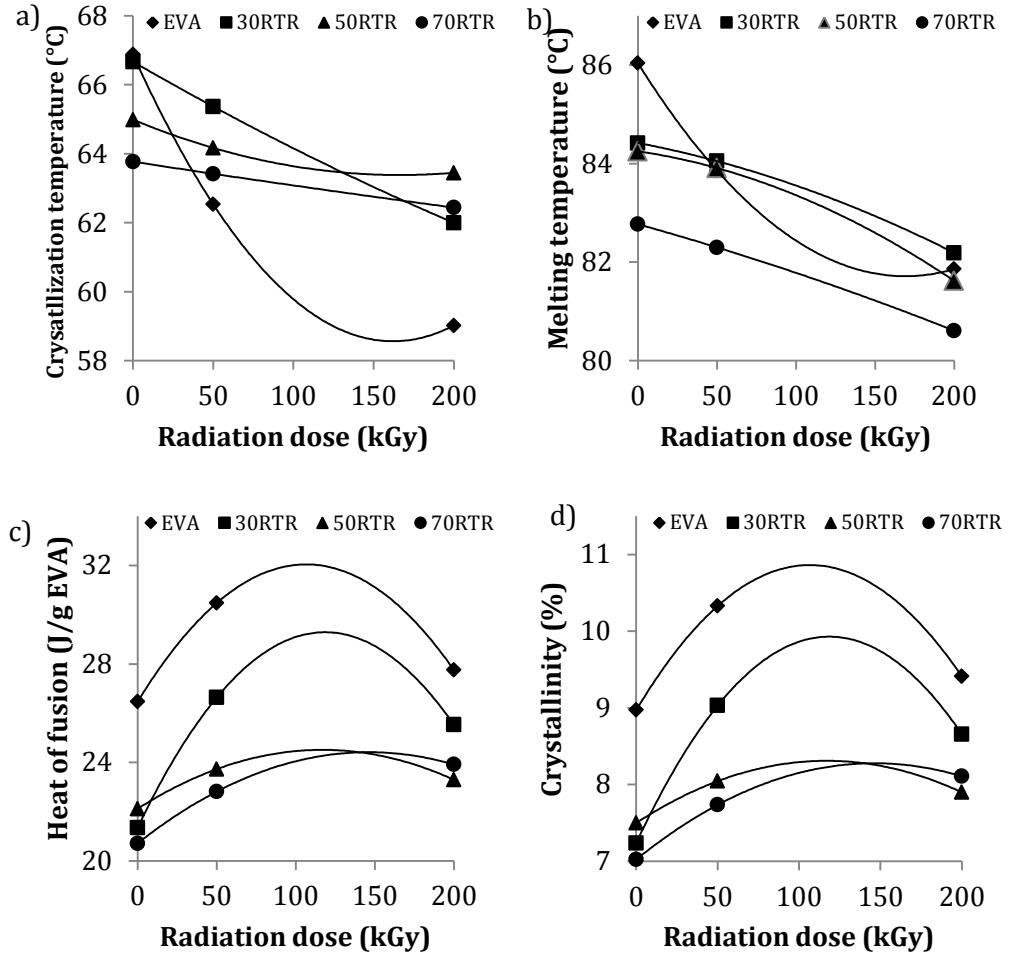


Figure 4.12 Effect of irradiation dose on a) crystallization temperature, b) melting temperature, c) heat of fusion and d) crystallinity of EVA and RTR/EVA blends

Figure 4.12b shows the influence of increasing irradiation dose on melting temperatures of EVA and RTR/EVA blends. The pattern of changes in melting temperature was very much similar to the pattern of changes in crystallization temperature. Melting temperature of EVA decreased from 86 °C to 82.77 °C (70RTR, 0 kGy) with increasing RTR content. Grigoryeva et al. (2006) and Qin et al. (2008) discussed the depression of melting temperature of polymers in the RTR blends is caused by the formation of imperfect crystallites and/or by crystallites having smaller size. Melting temperature of EVA decreased by about 5 °C at 200 kGy irradiation dose as imperfect crystallite with smaller size and lesser amount being formed due to irradiation induced crosslinks which restricts the rearrangement of EVA chains (Dong et al., 2000). The magnitude of decrease in melting temperature of the blends with increasing irradiation dose

was less notable compared to EVA, similar to the observation with crystallization temperature. Though, it was interesting to note the changes in melting temperature with increasing irradiation dose was lying closely nearby for 30RTR and 50RTR blends, implying the presence of RTR has a significant effect on melting temperature than the content of RTR up to 50 wt% RTR in the blends. This might also suggest the distribution of size or amount of EVA crystallite is similar in these blends.

Figures 4.12c and 4.12d show the effect of irradiation on heat of fusion of crystallisable content (J/g of EVA) and crystallinity of EVA and RTR/EVA blends respectively. In EVA and EVA/RTR blends, both heat of fusion and crystallinity decreased in the presence of RTR and increased with increasing irradiation dose. A few studies have also noted similar observation in rubber/plastic blends (Varghese et al., 2002, Saleesung et al., 2010). Study conducted by Ratnam et al. (2014) concluded the presence of ground tire rubber in EVA matrix has a disrupting role in the EVA chain molecules arrangement when cooling from melt, thus reducing the crystallinity of the blend. RTR surface contains free chains (due to devulcanized structure of RTR) that allow intermingling of EVA chains with RTR, promoting the "amorphous state" in the space closest to RTR surface (Hassan et al., 2013c). Therefore, reducing the heat of fusion and crystallinity (at 0kGy) of the blends, regardless of RTR content.

Irradiation, however, improves the heat of fusion and crystallinity of EVA and RTR/EVA blends up to 100 kGy followed by a slight reduction. Reyes-Labarta et al. (2006) studied the blends of PP/EVA and indicated the presence of functional group produced upon irradiation leads to formation of more defective crystal in the crystalline phase of the blends. Similarly, Sujit et al. (1996) in their work noted higher amount of intermolecular interaction in EVA due to the formation of polar group such as C=O with increasing irradiation dose allows for closer packing of EVA chain, hence increasing the crystallinity. Beyond the optimum irradiation dose (100 kGy in this case), the decrease in the crystallinity is associated with the irradiation induced degradation of the crosslinked network structures along with the formation of crosslinks between readily present crosslinks that lead to more imperfect EVA crystal (Şen and Güven, 1995). Blends with more than 50 wt% RTR showed less remarkable changes in heat of fusion and crystallinity due to the presence of RTR playing more dominant role in disrupting the EVA chain rearrangement and recrystallization with increasing

irradiation dose. In view of this, the TEM micrographs in Figure 4.9 (c) indicate that the RTR are more evenly distributed in EVA matrix upon 200 kGy irradiation, and it is more difficult to distinguish the borders between the RTR and EVA phase. The redistribution of smaller RTR particles in EVA phase with increasing irradiation dose might have increased the effective surface area between RTR and EVA, thus, disrupting the EVA chain recrystallization and rearrangement (l'Abee et al., 2010). This phenomenon leads to less notable changes in heat of fusion and crystallinity of the blends containing higher amount of RTR.

4.7. Dynamic mechanical analysis

4.7.1. Storage modulus

Dynamic mechanical properties of RTR, 50RTR and EVA before and after 200 kGy irradiation are illustrated in Figure 4.13(a-c). Storage modulus determines the dynamic rigidity of a material, which originates from the elastic response of the material. All RTR, 50RTR and EVA storage modulus curves show three regions, namely, glass, transition and rubbery region. Storage modulus of RTR showed a substantial decrease in the glass and transition range upon 200 kGy irradiation compared to non-irradiated RTR. Such observation believed to be attributed to the occurrence of irradiation induced chain-scissioning in RTR. This finding is in agreement with gel content findings, where the gel content did not show any difference with increasing irradiation dose and yields high p_0/q_0 values. Macroradicals formed through irradiation are scavenged and stabilized by additives and residual reclaiming agents present in RTR matrix, leading to chain scissions, thereby decreasing the storage modulus in glassy and transition regions (Ratnam, 2001, Ratnam et al., 2001c). Although mechanical and thermal properties of RTR discussed in sections 4.4 and 4.6 did not show a substantial drop with increasing irradiation dose, storage modulus was clearly affected. There was no distinct difference in the storage modulus of RTR before and after irradiation upon reaching rubbery region. This is a common trait in amorphous polymer such as natural rubber which is one of the major components of RTR (Grigoryeva et al., 2006).

50RTR blend before irradiation, showed higher storage modulus values compared to EVA and RTR throughout the studied temperature range. Presence

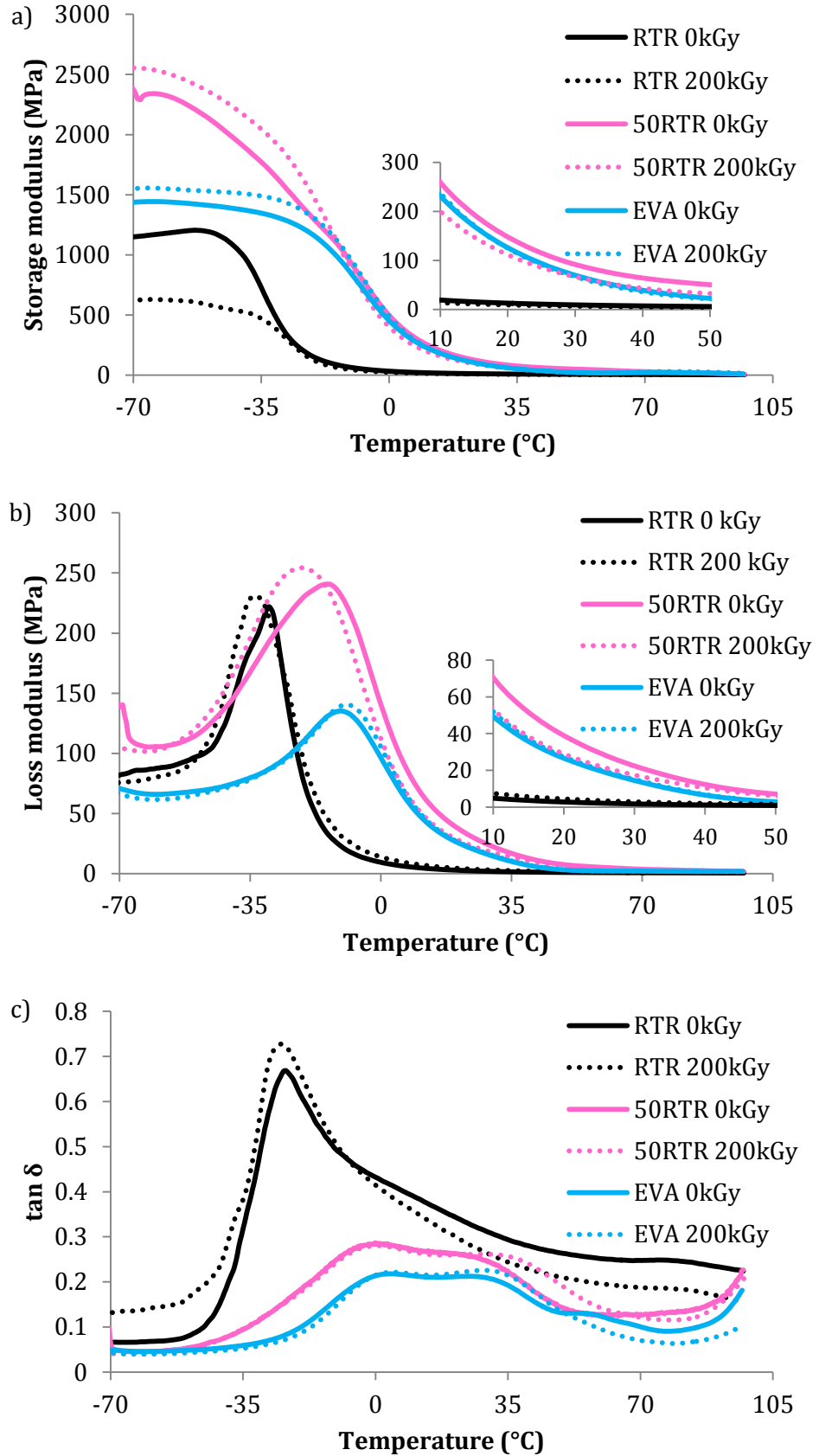


Figure 4.13 Dynamic mechanical properties; a) Storage modulus, b) Loss modulus and c) tan δ of RTR, EVA and 50RTR blend before and after irradiation

of crosslinked structure in RTR, capable of storing elastic capacity and rendering stiffness, could be responsible in enhancing the storage modulus of 50RTR blend. Additionally, the presence of carbon black and nano fillers in the blends, as evident from Figure 4.9; might enhance the stiffness of the 50RTR blend. The higher storage modulus values observed for the blends compared to the individual components (RTR and EVA) also suggests molecular level miscibility between these components have been achieved. Upon irradiation, storage modulus of 50RTR blend improved throughout, by about 10% up to -15 °C, after which the irradiated 50RTR blend shows lower storage modulus values compared to non-irradiated 50RTR blend. Such an increase in glassy region's storage modulus of 50RTR blend upon irradiation again validates the assumptions made in the gel content analysis where the gel content of the blends was found to increase more rapidly at higher doses upon consumption of the stabilizing and radical scavenging additives which present readily in RTR. After complete consumption of stabilizing and radical scavenging additives, irradiation induced crosslinks are deemed to happen in the blends. Radiation induced crosslinking in 50RTR blend upon 200 kGy irradiation improves the ability of the blend to store the elastic deformation, which translates to an increase in the storage modulus (Ratnam et al., 2001a). While the improvement in the storage modulus of glassy region is associated with the irradiation induced crosslinks, the decrease upon reaching transition region was associated with the loss of crystalline zone of EVA in the blend due to irradiation. In a semicrystalline polymer, contribution to storage modulus, above the glass transition temperature is associated with the crystalline region of the polymer (Mohamad et al., 2006, George et al., 1997, John et al., 2003). Irradiation induced redistribution of RTR, decreases the crystallinity of EVA in 50RTR blend, hence, a drop in the storage modulus was noted.

Similarly, irradiated EVA also showed about 8% increment in storage modulus up to 0 °C, upon which the storage modulus of both before and after irradiation remained the same. Smaller increment of glassy region's storage modulus of EVA might indeed be due to the formation of excessive crosslinking at 200 kGy irradiation which causes embrittlement of EVA. The insignificant difference in storage modulus at above 0 °C between non-irradiated and irradiated EVA is found to be in agreement with the crystallinity of EVA at 0 and 200 kGy

exhibiting similar values (Figure 4.12d). Therefore, it is evident that crystallinity has major influence on the storage modulus beyond the glassy region of EVA.

Entering the rubbery region (inset of Figure 4.13a), the sequence of storage modulus was 50RTR 0 kGy > EVA 0 kGy = EVA 200 kGy > 50RTR 200 kGy > RTR 0 kGy = RTR 200 kGy. 50RTR blend displayed about 10 fold improvement in storage modulus of rubbery region compared to RTR. Furthermore, most application of EVA based product falls within the rubbery region (temperature 10 to 50 °C). Therefore, substitution of 50 wt% of RTR with EVA would not affect the product performance in terms of dynamic mechanical properties.

4.7.2. Loss modulus

Figure 4.13b shows the temperature dependence of loss modulus of EVA, RTR and 50RTR blend before and after irradiation. Loss modulus is related to the work dissipated within the material during one load cycle. It is a measurement of the viscous component of the energy dissipated that is unrecoverable during a load cycle. Peak of loss modulus is associated with the glass transition temperature of the material (Ratnam et al., 2001a). RTR showed a peak around -30 °C with a modulus value of 221 MPa. Upon irradiation, the peak of loss modulus shifts to a lower temperature, -33 °C, recording a modulus value of 230 MPa. The observation in changes of loss modulus with irradiation of RTR supports the gel content analysis, where the dominance of chain scission over crosslinking process in RTR was deduced.

Peak of 50RTR blend's (0 kGy) loss modulus was higher than RTR and EVA, recording a value of 241 MPa at -14 °C. Similar to the observation of RTR, 50RTR blend showed an increase in loss modulus peak shifting to a lower temperature with 200 kGy irradiation. 50RTR blend recorded loss modulus peak value of 254 MPa at -21 °C at 200 kGy irradiation. An increase noted in the storage modulus of irradiated 50RTR was inferred to be related to occurrence of irradiation induced crosslinking in 50RTR. If crosslinking was the predominant process as per inference, the loss modulus peak is likely to decrease and shift towards higher temperature due to increased restriction of the polymeric chain resulting from the crosslinking. However, an opposite trend was found in loss modulus of 50RTR upon irradiation. A plausible reason could be breakdown of C-S crosslinks in RTR (which has lower bond energy compared to C-C bond energy)

along with the formation of C-C crosslinks induced by electron beam irradiation. This phenomenon could lead to overall increased energy loss and possibly shift the peak of loss modulus towards lower temperature. Furthermore, cleavage of C-S crosslinks and formation of C-C crosslinks in RTR will lead to a less elastic system which dissipates more energy as heat (Basfar et al., 2002, Hernández et al., 2015). Chakraborty et al. (2011) showed improvement in EB irradiated tire components (previously sulphur crosslinked) due to formation of C-C bond. Grobler and McGill (1994) in their work with different curing system in polyisoprene rubber, showed the glass transition temperature of conventionally cured rubber was higher than radiation cured rubber due to prevalence of network heterogeneity in conventionally cured rubber compared to radiation cured rubber. Moreover, recent study on electron beam irradiation of sulphur cured NR/SBR blend showed reduction of poly- and di-sulfide bonds to mono-sulfide and C-C bonds (Shen et al., 2013).

A minute changes in loss modulus of EVA was observed with irradiation, where the peak increased by 3.6 MPa and shifted to higher temperature by 2 °C. Such changes might be a result of the combined effect of crosslinking and scission reaction prevailing at 200 kGy irradiation, as well as perturbed relaxation of the chain molecules due to the structural changes (Vijayabaskar and Bhowmick, 2005).

4.7.3. Tan delta

Figure 4.13c shows the temperature dependence of tan delta of EVA, RTR and 50RTR blend before and after irradiation. Tan delta, also known as the damping factor, is defined as the ratio of loss modulus to storage modulus, measuring the energy loss in relation to the recoverable energy (Ratnam et al., 2001a). Damping pattern of all samples, EVA, RTR and 50RTR, before and after irradiation; goes through a maximum in the transition region and decreases in the rubbery region. Low damping characteristic below transition region are typical of frozen polymer chain segments, where deformation is primarily elastic and occurrence of molecular slip resulting in viscous flow is minimal. Whereas, low damping characteristic above transition region are typical of free to move molecular segments with little resistance to flow. Damping characteristics are the highest in the transition region due to initiation of micro-Brownian motion

of molecular chains (Vijayabaskar and Bhowmick, 2005). In this study, the position and the height of tan delta peak are indicative of the structure and the extent of crosslinking of the samples.

The peak of tan delta of RTR upon irradiation remained at -24 °C but increased by 0.058, again supporting the view of the probability of breakdown of C-S crosslinks dominance over C-C crosslinking in RTR upon irradiation. It is a common knowledge that tire rubber are blends of two or more rubber components showing separate tan delta peak as most rubber blends are immiscible. TGA analysis of RTR showed the presence of natural rubber (NR) and butadiene rubber (BR) or styrene butadiene rubber (SBR) at almost 50:50 composition in RTR. The glass transition temperature recorded for RTR in this study fits well to glass transition temperature of filled and cured NR. The glass transition temperature of SBR could not be seen as it overlaps with NR, whereas for the glass transition temperature of BR (-100 to -80 °C), the range of temperature used in this study was not sufficient to detect it (Bandyopadhyay et al., 2010, George et al., 2000b, Sircar et al., 1997).

Tan delta curve of EVA peaks at 4 °C showing a peak shoulder appearance due to motion of side chains which is common in semicrystalline polymers. Upon 200 kGy irradiation, no changes were observed in the position and height of tan delta peak; however, broadening of the tan delta curve was obvious. This might be due to increased free side chains as a result of chain scission or oxidation of EVA (Giri et al., 2012, Munusamy et al., 2012) which introduces micro heterogeneity.

50RTR showed similar trends to EVA, displaying a peak at 0 °C with a peak shoulder appearance, suggesting the presence of side chains. It was interesting to note the appearance of single peak of tan delta, which was very much closer to EVA, rather than taking mid-way between EVA and RTR. Although the similar appearance of 50RTR tan delta peak to EVA's peak suggests that EVA and RTR are compatible blends; the broadening of tan delta curve compared to EVA suggest the presence of only partial miscibility in the blends (George et al., 2000b). Upon irradiation of 50RTR, again similar to EVA, only broadening of the tan delta curve was observed. This could be due to the formation of more free side chains and increased heterogeneity between EVA and RTR due to irradiation induced redistribution of RTR phase in the blends.

4.8. Equilibrium swelling

The sorption behavior of RTR, EVA and RTR/EVA blends are presented as mol uptake, Q_t , of toluene by 100g of the polymer as a function of square root of time in Figure 4.14. RTR, EVA and all the blends presented similar sorption behavior even though the corresponding equilibrium uptake is different. Sigmoidal curve was observed at the beginning of the sorption time. Surface of polymer samples swells immediately upon contact with the solvent. However, material deeper within the sample, which has yet to come in contact with the solvent and swell, prevents further swelling of the polymer sample. Hence, a two-dimensional compression stress is produced on the sample surface. The swelling stresses are either relaxed or dissipated by further swelling and rearrangement by polymer segmental movement (George et al., 2000b). Figure 4.14a shows sorption behavior of EVA and RTR/EVA blends before irradiation. Sorption behavior of RTR before irradiation could not be charted as RTR turned fragile and broke into pieces after about 60 minutes of immersion in toluene.

EVA showed the maximum equilibrium uptake and 70RTR the lowest equilibrium uptake. Equilibrium uptake decreases with increasing RTR content in the blends. This was due to the presence of crosslinked structure and filler within RTR matrix; which restricts the molecular motion of the polymer segments by creating a more rigorous path for penetration of toluene molecules through the sample (Kumnuantip and Sombatsompop, 2003, De et al., 2007). As the RTR content in the blend increases, the filler (such as carbon black and silica) content increases. Migration of some filler particles from RTR into EVA matrix was also observed in TEM micrographs in section 4.5. These filler fills up the free volume or micro voids within the blends. The increase in filler content restricts the molecular motion of the polymeric chain resulting in a torturous path for solvent penetration and diffusion (Sujith et al., 2007).

Figure 4.14 (b – d) shows the changes in sorption behavior of EVA, 50RTR and RTR with increasing irradiation dose. Equilibrium uptake of EVA dropped by 25% upon irradiation and remained the same with further increase in irradiation dose. All irradiated EVA showed similar steeper sigmoidal curve in the beginning of sorption and attained equilibrium faster compared to non-irradiated EVA. Formation of crosslinked network in EVA matrix upon irradiation hinders the molecular motion of EVA chains and penetration of

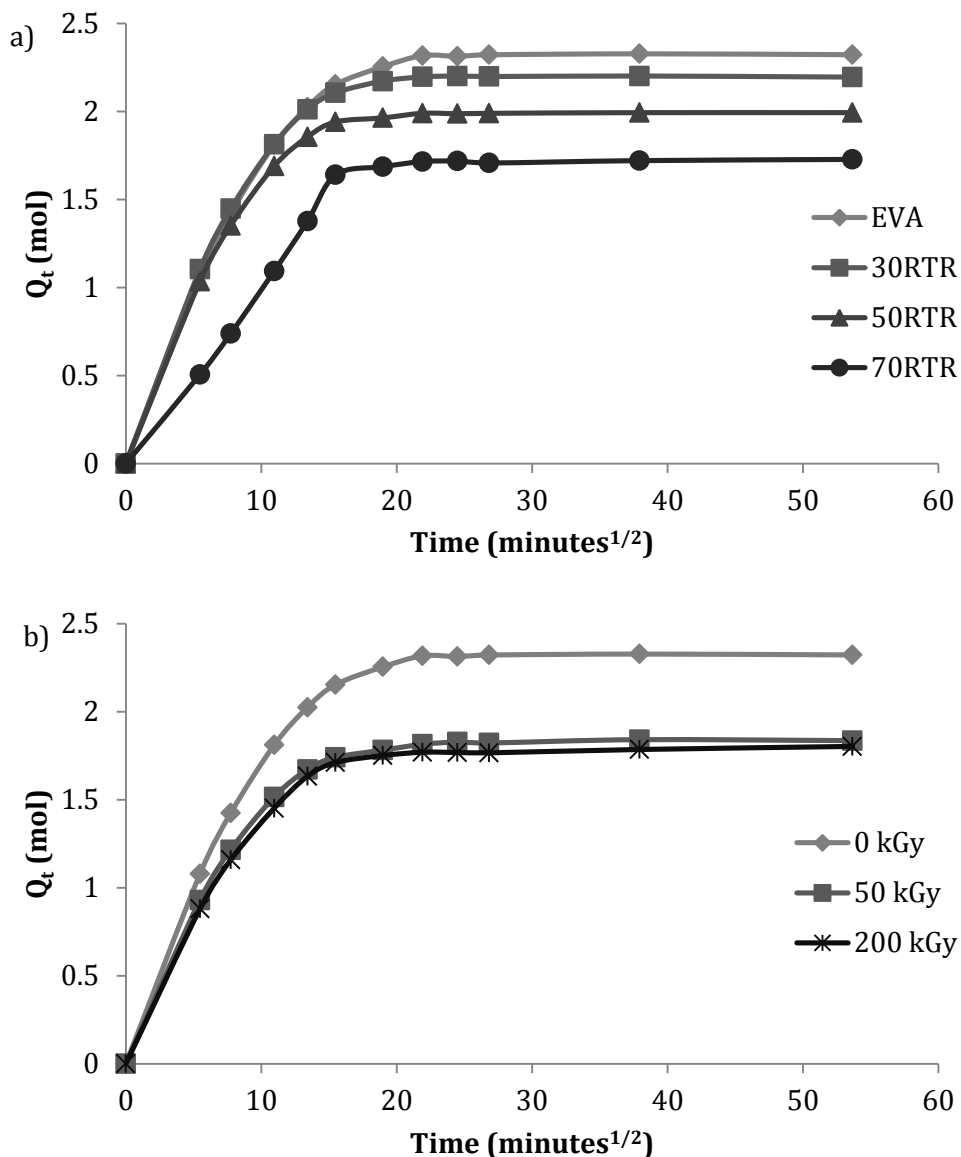


Figure 4.14 Mol percent toluene uptake of a) EVA and RTR/EVA blends at 0 kGy, b) EVA at 0, 50 and 200 kGy, c) 50RTR blend at 0, 50 and 200 kGy; and d) RTR at 50 and 200 kGy irradiation doses

toluene molecules, which helps to reduce the equilibrium uptake of the irradiated EVA sample. However, it was interesting to note, with further increase in irradiation dose; which corresponds to increase in crosslinked network, no influence on the sorption behavior of EVA was observed.

Contrary to EVA, all RTR/EVA blends and RTR did not show a significant difference or pattern in sorption behavior with increasing irradiation dosage. Referring to gel content analysis, presented in section 4.3, crosslinking efficiency was retarded in RTR and RTR/EVA blends as compared to EVA. This suggests

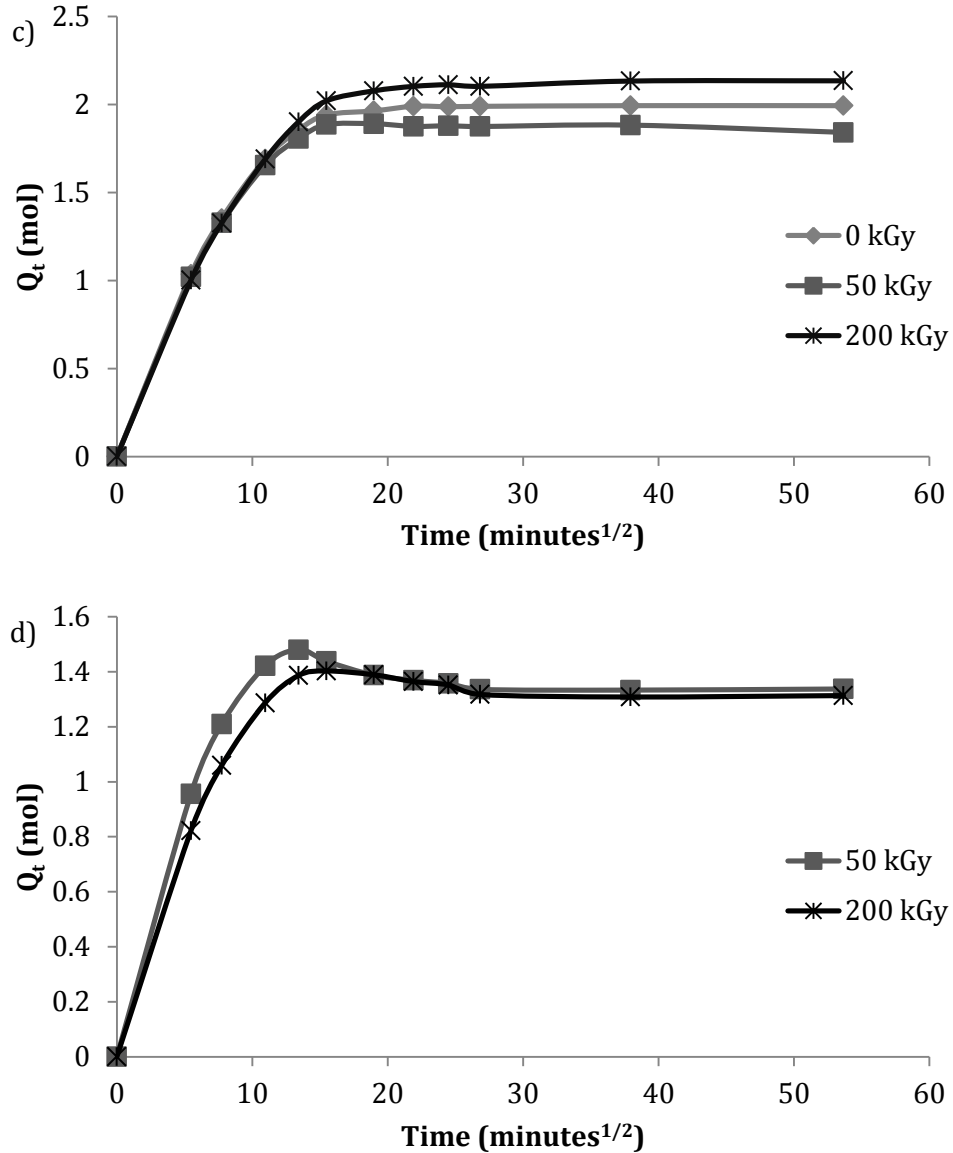


Figure 4.14 Mol percent toluene uptake of a) EVA and RTR/EVA blends at 0 kGy, b) EVA at 0, 50 and 200 kGy, c) 50RTR blend at 0, 50 and 200 kGy; and d) RTR at 50 and 200 kGy irradiation doses

the crosslinked network in RTR and RTR/EVA blends only differed marginally with increasing irradiation dosage; leading to insignificant changes in the sorption behavior of the blends and RTR. This is also in line with the sorption behavior observed with increasing irradiation dosage of EVA, suggesting feasibility of changes in sorption behavior up to a certain level of irradiation induced crosslinked network structure, upon which, no significant changes will be observed. Another interesting point of consideration is the fact that RTR before irradiation which was fragile upon immersion in toluene; turned into sturdy sample which lasted 3 days without breaking apart upon irradiation.

Though dynamic mechanical analysis in section 4.7 clearly showed domination of chain scissions in RTR sample, clearly some deeper changes are ought to have happened in the irradiated RTR sample, which improved the ability of RTR to endure toluene immersion.

4.8.1. Empirical analysis

Table 4.3 lists the n , k , diffusion, sorption and permeability coefficient of RTR, EVA and RTR/EVA blends. The value of n indicates the mechanism of sorption in the samples. If $n=0.5$ the mechanism of sorption is termed as Fickian which occurs when the rate of diffusion of permeant molecules is less than the polymer segmental mobility. If $n=1$ the mechanism of sorption is termed as case II whereby, the rate of diffusion of permeant molecules is much greater than polymer segmental mobility. If n lies between 0.5 and 1 then the mechanism of sorption follows an anomalous trend. In this case, the permeant molecules mobility and polymer segmental relaxation rates are similar. In this study, the n values for all RTR, EVA and RTR/EVA blends ranges from 0.49 to 0.67 indicating the anomalous sorption trend. There was slight inclination of decrease in n values with increasing RTR content.

Table 4.3 Different parameters of sorption behavior of RTR, EVA and RTR/EVA blends before and after irradiation. (n , $\log \text{min}^{1/2}$; k , unitless; D , $\times 10^5 \text{ cm}^2\text{min}^{-1}$; S , unitless; P , $\times 10^4 \text{ cm}^2\text{min}^{-1}$)

Designation	n		k		D		S		P	
	0kGy	50kGy								
RTR	-	0.49	-	0.31	-	7.18	-	2.25	-	1.62
70RTR	0.61	0.56	0.19	0.24	4.65	5.76	2.58	2.66	1.20	1.53
50RTR	0.66	0.64	0.17	0.18	4.73	5.07	2.83	2.73	1.34	1.39
30RTR	0.63	0.61	0.18	0.19	4.44	4.53	3.03	2.96	1.35	1.34
EVA	0.67	0.61	0.16	0.19	4.01	4.50	3.13	2.68	1.26	1.21

The value of k depends on the structural features of polymer and its interaction with the solvent. The k values showed a slight increase with increasing RTR content. Similar observations on n and k values have been reported in the literature (Kumnuantip and Sombatsompop, 2003, De et al., 2007, Joseph et al.,

2003, Sujith et al., 2003). These findings suggest that with increasing RTR content; there is increased restriction on the diffusion of toluene molecules into the sample resulting in lower equilibrium uptake and increased interaction between toluene molecules and sample allowing for faster reach to equilibrium. As discussed earlier, no significant pattern was observed in the changes of n and k values before and after irradiation.

Diffusivity is a kinetic parameter, which depends on the polymer segmental mobility (Joseph et al., 2003). The values of diffusion coefficient of RTR, EVA and RTR/EVA blends before and after irradiation can be found in Table 4.3. Diffusion coefficient increases with increasing RTR content, indicating quick attainment of equilibrium uptake. Sorption coefficient is defined as the ability of penetrant molecules to diffuse into sample (George et al., 2000b) and was found to decrease with increasing RTR content in the blends. This leads to lower values of equilibrium uptake in blends with higher RTR content. Permeability is defined as the net effect of diffusion and sorption coefficient on the sample. Toluene permeability in RTR/EVA blends however, did not show a systematic trend. Both sorption parameter analysis (n, k and D, S) leads to similar conclusion whereby, increasing the RTR content in RTR/EVA blends allows for faster reach and lower equilibrium uptake.

4.9. Summary

Addition of EVA improved crosslinking efficiency, mechanical and swelling properties of RTR/EVA blends. Results on TGA and DMA revealed that the thermal stability, storage modulus and loss modulus exhibited a significant enhancement. However, crystallinity was observed to be affected due to entrapment of EVA chain within RTR domain while morphological analysis showed lack of adhesion between EVA and RTR. Crosslinking efficiency was found to be depressed in RTR and RTR/EVA blends due to presence of radical scavenging additives which readily present in RTR.

CHAPTER 5. EFFECT OF DIFFERENT COMPATIBILIZATION STRATEGIES ON THE PROPERTIES OF RTR/EVA BLEND

5.1. Introduction

In this chapter, the second aim of this study is addressed, whereby the compatibilization strategies of RTR/EVA blend is discussed. Judging from mechanical, morphological, thermal and dynamic mechanical analysis of RTR/EVA blends, it is evident that the interfacial properties of these two components were poor. Thus, it is important to enhance the interfacial properties by compatibilization in order to yield a blend with enhanced properties. 50RTR blend is used as control sample in this phase of study. Both reactive and non-reactive compatibilization strategy has been employed. Figure 5.1 shows the representation of reactive and non-reactive compatibilization strategy. Three different types of compatibilizer were used, namely, (3-Aminopropyl)triethoxy silane (APS), liquid styrene butadiene rubber (LR) and maleic anhydride grafted EVA (MAEVA). APS has acted as a reactive compatibilizer, where the amine and ethoxy group from APS poses potential to chemically react with both RTR and EVA. The LR acts as non-reactive compatibilizing agent and likely to encapsulate RTR particles, effectively reducing the interfacial tension of the blends. MAEVA on the other hand, employs a combination of reactive and non-reactive methods. MAEVA contain maleic anhydride groups which is likely to react with carbonyl or hydroxyl group (reactive) from RTR surface; whereas the EVA chains of MAEVA will be wetting (non-reactive) itself into the EVA matrix. Processing, mechanical, morphological, thermal, dynamic mechanical and swelling properties of the compatibilized blends are discussed here.

5.2. Processing characteristics

Figure 5.2 shows the torque-time profile of the compatibilized blends at different compatibilizer loading. The peak at twenty seconds and two minutes represents the loading peak of EVA (loading torque) and RTR (maximum torque), respectively. The absence of rising torque and the presence of a

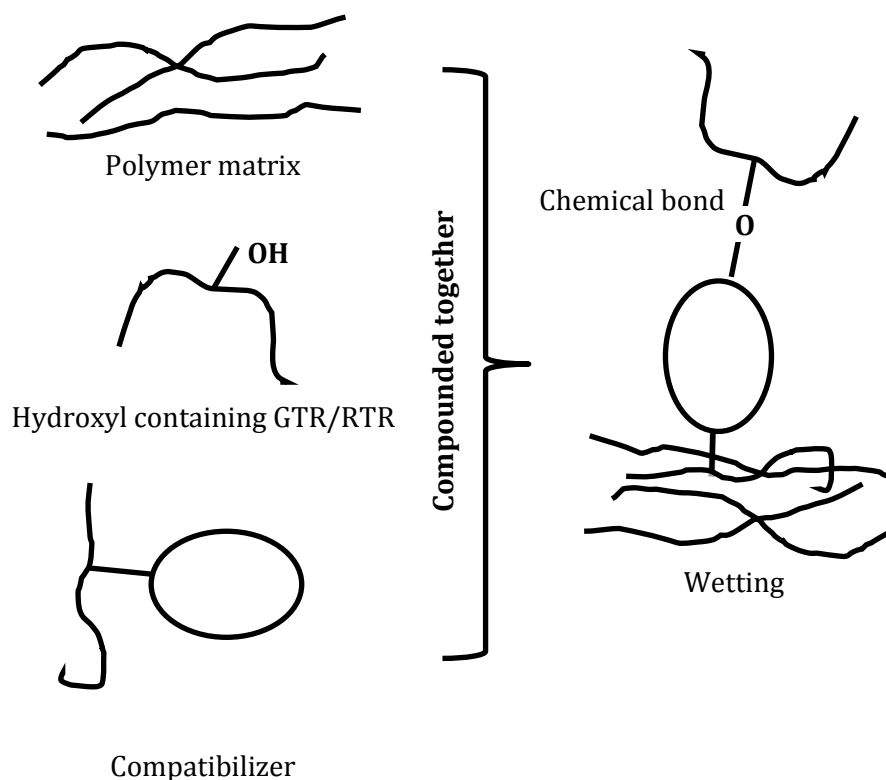


Figure 5.1 Illustration of reactive (chemical bond) and non-reactive (wetting) compatibilization strategy

stabilization zone were observed for all the compatibilized blends after four minutes, indicating the blends have essentially achieved homogenous state. All the blends compatibilized by APS, LR and MAEVA displayed similar torque profile at EVA loading point and complete EVA melting (minimum torque). This is clearly due to the similar amount of EVA loading in all the compatibilized blends. However, RTR loading torque profile was found to record a decrease with increasing APS content. This observation was even more prominent in LR compatibilized blends. The respective liquid and viscous liquid state of APS and LR allows it to acts as plasticizer and reduces the torque reading upon introduction into the mixing chamber (Pechurai et al., 2008). MAEVA compatibilized blends did not show such decrease as they exist in pellets form with MFI values almost similar to EVA matrix. End of the mixing torque was also decreasing with increasing compatibilizer loading in APS and LR compatibilized blends due to plasticization effect rendered by the compatibilizer.

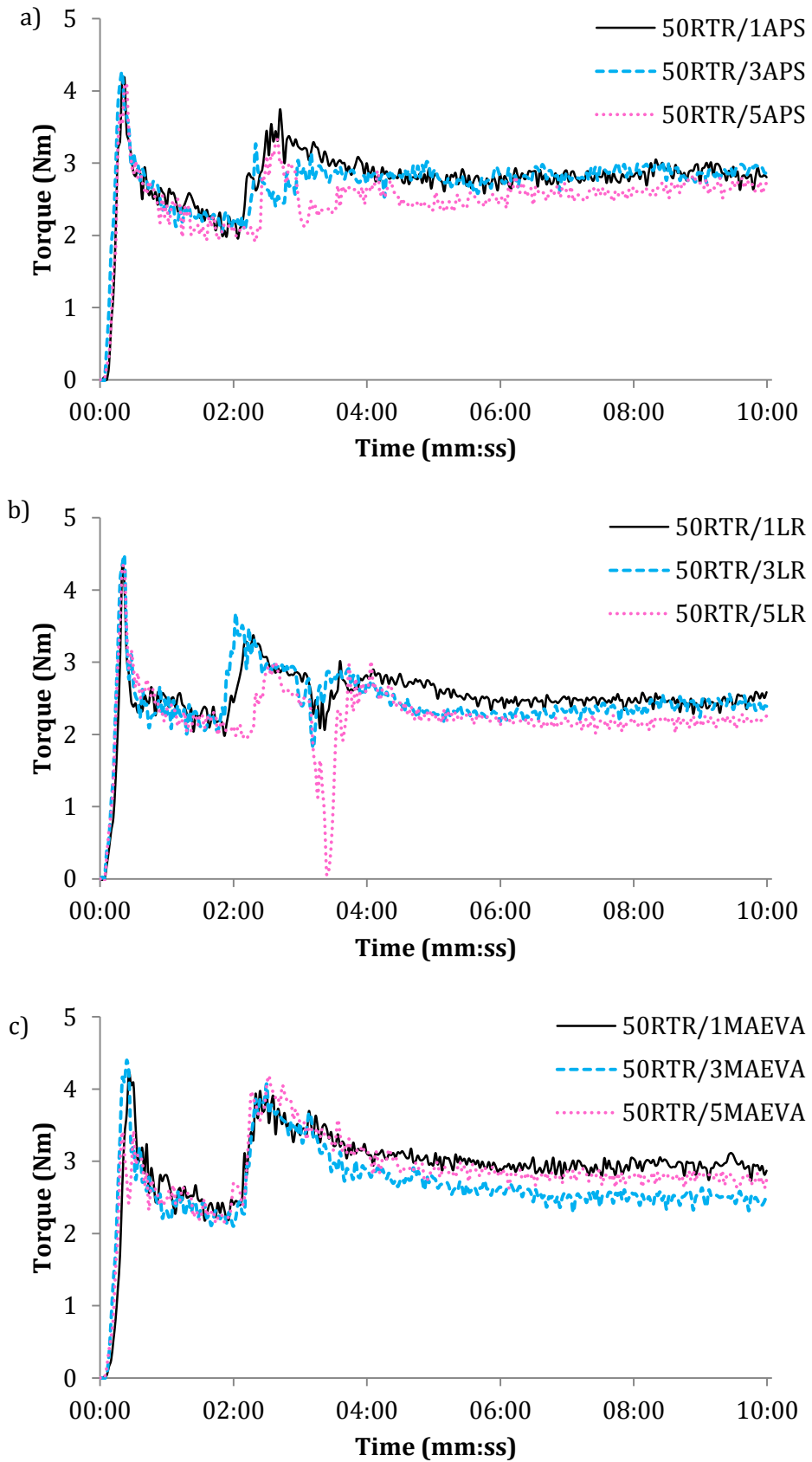


Figure 5.2 Torque vs time profile of a) APS, b) LR and c) MAEVA compatibilized blends at different compatibilizer loading

Figure 5.3 shows the influence of different types and loading of compatibilizer on loading, minimum, maximum and end mixing torques of the blends. As mentioned earlier, the loading and minimum torques of the compatibilized blends remained similar to 50RTR blend as it is only influenced by the amount of EVA, which is the same in all the blends. However, maximum and ending torque are clearly affected by the compatibilization. Maximum torque of APS compatibilized blends decreased with increasing APS loading. This is apparently due to ability of APS to further reclaim the RTR, hence, reducing the viscosity of the blends. This interaction will be further detailed in the following sections. The LR compatibilized blends did not show apparent changes in the maximum torque. Maximum torque was the torque reading taken at point of RTR introduction into the mixing chamber. This contradicts with the observation from Figure 5.2, where there was a significant drop in the torque reading with addition of LR. Though LR was added simultaneously with RTR, there was about 1.5 minute lag in LR reaching the bottom of mixing chamber where the transducer was positioned. This lag might be due to the viscous nature of LR. Maximum torque values of MAEVA compatibilized blends increased with increasing MAEVA loading. This is due to the chemical interactions taking place in the compound, increasing the viscosity of the blends. Ending torque of APS and MAEVA compatibilized blends increased slightly compared to 50RTR, however no influence of the compatibilizer loading was observed. Compared to 50RTR, only 1 wt% LR loading showed a slight increase, whereas 3 and 5 wt% LR blends displayed almost similar values.

Table 5.1 shows the total mixing energy of 50RTR (0 wt%) and compatibilized blends. All the blends showed an increase in total mixing energy at some point of loading. Highest increase for APS compatibilized blends was observed at 3 and 5 wt% loading corresponding to 6.6% increase compared to 50RTR. Similarly, MAEVA compatibilized blends increased by 13.9% at 5 wt% loading. LR showed the most nominal increase of 4.1% at 1 wt% loading. Only 5 wt% LR compatibilized blend displayed lower mixing energy consumption of 7.08 kNm. Hence, it is obvious that the compatibilization increases the mixing energy of the blends (Pechurai et al., 2008). In this study, chemical compatibilization using APS and MAEVA recorded slightly higher mixing energy values compared to physical compatibilizing using LR.

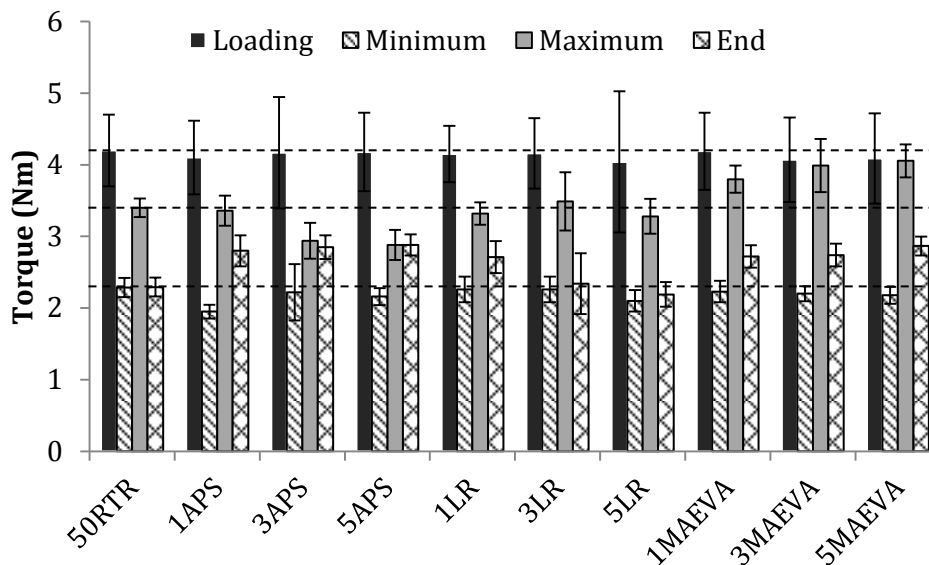


Figure 5.3 Mixing torque values of APS, LR and MAEVA compatibilized 50RTR blends

Table 5.1 Total mixing energy (kJNm) of 50RTR and compatibilized blends

Designation/loading	0 wt%	1 wt%	3 wt%	5 wt%
50RTR/APS		8.16 ± 0.45	8.23 ± 0.33	8.23 ± 0.34
50RTR/LR	7.72 ± 0.29	8.04 ± 0.40	7.94 ± 0.44	7.08 ± 0.40
50RTR/MAEVA		8.65 ± 0.40	8.59 ± 0.33	8.80 ± 0.27

5.3. Gel content

Figure 5.4 shows the influence of the types and loadings of compatibilizer, as well as irradiation on the gel content of 50RTR blend. All APS compatibilized blends showed an interesting result where the gel content before irradiation (0 kGy) recorded lower values compared to the control, 50RTR blend. There was a gradual reduction on gel content with increasing APS loading before irradiation. It was discussed in section 4.3 that the gel content observed before irradiation was a contribution from the partially devulcanized structure of RTR. An obvious reduction in the gel values of APS compatibilized blends suggests that APS plays major role in further devulcanizing or reclaiming the RTR. One of the oldest rubber reclaiming method, known as the pan and digester process, utilizes amines as reclaiming agent (Myhre et al., 2012). Amines function as reclaiming agent, where it cleaves the crosslinks in vulcanized rubber by nucleophilic

mechanism as they contain a lone pair of electrons (displaying strong nucleophile nature). A few types of amines have been successfully used as reclaiming agents for EPDM rubber (Dijkhuis, 2008, Dijkhuis et al., 2005, Sutanto et al., 2006). APS containing an aliphatic primary amine group might also act as an effective reclaiming agent for crosslinked tire rubbers. To evaluate the reclamation of RTR by APS, a mixture of RTR with 3 wt% APS (RTR/3APS) was prepared in internal mixer. As detailed in section 3.6, soluble fraction of RTR and RTR/3APS was subjected to gel permeation chromatography to obtain the information on molar mass distribution. Table 5.2 lists the weight average molecular weight (M_w), number average molecular weight (M_n) and polydispersity index (PDI) of the samples obtained through GPC analysis. Addition of APS to RTR clearly reduces the molecular weight of RTR. M_w , M_n and PDI decreased by 33%, 11% and 24.5% respectively. These observations confirm that APS do participate in the scission of three dimensional networks in RTR, similar to commercial reclaiming agents.

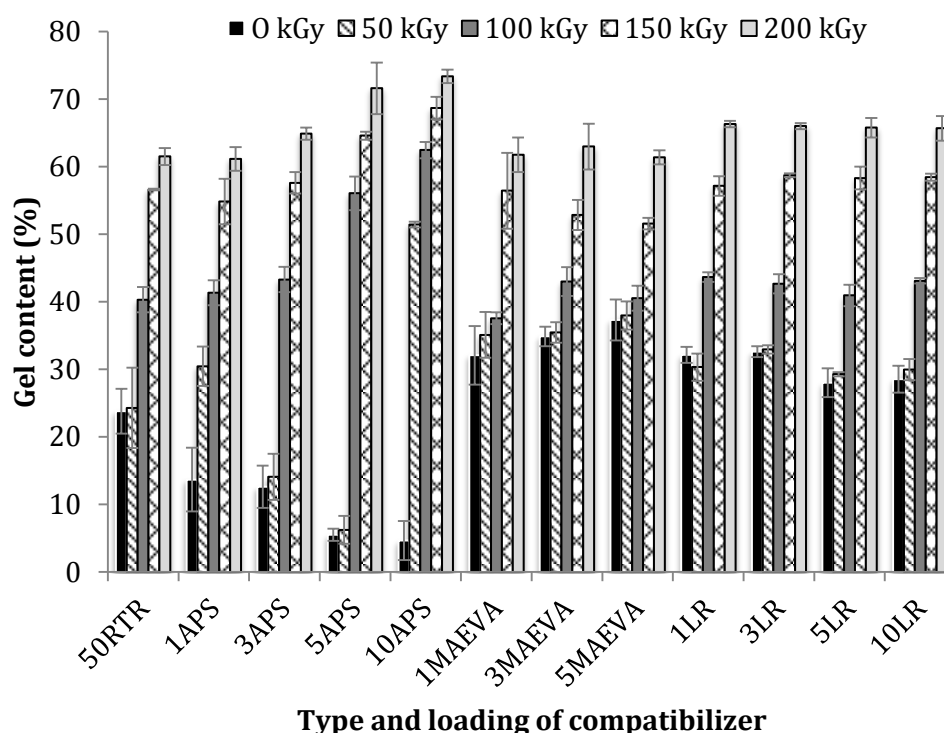


Figure 5.4 Gel content of 50RTR blend as a function of compatibilizer type, compatibilizer loading and irradiation dose

Table 5.2 Weight average molecular weight (M_w), number average molecular weight (M_n) and polydispersity index (PDI) of RTR and RTR with 3wt% APS (RTR/3APS)

	M_w	M_n	PDI
RTR	179,318	68,603	2.61
RTR/3APS	119,809	60,798	1.97

The efficiency of crosslinking in APS compatibilized blends was also improved with increasing irradiation dose. At the similar irradiation dose, the percentage of gel formation was higher in blends with higher loadings of APS. The delayed crosslinking yield up to 50 kGy was completely resolved with the use of 10wt% APS. These could be the result of interaction between the APS and tire additives or residual radical scavenging reclaiming agents, which then allows the blends to crosslink.

LR and MAEVA compatibilized blends showed slightly higher gel content before irradiation (0 kGy) compared to the control, 50RTR blend. This is due to the batch variation of the RTR used in this study. LR compatibilized blends, though had slightly higher gel content before irradiation, resulted in similar gel content yield to control blend from 100 up to 200 kGy irradiation dose. This clearly shows, LR acted as a physical compatibilizer and did not participate in the chemical crosslinking process of the blends. The gel content of MAEVA at 0 kGy was increasing with increasing MAEVA loadings. MAEVA acts as an intermediate between RTR and EVA by forming a chemical link with RTR and physically intermingling with EVA chains. This would allow some amount of MAEVA with chemical attachment to RTR to have remained insoluble in toluene, hence, increasing the gel content with increasing MAEVA loading. MAEVA compatibilized blends also showed a delayed crosslinking yield up to 100 kGy, one dose higher than the control. However, the yield of crosslinking remained similar to control at 150 and 200 kGy. The presence of MAEVA further decrease the interaction probability between close lying macroradicals, compared to control blend, resulting in the delayed crosslinking yield up to 100 kGy. The loadings of LR and MAEVA did not cause a significant effect on the gel content of the irradiated blend.

Charlesby-Pinner equation was used to determine the crosslinking and chain scission yield of the compatibilized blend. The ratio of chain scission to

crosslinking, p_0/q_0 values, were obtained and tabulated in Table 5.3. Addition of APS clearly decreases the p_0/q_0 values, suggesting crosslinking efficiency was improved by incorporation of APS. At 5 wt% APS loading, the p_0/q_0 value was reduced to half the control's (5ORTR) p_0/q_0 value. Such increase in irradiation induced crosslinking in the presence of APS is believed to be associated with the increase in free radicals which form crosslinks. This observation is ascribed as a consequence of an efficient devulcanization or reclaiming of RTR by the added APS, along with the ability of APS to react with the residual radical scavenging additives. The deactivation of irradiation induced free radical within the blends by the residual radical scavengers has been described in CHAPTER 4.

Table 5.3 Values of p_0/q_0 of compatibilized blends

Type of compatibilizer	Loading	p_0/q_0
Control	-	1.2669
APS	1	1.1574
	3	0.9411
	5	0.5478
	10	0.7853
LR	1	1.3768
	3	1.3978
	5	1.3093
	10	1.3139
MAEVA	1	1.4921
	3	1.5336
	5	1.6281

MAEVA showed the highest p_0/q_0 values among the three compatibilizers used, and the values kept increasing with the increasing MAEVA loading. This observation tends to suggest that the addition of MAEVA is further aggravating the crosslinking process in the blend and needs to be further studied. Addition of LR on the other hand, showed a small increase in the p_0/q_0 values. This might be due to the higher gel content of LR blends before irradiation. However, no distinct pattern was observed with the increase in LR loading, which again strengthens the physical compatibilizing function of LR.

5.4. Mechanical properties

5.4.1. Tensile properties

Figure 5.5 shows the stress-strain curve of compatibilized 50RTR blends before irradiation (0 kGy). All the compatibilized blends represent flexible and tough characteristic curve with elastic deformation occurring up to yield point and thereafter, irreversible plastic deformation occurs until it fractures. Addition of APS increases the strength of the blend at the cost of elongation at break. Whereas, the addition of LR showed a slight diminution in the blend strength, without affecting the elongation at break. MAEVA on the other hand did not show any difference to 50RTR blend, even with increasing MAEVA loadings. Information gathered from the stress vs strain curve of compatibilized blends before and after irradiation has been charted in for better understanding.

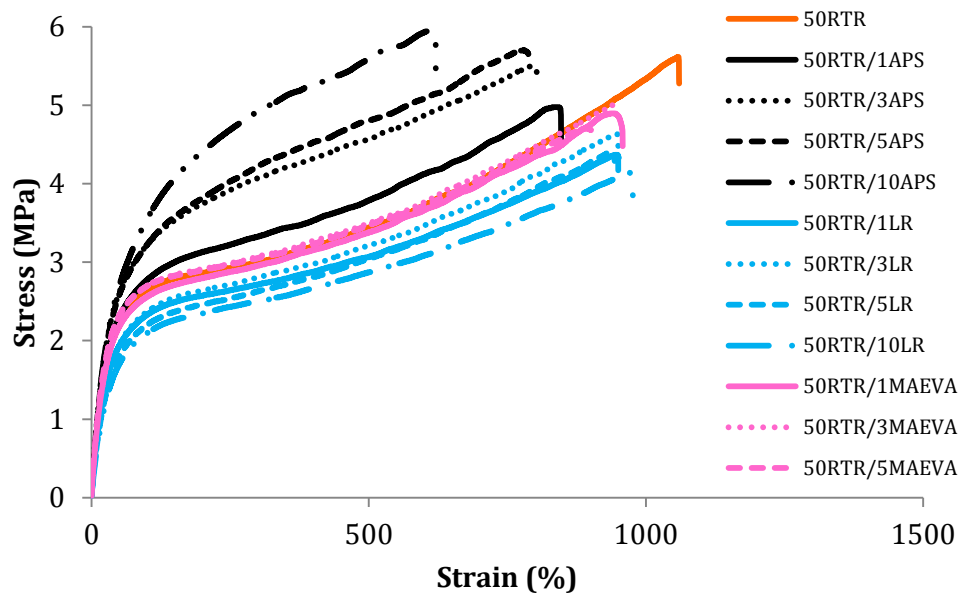


Figure 5.5 Stress vs strain plot of 50RTR and compatibilized blends at different loading before irradiation

Figure 5.6 shows the influence of types and loading of compatibilizer, as well as irradiation dose on tensile properties of compatibilized 50RTR blends. Prior to irradiation, tensile strength of APS compatibilized blends increased by 15.26% at 10wt% APS as compared to the control blend. It was interesting to note that the improvement in tensile strength of samples before irradiation, although the gel content was found to decrease in APS compatibilized blends. Such

observation reflects that the effective improvement in tensile strength of the blend with the incorporation of APS is due to effective interphase formation between EVA and RTR components (Pichaiyut et al., 2008). Good interphase ensures efficient stress transfer between components, hence allowing for the material to withstand higher amount of stress before failure. Furthermore, use of APS has enabled the rubber particles to be dispersed in smaller size in the blend. This increases the effective surface area of interaction between RTR and EVA as evident from SEM micrographs of tensile fractured surfaces (these changes has been clearly elaborated in section 5.6). Increased surface area of interaction along with good interphase formation, increases stress transfer feasibility between the components, resulting in improved tensile strength.

Effect of irradiation on tensile strength of APS compatibilized blends can be deduced from Figure 5.6a and Table 5.4. Improvement was noted in the tensile strength of APS compatibilized blends at all four different loadings, with increase in irradiation dose. However, Table 5.4 shows the efficiency of irradiation induced improvement in tensile strength of APS compatibilized blends decreases with increasing APS loading. This trend of result is related to effectiveness of APS as reclaiming agent of RTR that leads to a substantial increase in tensile strength before irradiation. Also it is noteworthy that the yield of gel content upon irradiation was improved with increasing APS loading, suggesting formation of more irradiation induced crosslinks in blends with higher loading of APS. Moreover, increasing crosslinks, increase the stiffness of the blends, hence, a reduction in the efficiency of irradiation induced improvement in tensile strength with increasing APS loading.

At 0 kGy, LR compatibilized blends recorded lower tensile strength values compared to control blend. The lower values are attributed to the presence of LR which is a low molecular weight substance. A small decrease in tensile strength was also noticed with increasing LR loadings. Similar observation was also reported on liquid natural rubber compatibilized NR/LLDPE blends and NR/HDPE blends (Dahlan et al., 2002a, Nakason et al., 2006). Dispersion of LR into EVA chains might indeed decrease the crystallinity of the EVA phase resulting in the decreasing trend of tensile strength with increasing LR loading. Table 5.4 shows the improvement in tensile strength with increasing irradiation dose was not influenced by LR loading. This again strengthens the role of LR as physical compatibilizer, whereby, LR does not affect the irradiation induced

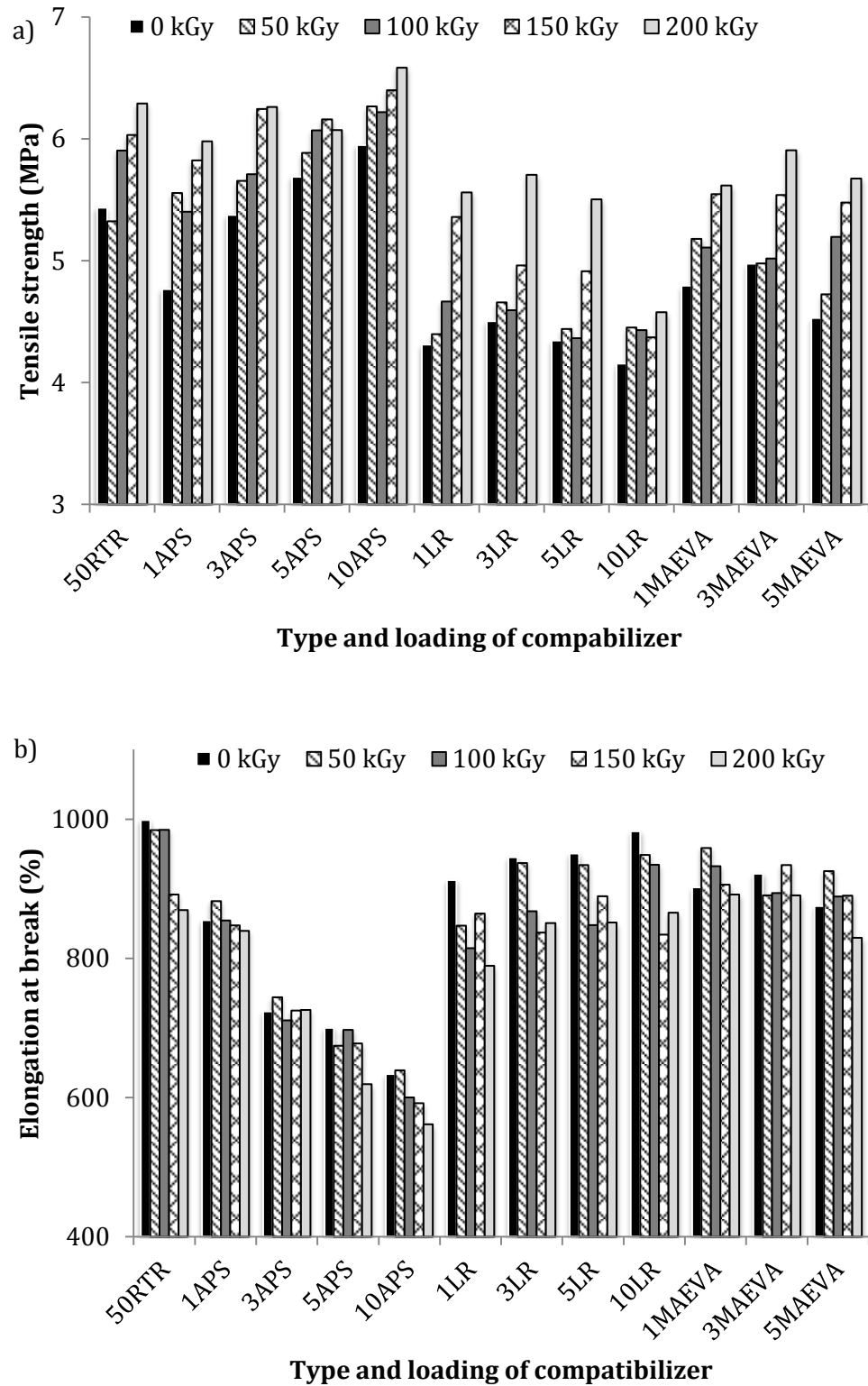


Figure 5.6 Representation of a) tensile strength, b) elongation at break and c) modulus 100 of compatibilized blends before and after irradiation

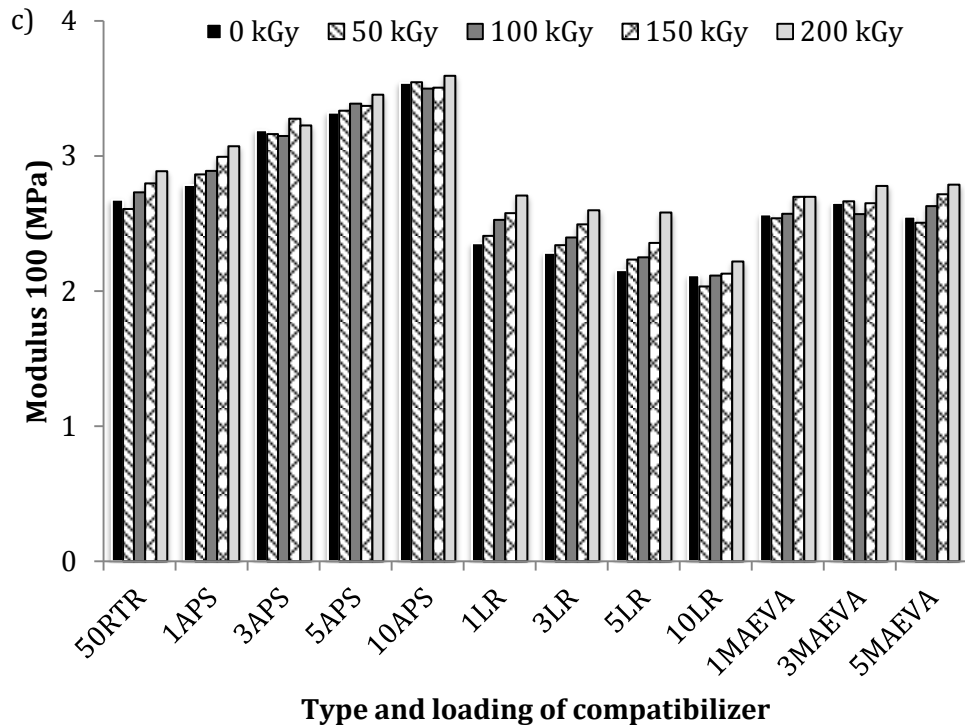


Figure 5.6 Representation of a) tensile strength, b) elongation at break and c) modulus 100 of compatibilized blends before and after irradiation

crosslinking process of the blends. However, the percentage of improvement in tensile strength with irradiation in the presence of LR was higher than 50RTR. Such observation is attributed to the self-crosslinking ability of LR upon exposure to irradiation.

Tensile strength of MAEVA compatibilized blends before irradiation, showed lower values compared to 50RTR. Though the lower tensile strength reading before irradiation could have been a factor of batch difference of the RTR used, it is apparent there was no significance of MAEVA loading, nevertheless, the presence of MAEVA on tensile strength properties. Therefore, it can be concluded that in this study, MAEVA did not play the compatibilizing agent role (Pichaiyut et al., 2008). This could be due to such small amount of MAEVA used. Apparently most of the successful studies utilized more than 10 wt% compatibilizer or the complete (100%) matrix out of maleic anhydride grafted polymer for improvement in tensile properties of GTR or RTR containing polyolefin (Lee et al., 2007, Lee et al., 2009, Punarak et al., 2006). In agreement

with gel content observation, tensile strength of MAEVA compatibilized blends displayed delayed effect up to 100 kGy irradiation dose, and increased only beyond it. However, no distinct improvement was noticed in tensile strength of irradiated blends with increasing MAEVA loading (Table 5.4). These observations are in line with the conclusion made in gel content analysis detailed in section 5.3.

Table 5.4 Percentage of changes in tensile properties of blends at 200 kGy irradiation compared to non-irradiated blends

Compatibilizer loading (wt%)	50RTR (control)	APS	MAEVA	LR
Changes in tensile strength (%)				
1	15.69	25.40	17.14	26.50
3		18.69	18.73	26.64
5		6.71	25.3	26.65
10		5.06	-	12.85
Changes in elongation at break (%)				
1	12.96	1.83	1.14	13.47
3		0.30	3.36	9.97
5		11.58	5.21	10.46
10		11.38	-	11.89

Figure 5.6b shows the changes in elongation at break of blends with different type and loading of compatibilizer and irradiation dose. Elongation at break of 10 wt% APS compatibilized blends dropped by 42% compared to 50RTR before irradiation. Systematic drop in the elongation at break values with increasing APS was noted for samples before irradiation. Improved interphase adhesion would lead to increased resistance of matrix to flow resulting in a drop of elongation at break. However, the drop noticed with the addition of APS was very prominent. The discussion in section 4.4 clearly indicated the elongation at break of RTR/EVA blends were mainly the contribution of EVA matrix. Therefore, it is appropriate to infer that the properties of EVA matrix have been changed due to interaction between the vinyl acetate group of EVA and amine group of APS. In order to confirm this assumption, EVA was prepared with 3 wt% APS and subjected to tensile testing. The elongation at break of EVA/3APS showed a value of 1195.36%, a distinct 39% drop compared to pure EVA. This deduces the chemical interaction between EVA and APS changes the microstructure of EVA, hence, resulting in deterioration of elongation at break. However, the drop in elongation at break of 50RTR/3APS blend was only

27.54%, about one third lesser than EVA/3APS. This is because in the blends, APS is consumed as the reclaiming agent in RTR, leaving relatively lesser APS to react with EVA as compared to 100% EVA matrix. Generally, elongation at break show a decline with the increase of irradiation dose in APS compatibilized blends. Table 5.4 shows that at lower APS loading (1 and 3 wt%), no significant changes was observed in percentage of changes of elongation at break with increasing irradiation dose. At higher APS loading (5 and 10 wt%), the drop in percentage of changes of elongation at break was about 11 to 12%. Higher gel content yield with increasing irradiation dose was observed at higher APS loading, suggesting the presence of more irradiation induced crosslinks in the blends. The significant difference is seen between gel content before and after irradiation at higher APS loading, leading to a larger difference in the elongation at break of blends with higher APS loading. These observations attributed to the efficiency of APS in improving crosslinking over chain-scission as shown by p_0/q_0 values obtained using Charlesby Pinner equation.

LR on the other hand, showed increase in elongation at break of non-irradiated blend with increasing LR loading. LR is a low molecular weight rubber, which presents itself in the interphase area of RTR/EVA blend, reducing the interfacial tension and improving RTR dispersion, thereby allowing the matrix to elongate a little further before rupture (Moly et al., 2006). Furthermore, LR could also act as plasticizer within EVA matrix, increasing the plasticity of the matrix and improving the elongation at break. Increasing the irradiation dose, decreases the elongation at break of LR compatibilized blends. Formation of crosslinks induced by irradiation increases the stiffness of the blends resulting in a decrease of elongation at break. However, Table 5.4 shows the loading of LR did not influence the changes in the elongation at break of the blends with increasing LR loading. This is, again, due to the physical compatibilizing role played by LR which does not change the chemistry behind the crosslinking process.

All MAEVA compatibilized blends showed elongation at break values lower than 50RTR before and after irradiation. Lower elongation at break values of non-irradiated MAEVA and LR compatibilized blends compared to 50RTR are due to the presence of low molecular weight compatibilizer in the blends. As discussed previously, MAEVA retards the crosslinking process in the blends, leading to only a small amount of crosslinks being formed with irradiation. Hence,

negligible changes in elongation at break (Table 5.4) were noted upon irradiation of the blends in the presence of MAEVA.

Figure 5.6c shows the influence of irradiation and compatibilizers on modulus at 100% elongation of 50RTR blends. Modulus increased by 147% with 10 wt% APS loading compared to control blend. Gel content findings in section 5.3 showed APS functions as reclaiming agent, breaking down the crosslinks in RTR, which should decrease the modulus value of the blend as the rubber is softer now. However, an opposite trend is observed due to the dominance of microstructural modification of EVA by interaction with APS, leading to increased modulus of the matrix. This effect is more prominent with increasing APS loading. Moreover, increasing the irradiation dose results in an increase of modulus values of APS compatibilized blends, which is an attribute of increased stiffness as a result of irradiation induced crosslinking.

On the other hand, LR showed decreasing modulus values with increasing LR loading. LR is a low modulus substance which acts as plasticizer as well as compatibilizer, hence, a drop in the modulus values was observed. Irradiation increases the modulus values of the LR compatibilized blends at all studied loading, as a result of irradiation induced crosslinking. Addition of MAEVA to 50RTR blend did not change the modulus values, even with increasing MAEVA loading or irradiation dose. This further supports the observation on the inefficiency of MAEVA to act as a compatibilizing agent between RTR and EVA at 1 to 5 wt% loading.

5.4.2. Tear and hardness

Figure 5.7a shows the influence of compatibilizers and irradiation on the tear strength of 50RTR blends. This study uses Type C tear test specimens which measures rupture, or tear initiation strength at stress concentration area. Tear strength of APS compatibilized blends improved up to 5 wt% APS loading and stabilized thereon. Non-irradiated 50RTR/5APS blends showed an improvement of 19.54% in tear strength compared to control blend. Improved reclamation of RTR particles coupled with enhanced interfacial adhesion could account for such observation. Stabilization of tear strength beyond 5 wt% APS loading suggests that the compatibility of 50RTR blends at 5 wt% APS is sufficient to reach maximum tear strength.

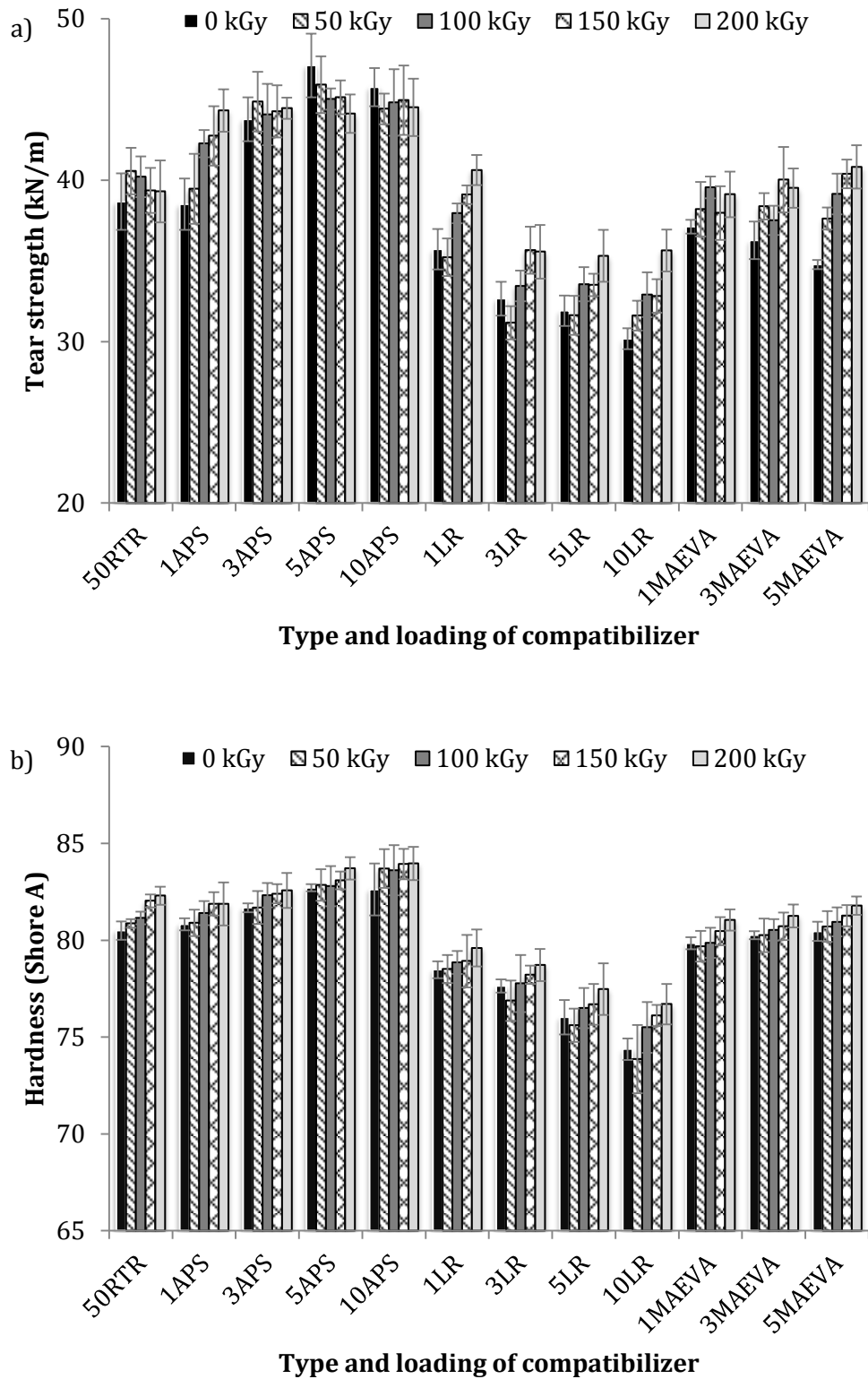


Figure 5.7 Influence of irradiation dose, compatibilizer type and loading on a)tear strength and b) hardness of compatibilized 50RTR blends

Han and Han (2002) in their work described an increase in tear energy of filled system is contribution of increased intrinsic strength due to enhanced energy dissipation and/or deviation of tear path. The initiation and propagation of cracks through the bulk is efficiently arrested or deflected by the improved dispersion of smaller RTR particles. This also explains the increase in the tear strength of the APS compatibilized blends. At 5 wt% APS loading, the dispersion of RTR might have been the optimum resulting in stabilized tear strength thereon. Irradiation on the other hand only improves the tear strength of 1 wt% APS blends but did not show a significant difference at higher APS loading. LR on the other hand showed slight diminution of tear strength with increasing LR loading due to the presence of LR, which is soft and acts as a plasticizer for EVA matrix. However, gradual increase in tear strength with increasing irradiation dose was observed due to radiation induced crosslinks which enhances the intrinsic strength of the blends. Similar to tensile properties, tear strength of MAEVA compatibilized blends before irradiation remained the same with increasing MAEVA loading due to the inability of MAEVA to perform as compatibilizer. Whereas, changes in tear strength with increasing irradiation dose was similar to the trend observed with LR compatibilized blends.

Figure 5.7b illustrates the influence of irradiation dose and compatibilizers on the hardness of 50RTR blend. Hardness of APS compatibilized blends increased up to 5 wt% loading, upon which saturation was observed for non-irradiated blends. This could be due to changes in the microstructure of EVA due to interaction with APS, hence, increasing the hardness of the blends. Irradiation improved the hardness of all the APS compatibilized blends by a meagre 1 to 3%. MAEVA compatibilized blends showed similar trend to the one observed with modulus, where the hardness values of the non-irradiated blends were lower than 50RTR and improved with increasing irradiation dose. LR also showed similar trend as per modulus.

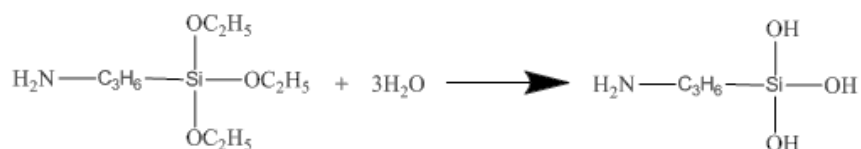
5.5. Compatibilization mechanism

As explained earlier, APS, MAEVA and LR were used for reactive, non-reactive and combination compatibilization mechanism, respectively. Each had a different compatibilization mechanism, rendering variation in the mechanical properties. The compatibilization mechanism has been detailed in this section.

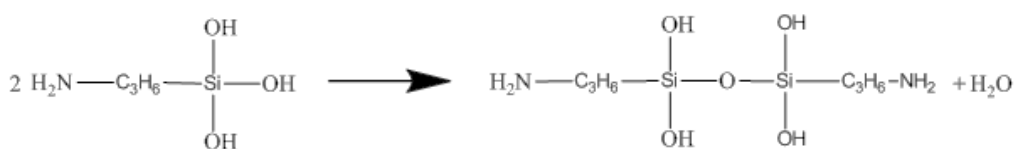
5.5.1. APS

APS is a type of silane coupling agent. Silane coupling agents are frequently used as compatibilizers in natural fiber, glass fiber and mineral filler containing polymer system. Silane coupling agents are generally present in $R_{(4-n)}\text{—Si—(R'X)}_n$ ($n=1,2$), where R represents the alkoxy group, X represents the organofunctionality and R' is the alkyl bridge or spacer connecting the organofunctionality to the silane atom (Xie et al., 2010). In this study, the APS used contains three ethoxy groups and a primary amine as the organofunctional group with a propyl spacer connected to the silane atom. Scheme 5.1 shows the hydrolysis process which readily happens when APS reacts with moisture present in the system and atmosphere. In this process, ethoxysilanes are hydrolysed into silanols which are more reactive groups (Zhang et al., 2014). Once silanols are formed, self-condensation of silanols takes place, forming polysiloxane network structure (Xie et al., 2010, Aviles et al., 2011).

a) Hydrolysis



b) Self-condensation

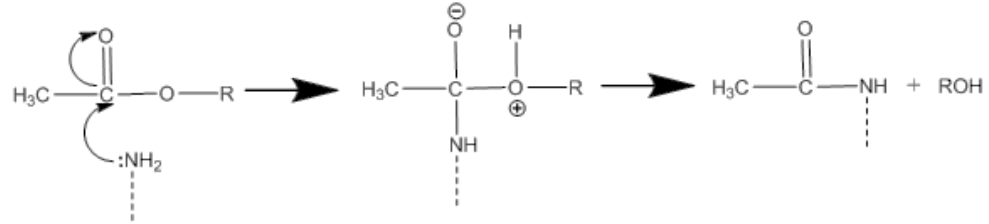


Scheme 5.1 Hydrolysis and self-condensation reaction in APS

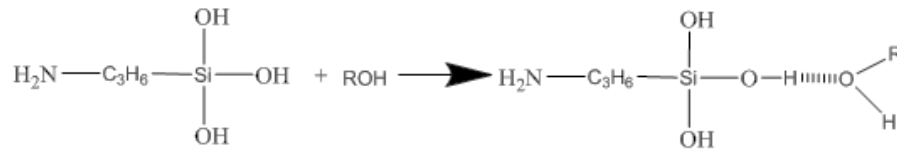
It is preferred to reclaim crosslinked rubber by the combination of mechanical shearing and chemical aid as it produces rubber with better properties compared to rubber reclaimed by mechanical shearing alone. Chemical aided reclaiming by scavenging the radicals formed during mechanical shearing using chemicals such as disulphides, thiols and phenols is the most studied and common method for reclaiming vulcanized natural rubber (Adhikari et al., 2000, Myhre et al., 2012). Whereas, reclaiming by nucleophilic mechanism using amines are more common in EPDM rubber (Dijkhuis, 2008, Dijkhuis et al., 2005).

in this study was 120 °C which could have easily facilitated the proposed reaction. This reaction produces EVA macromolecules with some –OH groups within its backbone, which could further react with silanol groups of hydrolysed APS and silanol groups of condensed APS (polysiloxanes). These reactions are shown in Scheme 5.3 b and c as adsorption and chemical grafting of APTES and altered EVA.

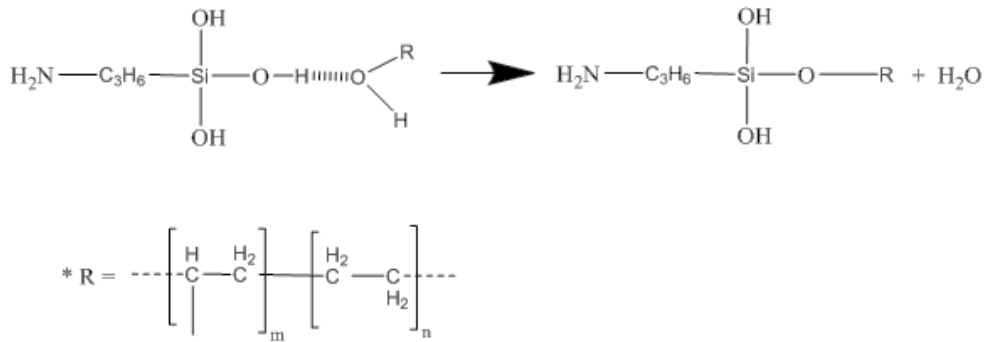
a) Interaction between carboxylate ester and amine



b) Adsorption



c) Chemical grafting



Scheme 5.3 Interaction between APS and EVA

Strong interfacial adhesion can be achieved between EVA and RTR with the aid of reactive compatibilization by APS (Colom et al., 2006). A combination of APS reaction with RTR (Scheme 5.2(b)) and EVA (Scheme 5.3(b) and (c)) can possibly covalently attach RTR and EVA forming a strong interphase. The formation of good interphase is believed to be one of the reasons behind

improved mechanical properties of APTES compatibilized blends before irradiation (Colom et al., 2006).

FTIR analysis was conducted on EVA and EVA/3APS films as described in section 3.17 and the spectra's are represented in Figure 5.8. Relating to Scheme 5.3a, the absorption peak associated to bending of $-\text{CH}_3$ group (Figure 5.8) was only present in EVA spectra and not in EVA/3APS spectra. This confirms the reduction of carboxylate ester group of EVA in the presence of APS. Whereas, increase in the absorbance of EVA/3APS spectra compared to EVA spectra as shown in Figure 5.8b, c and d indicates the presence of Silane and primary amine group on EVA structure. These findings relate to the proposed adsorption and chemical grafting interactions shown in Scheme 5.3b and d.

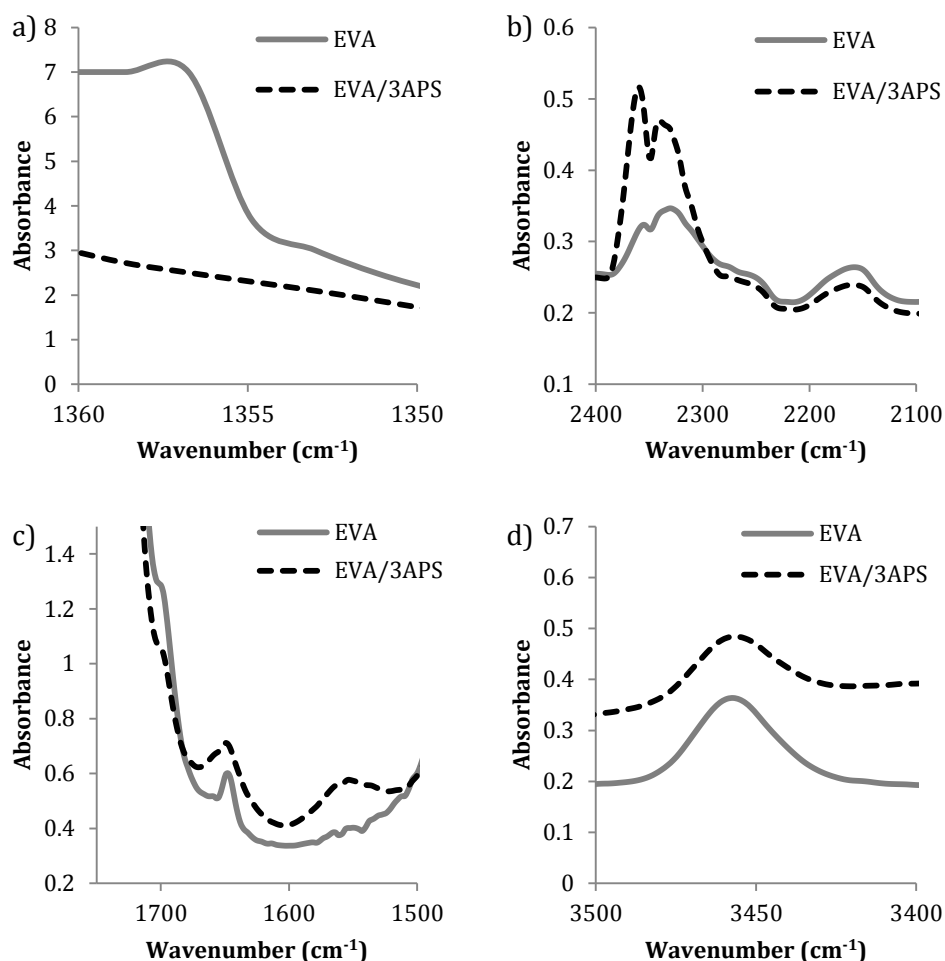


Figure 5.8 FTIR representation of EVA and EVA/3APS indicating a) bending of $-\text{CH}_3$ group (1350 – 1360 cm^{-1}), b) Silane group (2100 – 2360 cm^{-1}), c) bending of primary amine group (1550 – 1650 cm^{-1}) and d) stretching of primary amine (3400 – 3500 cm^{-1})

5.5.2. Liquid rubber (LR)

Liquid rubber such as liquid natural rubber has been successfully used as a compatibilizer in thermoplastic elastomer blends (Dahlan et al., 2002a, Shashidhara and Pradeepa, 2014). Also, studies utilizing GTR in thermoplastic elastomer observed the encapsulation of GTR by the rubber component and observed good mechanical properties (Naskar et al., 2001, Cañavate et al., 2011, Abou Zeid et al., 2008, Li et al., 2003b). In this study, low molecular weight liquid styrene butadiene rubber (LR) was used instead of a high molecular weight rubber, to improve the adhesion between RTR and EVA. Figure 5.9 shows the schematic representation of RTR/EVA blend compatibilization by LR. RTR phase is encapsulated by LR, efficiently decreasing the interfacial tension. This improves the dispersion of RTR in EVA matrix. Similar observation was also reported in GTR/LDPE blends compatibilized by elastomers (Formela et al., 2015). Furthermore, the free chains of LR can co-mingle with both free devulcanized chains of RTR and EVA matrix, improving the interfacial adhesion. Upon irradiation, both EVA and RTR can be adhered together through formation of crosslinks between these co-mingling chains (Dahlan et al., 2002b, Noriman et al., 2012).

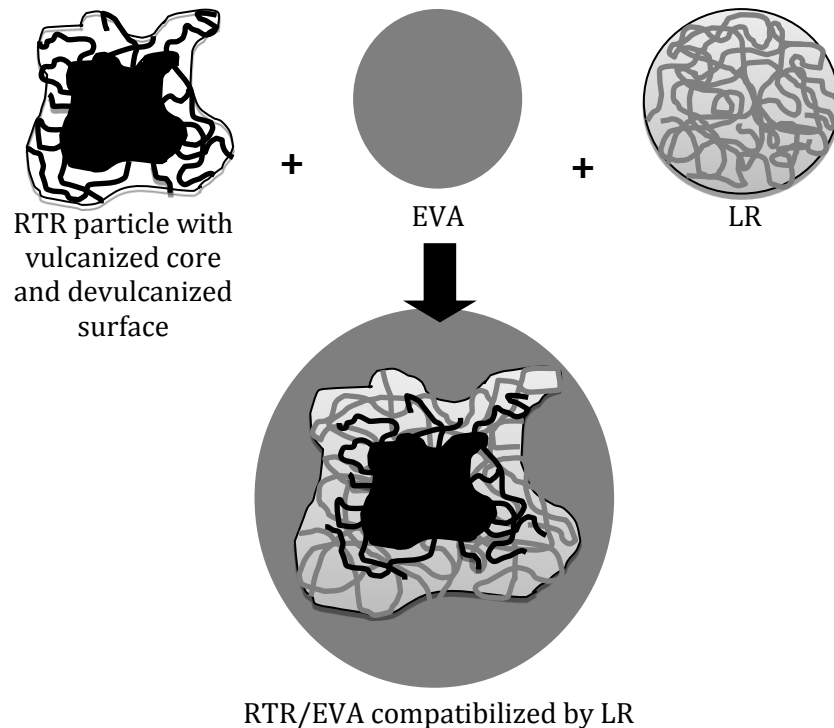


Figure 5.9 Schematic representation of RTR/EVA blend compatibilization by LR

5.5.3. Maleic anhydride grafted EVA (MAEVA)

Maleic anhydride grafted polymers have been heavily used in compatibilization of polymeric blends and composites (Xanthos and Dagli, 1991, Al-Malaika, 2012). The maleic anhydride (MA) group is often responsible in reactive interaction with specific component of polymer blend or composite (Ramesh et al., 2014, Rajan et al., 2014, Wu et al., 1993). The MA group has potential to reactively interact with hydroxyl groups forming a covalent bond. Carbonyl oxygen in MA group could also form intermolecular dipole-dipole interaction with hydrogen in the hydroxyl group (Kim et al., 2001, Formela et al., 2015). Presence of hydroxyl group on RTR was confirmed by FTIR analysis as shown in Figure 5.10. The interactions between MAEVA and RTR are shown in Scheme 5.4. Whereas, the polymer section of an MA grafted polymer will be able to physically wet into the polymer matrix (Chang et al., 2006). As for this study, MA group of MAEVA could interact with hydroxyl groups available on the RTR and carbon black surfaces, while the EVA group of MAEVA physically wets into the EVA matrix. This should improve the compatibility and interfacial adhesion between RTR and EVA components of the blends.

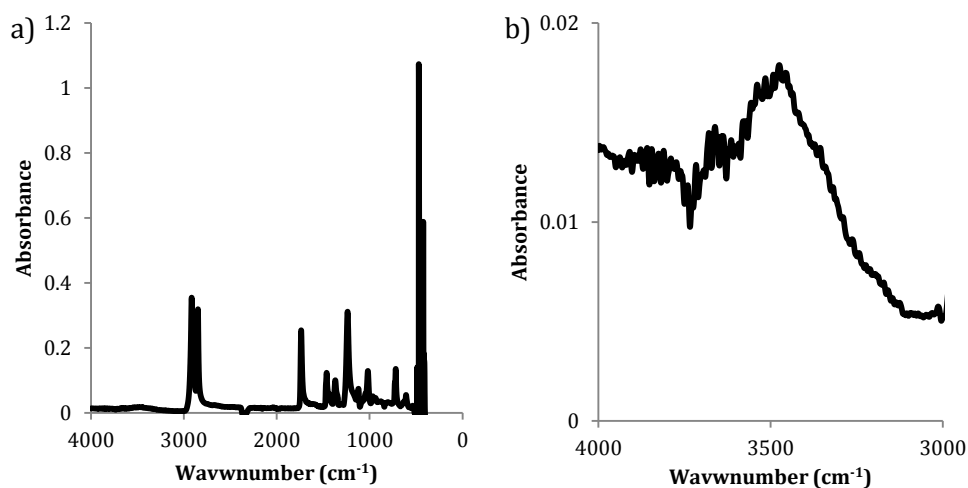
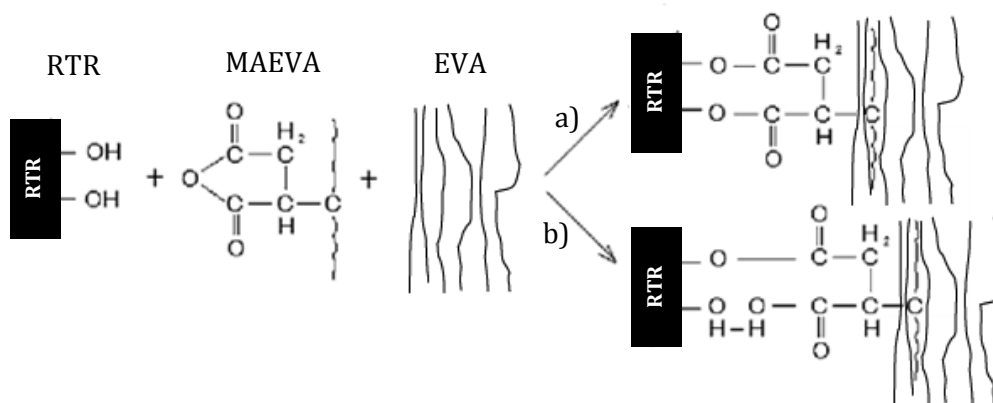


Figure 5.10 FTIR spectra representation of RTR, a) full spectrum and b) enlargement of wavenumber 3000 to 4000 cm⁻¹ which shows a broad peak indicating stretching of —OH group



Scheme 5.4 Interaction between MAEVA and RTR through a) covalent bond, b) intermolecular dipole-dipole interaction, as well as representation of EVA chain of MAEVA wetting into EVA matrix

5.6. Morphological study

5.6.1. SEM

Figure 5.11a, c and e show the overview of tensile fractured surfaces of APS, LR and MAEVA compatibilized blends at 1000x magnification, respectively. Figure 5.11b, d and f show the focus on the RTR particle to observe the interfacial properties of the compatibilized blends.

APS compatibilized blends showed a good dispersion of RTR particle in EVA matrix. RTR particles were also found to be smaller in APS (Figure 5.11a) compatibilized blend than LR (Figure 5.11c) and MAEVA (Figure 5.11e) compatibilized blends. The arrows in lower magnification SEM micrographs indicate the rubber particles. The function of APS to further reclaim the RTR is evident from the dispersion of the smaller rubber particle. Reclaiming of RTR by APS makes the rubber softer hence easier breakdown into smaller particle with applied stress during compounding and compression molding. This leads to smaller RTR particle being well dispersed in EVA matrix. At higher magnification, fully embedded RTR particle with fibrils interlocking EVA and RTR together was observed. It is obvious that the stress was also supported by the rubber particles as evident from the fractured rubber particle in Figure 5.11b. This confirms the effective formation of interphase in APS compatibilized blend allowing for improvement in tensile properties before irradiation (Wang et al., 2012). Another salient point to note is the appearance of EVA matrix in APS compatibilized blend was found to be different from control (Figure 4.7a),

LR or MAEVA compatibilized blends. No signs of fibrillation were observed on the matrix surface. This supports the discussion in section 5.4 where the microstructure of EVA was inferred to be affected due to interaction with APS.

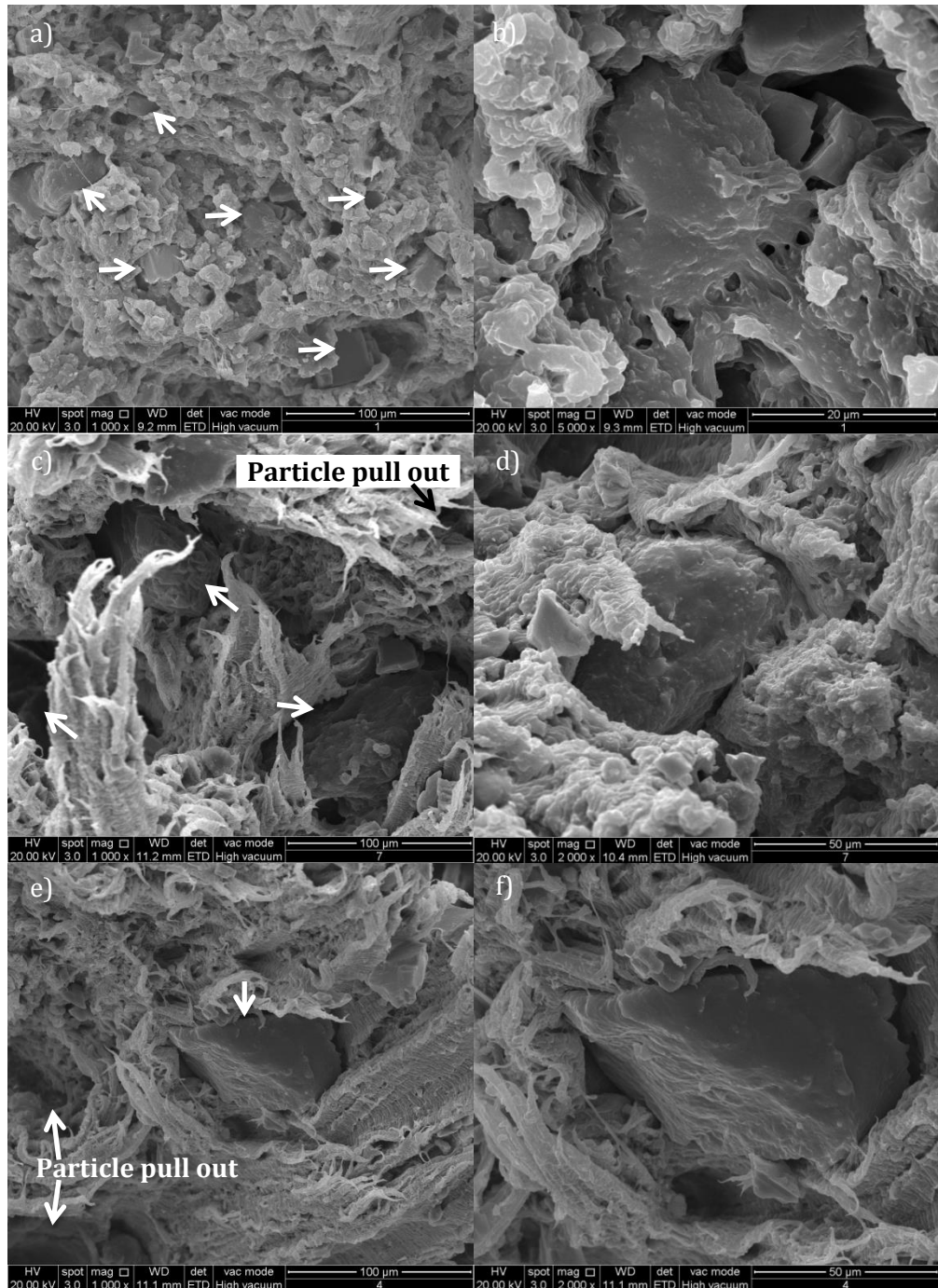


Figure 5.11 SEM micrographs of (a,b)3APS, (c,d)3LR, (e,f)3MAEVA compatibilized 50RTR blends before irradiation (0 kGy) showing overview at (a,c,e) 1000x magnification; as well as focused RTR particle at (d,f) 2000x and (b)5000x magnification

Overview of LR compatibilized blends can be seen in Figure 5.11c. RTR particles were found buried deep down in the EVA matrix with fibrils elongating around it. Very little particle pull out was observed in LR compatibilized blends. Figure 5.11d shows absence of voids around the rubber particle, which has a thin coating on it. However, no evidence of chemical interaction between RTR and EVA was observed. These observations support that LR functions as a physical compatibilizer by reducing the stress in the RTR, EVA interphase as discussed in sections 5.3 and 5.4.

The micrograph of MAEVA compatibilized blend indicating multiple particle pull out and matrix failure around the RTR particles can be observed in Figure 5.11e. Inefficiency of MAEVA as compatibilizer is depicted on Figure 5.11f, where voids were present around the rubber particle. In this blend, the continuous matrix EVA was solely responsible for the resulting mechanical properties. RTR acts as stress concentrating agents in the blend, leading to low elongation at break.

5.6.2. TEM

Figure 5.12 and Figure 5.13 show the TEM micrographs of APS and LR compatibilized 50RTR blends respectively. Similar to 50RTR blend (section 4.5), compatibilized blends also contained domains of RTR (darker grey shade) distributed in EVA matrix (lighter grey shade). RTR domain in APS compatibilized blends before irradiation measured between 0.3 to 1.0 μm , about 50% smaller than RTR domain sizes in non-irradiated 50RTR blend. This is again, in accordance to the previous discussion on the further reclaiming of RTR by APS which results in distribution of RTR in smaller domain sizes within EVA matrix. Lesser contrast between RTR domain and EVA matrix suggest good compatibility in APS compatibilized blends. Upon irradiation the domain sizes of RTR were further reduced to 0.1 to 0.5 μm . Notably, higher contrast between RTR domains and EVA matrix was observed after irradiation. These suggest distinct phase separation/heterogeneity in APS compatibilized blends upon irradiation, which could have been due to increased efficiency in crosslinks formation induced by irradiation in these samples.

The difference in the RTR domain of APS compatibilized samples, before and after irradiation, can be clearly drawn from Figure 5.12b and d respectively. Patches of different grey shades within RTR domain before irradiation indicates

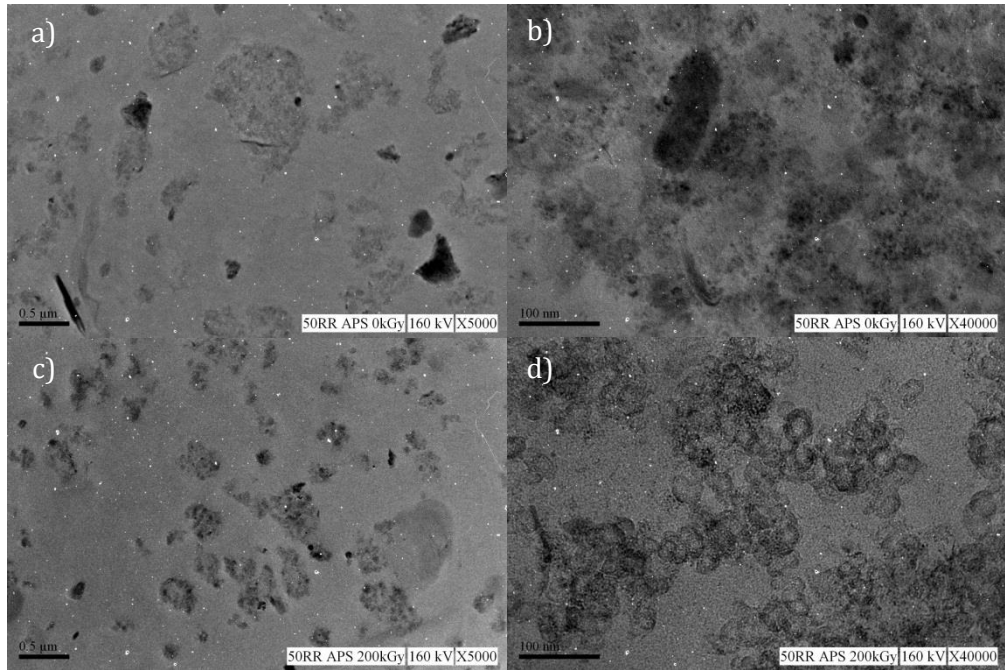


Figure 5.12 TEM micrographs of APS compatibilized blend before (a,b) and after 200 kGy irradiation (c,d) at 5000x (a,c) and 40000x (b,d) magnification

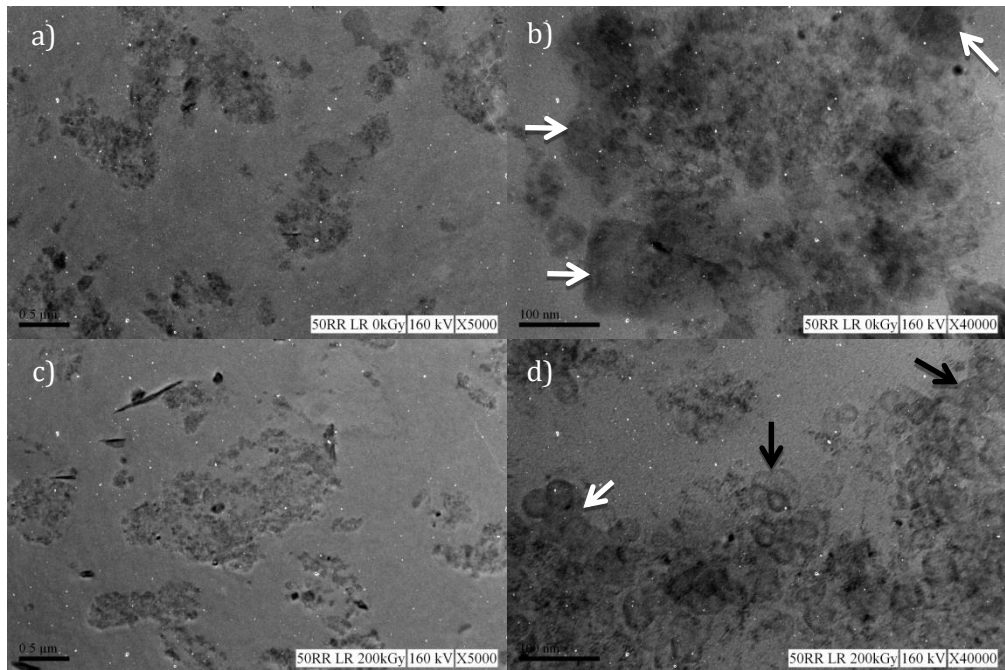


Figure 5.13 TEM micrographs of LR compatibilized blend before (a,b) and after 200 kGy irradiation (c,d) at 5000x (a,c) and 40000x (b,d) magnification

the partial devulcanized state of the rubber. The darker grey indicating crosslinked rubber whereas the lighter grey shades indicating amorphous/free rubber chains. Upon irradiation, the patches of different grey shades changes to

distinct, overlapping spherical shapes in different grey shades. This change was not observed in control, 50RTR blend. Hence, it is due to the efficient crosslink formation in APS compatibilized blends.

RTR domain in LR compatibilized blends measured around 0.4 to 1.8 μm before irradiation and reduced to around 0.1 to 1.1 μm after irradiation. Both the ranges of RTR domain in LR compatibilized blends are very similar to the control blend, 50RTR, which again indicates the physical compatibilizing properties of LR. The contrast in irradiated LR compatibilized blends was less compared to sample before irradiation, suggesting better compatibility in irradiated blends.

At higher magnification into RTR domain, similar observation to APS compatibilized blend was noted in LR compatibilized blends before and after irradiation. However, the overlapping spherical shapes in different grey shades of irradiated LR compatibilized blend were not as distinct as APS compatibilized blend. This could be due to lower efficiency in crosslink formation in LR compatibilized blends upon irradiation. Presence of LR partly encapsulating RTR surface could also be observed at higher magnification of TEM micrographs (indicated by arrows).

5.7. Thermal properties

5.7.1. TGA analysis

Figure 5.14 illustrates the thermal stability of 50RTR and compatibilized blends. The mass loss and derivative curves clearly indicate the thermal stability of 50RTR blend was not severely affected by compatibilization. Even in the case of APS compatibilized blends where EVA was believed to have structural changes due to interaction with APS, the thermal stability remained similar to the control blend (50RTR). Data from Figure 5.14 has been tabulated in Table 5.5. $T_{\text{max}1}$ and $T_{\text{max}2}$ of the all compatibilized blends was 357.5 $^{\circ}\text{C}$ and 474.2 $^{\circ}\text{C}$ which showed a reduction of 3 $^{\circ}\text{C}$ and 5 $^{\circ}\text{C}$ respectively, compared to 50RTR blend. As discussed earlier, this could be due to batch difference in the RTR used. Total mass loss in the first degradation step of the 50RTR and compatibilized blends was around 19% corresponding to degradation of vinyl acetate (from EVA) and NR (from RTR). However, the mass loss associated to second degradation step is 51.98%, 51.66%, 54.55% and 53.51% for 50RTR, 50RTR/5APS, 50RTR/5LR and 50RTR/5MAEVA blends respectively. Second degradation step is related to degradation of polyethylene chain (from EVA) and BR/SBR (from RTR).

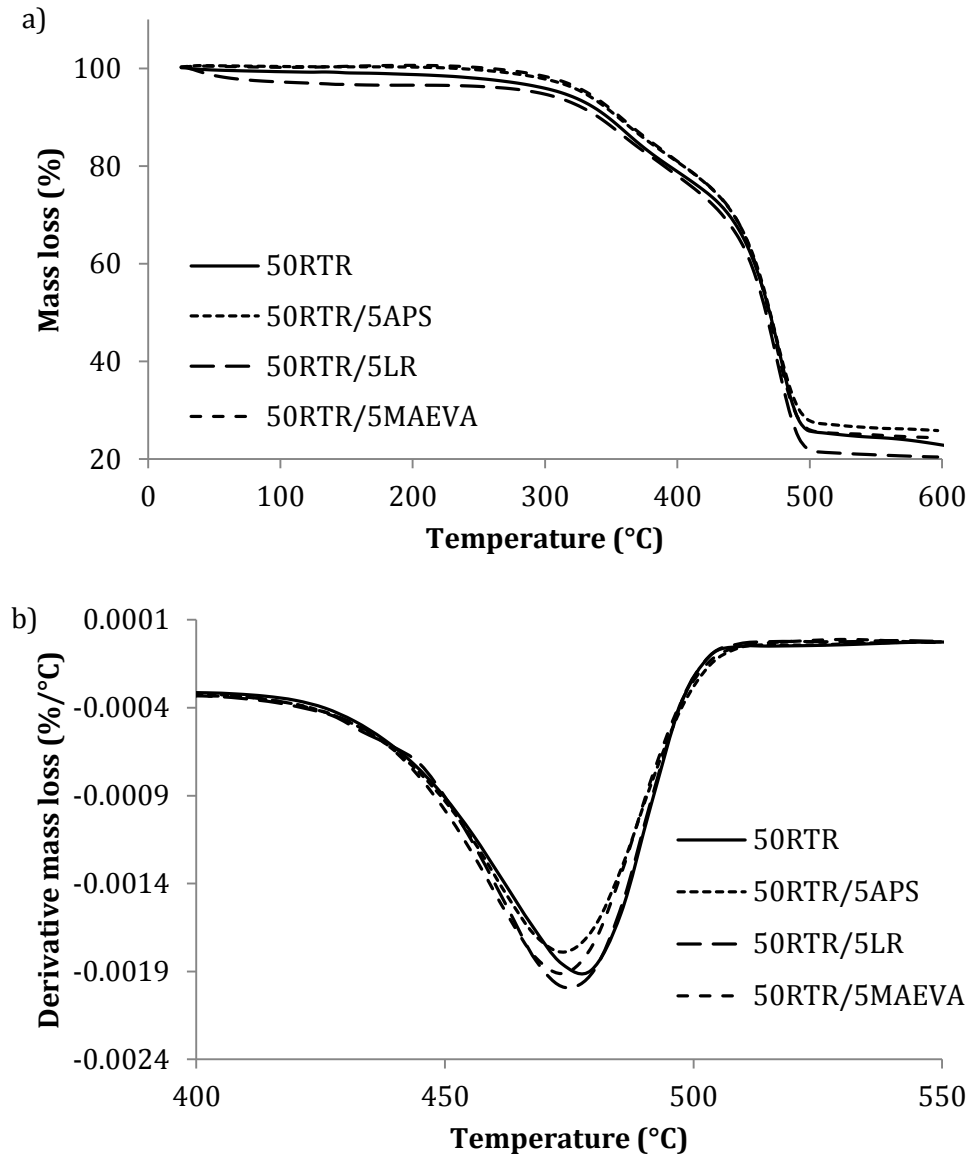


Figure 5.14 Typical TGA curves of 50RTR, 50RTR/5APS, 50RTR/5LR and 50RTR/5MAEVA samples, a) Mass loss curve, b) Derivative curve

Table 5.5 Degradation temperatures and residual weights of 50RTR and compatibilized blends before irradiation

Sample designation	Volatile content wt (%)	Degradation temperature (°C)						Residual wt (%)
		T _{5%}	T _{10%}	T _{25%}	T _{50%}	T _{max1}	T _{max2}	
50RTR	4.06	312.0	348.2	419.9	471.5	360.3	479.4	23.0
5APS	2.12	328.3	351.7	427.5	468.3	357.5	474.2	26.8
5LR	5.22	299.2	340.0	415.8	468.3	357.5	474.2	20.9
5MAEVA	1.59	328.3	351.7	427.5	468.3	357.5	474.2	25.0

Compared to control blend, APS and MAEVA compatibilized blends showed slightly better thermal stability up to 450 °C ($T_{5\%}$, $T_{10\%}$ and $T_{25\%}$); higher residual weight and 50% lesser volatile content. However, it is difficult to determine if the improved thermal stability was related to effectiveness of compatibilization or the influence of RTR batch difference. LR on the other hand, recorded lower thermal stability, residual weight and higher volatile content compared to control blend (refer to Table 5.5). This is obviously due to LR being a low molecular weight substance. Moreover, LR degrades early contributing to the volatile lost in the blend and lower residual weight in LR compatibilized blend.

Apparently, the lag in thermal stability becomes smaller with increasing temperature as LR degrades early on. In a compatibilized blend system, though chemical interaction or physical intermingling of chain happens at the interphase; the bulk of the polymers remain uninfluenced. Hence, individual polymeric systems tend to follow their own degradation route. This explains why the compatibilizers did not significantly improve the thermal stability of the blends (Jana and Nando, 2003).

Similar to 50RTR blend, the thermal stability of APS and MAEVA compatibilized blends remained unchanged upon irradiation. However, LR compatibilized blends (Figure 5.15) showed improved thermal stability due to irradiation induced crosslinks in LR which prevents early degradation. Thermal stability of irradiated LR compatibilized blends increased by about 4 °C up to first degradation step compared to non-irradiated 50RTR/LR blend. Residual weight also increased from 21% before irradiation to 23% after irradiation. $T_{\max 1}$ and $T_{\max 2}$ remained unchanged indicating the improvement in thermal stability was linked to only LR crosslinking.

5.7.1. DSC analysis

DSC thermograms of 50RTR and APS, LR and MAEVA compatibilized blends before irradiation are shown in Figure 5.16. It is obvious that the changes in crystallinity of the compatibilized blends only differed minutely compared to control, 50RTR blend. To aid the discussion, data from DSC thermograms of blends before and after irradiation have been charted in Figures 5.16a-d.

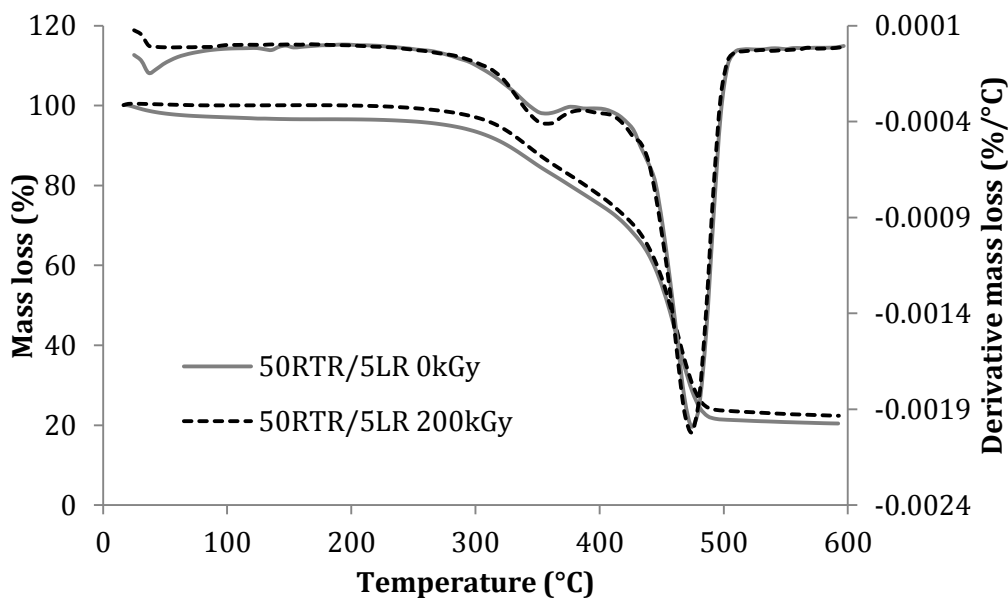


Figure 5.15 TGA curves of 50RTR/5LR blends before and after 200 kGy irradiation

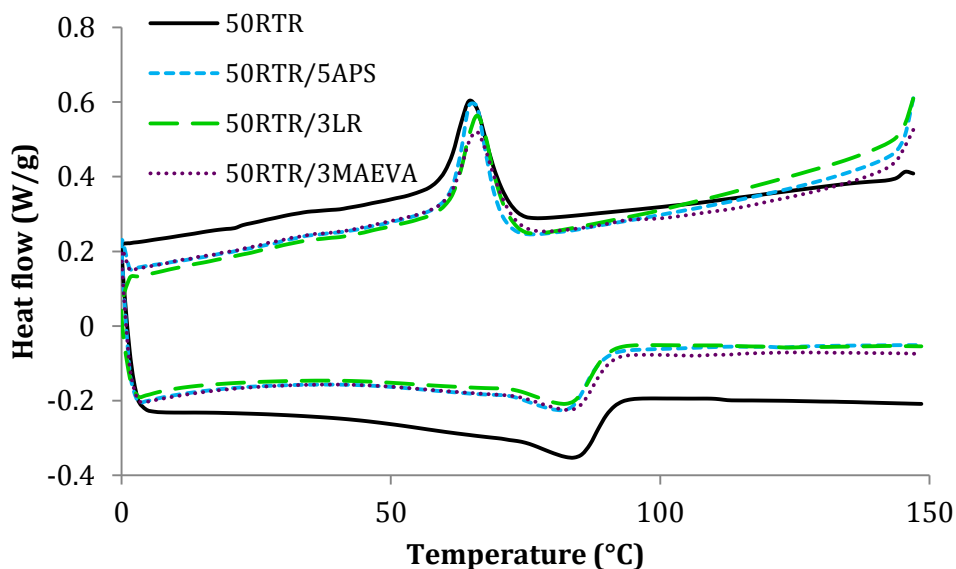


Figure 5.16 Heating and cooling DSC thermograms of 50RTR and compatibilized 50RTR blends before irradiation

Crystallization temperature of the blends before irradiation (0 kGy) increased with the addition of the compatibilizers (Figure 5.17a). 50RTR, APS, LR and MAEVA blends recorded crystallization temperatures of 65.0, 65.5, 66.3 and 66.0 °C respectively. The reduction in interfacial tension between RTR and EVA

believed to facilitate the nucleating capacity of RTR. Hence, this increases the nucleation effect rendered by RTR, leading to increased need for energy to form crystal (Tao and Mai, 2007). This translates to increased crystallization temperature in the compatibilized blends. Increasing the irradiation dose leads to decrease in the crystallization temperature of APS and LR compatibilized blends, similar to 50RTR blend. Irradiation induced crosslinks in the blends, decreases the net amount of EVA chains involved in chain rearrangement to form crystals, which leads to decrease in crystallization temperature with increasing irradiation dose. MAEVA compatibilized blends showed a stagnant effect in changes of crystallization temperature at 50 kGy irradiation, possibly due to aggravated crosslink efficiency as detailed in section 5.3.

All compatibilized blends recorded melting temperature lower than control, 50RTR blend (Figure 5.17b). Before irradiation (0 kGy) 50RTR, 50RTR/5APS, 50RTR/3LR and 50RTR/3MAEVA blends showed melting temperature of 84.2, 82.8, 83.3 and 84.0 °C respectively. Lower melting temperature of the compatibilized blends suggests lesser amount and/or imperfect crystals are formed as compared to 50RTR blend. This is an indication of good interfacial adhesion between EVA and RTR, which retards and prevents the formation of EVA crystals (Grigoryeva et al., 2004). Melting temperatures of all the compatibilized blends decreased with increasing irradiation dose. However, the magnitude of decrease in melting temperature at 200 kGy in APS (1.4%) and LR (1.6%) compatibilized blends was lower compared to 50RTR blend (3.0%). Compatibilization leads to lower amount and/or smaller crystals formed in the initial blend (0 kGy). However, in 50RTR blend, the feasibility of EVA chain movements was higher (due to lower crosslinking efficiency) leading to more crystal formation as compared to the compatibilized blends. The difference in blend's crosslinking efficiency causes less prominent changes in melting temperatures upon irradiation. In contrast, melting temperatures of MEAVA compatibilized blend decreased substantially with an increase in irradiation dose.

Figures 5.17 c and d show the influence of irradiation dose on the heat of fusion and crystallinity of the compatibilized blends, respectively. Interestingly, before irradiation, both APS and LR compatibilized blends had higher heat of fusion and crystallinity compared to 50RTR blend. Similar observation has been reported for compatibilized PP/NBR blends (George et al., 2000a) and PA6/SEBS blends

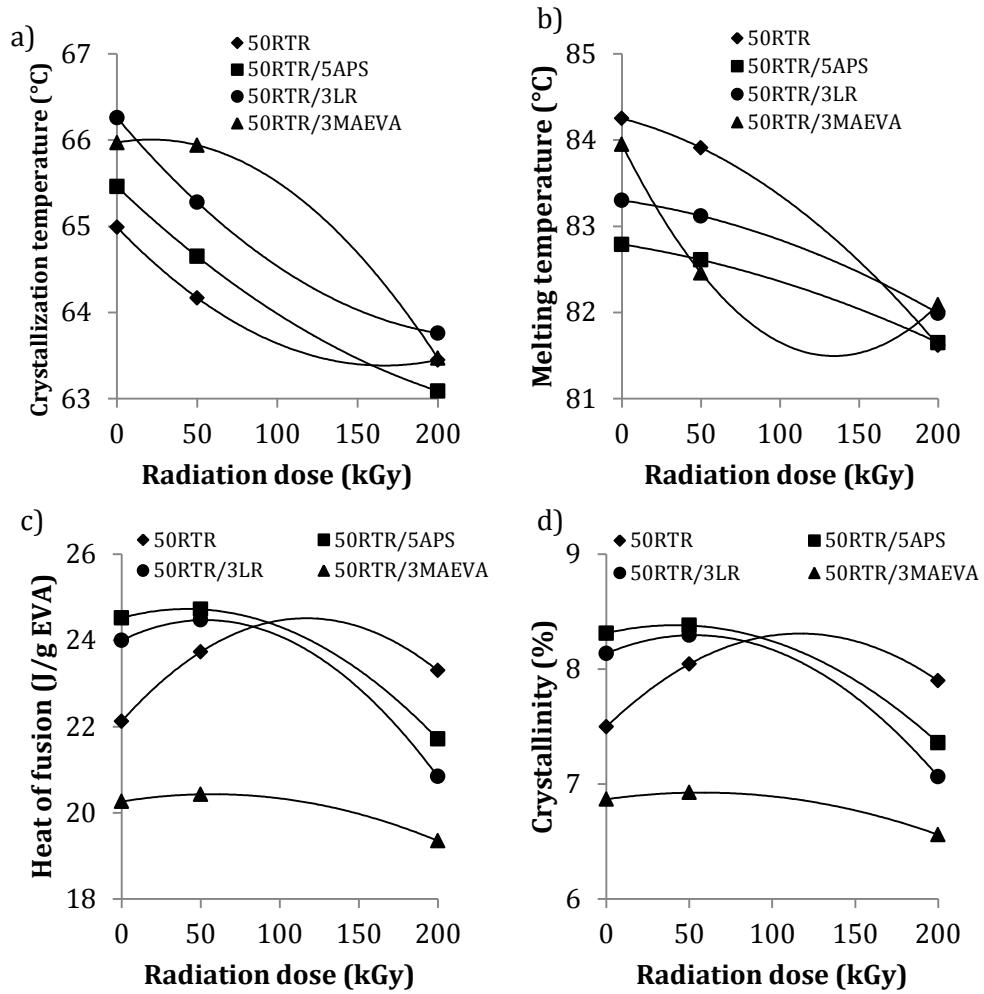


Figure 5.17 Effect of irradiation dose on a) crystallization temperature, b) melting temperature, c) heat of fusion and d) crystallinity of 50RTR and compatibilized 50RTR blends

(Wu et al., 1993). Increased crystallinity of APS compatibilized blends are in line with improvement in tensile and tear strength of the blend. Improved interfacial adhesion, increased nucleating capacity of the blends, resulting in higher heat of fusion and crystallinity of the blends (Tao and Mai, 2007). Microstructural changes in EVA could also be the reasoning for improved crystallinity of APS compatibilized blend. Whereas, in LR compatibilized blends, plasticization effect by LR improves chain rearrangement in EVA facilitating crystallization process (Hassan et al., 2015).

Increasing irradiation dose resulted in decrease in heat of fusion and crystallinity of the blends. This is contrary to 50RTR blends, which recorded higher heat of fusion and crystallinity with irradiated blends compared to non-

irradiated 50RTR blend. In 50RTR blend, redistribution of RTR and lower crosslinking efficiency results in increased flexibility for EVA chain rearrangements and recrystallization. Gel content analysis of compatibilized blends in section 5.3 confirmed increased efficiency of crosslinking in APS compatibilized blends. More crosslinks were formed in APS compatibilized blends compared to 50RTR blends upon irradiation. Hence, higher degree of decrease in crystallinity upon irradiation is due to lower degree of EVA chain rearrangement to form crystals in APS compatibilized blends. Whereas in LR compatibilized blends, though the crosslinking efficiency was similar to 50RTR blend, LR was effectively crosslinked as evident from thermogravimetry analysis. LR is believed to function as co-crosslinking agent between RTR and EVA which again limits EVA chain rearrangement and re-crystallization. This is evident from TEM micrograph in Figure 5.13 indicating improved compatibility in irradiated LR compatibilized blend upon irradiation. The maximum value of heat of fusion and crystallinity of 50RTR was achieved at 100 kGy. These values shifted lower to 50 kGy in APS and LR compatibilized blends due to improved crosslinking efficiency. MAEVA showed lower heat of fusion and crystallinity before and after irradiation as opposed to all the other blends.

5.8. Dynamic mechanical analysis

5.8.1. Storage modulus

Figures 5.18, 5.19 and 5.20 illustrate the storage modulus, loss modulus and tan delta profiles of 50RTR and compatibilized blends, before and after irradiation, respectively. All the blends, before and after irradiation clearly displayed glass, transition and rubbery characteristics in the storage modulus curve. Storage modulus was highest in the glassy region and rapidly decreases from transition region and displayed a plateau rubbery curve. Before irradiation, APS and MAEVA compatibilized blends showed slight improvement whereas LR compatibilized blend showed decrease in the storage modulus of glass and transition region compared to 50RTR blend.

Table 5.6 lists storage modulus values of the blends, before and after irradiation, at different temperatures. APS compatibilized blends, before and after irradiation, showed improved storage modulus values at low temperatures due to efficient interphase formation in the blend (Pichaiyut et al., 2008). Whereas,

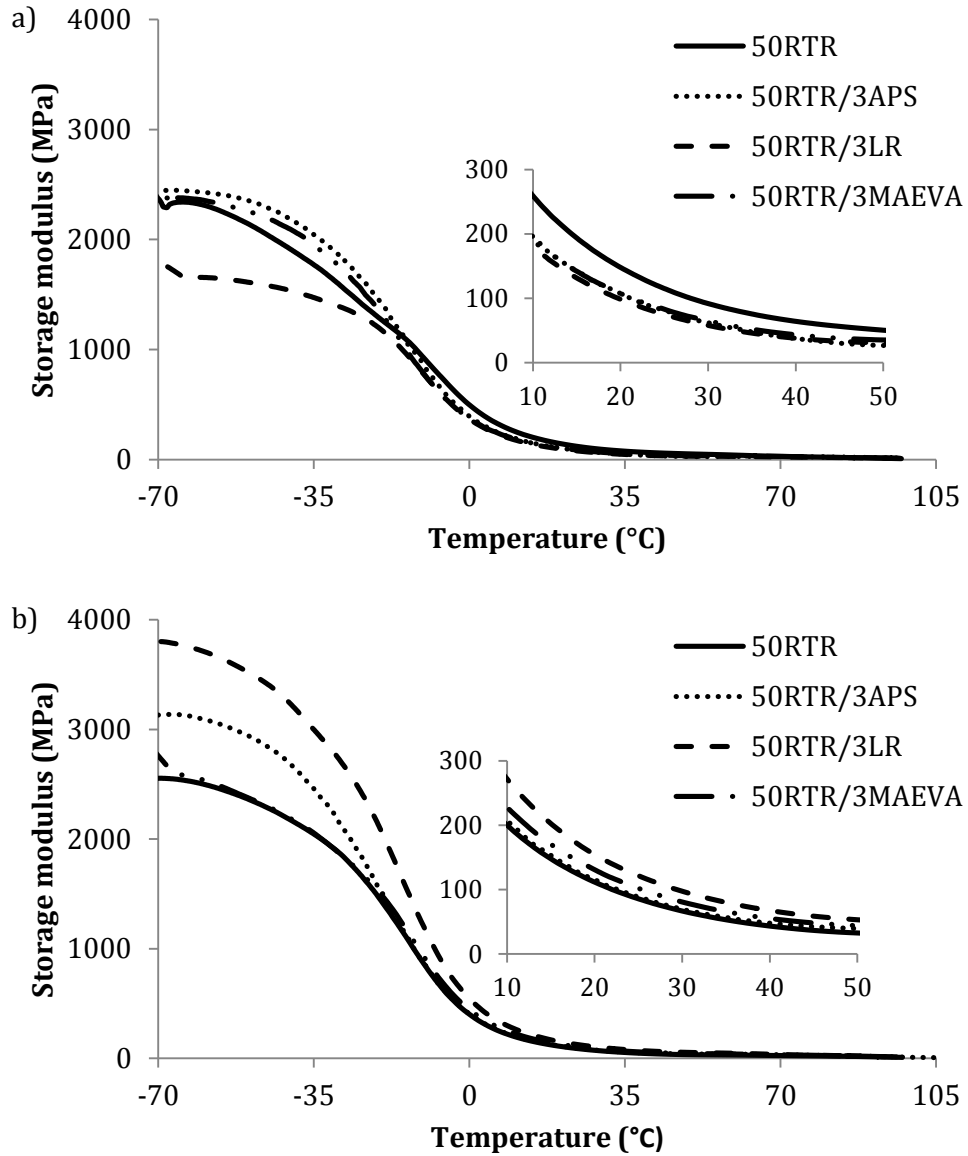


Figure 5.18 Storage modulus of 50RTR, 50RTR/3APS, 50RTR/3LR and 50RTR/3MAEVA a) before and b) after irradiation

Table 5.6 Storage modulus (MPa) of control and compatibilized blends at different temperatures, before and after irradiation

Temperature (°C)	Storage Modulus (MPa)							
	-25		0		20		40	
	0	200	0	200	0	200	0	200
50RTR	1446	1701	491.7	392.5	147.1	111.7	64.07	43.27
50RTR/3APS	1688	1896	390.3	398.8	106.8	115.0	37.46	47.73
50RTR/3LR	1323	2474	362.6	539.1	97.03	154.1	38.00	67.37
50RTR/3MAEVA	1587	1721	359.9	435.1	106.6	128.7	43.46	54.99

LR which showed diminution in storage modulus before irradiation (due to plasticizing effect of LR), improved tremendously upon irradiation; as the elasticity of the blend increases with efficient crosslink formation in LR. Storage modulus before irradiation could be ranked as 3APS>3MAEVA>50RTR>3LR; 50RTR>3APS≈3MAEVA>3LR and 50RTR>3LR≈3APS≈3MAEVA in glass, transition and rubbery regions respectively (inset of Figures 5.18a and b). Previous studies have shown an increase in interphase thickness in the presence of compatibilizer (Moly et al., 2006). Compatibilizer with higher molecular weight tends to form thicker interphase compared to the fully stretched length of the compatibilizer chain. These findings enhance the fact that presence of an effective compatibilizer restricts the mobility of the matrix chains. Thus, effective compatibilization renders a composite stiffer recording higher storage modulus.

Upon irradiation, APS compatibilized blends showed about 30% increment in storage modulus within the glassy region. Whereas, LR showed two fold increments compared to respective non-irradiated blend. MAEVA on the other hand showed only about 10% improvement in storage modulus within the glassy region compared to non-irradiated blend. Irradiated APS and LR showed 1 and 1.5 times higher storage modulus value in glassy region compared to irradiated 50RTR blend. However, irradiated MAEVA did not show any distinct difference in storage modulus compared to irradiated 50RTR. All the blends displayed almost similar storage modulus values at rubbery region.

5.8.2. Loss modulus

Figure 5.19 shows the loss modulus curve of 50RTR, 50RTR/3APS, 50RTR/3LR and 50RTR/3MAEVA blends before and after irradiation. In this discussion, the apparent loss modulus peak height and the peak temperature will be used to study the extent of compatibilization and the values have been listed in Table 5.7.

All the compatibilized blends, before irradiation, displayed shifting of loss modulus peak towards lower temperature. In APS compatibilized blend, the loss modulus peak shifted towards lower temperature from 9 °C to -23.2 °C, while the peak height resumed higher to 288.7 MPa compared to 50RTR. This clearly indicates increasing viscous component of APS compatibilized blend due to

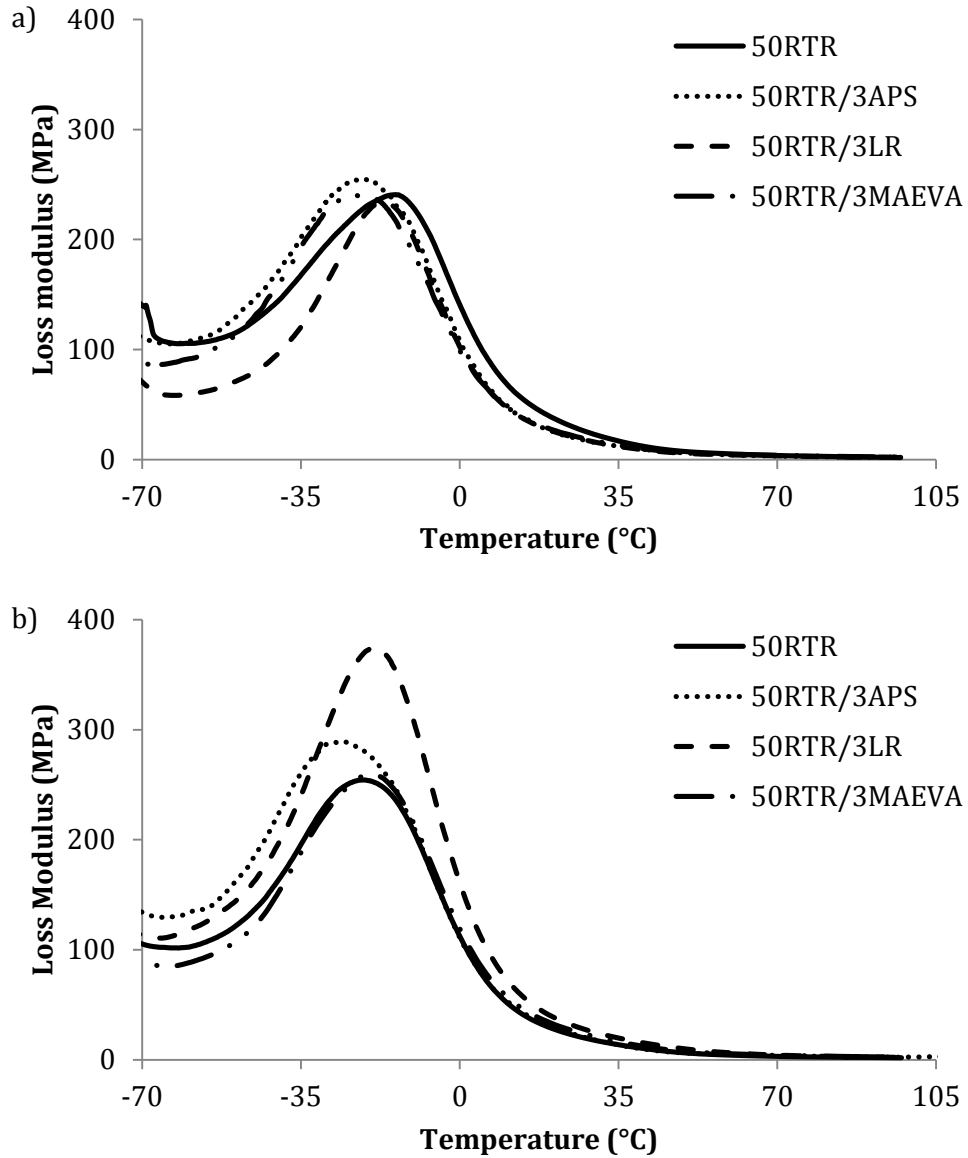


Figure 5.19 Loss modulus of 50RTR, 50RTR/3APS, 50RTR/3LR and 50RTR/3MAEVA blends a) before and b) after irradiation (200 kGy)

Table 5.7 Values corresponding to peak of loss modulus and tan delta curve of 50RTR and compatibilized blends

DMA properties	Loss modulus				Tan delta			
	Temperature (°C)		Height (MPa)		Temperature (°C)		Height	
Radiation dose (kGy)	0	200	0	200	0	200	0	200
50RTR	-14.0	-21.5	240.8	524.4	-0.19	0.9	0.286	0.280
50RTR/3APS	-23.2	-27.6	288.7	254.6	-0.56	-0.20	0.277	0.274
50RTR/3LR	-16.8	-18.2	234.0	374.5	-0.73	0.3	0.286	0.296
50RTR/3MAEVA	-21.1	-19.9	240.5	259.8	-0.48	0.61	0.269	0.269

reclamation of RTR by APS. LR and MAEVA compatibilized blends recorded a peak temperature of -16.8 and -21.1 °C, a slight decrease by 3 and 7 °C respectively, compared to 50RTR. However, no distinct change was observed in the loss modulus peak height. This is again due to physical compatibilizing nature of LR and inefficiency of MAEVA to perform as compatibilizer. The slight reduction in loss modulus peak temperature in these two blends might possibly be due to the contribution of lower T_g values of LR and MAEVA used.

Upon irradiation, APS compatibilized blend showed loss modulus peak shifting to higher temperature with a decrease in the height, compared to non-irradiated blend. These changes are due to effective formation of crosslinking in APS compatibilized blends (Benmesli and Riahi, 2014). Interestingly, LR compatibilized blend, upon irradiation, showed shifting of loss modulus peak temperature and height to -18.2 °C (increased by 1.4 °C) and 374.5 MPa (increased by 140.5 MPa), respectively, compared to non-irradiated counterpart. Apparently, irradiation induced crosslinking of LR in LR compatibilized blends increases the portion of viscous component in the blend, resulting in increased energy loss in the blend. However, MAEVA compatibilized blend did not show any difference in loss modulus of irradiated blend compared to non-irradiated blend, further enhancing the lack of crosslinking efficiency in the blend.

As compared to irradiated 50RTR, irradiated APS compatibilized blends displayed enhanced loss modulus up to the transition region (-10°C). Similarly, irradiated LR displayed enhanced loss modulus up to rubbery region (50 °C). Whereas, irradiated MAEVA did not display any difference in loss modulus compared to irradiated 50RTR. This clearly indicates that APS and LR have effectively compatibilized the blends and enhanced the dynamic mechanical properties upon irradiation.

5.8.3. *Tan delta*

Tan delta curve of 50RTR and compatibilized blends, before and after irradiation are illustrated in Figure 5.20. The corresponding tan delta peak temperature and height have been tabulated in Table 5.7. Tan delta properties was the least affected by compatibilization and irradiation of 50RTR blend as the peak temperature and height remained around 0 °C and 0.3 respectively. Similar

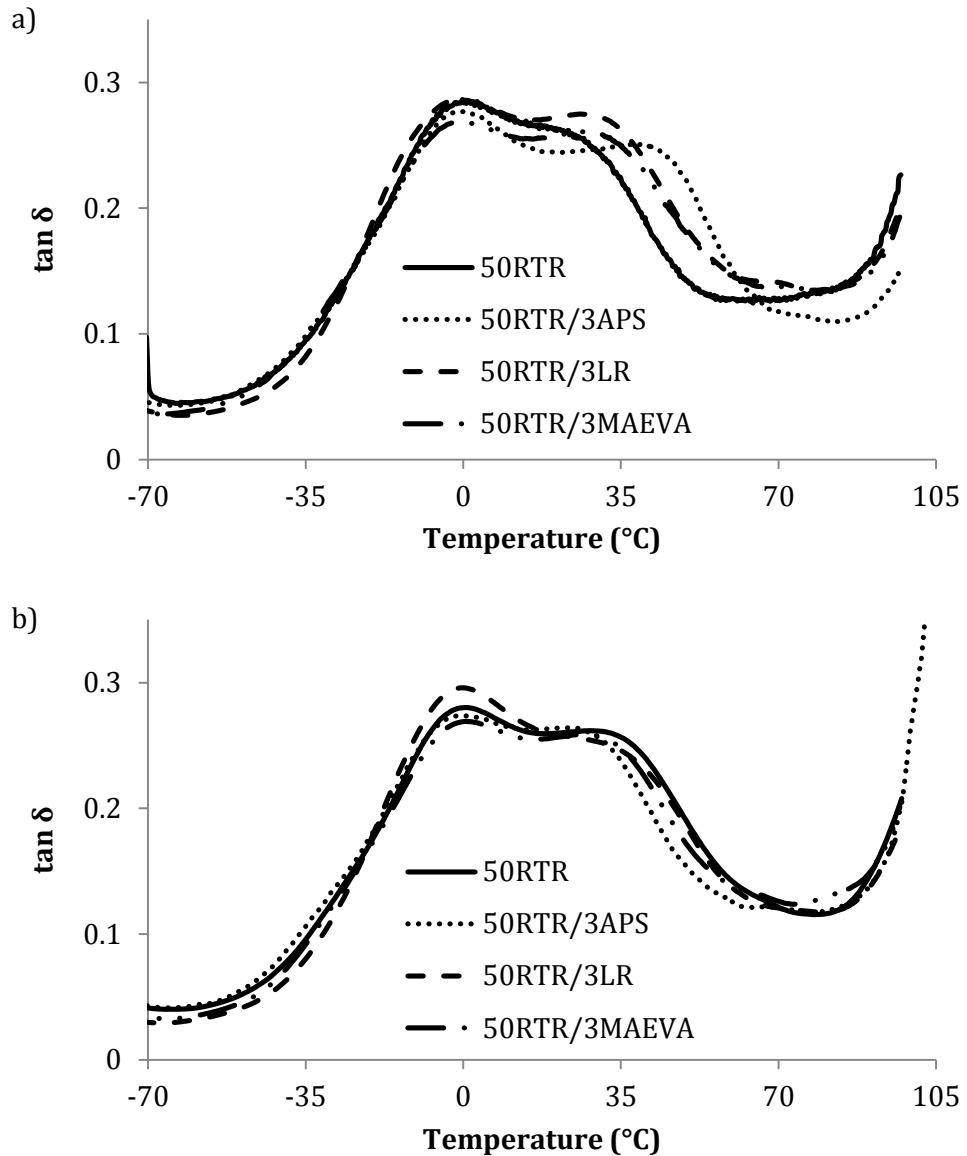


Figure 5.20 Tan delta of 50RTR, 50RTR/3APS, 50RTR/3LR and 50RTR/3MAEVA blends a) before and b) after irradiation (200 kGy)

observation was also reported for NBR/EVA blends (Jansen et al., 2003) and PP/NR blends (George et al., 1997).

The breadth of tan delta curve, before irradiation, increased with compatibilization. The broadening was most obvious in APS compatibilized blends. Compatibilization leads to improved dispersion of RTR in EVA matrix, resulting in increased heterogeneity of the blends. Similar to 50RTR blend, increased broadening was observed in all the compatibilized blends at 200 kGy, suggesting even higher heterogeneity or presence of side chains in irradiated blends. In a two phase system, where two polymers are far from being

completely miscible, no compatibilizer is likely to change it into one phase system. However, APS and LR compatibilizers act only as interfacial agents by effectively improving RTR dispersion in EVA, preventing coalescence of RTR particles and reducing interfacial tension (Moly et al., 2006, John et al., 2003).

5.9. Equilibrium swelling

Figure 5.21 shows the toluene sorption behavior of 50RTR and compatibilized blends before and after irradiation. Before irradiation, APS compatibilized blend showed lower equilibrium toluene uptake; while LR and MAEVA compatibilized blends showed comparable sorption characteristics as compared to 50RTR. Decrease in equilibrium uptake of APS compatibilized blend is due to formation of interphase with chemical links between RTR and EVA matrix. LR compatibilization did not affect the sorption characteristics as it performs only as physical compatibilizing agent. MAEVA on the other hand, did not effectively perform as compatibilizer in this study.

Upon increasing irradiation dose, equilibrium toluene uptake of, APS compatibilized blends showed a decrease; LR showed a distinct increase followed by a decrease at 200 kGy; while MAEVA showed an increase followed by stabilization. Trends observed in irradiated APS blends are in line with observation with irradiated EVA discussed in section 4.8. This is related to more compact network formation in APS compatibilized blends due to irradiation induced crosslinks. In LR compatibilized blends, however, crosslinks formed within LR increases the molecular weight of LR, thereby increases the viscous and elastic components of the irradiated blend as evident from DMA analysis detailed in section 5.8. This accounts for more free volume in irradiated LR compatibilized blends, resulting in higher equilibrium uptake.

5.9.1. Empirical analysis

Table 5.8 lists the sorption parameters of 50RTR, 50RTR/5APS, 50RTR/3LR and 50RTR/3MAEVA blends at 0, 50 and 200 kGy irradiation. All the compatibilized blends, before and after irradiation, had n values in the range of 0.61 to 0.82, implying the blends followed anomalous sorption mechanism similar to 50RTR.

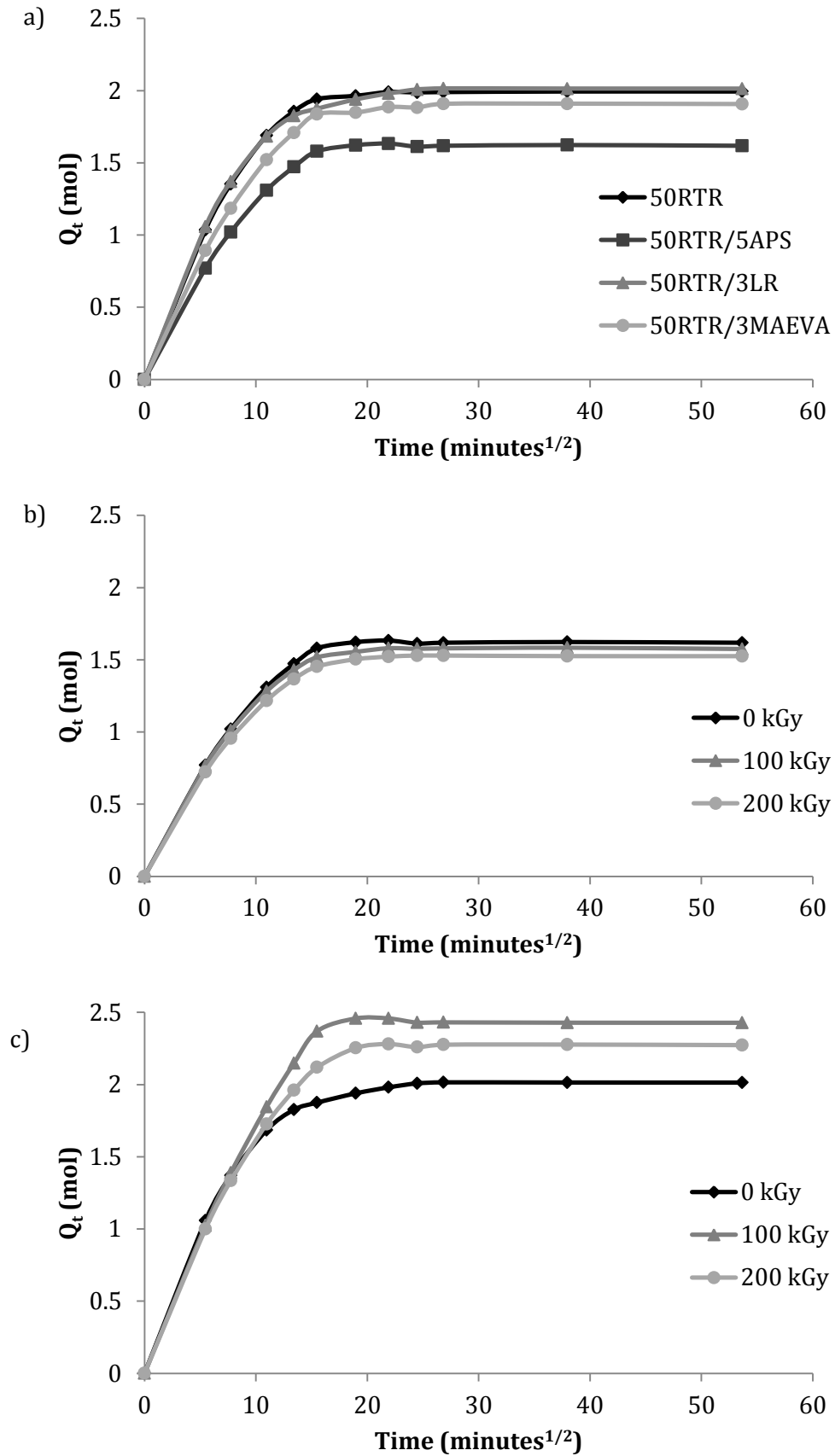


Figure 5.21 Sorption behavior of a) 50RTR and compatibilized blends before irradiation, b) APS compatibilized blends, c) LR compatibilized blends and d) MAEVA compatibilized blends with irradiation.

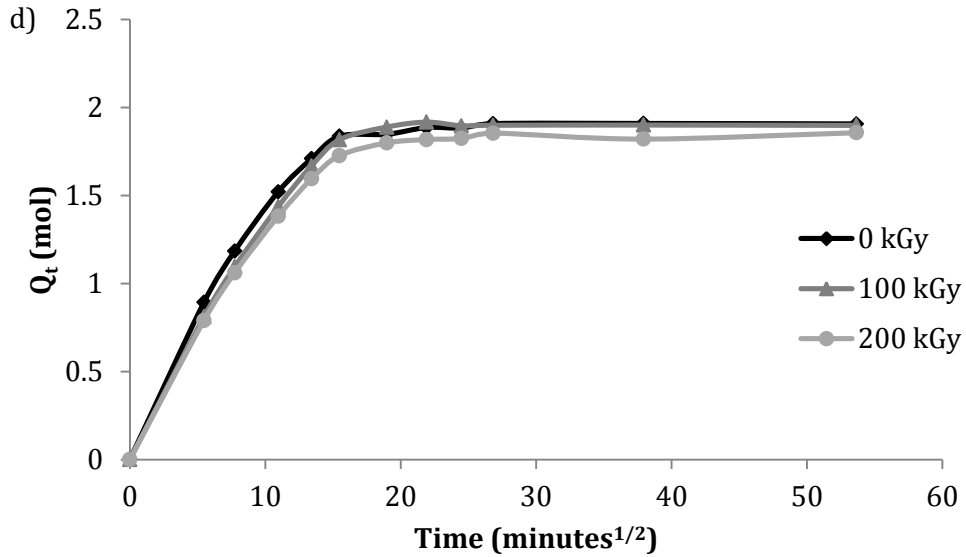


Figure 5.21 Sorption behavior of a) 50RTR and compatibilized blends before irradiation, b) APS compatibilized blends, c) LR compatibilized blends and d) MAEVA compatibilized blends with irradiation

However, it's worth noticing all the compatibilized blends showed lower n values compared to 50RTR blends before irradiation. Upon irradiation, n values of APS remained unchanged, whereas LR and MAEVA compatibilized blends showed an increase at 50 kGy followed by a decrease at 200 kGy. Generally, decrease observed in n values of compatibilized blends and higher irradiation dose suggest diffusion of toluene into samples is restricted. This is due to the improved interfacial adhesion and effective crosslink formation in the blends. An initial increase in n values of LR and MAEVA compatibilized blends upon 50 kGy irradiation might be due to tendency of chain scission domination at lower irradiation doses which has been discussed in sections 4.3 and 5.3. This was not observed in APS compatibilized blends as crosslinking efficiency was improved due to reclamation of RTR and reaction of APS with radical scavenging additives.

Values of k , related to structural features of polymer and its interaction with solvent, was found to differ only slightly in compatibilized blends. However, no distinct pattern was observed with increasing irradiation dose.

Diffusion coefficient (D) showed smaller values in all the compatibilized blends compared to 50RTR. Improved interfacial adhesion limits the molecular motion of the sample and hence, decreasing polymer segmental mobility. However,

Table 5.8 Effect of compatibilizers and irradiation on different parameters of sorption behavior of 50RTR blends

Parameter	Radiation	Designation			
	dose	50RTR	5APS	3LR	3MAEVA
n (log min ^{1/2})	0	0.66	0.62	0.61	0.62
	50	0.64	0.62	0.82	0.72
	200	0.71	0.61	0.75	0.69
k	0	0.17	0.17	0.19	0.18
	50	0.18	0.17	0.11	0.14
	200	0.14	0.18	0.12	0.14
D (cm ² min ⁻¹)	0	4.73	4.32	4.60	4.27
	50	5.07	4.12	4.08	3.99
	200	4.12	4.14	3.82	3.76
S	0	2.83	2.48	2.85	2.74
	50	2.73	2.48	3.18	2.76
	200	2.95	2.41	3.08	2.68
P (cm ² min ⁻¹)	0	1.34	1.07	1.31	1.17
	50	1.39	1.02	1.29	1.10
	200	1.23	1.00	1.18	1.01

upon irradiation, APS showed stabilized D values, whereas in LR and MAEVA compatibilized blends a continuous decrease was observed.

Sorption coefficient (S) of APS and MAEVA compatibilized blends showed lower values. While LR compatibilized blend showed almost similar values as compared to 50RTR blend. Upon irradiation, sorption coefficient of APS compatibilized blends differed only minimally, whereas LR and MAEVA blends showed an increase at 50 kGy followed by a decrease at 200 kGy. This is linked to the difference in crosslink density of the compatibilized 50RTR blends upon irradiation.

Permeability coefficient (P) of compatibilized blends was lower compared to 50RTR blend. Increasing irradiation dose also results in decrease in permeability coefficient. This clearly indicates compatibilization and irradiation improves chemical stability of 50RTR blend (towards toluene).

5.10. Summary

APS has efficiently functioned as compatibilizer of 50RTR blend and performed as reclaiming agent for RTR component of 50RTR blend. LR has also functioned as physical compatibilizer and improved dispersion of RTR in EVA matrix. MAEVA, however, failed to function as a compatibilizing agent in this study. Judging from mechanical properties, 5 and 3 wt% was found to be the optimum amount of compatibilizer loading for APS and LR respectively.

Irradiation enhanced the mechanical properties of the compatibilized blends slightly. However, only LR compatibilized blends displayed improved thermal stability. Irradiation also affected the crystallization of EVA matrix in the compatibilized blends. Irradiated APS and LR compatibilized blends revealed good dynamic mechanical properties enhancement, particularly LR compatibilized blend.

CHAPTER 6. EFFECT OF DIFFERENT RADIATION SENSITIZERS ON THE PROPERTIES OF RTR/EVA BLEND

6.1. Introduction

Ionizing radiation is an upcoming powerful technology in addressing polymeric waste issues. The extent of irradiation can be controlled to introduce chain crosslinking or scission to tweak a recycle material's properties as desired. Previous chapters have addressed the lack of efficiency in radiation induced crosslink formation in RTR/EVA blends due to readily present radical stabilizing and scavenging additives in RTR. This chapter is dedicated to the use of different radiation sensitizers to accelerate radiation induced crosslinks in RTR/EVA blends. The three radiation sensitizers used are HVA2, TMPTA and TPGDA with two, three and two functional sites, respectively. The chemical structure of all three radiation sensitizers are shown in Figure 6.1. The loading of the radiation sensitizers has been set to 4 phr based on previous studies (Du et al., 2005, Yin et al., 2013, Dutta et al., 1996). Presence of radiation sensitizers would allow for faster reach to optimal irradiation dose and also reduce the undesired effect of oxidative degradation. The influence of radiation sensitizers and crosslink network density on the gel, mechanical, morphological, thermal, dynamic mechanical and sorption properties are reported in this chapter.

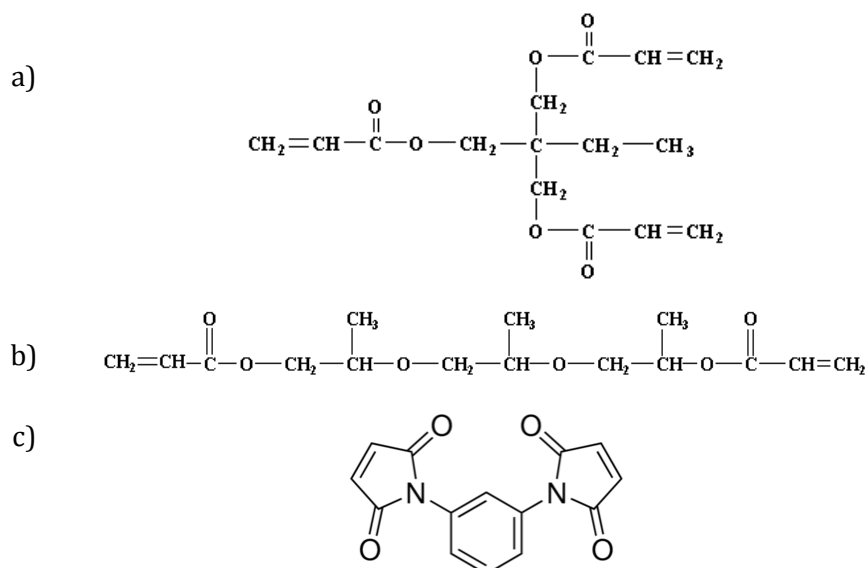


Figure 6.1 Chemical structure of a) TMPTA, b) TPGDA and c) HVA2

6.2. Processing characteristics

Figure 6.2 shows the evolution of processing torque over time for RTR, EVA and 50RTR/5APS blends in the presence of radiation sensitizers. In RTR, addition of TMPTA and TPGDA at about the fourth minute decreased the torque. The torque readings stabilize again after about 30 seconds and remains so until the end of mixing process. The drop in the torque is an attribute of lubricating effects rendered by liquid TMPTA and TPGDA. End of mixing torque was lower in RTR/TPGDA composition compared to RTR/TMPTA composition. This suggests that TPGDA has higher lubricating capacity in RTR system. In the case of HVA2 addition at about the seventh minute, the torque of RTR increases for 30 seconds and reaches a maximum. After the maximal torque reading, a gradual decrease was noticed in RTR/HVA2 torque profile. HVA2 is in powder form; hence addition of powder to a RTR increases the viscosity of the RTR/HVA2 compound. Additionally, the dynamic vulcanization of RTR in the presence of HVA2 is also responsible for the observed increase in the viscosity of the RTR/HVA2 compound (He et al., 2014, Awang and Ismail, 2008). However the drop in torque value after reaching the maximum suggests that the dynamically vulcanized RTR undergoes degradation (Magioli et al., 2010). RTR/HVA2 also had the highest end of mixing torque values suggesting highest viscosity of RTR in the presence of HVA2 compared to TMPTA and TPGDA compositions.

Figure 6.2b depicts the evolution of torque-time profile of EVA in the presence of TMPTA, TPGDA and HVA2. A sharp increase in the start of mixing indicates melting of EVA and stabilization attainment at about the second minute. The beginning of torque profile was similar for all the three systems studied. Addition of TMPTA and TPGDA at about the fourth minute resulted in a sharp dip, followed by an increase in the torque value and stabilized from there on. The torque profile of EVA after the addition of TMPTA and TPGDA upon reaching the stabilization was relatively smoother than before the addition of the radiation sensitizers. The dip and smoother torque profile observed were due to the lubricating nature of TMPTA and TPGDA. The end of mixing torque of EVA/TMPTA and EVA/TPGDA was similar, suggesting similar level of lubricating nature offered by the two radiation sensitizers on EVA system. Surprisingly, addition of HVA2 to EVA mixture at about the sixth minute sharply decreased the torque reading and stabilized thereon. Stabilization of the torque profile until the end of mixing suggests little to no dynamic vulcanization has occurred

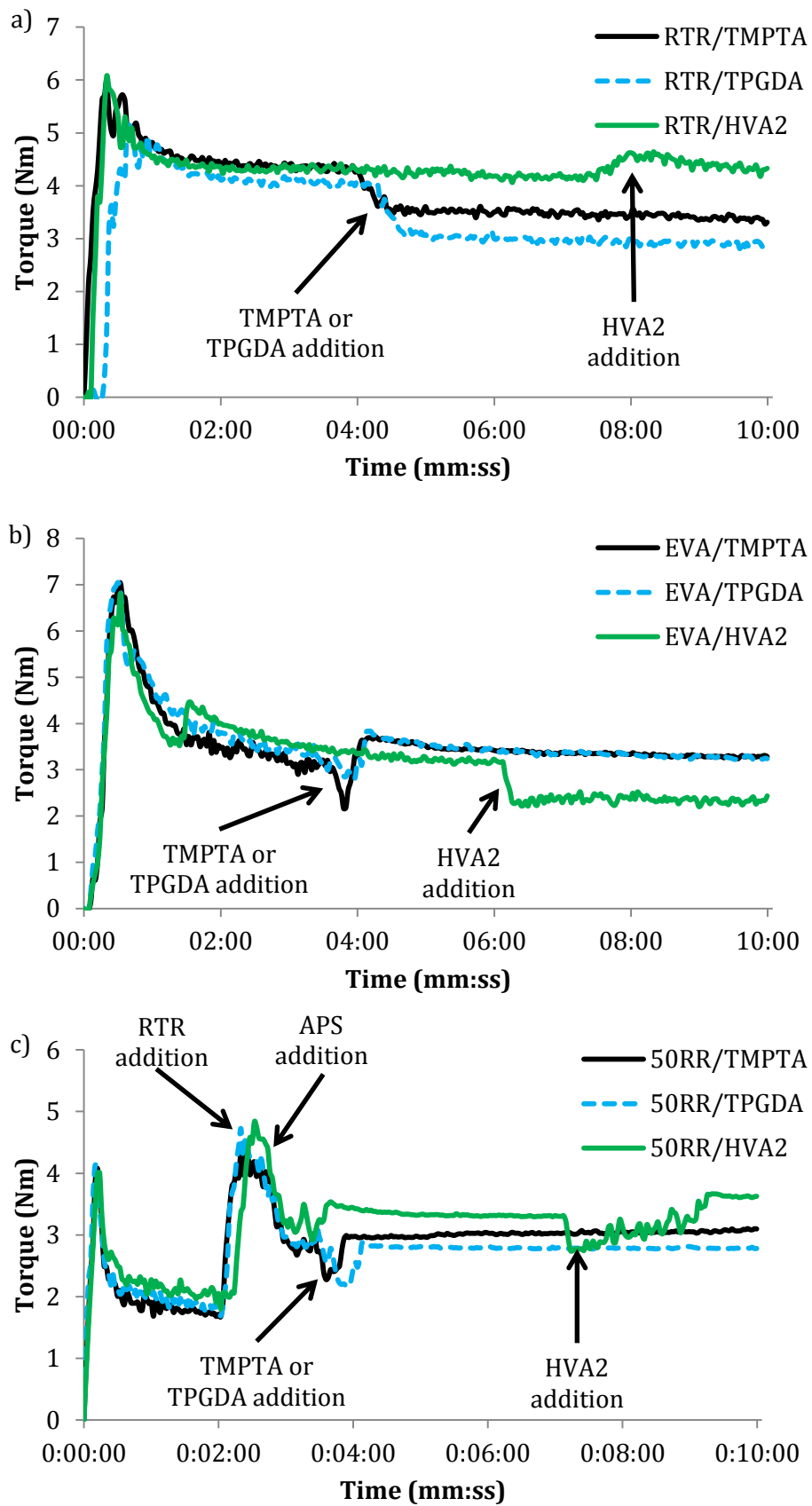


Figure 6.2 Torque-time curve of a) RTR, b) EVA and c) 50RTR/5APS blend; in the presence of radiation sensitizers

in the EVA mixture. It was also interesting to note the ending torque of EVA/HVA2 was lower by about 1 Nm compared to TMPTA or TPGDA compositions.

Figure 6.2c displays the influence of TMPTA, TPGDA and HVA2 addition to the torque-time profile of 50RTR/5APS blends. A sharp increase at time 0 and 2 minutes is subject to EVA and RTR loading, respectively. A slight drop in torque profile subsequent to the addition of RTR is due to introduction of APS into the system. It is apparent that all the compositions exhibit similar torque profile up to this point. Similar to EVA torque profile, addition of TMPTA and TPGDA into the 50RTR/5APS blends mixture at about the fourth minute showed a sharp decrease in the torque profile, which later increases to a maximal value and stabilizes thereon. However, similar to observation with RTR compositions, the stabilization and end of mixing torque of 50RTR/5APS was lower in TPGDA composition than in TMPTA composition. This could be an attribute of better lubricating function of TPGDA in the RTR phase of the blend. Addition of HVA2 at about the seventh minute to the blend mixture results in a sharp decrease in the torque readings. Thereon, torque readings kept increasing for about two minutes (ninth minute of mixing), after which, end of mixing torque was observed. Here again, the increasing torque readings of the blends in the presence of HVA2 suggests increase in the blends system's viscosity due to dynamic vulcanization in the blend composition (Magioli et al., 2010). Similar to end of mixing torque noted in RTR compositions, the highest end of mixing torque was recorded by HVA2 composition, followed by TMPTA composition and later by TPGDA composition. This is related to the viscosity of the blends in the presence of radiation sensitizers. TPGDA records the lowest torque readings due to the distinct lubricating nature which effectively decreases the viscosity of the blends.

6.3. Gel content

Figure 6.3 shows the influence of TMPTA, TPGDA and HVA2 on radiation induced gel formation in RTR, EVA and 50RTR/5APS blend as a function of irradiation dose. RTR/HVA2 shows about 20% increase in gel content compared to neat RTR at equivalent irradiation dose, netting a maximum value of 91% gel content at 200 kGy irradiation dose. Addition of HVA2 proves to be efficiently

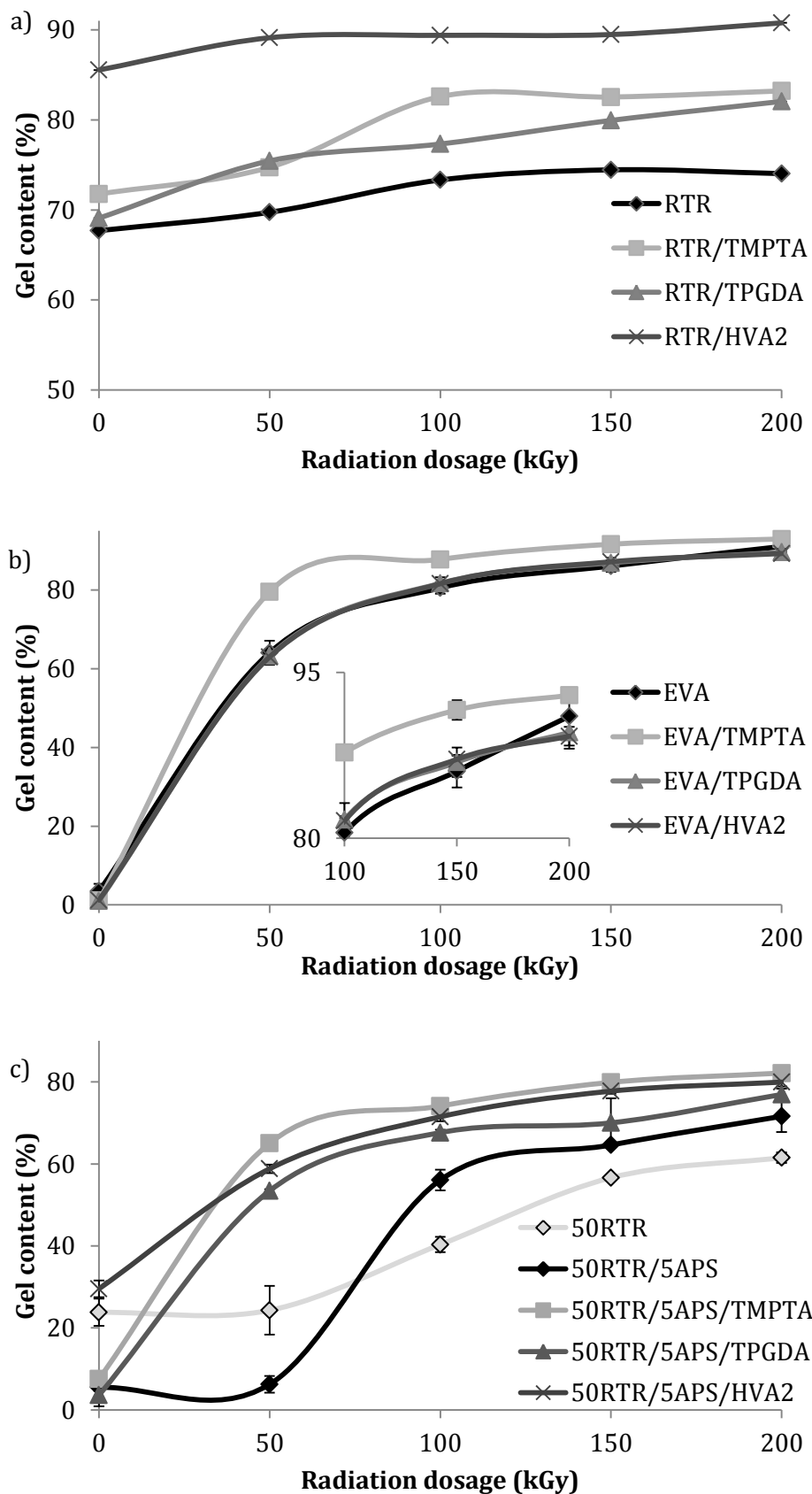


Figure 6.3 Gel content values of a) RTR, b) EVA and c) 50RTR/5APS blends as a function of radiation sensitizers and radiation dose

introducing crosslinking in RTR sample. Similar observation has also been reported in EVA/NR study (Zurina et al., 2008). However, as evident from torque-time study in section 6.2, dynamically vulcanized RTR/HVA2 samples were found to undergo degradation during blending process. Thus, these made it difficult for RTR/HVA2 formulation to be compression molded into testing specimens. Hence, influence of HVA2 on RTR properties could not be verified. TMPTA and TPGDA containing RTR sample also displayed higher gel content than neat RTR. This indicates that presence of TMPTA and TPGDA accelerates irradiation induced crosslinking in RTR (Yasin et al., 2015). RTR/TMPTA records higher gel content values as compared to RTR/TPGDA. This is due to the higher number of functionality in TMPTA (trifunctional) contrast to TPGDA (difunctional) (Ratnam et al., 2014, Banik et al., 1999). TMPTA is capable of forming more crosslink bridges due to higher functionality resulting in higher gel content values.

Figure 6.3b shows the influence of TMPTA, TPGDA and HVA2 on gel formation of EVA matrix. TMPTA was found to be the most efficient radiation sensitizer in accelerating formation of the crosslinks on EVA matrix compared to TPGDA, HVA2 and neat EVA. TPGDA and HVA2 only displayed slight increase in gel content values compared to neat EVA (inset of Figure 6.3b). These findings suggest the efficiency of crosslink formation in EVA matrix are in the order of TMPTA > TPGDA = HVA2. This is again due to difference in the functionality of radiation sensitizers as mentioned earlier. Unlike RTR/HVA2, no crosslink formation was observed in EVA/HVA2 composition before irradiation. HVA2 with multi-radical accepting capabilities interacts with radicals to stabilize the overall reaction. This suggests the presence or formations of radicals are more likely happening in RTR aided by the heat energy available during blending and compression molding process. Whereas, EVA is accounted as more stable at the processing temperature, leading to lower possibility for crosslink formation in EVA/HVA2 composition before irradiation. Similar observation has also been reported by Zurina et al. (2008). Moreover, previous work has shown that HVA2 have higher tendency to interact with rubber component than the thermoplastic matrix used in the study (Awang and Ismail, 2008, Zurina et al., 2008).

Figure 6.3c shows the influence of TMPTA, TPGDA and HVA2 on gel formation of 50RTR/5APS blend. Gel content yield of neat 50RTR blend was also shown on the figure for comparison. Presence of radiation sensitizers has completely

resolved the delay in crosslink formation observed in neat 50RTR and 50RTR/5APS blends. Upon irradiation of the 50RTR/5APS blends, TMPTA was found to yield the highest gel content values, closely followed by HVA2 and TPGDA. Before irradiation (0 kGy), a gel content value of 29.5% was observed in 50RTR/5APS/HVA2 composition. Judging from the gel content analysis of RTR and EVA in the presence of HVA2, the gel value observed in 50RTR/5APS/HVA2 composition could be mostly due to crosslink formation in RTR component of the blend.

Charlesby-Pinner equation was used to determine the ratio of chain scission to crosslinking (p_0/q_0) in RTR, EVA and 50RTR/5APS blends in the presence of radiation sensitizers. The p_0/q_0 values have been listed in Table 6.1. Presence of TMPTA and TPGDA in RTR decreased, while HVA2 further increased the p_0/q_0 values. The p_0/q_0 value of RTR/HVA2 was 1.93 indicating about 2 scissions could be happening per crosslinking in the RTR matrix, which would lead to substantial decrease in the molecular weight of RTR matrix. This further corroborates the reasons for difficulties in molding RTR/HVA2 samples. Although RTR/TMPTA and RTR/TPGDA recorded a decline, the p_0/q_0 values were still higher than 1, indicating chain scissioning dominates over crosslinking in the RTR matrix.

Table 6.1 Values p_0/q_0 of RTR, EVA and 50RTR/5APS blends in the presence of radiation sensitizers

	Nil	TMPTA	TPGDA	HVA2
RTR	1.8724	1.7718	1.7920	1.9255
EVA	0.2473	0.2723	0.2740	0.2805
50RTR/5APS	0.5478	0.6700	0.6960	1.0908

Both EVA and 50RTR/5APS blends displayed a slight increase in p_0/q_0 values in the presence of all three radiation sensitizers. This is to be expected as crosslinking process was found to have already effectively take place in the neat EVA and 50RTR/5APS matrix upon irradiation. Whereas, the addition of radiation sensitizers would enhance the crosslinking process to a certain absorbed radiation dosage, upon which, chain scission are deemed to prevail. Presence of radiation sensitizers would allow for optimal crosslinking to be

achieved at a lower absorbed dose of irradiation (Burillo et al., 2001, Vijayabaskar et al., 2004, Ng et al., 2014). Among all the three radiation sensitizers, HVA2 recorded p_0/q_0 values above 1 for RTR and 50RTR/5APS blends. This indicates the 4phr of HVA2 loading used in this study is more than sufficient for RTR based system, leading to domination of chain scission. Optimization of HVA2 loading and blending parameters is essential to observe neat crosslink formation in irradiated 50RTR/5APS/HVA2 blends.

6.4. Mechanical properties

6.4.1. Tensile strength

Figure 6.4 details the influence of radiation sensitizer on tensile strength of RTR, EVA and 50RTR/5APS blends upon irradiation. Figure 6.4a clearly indicates the addition of TMPTA and TPGDA to RTR enhances the blend's tensile strength, especially at higher irradiation doses (150 to 200 kGy). The increase noted in tensile strength is due to three dimensional network formation through greater number of C-C interchain crosslinks initiated by the radiation sensitizers in presence of electron beam irradiation (Mitra et al., 2010). Before irradiation, both TMPTA and TPGDA composition of RTR recorded lower tensile strength values due to the lubrication effect rendered by the radiation sensitizers. RTR/TMPTA composition showed 41% enhancement in tensile strength at 50 kGy irradiation dose, which further improved by 106% at 200 kGy irradiation dose compared to neat RTR at equivalent irradiation dose. RTR/TPGDA on the other hand only shows enhancement in tensile strength from 150 kGy irradiation dose onwards. It is our assumption that TMPTA and TPGDA are involved in the consumption of the radical stabilizing and scavenging additives readily present within RTR. Due to higher functionality of TMPTA, all additives are consumed earlier, allowing for TMPTA to aid crosslinking process at lower irradiation dose. Whereas, TPGDA with lower functionality, requires a higher dose of irradiation to effectively aid crosslinking process in RTR (Patacz et al., 2001). Also, it is contradictory to observe a clear enhancement in tensile strength of RTR/TMPTA and RTR/TPGDA even though the gel values and p_0/q_0 values were indicating chain scissioning. This could probably be explained based on the dynamic mechanical findings in section 4.7, indicating the scissions of S-S and S-C crosslinks being replaced with higher energy C-C crosslinks. Hence, the enhancement in tensile strength is observed in RTR/TMPTA and RTR/TPGDA compositions.

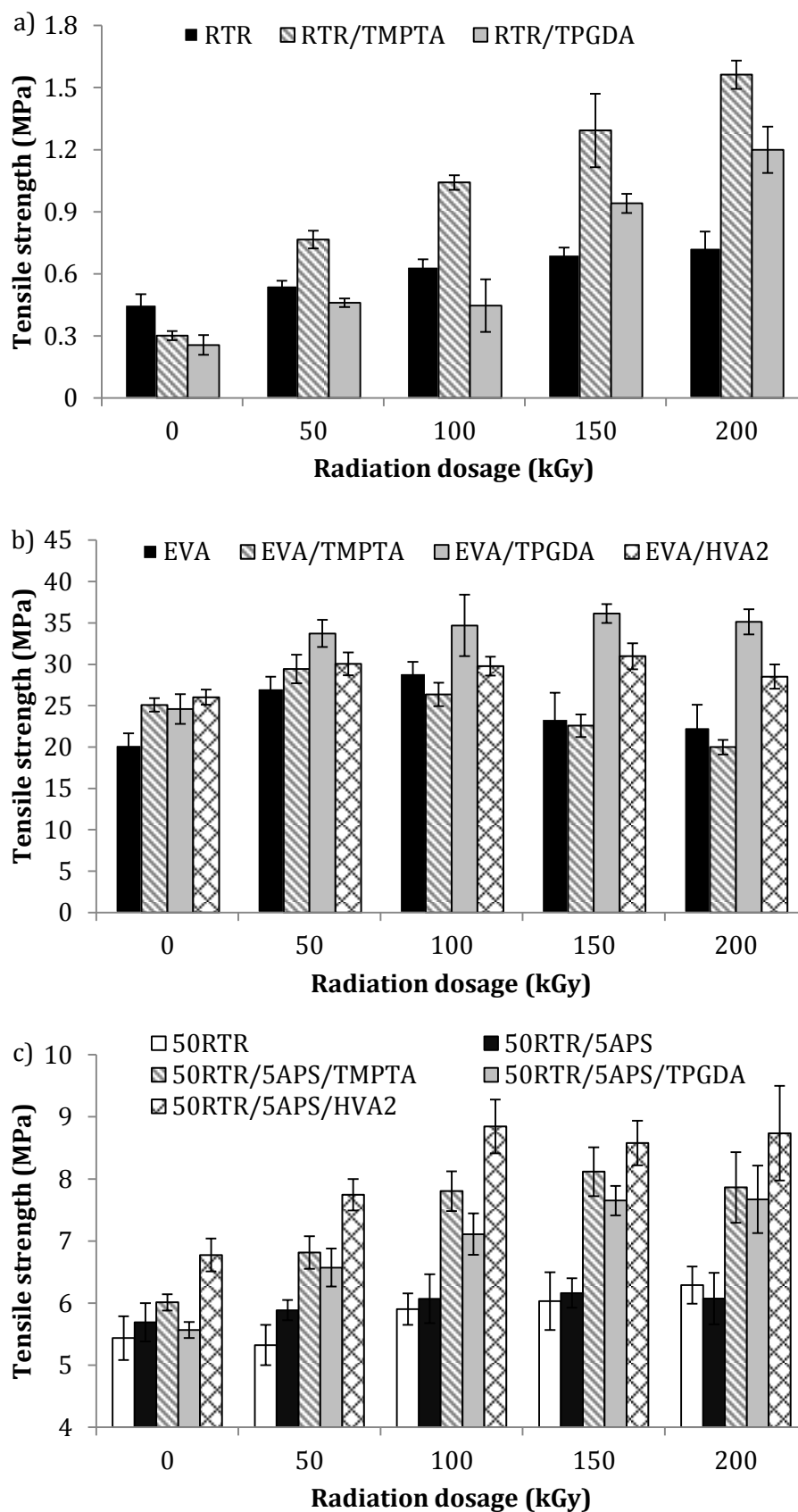


Figure 6.4 Effect of radiation sensitizers on tensile strength of a) RTR, b) EVA and c) 50RTR/5APS blends at various radiation doses

Figure 6.4b shows the influence of radiation sensitizers on tensile strength of EVA upon irradiation. For EVA system, all the three radiation sensitizers, TMPTA, TPGDA and HVA2, were capable of enhancing the tensile strength of EVA. Such enhancement in tensile strength upon irradiation is an indication of successful acceleration of irradiation induced crosslinking due to presence of radiation sensitizers (Yasin et al., 2002, Maziad and Hassan, 2007). However, EVA/TPGDA composition recorded the highest tensile strength of 36 MPa at 150 kGy irradiation dose. This is followed by EVA/HVA2 and EVA/TMPTA composition with a value of 31 MPa (at 150 kGy) and 29 MPa (at 50 kGy), respectively. Similar observations have been reported by previous studies (Ratnam et al., 2014, Sakinah et al., 2011). The faster reach to highest tensile strength values recorded by EVA/TMPTA is due to relatively high reactivity of trifunctional acrylates (Yin et al., 2013). Drastic drop in tensile strength of EVA/TMPTA after the optimal irradiation dose of 50 kGy was observed due to higher extent of crosslinking, causing embrittlement of EVA matrix (Sujit et al., 1996, Martínez-Pardo and Vera-Graziano, 1995). The drop in tensile strength of EVA/TPGDA and EVA/HVA2 is less vigorous due to lower crosslink density of the composition as compared to EVA/TMPTA (Patacz et al., 2001). Interestingly, tensile strength values of EVA/TPGDA were always higher than EVA/HVA2, even though both compositions had very similar gel content values. EVA/TPGDA recorded lower p_0/q_0 values suggesting higher efficiency of crosslinking of EVA in the presence of TPGDA compared to HVA2, resulting in higher tensile strength values in EVA/TPGDA composition. These findings suggest the efficiency of radiation sensitizer with respect to tensile strength enhancement of EVA matrix follows the order of TPGDA>HVA2>TMPTA.

Figure 6.4c displays the influence of radiation sensitizers on tensile strength of 50RTR/5APS blends upon irradiation. Changes in tensile strength of 50RTR blend have also been charted in for comparison. All blends containing radiation sensitizers recorded higher tensile strength values than 50RTR and 50RTR/5APS throughout the studied irradiation doses. This again agrees with earlier findings where, the addition of radiation sensitizers was accounted for acceleration and efficiency of irradiation induced crosslinking in the blends. The best tensile strength value of 8.8 MPa at 100 kGy irradiation dose was obtained with 50RTR/5APS/HVA2, followed by 50RTR/5APS/TMPTA composition with a value of 8.1 MPa at 150 kGy irradiation dose. 50RTR/5APS/TPGDA composition

recorded the least optimal tensile strength value of 7.7 MPa at 200 kGy irradiation dose. Tensile strength of 50RTR/5APS/HVA2 composition was higher than neat 50RTR/5APS blend before irradiation (0 kGy) due to the formation of crosslinks during the blending and compression molding processes as explained in section 6.3. The efficiency of tensile strength enhancement of radiation sensitizers in 50RTR/5APS blends follows the order of HVA2>TMPTA>TPGDA. These findings are believed to be associated with the tendency of radiation sensitizers to form crosslinking in the RTR regions of 50RTR/5APS blends. Also to be noted, the trend of higher percentage of enhancement in tensile strength at higher irradiation doses in the blends was similar to the observation with RTR composition with radiation sensitizers. Interestingly, 50RTR/5APS/HVA2 composition recorded enhancement in tensile strength despite gel content analysis suggesting prevalence of chain scissions in this blend. Again, this observation is similar to the trend observed with RTR compositions, suggesting scissions of S-S and S-C bonds being replaced with higher energy C-C bonds in the RTR matrix.

6.4.2. Elongation at break

Figure 6.5 shows the influence of radiation sensitizers on elongation at break of RTR, EVA and 50RTR/5APS blends. Addition of TMPTA and TPGDA to RTR increases the elongation at break of RTR throughout the studied irradiation dose. The increase noted before irradiation is an attribute of lubrication effect rendered by the radiation sensitizers (Ratnam and Zaman, 1999b). Increase noted upon irradiation could be due to efficient crosslinking of short RTR chains by radiation sensitizers hence, restoring the elastic capacity of the rubber. TPGDA was more efficient in restoring the elasticity of RTR compared to TMPTA. The drop in elongation at break with increasing irradiation dose was also more prominent in RTR/TMPTA. These are due to denser crosslink formations by trifunctional TMPTA compared to difunctional TPGDA (Vijayabaskar et al., 2004).

In EVA composition, with increasing irradiation dose, presence of TMPTA and TPGDA caused the most and least rigorous drop in elongation at break, respectively (Figure 6.5b). Whereas, in EVA/HVA2 composition, almost comparable elongation at break values to neat EVA was observed throughout the

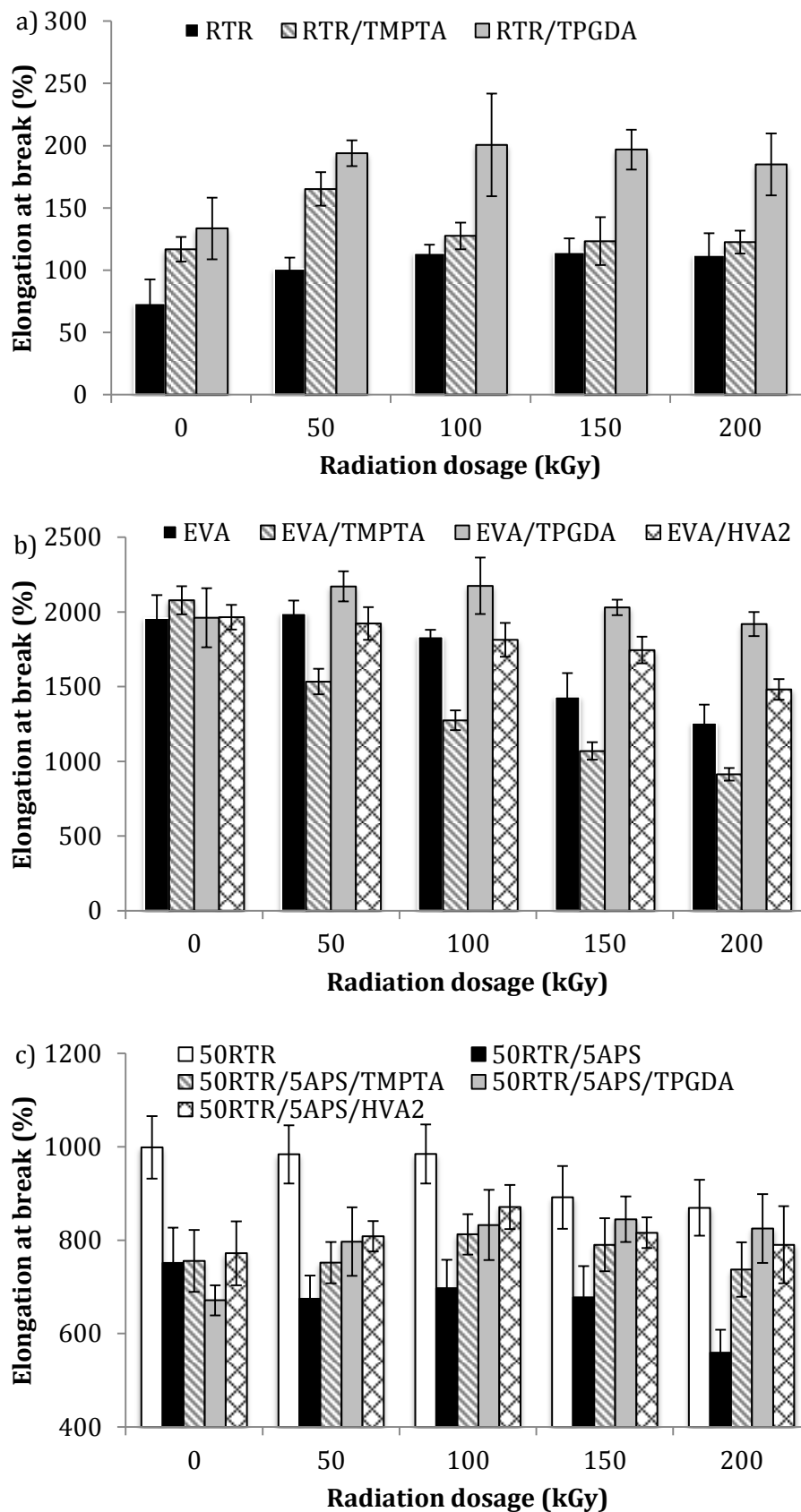


Figure 6.5 Effect of radiation sensitizers on elongation at break of a) RTR, b) EVA and c) 50RTR/5APS blends at various radiation doses

studied irradiation doses. The drop in elongation at break with increasing irradiation dose is an indication of loss of elastic properties (or increasing brittle behavior) as a consequence of increased crosslink density upon irradiation (Yasin et al., 2002, Ratnam and Zaman, 1999b). EVA/TMPTA has the highest gel content, hence, the densest crosslink network, causing the more drastic deterioration in the elongation at break of EVA matrix (Shirodkar and Burford, 2001). The best retention of elongation at break can be ranked as follows: EVA/TPGDA>EVA/HVA2=neat EVA>EVA/TMPTA.

Figure 6.5c shows the influence of radiation sensitizers on elongation at break of 50RTR/5APS blends as a function of irradiation dose. The elongation at break of 50RTR blends have also been charted in for comparison. Upon irradiation, all composition of 50RTR/5APS with radiation sensitizers had higher elongation at break values compared to neat 50RTR/5APS. The highest elongation at break values of 50RTR/5APS/HVA2 was recorded between 50 to 100 kGy, while 50RTR/5APS/TPGDA recorded the highest values between 150 to 200 kGy. At 200 kGy, TPGDA and HVA2 composition had almost 50% higher elongation at break values compared to neat 50RTR/5APS blend and these values were almost comparable to 50RTR blend (at 200 kGy irradiation dose). These findings relay that the RTR component of the blend is efficiently crosslinked by the radiation sensitizers, resulting in the increase of blend ductility. However, the elongation at break of 50RTR/5APS in the presence of radiation sensitizers did not exceed the elongation at break value of 50RTR blend. It was interesting to note improvements in tensile strength and elongation at break of the blends in the presence of radiation sensitizer. Xu et al. (2013) discussed simultaneous improvement in elongation at break and tensile strength of a blend are due to efficient co-crosslinking of the blend components at interfacial regions.

6.4.3. Tensile modulus

Figure 6.6 shows the influence of TMPTA, TPGDA and HVA2 on modulus at 100% elongation of RTR, EVA and 50RTR/5APS blends as a function of irradiation dose. In all RTR composition (Figure 6.6a), modulus increased with increasing irradiation dose. RTR/TMPTA recorded the highest modulus values throughout the studied irradiation doses. At 200 kGy irradiation dose, RTR/TMPTA recorded 407% and 90% higher values compared to RTR/TMPTA

(0 kGy) and neat RTR (200 kGy), respectively. Whereas, RTR/TPGDA composition, displayed lower modulus values compared to neat RTR, up to 150 kGy irradiation dose. The increase noted in modulus of all RTR composition with increasing irradiation dose is an attribute of increasing crosslink density of the matrix (Vijayabaskar et al., 2004). The superior modulus values of RTR/TMPTA composition is validating the earlier finding where TMPTA was found as a radiation sensitizer capable of producing denser crosslinks in RTR matrix due to higher functionality and reactivity of TMPTA. RTR/TPGDA recorded lower values compared to neat RTR due to the lubricating effects, which was resolved at higher irradiation dose. The later increase in modulus value of RTR/TPGDA composition (as compared to neat RTR at equivalent irradiation dose) is due to lower functionality of TPGDA that requires higher doses of irradiation to reach optimal crosslink density in RTR matrix.

Influence of TMPTA, TPGDA and HVA2 on modulus at 100% elongation of EVA in relation to irradiation dosage is depicted in Figure 6.6b. EVA/TMPTA and EVA/TPGDA composition recorded a slight decline in modulus before irradiation, compared to neat EVA. This is owing to the lubricating nature of these radiation sensitizers. However, the modulus values increased upon 50 kGy irradiation and level off at higher irradiation doses. On the other hand, modulus values of EVA/HVA2 neither increased nor decreased throughout the studied irradiation dose. This is in agreement with the gel content analysis, where the gel content of EVA with radiation sensitizers reached optimal values at 50 kGy irradiation and increased slowly thereon. Moreover, throughout the studied irradiation dose, TMPTA had highest modulus values followed by HVA2 and TPGDA, which is also in agreement with gel content values. This finding further corroborates the influence of crosslink density on modulus values of EVA compounds.

Figure 6.6c depicts the influence of radiation sensitizers on the modulus at 100% elongation of 50RTR/5APS blends in relation to increasing irradiation dose. All 50RTR/5APS blends show a slow rate of increase in modulus values with increasing irradiation dosage. Upon irradiation, HVA2 composition had higher modulus values compared to neat 50RTR/5APS blends at equivalent irradiation dose. On the other hand, TMPTA and TPGDA compositions had lower modulus values up to 100 and 200 kGy irradiation dose, respectively (compared to neat 50RTR/5APS blends at equivalent irradiation dose). Though the increase in

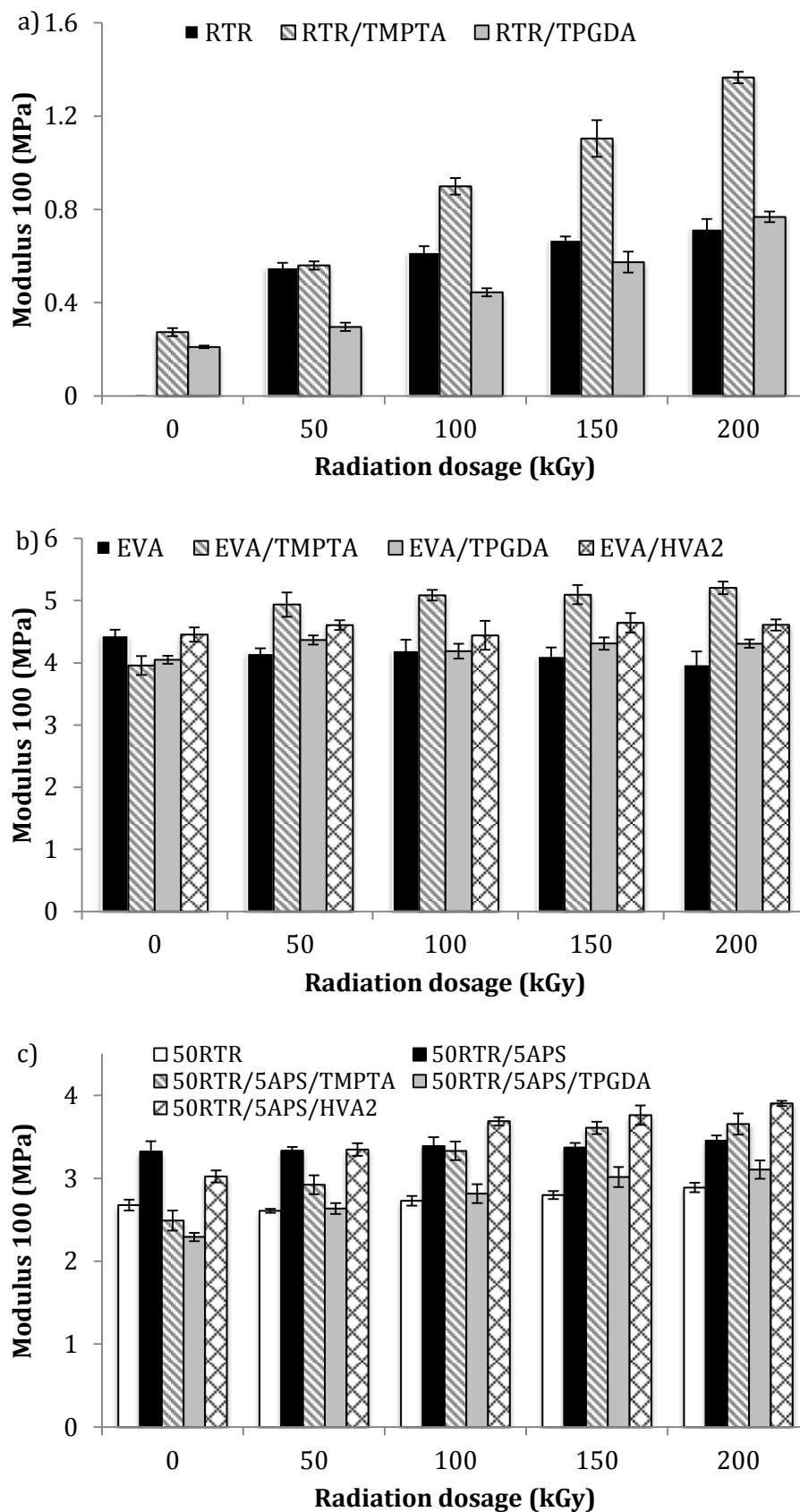


Figure 6.6 Effect of radiation sensitizers on modulus at 100% elongation of a) RTR, b) EVA and c) 50RTR/5APS blends at various radiation doses

modulus values relates to increase in irradiation induced crosslinks with the matrix, the lower modulus values recorded for TMPTA and TPGDA composition are in agreement with lubrication properties of the radiation sensitizers and restoration of elasticity (or ductility) of the RTR component of the blend.

6.4.4. Tear strength

Tremendous improvement was noted in tear strength of RTR in the presence of radiation sensitizer as depicted in Figure 6.7a. Restoration of elasticity of RTR by effective crosslink formation between two short rubber chains are the founding reasons for increased tear strength in RTR/TMPTA and RTR/TPGDA composition.

Similar to neat EVA, all the composition of EVA with radiation sensitizers displayed an increase at 50 kGy irradiation dose followed by a gradual drop with subsequent increase in irradiation dose (Figure 6.7). Excessive crosslink formation causes embrittlement of EVA matrix leading to the drop in tear strength beyond 50 kGy. As expected, the most and least prominent drop is observed in TMPTA and TPGDA, correlating to the crosslink density in the composition.

All 50RTR/5APS composition with radiation sensitizers displayed a slow rate of increase in tear strength up to 150 kGy irradiation dose, before falling slightly at 200 kGy irradiation dose. Similar to the trend observed in EVA, all the blends with radiation sensitizers had comparable tear strength values. This leads to an assumption that the tear strength of the blends are closely dependent on the EVA component. It is also contrary to the tensile properties of the blends, which were more dependent on the RTR component.

6.4.5. Hardness

Figure 6.8a shows the influence of radiation sensitizers on the hardness of RTR as a function of irradiation dose. The trend observed here was very similar to tensile modulus properties discussed earlier. TMPTA recorded higher hardness values compared to TPGDA. This is due to higher functionality of TMPTA attributing to higher crosslink density.

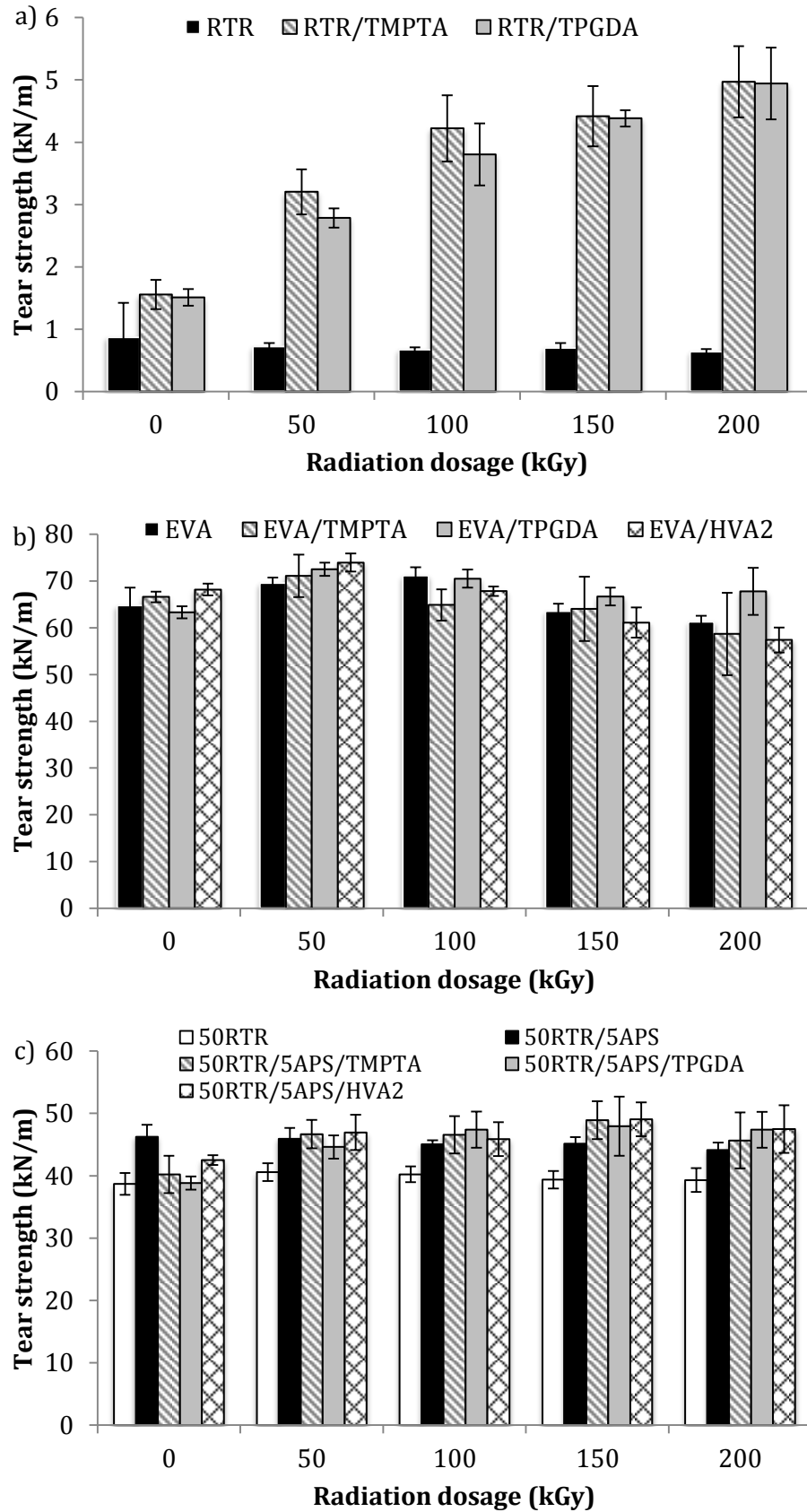


Figure 6.7 Effect of radiation sensitizer on tear strength of a) RTR, b) EVA and c) 50RTR/5APS blends at various radiation doses

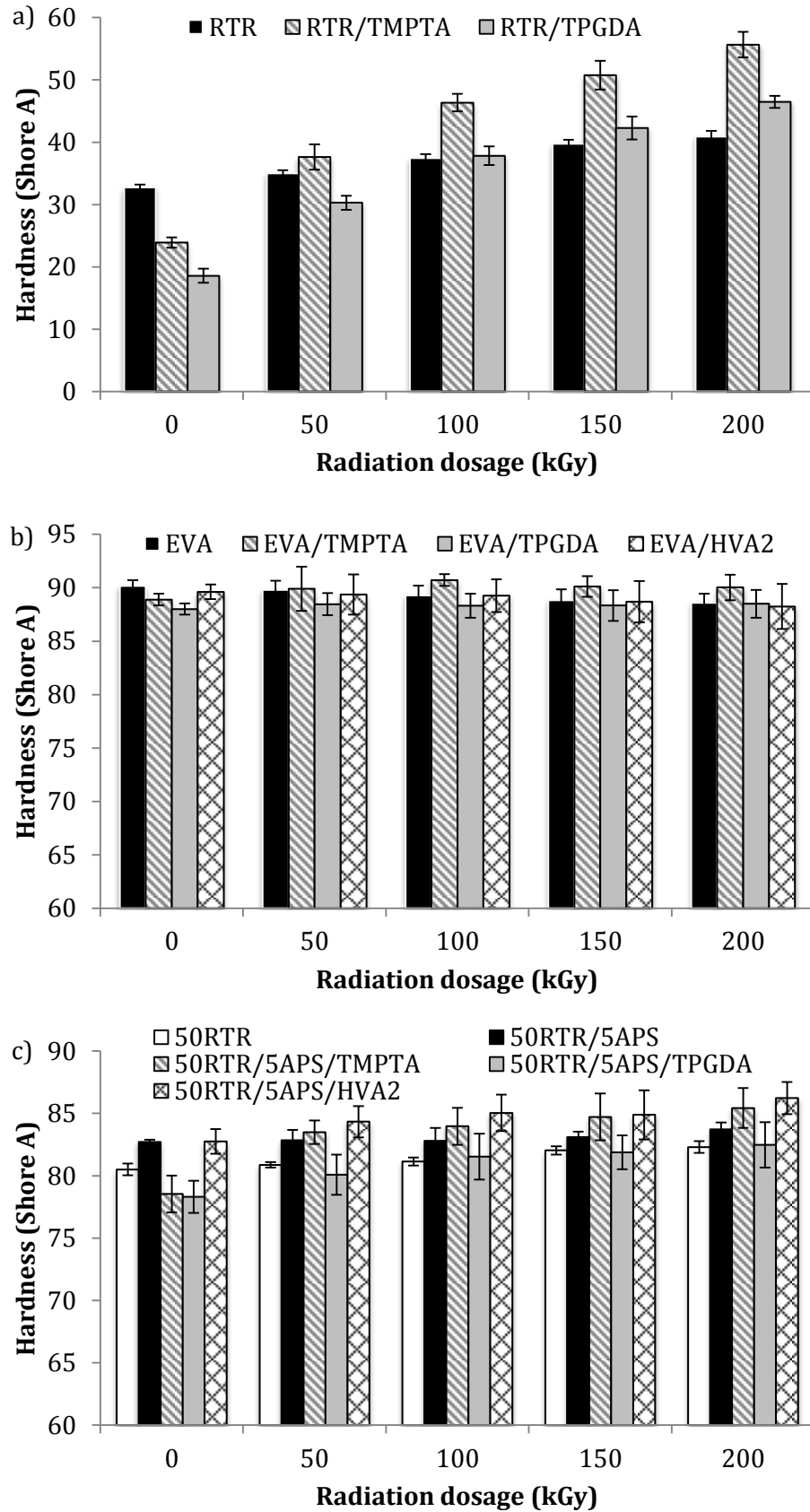


Figure 6.8 Effect of radiation sensitizers on hardness of a) RTR, b) EVA and c) 50RTR/5APS blends at various radiation doses

Influence of TMPTA, TPGDA and HVA2 on the hardness of EVA as a function of irradiation dose is depicted in Figure 6.8b. All composition of EVA with radiation sensitizers had comparable hardness values to EVA throughout the studied irradiation dose. Shore A hardness is less sensitive towards the changes of crosslink network in EVA matrix. Shore D hardness values might be more appropriate for irradiation crosslinked EVA in the presence of radiation sensitizers. However, it should be noted that the trend observed here is similar to the trend observed in tensile modulus of EVA.

Figure 6.8c depicts the hardness of 50RTR/5APS blends as a function of radiation sensitizers and irradiation dose. Again here, the trend observed is very similar to the trend in tensile modulus of 50RTR/5APS blends. 50RTR/5APS compositions with TMPTA recorded the highest hardness values closely followed by HVA2 and TPGDA. The reasons are similar to the discussion in tensile modulus section.

6.5. Morphological study

Figure 6.9 depicts the SEM micrographs of tensile fractured surface of RTR with TMPTA and TPGDA at 50 and 200 kGy irradiation doses. Similar to neat RTR (Figure 4.6), presence of filler was observed in both RTR/TMPTA and RTR/TPGDA (indicated by arrows). However, the filler particles are well embedded in the matrix unlike neat RTR (Figure 4.6) where voids were observed around the filler particles. Effective crosslink formation by TMPTA and TPGDA encapsulates the filler particles with the matrix thereby effectively increasing the tensile strength of RTR (Shen et al., 2013). Moreover, this could also be one of the reasons for dramatic improvement in the tear strength of RTR/TMPTA and RTR/TPGDA. The well embedded filler particle could restrict/arrest the propagation of tear leading to enhancement in tear strength. For RTR/TMPTA, the fracture surface displayed similar profile to that of neat RTR; whereby multiple irregular crack paths diverging in different direction were observed. However, the pattern of crack was less sharp and slightly tapered at different angles indicating more elastic nature compared to neat RTR (Figure 4.6). RTR/TPGDA on the other hand displayed better plastic fracture behavior compared to RTR/TMPTA with longer crack path diverging in one direction, less sharp and clear tapered angles. At 200 kGy, fracture surface

appeared much smoother than at 50 kGy, indicating decreasing elastic nature. However, the decrease is much noticeable in RTR/TMPTA than RTR/TPGDA. These again agrees well with discussion in sections 6.3 and 6.4 whereby TMPTA is found to have denser crosslink network upon irradiation leading to less ductile fracture at 200 kGy, as compared to TPGDA.

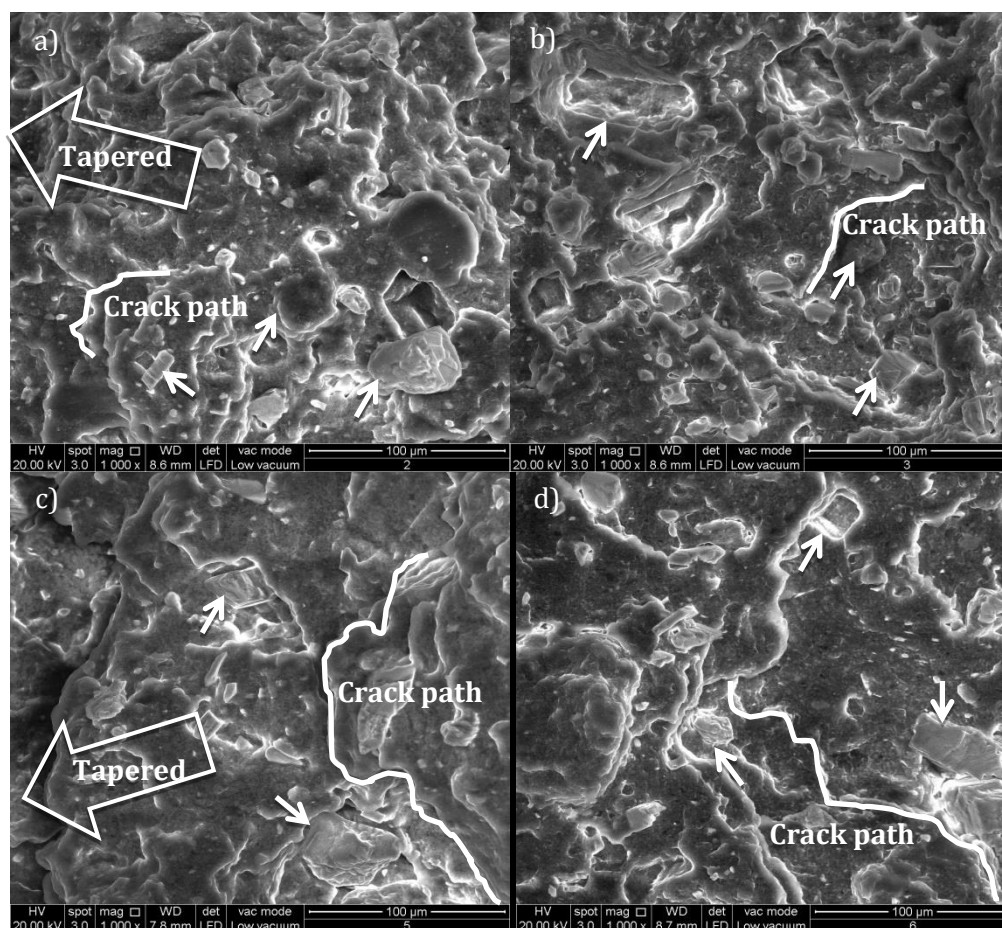


Figure 6.9 SEM micrographs of RTR composition with TMPTA (a,b) and TPGDA (c,d) at 50 kGy (a,c) and 200 kGy (b,d) irradiation doses

Figure 6.10 depicts the tensile fracture surface of EVA/TMPTA, EVA/TPGDA and EVA/HVA2 at 50 and 200 kGy irradiation doses. All EVA composition with radiation sensitizers displayed different fracture morphology compared to neat EVA matrix (Figure 4.8). Hence, one can conclude that addition of radiation sensitizers changes the molecular structure of EVA matrix through crosslink formation. The difference in crosslink network structures is responsible for the different types of fracture morphology of EVA matrix observed. EVA/TMPTA at

50 kGy irradiation dose displayed fibrillated waves elongating in specific direction. In neat EVA, tinier and lesser fibril structure was observed along the wavy lines. In EVA/TMPTA, however, heavy fibrillations were observed along the wavy lines ranging from tiny to larger sizes. Optimal tensile properties for EVA/TMPTA were observed at 50 kGy suggesting improvement in load bearing capacity due to formation of irradiation induced crosslinks. Upon 200 kGy irradiation, the fracture surface was smoother with minimal wavy lines accommodating large fibril structures. This is an indication of decreased ductility owing to increased crosslink density of EVA/TMPTA at 200 kGy irradiation dose.

EVA/TPGDA morphology had the closest resemblance to neat EVA (Figure 4.8). The fracture surface at 50 kGy irradiation dose displayed extensive formation of wavy lines with tiny fibril structures observed along the lines. Some of the fibrils did show extension, however it was thicker than the extended fibrils observed in neat EVA. Upon 200 kGy irradiation dose, the fracture surface of EVA/TPGDA was smoother with lesser wavy lines. This is associated with the increasing crosslink density which increases the brittleness of the matrix. However, presence of fibrils could still be observed along the available wavy lines. Furthermore, the formation of wavy lines was still unidirectional, which could be the reason behind good retention in elongation at break of EVA/TPGDA composition.

EVA/HVA2 composition had the most different fracture morphology in contrast to neat EVA (Figure 4.8). Though the tensile fracture surface also indicates ductile type failure, the formation of fibrils was inconsistent. There were several void on the fracture surface indicating regions of low strength in the EVA matrix. As speculated in section 6.3, the 4phr loading of HVA2 used in this study might be too high, creating highly crosslinked regions in the matrix. This highly crosslinked regions are stress concentration points appearing as voids observed on the fracture surface. Upon 200 kGy irradiation, fracture surface of EVA/HVA2 evolved into irregular discontinuous fracture paths with no fibril formation. Absence of fibril formation is an indication of decreased ductility of EVA/HVA2 composition, explaining the observed decrease in tensile strength and elongation at break.

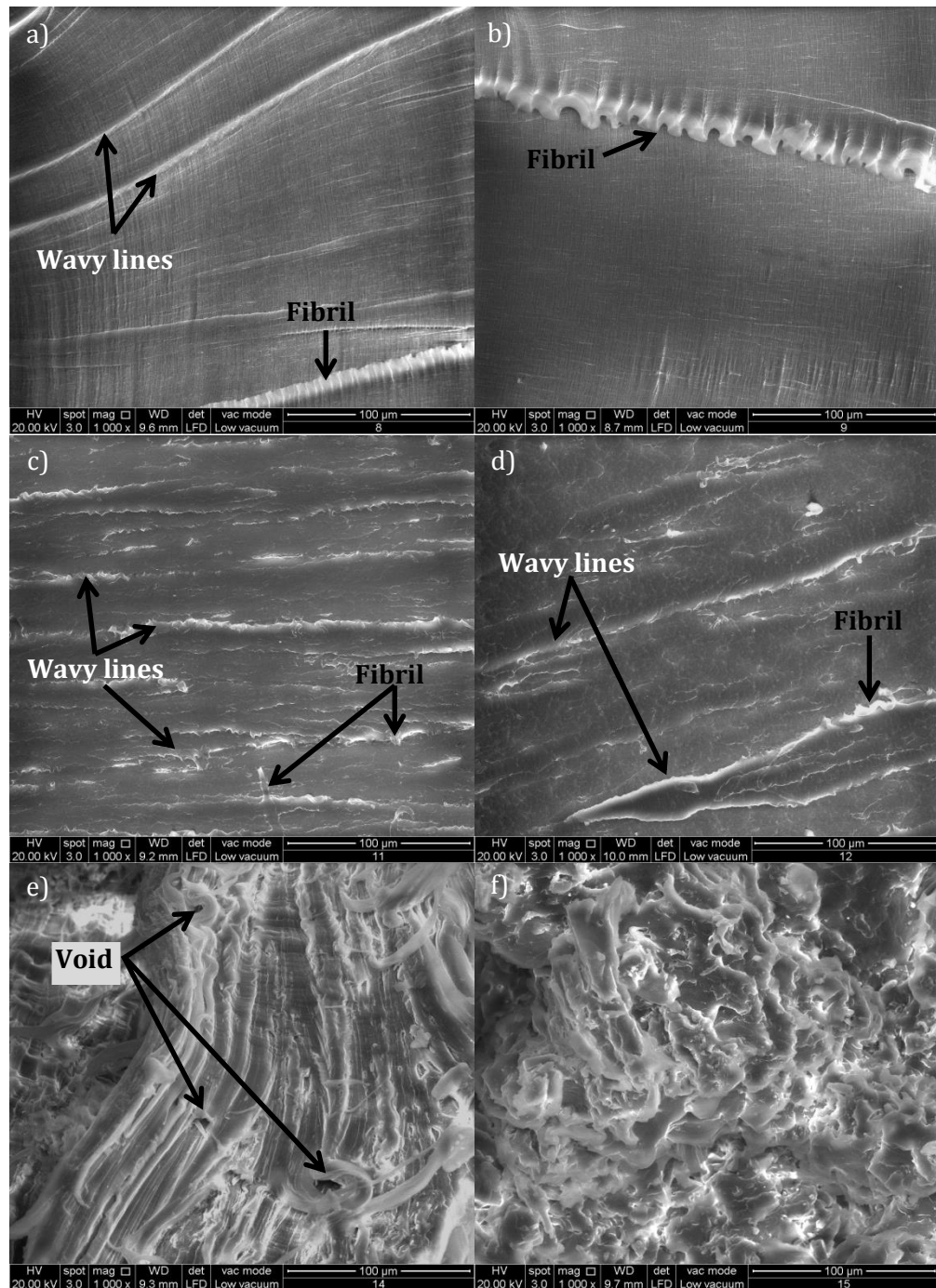


Figure 6.10 SEM micrographs of EVA composition with TMPTA (a,b), TPGDA (c,d) and HVA2 (e,f) at 50 kGy (a,c,e) and 200 kGy (b,d,f) irradiation doses

Figure 6.11 shows the tensile fracture surface of 50RTR/5APS in the presence of radiation sensitizers at 50 and 200 kGy irradiation doses. Morphological observation shows minimal changes occurred on EVA matrix of the blends at lower irradiation dose. No RTR particle pull out was observed, instead heavily embedded particle structures with some fracture characteristic was found on all

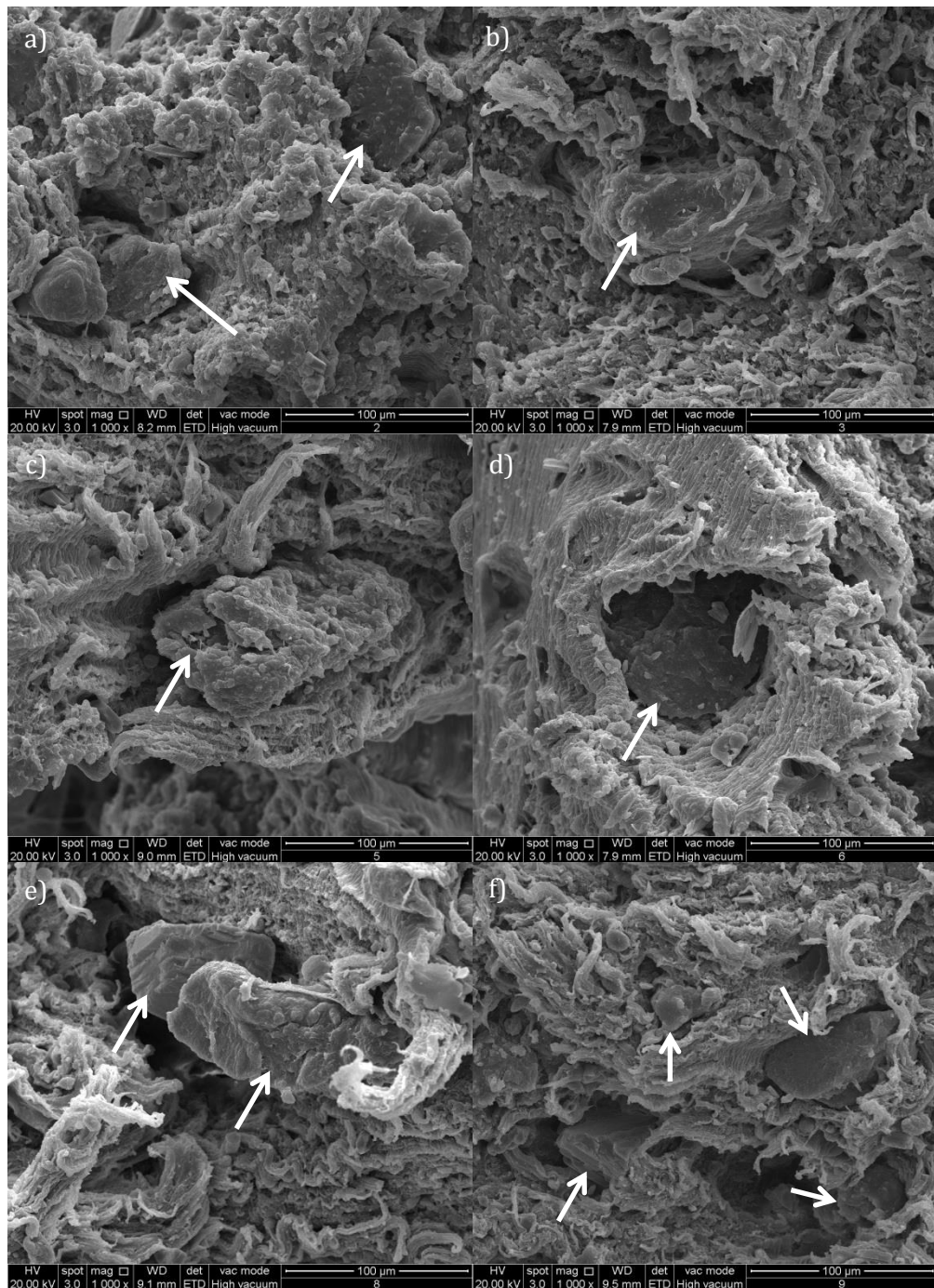


Figure 6.11 SEM micrographs of 50RTR/5APS composition with TMPTA (a,b), TPGDA (c,d) and HVA2 (e,f) at 50 kGy (a,c,e) and 200 kGy (b,d,f) irradiation doses

the blends at lower irradiation dose (indicated by arrows). This suggests the radiation sensitizers efficiently functions at the interface and the RTR regions of the blends (He et al., 2014). Enhanced compatibilization between two phases can be achieved with efficient placement of radiation sensitizers in the interphase

regions (Shin and Han, 2013). Radiation sensitizers' placed in the interphase regions form crosslinks between EVA matrix and RTR particles leading to more efficient stress transfer observed through the multiple fractured particles in the SEM micrographs. Fractured RTR particles with heavy coating and fully embedded RTR particles within EVA matrix are indications of well bonded phases (indicated by arrows). These lead to enhancement of the blends tensile strength in the presence of radiation sensitizers. HVA2 resembled the most ductile fracture with longer and finer fibril formations on EVA matrix at lower irradiation dose. At 200 kGy irradiation dose, all blends with radiation sensitizers displayed smoother fracture surface with lesser and thinner fibril formations. However, presence of embedded and fractured RTR particles could still be observed. Hence, at higher irradiation dose, the decrease observed in mechanical properties is due to decrease in the ductility of EVA matrix (Hassan et al., 2013b).

6.6. Thermal properties

A common problem with embarking on recycling projects is the difference in the properties of every different batch of recycled products. Every tire manufacturers have different formulation for different types of tire. This makes recycling of the tires harder as at current state of supply chain management, it is impossible to collect tires only from single source of manufacturer and types. Hence, tires from different manufacturer and types are commonly shredded, pulverized and reclaimed together; in the hope that the mix will give as similar properties as possible at every different batches of recycling process. However, the hope is farfetched as one could only achieve similarities in the macro related properties but not the molecular related properties. Similar trouble was faced in this study as different batch of RTR was used for each phase of study. Though the gel, mechanical and swelling properties were comparable at every batch, the thermal and dynamic mechanical properties clearly differed. Table 6.2 shows the difference in degradation temperature of neat RTR (phase 1/Chapter 4) and RTR used in the third phase (RTR/TMPTA 0 kGy). Obviously, the RTR used in third phase had higher rubber content, lower filler content and lower thermal stability. It is our inference that the portion of SBR rubber present in RTR used in third phase is higher which will be further explained in section 5.8. Hence,

direct comparison to the neat RTR (phase 1/Chapter 4) or neat 50RTR/5APS (phase 2/Chapter 5) could not be done. Effectiveness of radiation sensitizers was detailed by comparing the properties of irradiated RTR and blends (50 and 200 kGy) to the non-irradiated RTR and blends (0 kGy).

6.6.1. TGA analysis

Thermal stability of non-irradiated and irradiated RTR/TMPTA and RTR/TPGDA is illustrated in Figure 6.12 and tabulated in Table 6.2. The figure illustrates a slight improvement in thermal stability of RTR matrix upon irradiation in the presence of radiation sensitizer. TMPTA was found to improve the thermal stability at lower irradiation dose (50 kGy); whereas, TPGDA showed improvement at higher irradiation dose (200 kGy). In the presence of TMPTA, $T_{5\%}$, $T_{10\%}$, $T_{25\%}$ and $T_{\max 2}$ increased by about 5 to 20 °C at 50 kGy followed by a slight drop at 200 kGy. Similar observation was also noted in the residual weight. However, the thermal stabilities of all irradiated RTR/TMPTA were better than non-irradiated RTR/TMPTA. TPGDA on the other hand, only increased the $T_{5\%}$, $T_{10\%}$ and $T_{\max 2}$ by 11, 12 and 6 °C respectively, at 200 kGy irradiation dose. This is due to lower functionality of TPGDA which requires higher irradiation dose in order to introduce substantial molecular changes within the RTR structure. In both RTR/TMPTA and RTR/TPGDA composition, no changes in $T_{50\%}$ and $T_{\max 1}$ were observed. These two degradation temperatures are associated to the NR component of RTR, suggesting TMPTA and TPGDA did not change the molecular structure of NR phase of RTR.

Figure 6.13 shows the relationship between mass loss and increasing temperature of EVA/TMPTA, EVA/TPGDA and EVA/HVA2 at different irradiation doses. The overview from the figure suggests that TMPTA does not change the thermal stability, TPGDA improves and HVA2 decreases the thermal stability of EVA matrix upon irradiation. The associated degradation temperatures of EVA composition with radiation sensitizers have been listed in Table 6.3. TMPTA was found to increase the degradation temperatures between 0 to 50 wt% mass loss by 3 to 10 °C upon irradiation. Non-irradiated TPGDA on the other hand, recorded lowest degradation temperature of $T_{5\%}$ and $T_{10\%}$ due to evaporation of unreacted liquid TPGDA. Upon irradiation a small increment in

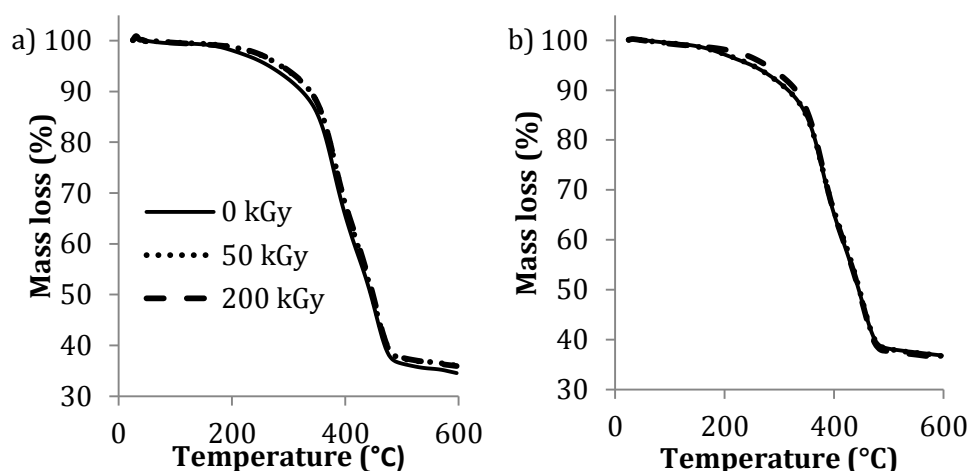


Figure 6.12 Typical TGA curve of a) RTR/TMPTA and b) RTR/TPGDA at different irradiation doses

Table 6.2 Degradation temperatures and residual weight of RTR, RTR/TMPTA and RTR/TPGDA at different irradiation doses

Designation	Radiation dose (kGy)	Degradation temperatures (°C)						Residual weight (wt%)
		T _{5%}	T _{10%}	T _{25%}	T _{50%}	T _{max1}	T _{max2}	
RTR	0	282.0	333.3	399.2	497.2	390.3	443.9	48.80
RTR/	0	264.2	322.5	380.0	445	380.3	450.3	34.55
TMPTA	50	287.5	340.0	392.5	445	380.3	456.7	36.01
	200	287.5	334.2	380.3	445	380.3	456.7	35.94
RTR/	0	264.7	316.7	375.0	445	380.3	450.3	36.81
TPGDA	50	264.7	316.7	375.0	445	380.3	450.3	36.71
	200	275.8	328.3	375.0	445	380.3	456.7	36.32

the degradation temperature was observed in EVA/TPGDA composition (Dutta et al., 1995). However, irradiation leads to decrease in the degradation temperatures of EVA/HVA2. Improvement in thermal stability in EVA/TMPTA and EVA/TPGDA is linked to irradiation induced crosslinking (El-Nemr, 2011). Whereas, the decrease observed in EVA/HVA2 sample is linked to prevalence of chain scissioning in EVA matrix in the presence of HVA2. This again suggests the 4phr loading of HVA2 used in this study might be too high for EVA system. Radiation sensitizers generate free radicals upon irradiation. These free radicals interact with polymer chains, to form crosslinking and/or chains scissions. However, excess amount of radiation sensitizers generates excess amount of free

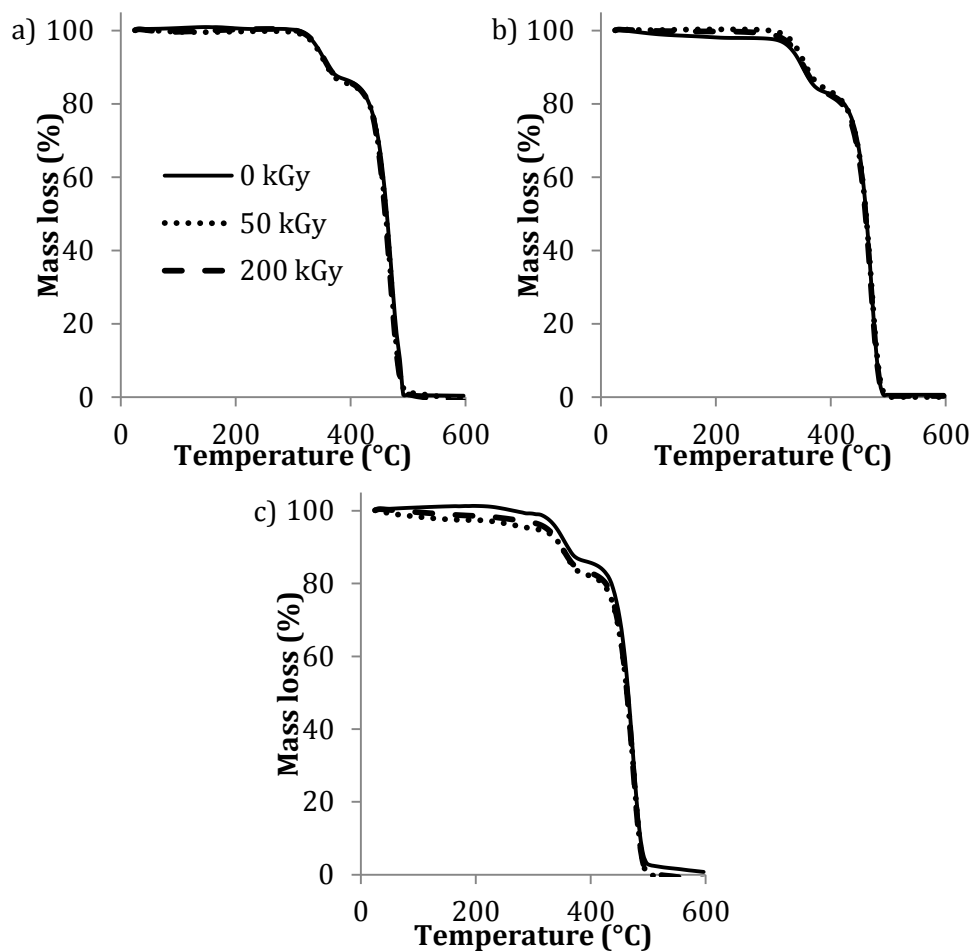


Figure 6.13 Typical TGA curve of a) EVA/TPMPTA, b) EVA/TPGDA and c) EVA/HVA2 compositions at different irradiation doses

Table 6.3 Degradation temperatures and residual weight of EVA/TMPTA and EVA/TPGDA and EVA/HVA2 at different irradiation doses

Designation	Radiation dose(kGy)	Degradation temperatures (°C)						Residual weight (wt%)
		T _{5%}	T _{10%}	T _{25%}	T _{50%}	T _{max1}	T _{max2}	
EVA/	0	340.0	360.3	431.5	462.5	351.7	468.3	0.4
TMPTA	50	345.8	363.3	442.5	465.0	351.7	468.3	0
	200	345.8	363.3	442.5	459.0	351.7	468.3	0
EVA/	0	328.3	351.7	431.7	462.5	351.7	468.3	0
TPGDA	50	340.0	357.5	439.7	462.5	351.7	468.3	0
	200	334.2	351.7	433.3	462.5	351.7	468.3	0
EVA/	0	340.0	357.5	445.0	465.0	351.7	474.2	0.8
HVA2	50	339.2	351.7	439.2	462.5	363.3	474.2	0
	200	322.5	351.7	439.2	462.5	351.7	474.2	0

radicals leading to prevalent scissions of the rubber chains. Therefore, crosslinks and chain scissions are associated with increased and decreased thermal stability, respectively (Ahmed et al., 2000, Hassan et al., 2013b, Wang et al., 2009b).

Figure 6.14 shows the typical TGA curve of 50RTR/5APS/TMPTA, 50RTR/5APS/TPGDA and 50RTR/5APS/HVA2 compositions. Overview of the figure suggests little to no influence of radiation sensitizers on thermal stability of 50RTR/5APS blends. Table 6.4 lists the degradation temperatures and residual weights of 50RTR/5APS blends in the presence of radiation sensitizers at different irradiation doses. Presence of TMPTA, TPGDA and HVA2 improved the thermal stability of 50RTR/5APS blends slightly. No decrease in degradation

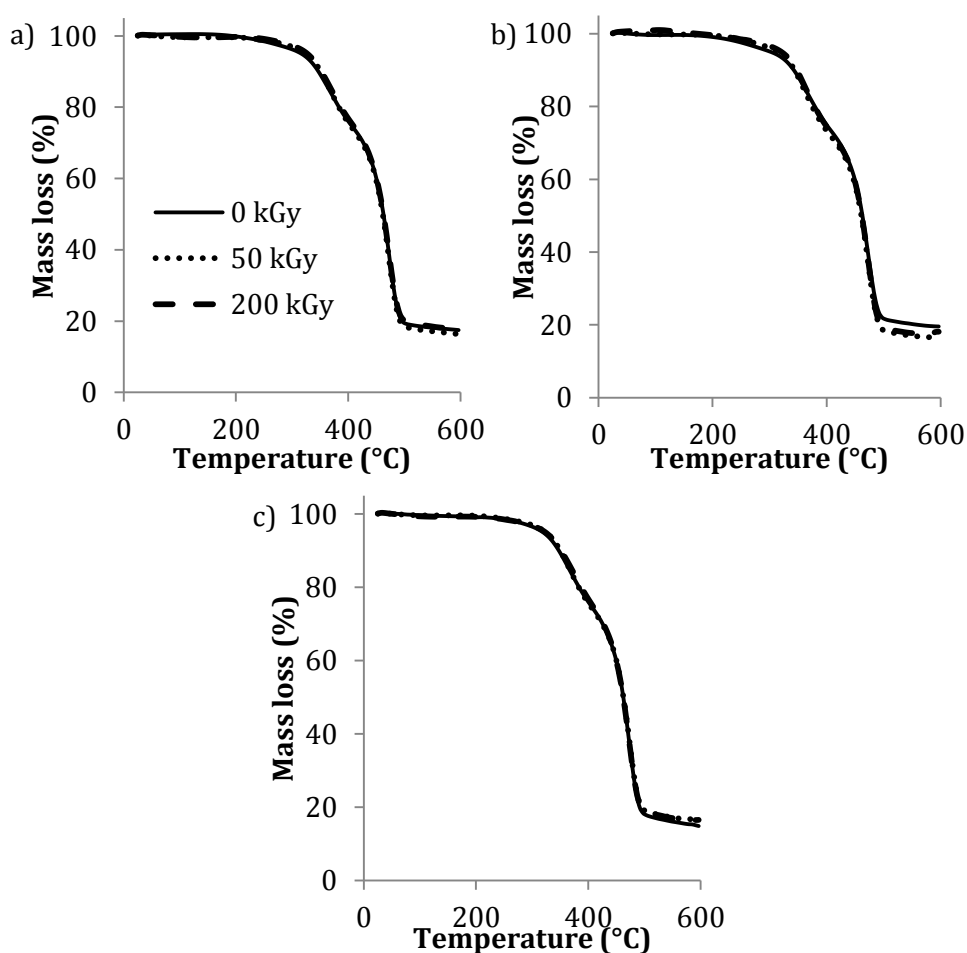


Figure 6.14 Typical TGA curve of a) 50RTR/5APS/TMPTA, b) 50RTR/5APS/TPGDA and c) 50RTR/5APS/HVA2 compositions at different irradiation doses

Table 6.4 Degradation temperatures and residual weight of 50RTR/5APS/TMPTA and 50RTR/5APS/TPGDA and 50RTR/5APS/HVA2 at different irradiation doses

Designation	Radiation dose(kGy)	Degradation temperatures (°C)						Residual weight (wt%)
		T _{5%}	T _{10%}	T _{25%}	T _{50%}	T _{max1}	T _{max2}	
50RTR/ 5APS/ TMPTA	0	316.7	345.8	404.2	462.5	375.0	474.2	17.4
	50	322.5	351.7	404.2	462.5	369.2	474.2	16.3
	200	328.3	351.7	410.0	462.5	369.2	474.2	17.8
50RTR/ 5APS/ TPGDA	0	299.2	340.0	398.3	462.5	369.2	474.2	19.6
	50	316.7	345.8	392.5	462.5	363.3	474.2	16.5
	200	322.5	345.8	398.3	462.5	363.3	474.2	18.1
50RTR/ 5APS/ HVA2	0	316.7	345.8	404.2	462.5	363.3	474.2	14.9
	50	322.5	351.7	404.2	462.5	363.3	474.2	16.7
	200	322.5	351.7	404.2	462.5	380.3	474.2	16.5

temperatures was observed indicating no substantial degradation has taken place in these blends (Noriman et al., 2010). HVA2 was more efficient in crosslinking the EVA and RTR components together as evident from increase in T_{max1} and T_{max2} of the blends upon irradiation (Shin and Han, 2013). While TPGDA was the least effective in increasing the thermal degradation temperatures owing to lower crosslink density observed in the 50RTR/5APS/TPGDA.

6.6.2. DSC analysis

Figure 6.15 illustrates the influence of radiation sensitizers on crystallization behavior of EVA as a function of irradiation dose. Trend observed in crystallization and melting temperature was rather similar. Before irradiation, presence of radiation sensitizers increased the crystallization temperature and decreased the melting temperature of EVA minutely. Before irradiation, radiation sensitizers were present as impurities in EVA matrix, performing as nucleating agent hence increasing the crystallization temperature minutely (Rytlewski et al., 2010). However, the presence of these radiation sensitizers as impurities also causes formation of imperfect crystals leading to lower melting temperatures of EVA (Maziad and Hassan, 2007). Upon irradiation, the

crystallization temperature decreased rapidly in all composition. However, TMPTA caused more rigorous drop, while TPGDA and HVA2 caused less rigorous drop (and higher crystallization temperature) in comparison to neat EVA. TMPTA was responsible of the denser crosslink formations in EVA matrix, hence, reducing the amount of free EVA chain capable/involved in the crystal formation process (Dutta et al., 1996). TPGDA was acting as lubricant within EVA chain, allowing increased flexibility of EVA chain to form crystals. Whereas, TGA analysis showed degradation of EVA in the presence of HVA2, leading to lower molecular weight EVA present in EVA/HVA2 composition during crystallization. These were the reasons driving the differences observed in crystallization temperature changes over increasing irradiation dose. Similar to crystallization temperature, rapid decrease in melting temperature was also observed with increasing irradiation dose. More rigorous decrease was observed in TMPTA and TPGDA composition compared to neat EVA. Whereas, drop in melting temperature of EVA/HVA2 followed closely behind neat EVA. These drops are associated with the increase in crosslink density which limits the amount of free EVA chains which could participate in chain re-arrangement and re-crystallization, causing formation of imperfect, smaller and lesser crystal in the EVA composition with radiation sensitizers. Interestingly, compared to neat EVA, melting temperature of EVA/TMPTA shows an increase at 200 kGy.

Heat of fusion and crystallinity of EVA markedly decreased with increasing irradiation dose in the presence of radiation sensitizers. Again, the most rigorous drop was observed in the presence of TMPTA, followed by HVA2 and TPGDA, which correlates to the crosslink density of EVA network in the respective composition (Dutta et al., 1996). EVA/TMPTA composition displayed a broad peak formation between 100 to 150 kGy beyond which, a slight increase in heat of fusion and crystallinity was observed. The peak formation signals the optimal crosslink formation in EVA/TMPTA. Whereas, the slight inclination in the increase of heat of fusion and crystallinity could be due to embrittlement of EVA network or increased formation of functional group. This allows closer packing of EVA chain, hence contributing to the observation noted at higher irradiation dose of EVA/TMPTA.

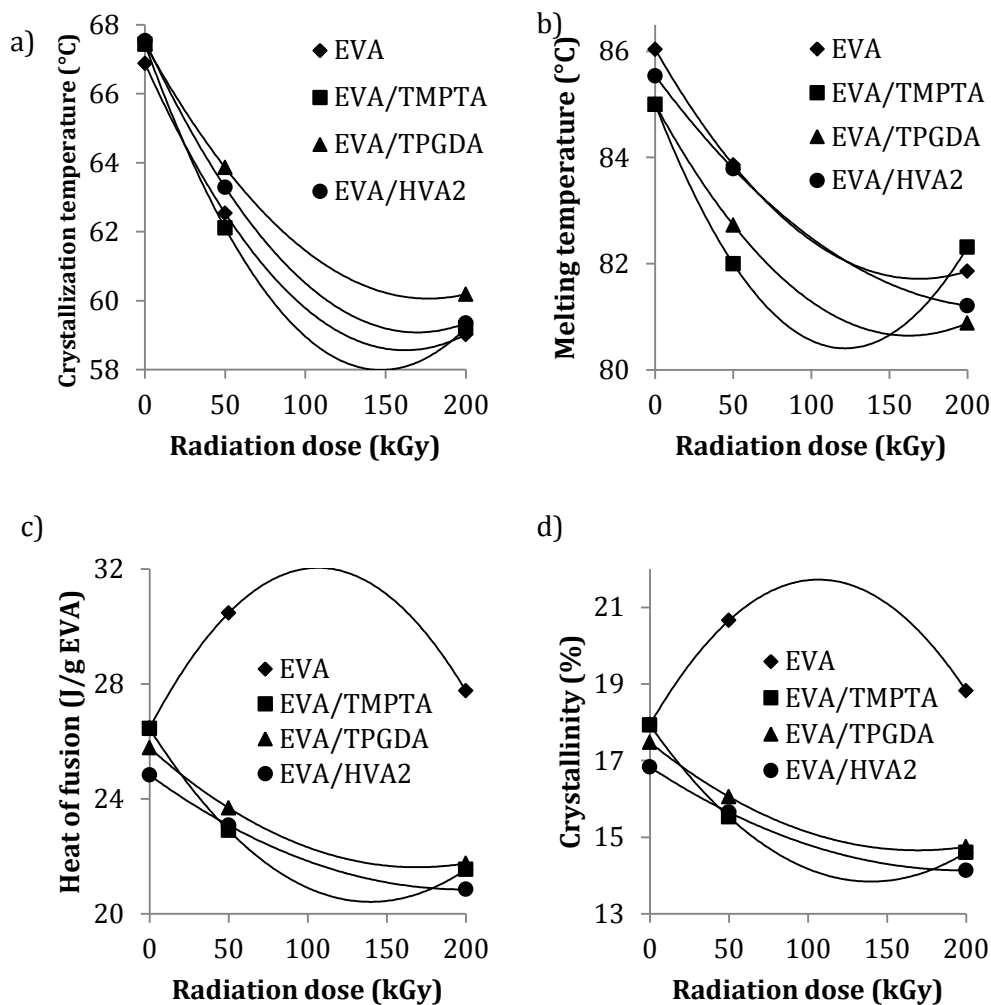


Figure 6.15 Effect of irradiation dose on a) crystallization temperature, b) melting temperature, c) heat of fusion and d) crystallinity of EVA in the presence of TMPTA, TPGDA and HVA2

Figure 6.16 depicts the effect of radiation sensitizers on crystallization behavior of 50RTR/5APS blend as a function of irradiation dose. All 50RTR/5APS compositions with radiation sensitizer recorded a decrease in the crystallization temperature compared to neat 50RTR/5APS blend throughout the studied radiation doses. The relationship between crystallization and irradiation dose was almost a linear. Presence of TMPTA and HVA2 caused a more rigorous drop in the crystallization temperature with increasing irradiation dose. Whereas, TPGDA displayed less rigorous drop in crystallization temperature at lower irradiation dose, which then was comparable to TMPTA and HVA2 composition at higher irradiation dose. Similar to crystallization temperature, melting temperature of 50RTR/5APS/radiation sensitizer compositions also displayed an almost linear like relationship with increasing irradiation dose. Generally,

increase in irradiation dose causes decrease in the melting temperature of the matrix (Hassan et al., 2014b). The rate of decrease can be listed as follows; TMPTA>HVA2>TPGDA. These are again, in relation to the crosslink density of the matrix, correlating to the functionality of the radiation sensitizers. A lower crosslink density is expected in TPGDA due to the presence of only two functional groups.

Figure 6.16 (c and d) depict the relationship between irradiation doses and presence of radiation sensitizers on the heat of fusion and crystallinity of 50RTR/5APS blends. Presence of TMPTA and HVA2 causes substantial decrease of heat of fusion and crystallinity of 50RTR/5APS blends. This is expected as crosslinking of the EVA component of 50RTR/5APS blend causes formation of lesser, defected and/or smaller crystals. TPGDA composition on the other hand displayed an increase in heat of fusion and crystallization at lower irradiation dose followed by a drop at higher irradiation dose with a broad peak at about 50 to 100 kGy. However, the recorded values were always lower than neat 50RTR/5APS. TPGDA is a linear difunctional substance, capable of connecting two EVA macromolecular chains through irradiation induced crosslinking. Hence, it is believed TPGDA could act as a tie molecule, effectively increasing the length of EVA chain involved in rearrangement and recrystallization process (Svoboda et al., 2010). However, at higher irradiation dose, extensive amount of crosslinks are formed between already crosslinked EVA chain causing embrittlement and restricts the mobility of EVA chain. These explain the observed increase and decrease of crystallinity at lower and higher irradiation doses, respectively. It has been reported that electron beam irradiation of EVA/GTR blend in the presence of TPGDA had higher amount of primary crystal formation due to increased EVA chain mobility and flexibility (Ratnam et al., 2014).

A special note goes to 50RTR/5APS/HVA2 composition as it records minimal changes in all studied crystallization behavior before irradiation (0 kGy), as compared to neat 50RTR/5APS. This observation suggests that little to no changes/crosslinking occurred in the EVA phase of the blends before irradiation. This further supports the earlier inference where the gel content observed before irradiation in this blends was believed to be a contribution of crosslinks formed within the RTR phase of the blend. It is interesting to note the melting temperature of this blend remaining close to the values noted in neat

50RTR/5APS blend though there was a substantial decrease in the crystallinity, especially at lower irradiation doses. Positioning of HVA2 in the interfacial regions, forming crosslinks between RTR and EVA phases could allow for primary crystal growth in the bulk of EVA phase, hence no remarkable effect noted on the melting temperature, especially at lower irradiation dose. At higher irradiation dose, crosslinking process believed to proceed in the bulk of EVA phase causing formation of imperfect crystals, lowering the melting temperature (Hassan et al., 2014b).

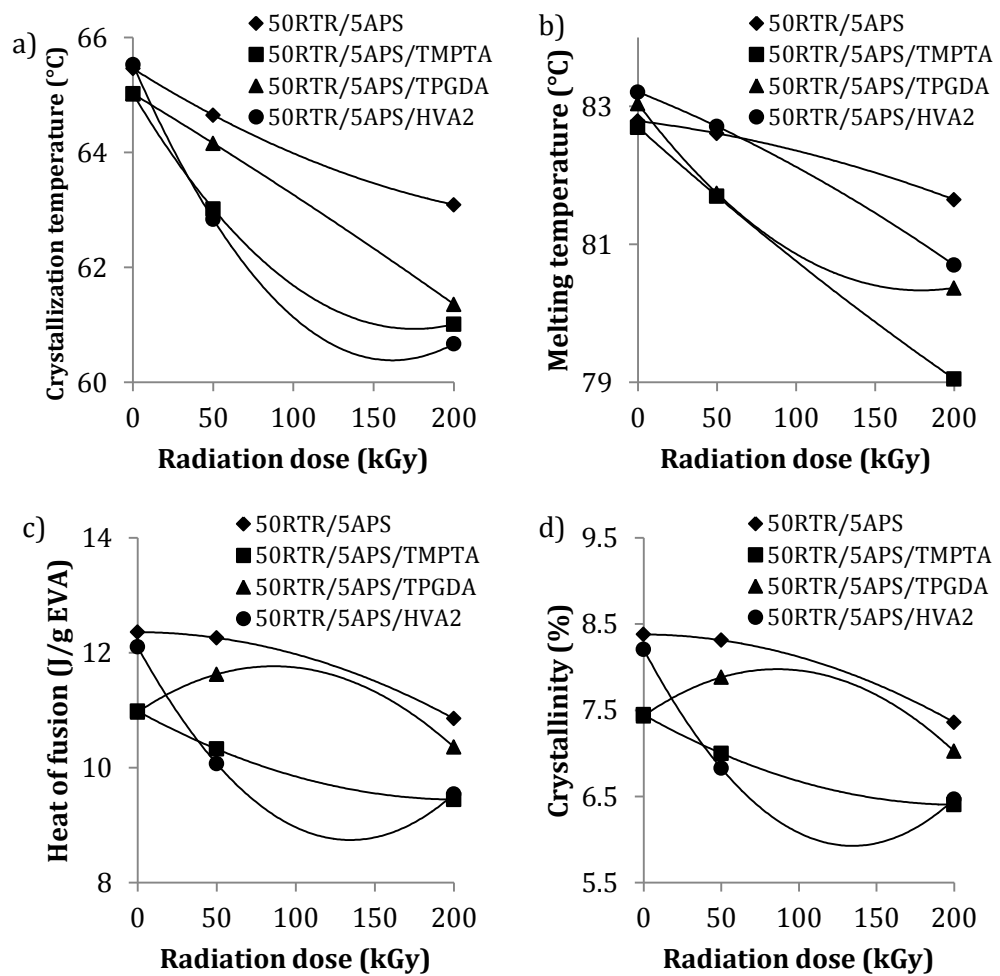


Figure 6.16 Effect of irradiation dose on a) crystallization temperature, b) melting temperature, c) heat of fusion and d) crystallinity of 50RTR/5APS blends in the presence of TMPTA, TPGDA and HVA2

6.7. Dynamic mechanical properties

6.7.1. Storage modulus

Figure 6.17a displays the influence of radiation sensitizers on the storage modulus of 50RTR/5APS before and after irradiation. All 50RTR/5APS blends in the presence of radiation sensitizers, before and after irradiation, displayed characteristic glassy, transition and rubbery regions of a typical storage modulus curve. Maximal glassy region storage modulus drops rapidly through transition region, which plateaus upon reaching rubbery regions. Table 6.5 summarizes storage modulus of the blends before and after irradiation, at different temperatures. The TPGDA composition before irradiation could not be tested as the sample deformed during cooling down to -100 °C, under minimal clamping force. Before irradiation, in comparison to 50RTR/5APS, TMPTA, composition recorded about 20% lower storage modulus in glassy and transition regions. The decrease was noted due to lubrication effect offered by TMPTA which decreases the bulk dynamic rigidity. HVA2 (0 kGy) blend composition, before irradiation displayed similar glassy region storage modulus which was lower in transition region and caught up back in the rubbery region as compared to non-irradiated neat 50RTR/5APS. Upon irradiation, storage modulus of TMPTA composition in glassy region improved by ≈ 1.5 times in view of TMPTA composition before irradiation. Whereas, in comparison to irradiated neat 50RTR/5APS blend, the glassy region storage modulus of TMPTA composition was higher by ≈ 350 MPa. The improvement in the storage modulus of blends in the presence of radiation sensitizer is due to acceleration of irradiation induced crosslinking of the blends (Vijayabaskar and Bhowmick, 2005). However, a dip was noticed in the storage modulus half way through transition region. Whereas, irradiated TPGDA composition had comparable storage modulus from -70 up to -25 °C, upon which the storage modulus was always superior to irradiated neat 50RTR/5APS. All blends with radiation sensitizers were found to have higher storage modulus in rubbery region. Changes noted half way through transition region through to rubbery regions was an effect of difference in the RTR used; which will be explained in more detail subsequently utilizing the loss modulus and tan delta values. Due to the difference in the RTR batch, direct correlations and comparison between the samples with radiation sensitizer to neat 50RTR/5APS is not feasible. Hence, discussion was focused on the influence of different radiation sensitizers on dynamic mechanical properties. Apparently, judging

from Table 6.5, irradiated HVA2 exhibits the highest storage modulus values followed by irradiated TPGDA and irradiated TMPTA compositions.

6.7.2. Loss modulus

Influence of radiation sensitizers on loss modulus of 50RTR/5APS blends before and after irradiation is depicted and listed in Figure 6.17b and Table 6.6, respectively. Loss modulus curve profile of blends with radiation sensitizers (utilizes RTR from phase 3), displayed formation of two peaks, each corresponding to either RTR (lower temperature) or EVA (higher temperature). This is contrary to findings in sections 4.7 and 5.8, whereby only single broad peak was observed due to partial miscibility of RTR and EVA. Past studies have shown that NR/EVA forms miscible to partially miscible blends (Yong, 2007, Mohamad et al., 2006) compared to SBR/EVA immiscible blend (Radhakrishnan et al., 2008, Soares et al., 2002). The RTR used in first and second phase of this work was rich in NR content while third phase RTR is suspected to have higher content of SBR, which results in immiscible blends of RTR/EVA. Hence, dual peak is observed on loss modulus curves in this third phase of work. SBR has higher rubbery region storage modulus compared to NR which explains the higher rubbery region storage modulus values observed in Figure 6.17a and Table 6.5 for blends with radiation sensitizer (utilizing RTR from third phase). 50RTR/5APS/TMPTA before irradiation displayed two peaks around -43 and -11 °C; corresponding to the glass transition temperature of RTR and EVA, respectively. The peak height recorded was 193 and 165 MPa, which is quite comparable in contrast to neat RTR and neat EVA (Phase 1/Chapter 4). Furthermore, presence of TMPTA causes difference in the segmental movement through promotion of matrix micro-heterogeneity, which could possibly cause a decrease in the loss modulus values (Ratnam et al., 2001b). Upon irradiation, a shift in the loss modulus peak temperature values towards the middle of both components, with almost two fold increase in the loss modulus values suggest improved compatibility between the two components. 50RTR/5APS/TPGDA upon irradiation displayed a distinct peak of RTR region with EVA peak appearing as a shoulder peak, similar to irradiated 50RTR/5APS/TMPTA. Though the peak temperature of irradiated TPGDA composition associates closely to irradiated TMPTA composition, the loss modulus values recorded for RTR phase was lower. This indicates irradiated TPGDA composition is less

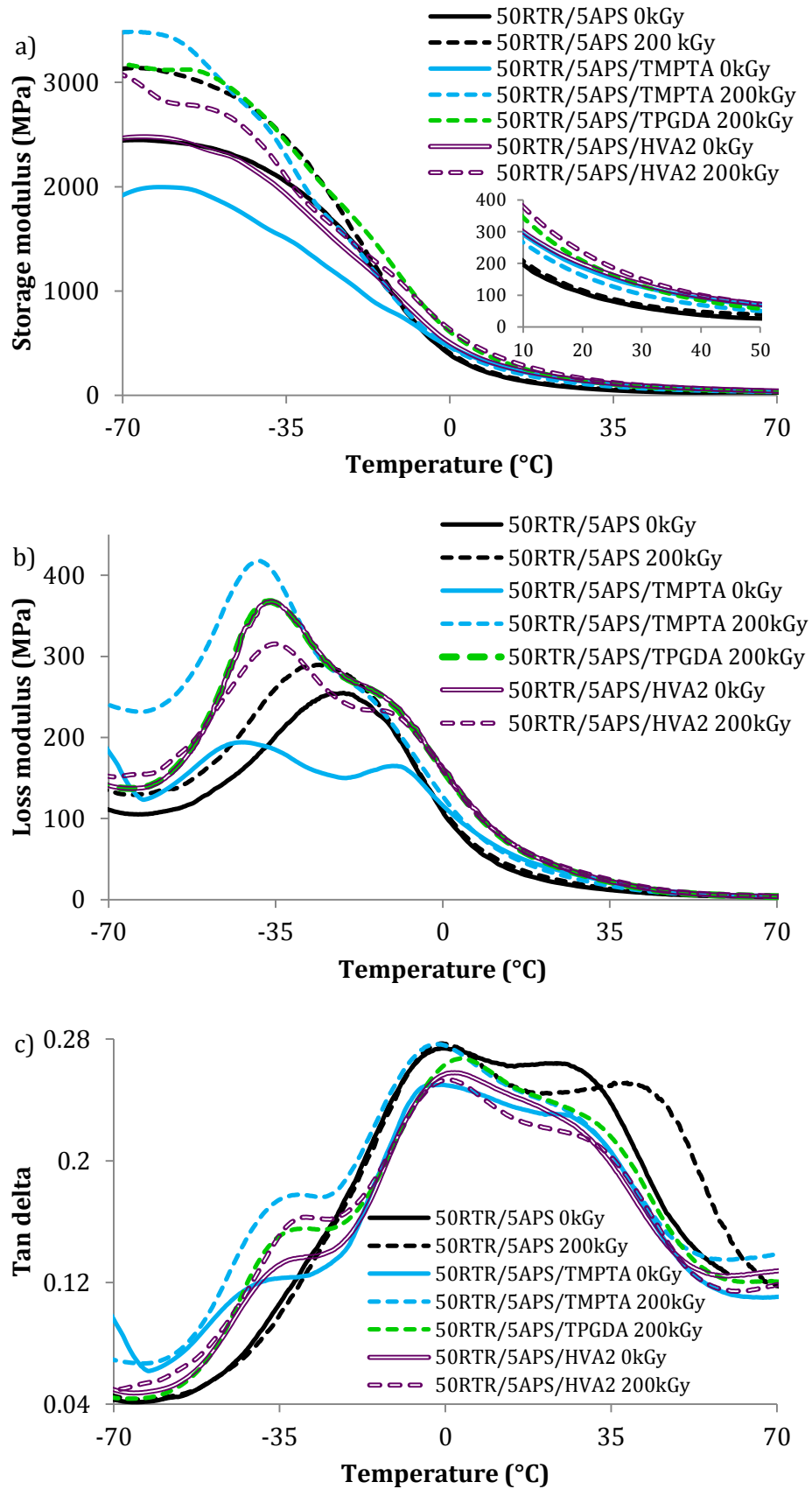


Figure 6.17 Dynamic mechanical properties; a) storage modulus, b) loss modulus and c) $\tan \delta$ of 50RTR/5APS in the presence of radiation sensitizer

Table 6.5 Storage modulus of 50RTR/5APS, 50RTR/5APS/TMPTA, 50RTR/5APS/TPGDA and 50RTR/5APS/HVA2 at different temperature, before and after irradiation

Temperature (°C)	Storage Modulus (MPa)							
	-25		0		20		40	
Radiation dose (kGy)	0	200	0	200	0	200	0	200
50RTR/5APS	1688	1896	390.3	398.8	106.8	115.0	37.46	47.73
50RTR/5APS/ TMPTA	1197	1658	466.2	460.5	187.6	162.2	90.96	69.15
50RTR/5APS/ TPGDA	-	1912	-	611.4	-	209.1	-	83.73
50RTR/5APS/ HVA2	1512	1623	500.7	620.4	198.3	234.1	95.67	99.24

Table 6.6 Values corresponding to peak of loss modulus and tan delta curve of 50RTR/5APS, 50RTR/5APS/TMPTA, 50RTR/5APS/TPGDA and 50RTR/5APS/HVA2

DMA properties	Loss modulus				Tan delta			
	Temperature (°C)		Height (MPa)		Temperature (°C)		Height	
Radiation dose (kGy)	0	200	0	200	0	200	0	200
50RTR/5APS	-23.2	-27.6	288.7	254.6	-0.56	-0.20	0.277	0.274
50RTR/5APS/ TMPTA	-43.7	-39.9	193.2	414.9	-39.6	-33.7	0.120	0.176
50RTR/5APS/ TPGDA	-10.9	-19.1	164.6	267.1	-3.7	-3.40	0.250	0.276
50RTR/5APS/ HVA2	-	-38.4	-	363.0	-	-34.4	-	0.152
		-15.9		261.4		1.57		0.266
50RTR/5APS/ HVA2	-37.8	-36.5	363.6	313.5	-34.2	-32.2	0.133	0.160
	-11.1	-13.4	245.7	233.5	0.15	-0.78	0.257	0.253

elastic compared to irradiated TMPTA composition which is contradictory to the observed gel values in section 6.3. Trifunctional TMPTA achieved optimal crosslink density upon 50 kGy irradiation dose and further increase in irradiation dose would promote crosslinking between already crosslinked macromolecular chains which causes matrix embrittlement (Peng et al., 1993). TPGDA is a difunctional monomer; higher irradiation dose is needed to attain optimal crosslink density. Since the DMA studies were conducted on samples

irradiated at 200 kGy, TPGDA composition displayed lower loss modulus peak values compared to TMPTA composition. At 200 kGy, TMPTA composition would have undergone far more severe embrittlement compared to equivalent TPGDA composition (Han et al., 2004). 50RTR/5APS/HVA2 before irradiation had almost identical loss modulus behavior as off irradiated 50RTR/5APS/TPGDA. The temperature corresponding to loss modulus peak of RTR phase in 50RTR/5APS/HVA2 composition before irradiation was -37.8 °C, nearly 7 °C higher than non-irradiated TMPTA composition. These findings are indicative of HVA2's potential to crosslink RTR rubber phase even before irradiation (Du et al., 2005, Magioli et al., 2010). HVA2 composition, upon irradiation, also showed tendency for the peak of loss modulus temperatures of RTR and EVA shifting towards each other. This indicates both RTR and EVA phase have been co-crosslinked upon irradiation in the presence of HVA2, improving the compatibility of the blends (Magioli et al., 2010). However, the loss modulus values corresponding to the peak of irradiated HVA2 composition decreased by 50 and 10 MPa for RTR and EVA phase, respectively, compared to their non-irradiated counterpart. Effective formation of irradiation induced crosslinking in the presence of HVA2 limits the mobility of the macromolecular chains, hence reducing the loss modulus properties of the blends.

6.7.3. *Tan delta*

Figure 6.17c displays the tan delta properties of 50RTR/5APS/radiation sensitizers' composition before and after irradiation. A peak formation between -50 to -24 °C in the composition with radiation sensitizers was noted, which was not present in the neat 50RTR/5APS blends. This peak is observed due to higher SBR percentage present in RTR which is immiscible with EVA. The height and temperature associated with the peak of tan delta profile has been summarized in Table 6.6. The observation was similar to observation reported in loss modulus properties. Tan delta values of irradiated 50RTR/5APS blends in the presence of radiation sensitizers increased in the order of: TMPTA < TPGDA < HVA2. The breadth of tan delta was neither affected in the presence of radiation sensitizers nor irradiation. Heterogeneity and oxidative degradation were limited due to efficiency of radiation induced crosslink formation in the blend composition with radiation sensitizers.

6.8. Equilibrium swelling

The sorption behavior of RTR, EVA and 50RTR/5APS blends in the presence of radiation sensitizers at 100 kGy irradiation dose are presented as mol uptake, Q_t , of toluene by 100g of the polymer as a function of square root of time in Figure 6.18. All blend compositions displayed a relatively fast initial rate of toluene uptake until attaining equilibrium uptake.

Upon 100 kGy irradiation dose, RTR/TMPTA and RTR/TPGDA recorded higher equilibrium uptake compared to RTR, even though both composition had higher gel content values. As explained in sections 6.6 and 6.7, higher percentage of SBR was speculated to be present in RTR used in this phase of study. SBR contains bulky aromatic styrene group, which restricts close packing of macromolecular chains. Hence, more free volumes are present in this sample for penetration of toluene molecules. This explains a rather high toluene uptake in RTR/TMPTA and RTR/TPGDA compositions. TPGDA composition's higher equilibrium uptake is bound to be due to lower crosslink density of the blend compared TMPTA composition.

All EVA composition with radiation sensitizers had lower toluene uptake compared to neat EVA at 100 kGy irradiation dose. The equilibrium toluene uptake followed a similar trend observed in gel content analysis. This enhances the fact that crosslink network structure greatly contributes to the sorption behavior of EVA (Yasin et al., 2002).

At 100 kGy irradiation dose, 50RTR/5APS/TMPTA and 50RTR/5APS/HVA2 composition had lower toluene uptake, while 50RTR/5APS/TPGDA had higher toluene uptake, compared to neat 50RTR/5APS blend. TMPTA and HVA2 had higher gel content indicating more crosslinks are formed in these compositions leading to lower mobility of macromolecular chains, creating a torturous path for toluene molecule diffusion. TPGDA composition, though displayed higher gel values than neat 50RTR/5APS, had high toluene uptake. TPGDA performs as a lubricating agent in the bulk matrix and also a linear reactive difunctional monomer that form linear crosslinks between macromolecular chains. Combination of chain mobility and linear crosslinks increases free volume in the sample facilitating toluene molecule diffusion, thereby, increasing the net toluene uptake.

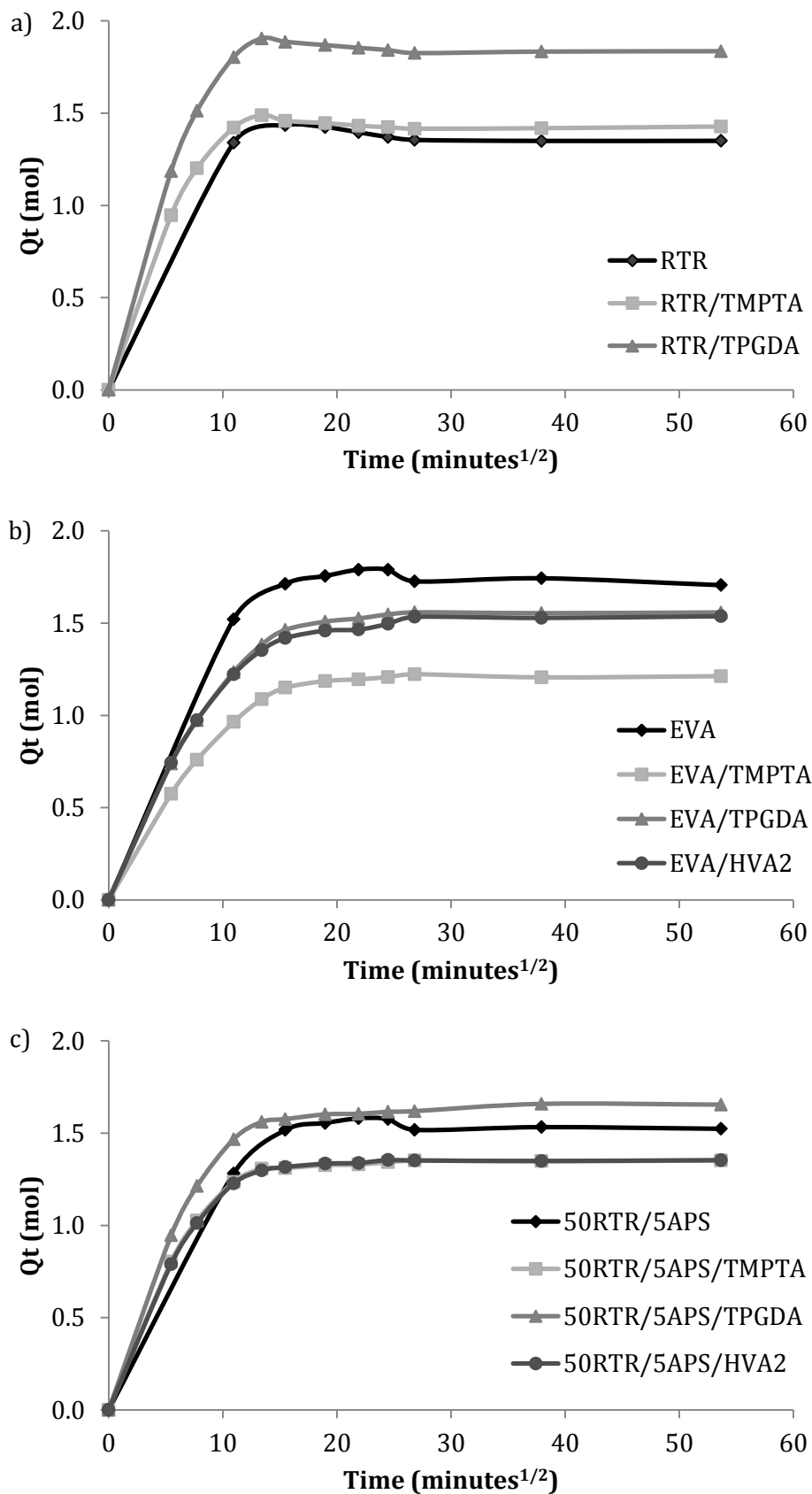


Figure 6.18 Sorption behaviour of a) RTR, b) EVA and c) 50RTR/5APS under the influence of TMPTA, TPGDA and HVA2 at 100 kGy irradiation dose

6.8.1. Empirical analysis

Table 6.7 lists the sorption parameters of 50RTR/5APS, 50RTR/5APS/TMPTA, 50RTR/5APS/TPGDA and 50RTR/5APS/HVA2 compositions at 0, 100 and 200 kGy irradiation dose. Values of n , remained between 0.5 to 1.0, indicating an anomalous sorption behavior. Throughout the studied irradiation doses, all radiation sensitizers' compositions recorded lower n values compared to neat 50RTR/5APS blend. Effective formation of irradiation induced crosslink in the presence of radiation sensitizers' forms dense network, thereby, decreasing penetration of toluene molecules into the samples. This leads to faster reach to equilibrium and translated as lower n values in irradiated samples. Whereas, values of k representing structural feature and matrix's interaction with toluene, recorded a decrease upon irradiation and stabilizes upon further increase in irradiation dose. However, all k values of radiation sensitizers' compositions were slightly higher than neat 50RTR/5APS blend, throughout the studied doses.

Table 6.7 Different sorption parameters of 50RTR/5APS, 50RTR/5APS/TMPTA, 50RTR/5APS/TPGDA and 50RTR/5APS/HVA2 compositions before and after irradiation

Parameter	Radiation dose	Designation			
		5APS	TMPTA	TPGDA	HVA2
n (log min ^{1/2})	0	0.62	0.53	0.55	0.44
	100	0.59	0.55	0.57	0.56
	200	0.61	0.54	0.54	0.56
k	0	0.17	0.26	0.25	0.41
	100	0.19	0.24	0.23	0.23
	200	0.18	0.25	0.24	0.23
D (cm ² min ⁻¹)	0	4.32	5.88	5.78	8.69
	100	4.33	5.53	5.40	5.37
	200	4.14	5.59	5.40	5.31
S	0	2.48	2.58	2.59	2.48
	100	2.45	2.24	2.49	2.24
	200	2.41	2.13	2.33	2.13
P (cm ² min ⁻¹)	0	1.07	1.52	1.50	2.15
	100	1.02	1.24	1.34	1.21
	200	1.00	1.19	1.26	1.13

Kinetic parameter defining polymer segmental mobility, diffusion coefficient (D), decreased upon irradiation and stabilized upon further increase in irradiation dose for all 50RTR/5APS/radiation sensitizer compositions. Also, upon irradiation, the D values of radiation sensitizers' compositions had almost comparable values. Sorption behavior of a substance is only affected up to a certain crosslink network formation, upon which, minimal changes is observed in the sorption behavior. This was also observed with neat EVA's sorption behavior reported in section 4.8. Upon irradiation, TMPTA composition had the highest D values, followed closely by TPGDA composition and later by HVA2 composition. TMPTA compositions exhibit a denser network formation as observed from gel content analysis that lead to lower level of mobility, restricting toluene molecules penetration and faster reach to equilibrium. Although HVA2 had almost similar gel values to TMPTA it still recorded the lowest D values. This could possibly be due to much more prominent chain scission in HVA2 compositions compared to TMPTA and TPGDA. Additionally, one could observe the D value of neat 50RTR/5APS blend was lower than all the compositions with radiation sensitizers, throughout the studied irradiation dose. This is believed to be a consequence of higher content of SBR rubber (RTR from Phase 3) present in the blends with radiation sensitizers leading to more free volume in the RTR phase due to presence of bulky styrene group.

Sorption coefficient (S), decreased continuously with increasing irradiation dose in all 50RTR/5APS/radiation sensitizer compositions. Crosslinked network limits the ability of toluene molecules to diffuse into the samples, leading to lower equilibrium uptake in the samples. However, the S values were comparable between TMPTA and HVA2 compositions, while TPGDA recording slightly higher values. Sorption behavior of 50RTR/5APS compositions with radiation sensitizers is influenced by the nature of matrix mobility. TPGDA compositions displayed higher matrix mobility due to the lubricating nature of TPGDA, consequently leading to easier interaction between toluene molecules and matrix network. This leads to higher equilibrium uptake observed in the samples with TPGDA as radiation sensitizers.

Permeability coefficient (P), describing the net effect of diffusion and sorption characteristics of a compound, was found to decrease with increasing irradiation dose in all 50RTR/5APS composition in the presence of radiation sensitizers. This indicates the improvement in chemical stability of 50RTR/5APS blends due

to irradiation induced crosslinks in the presence of radiation sensitizers. However, the P values recorded were higher than neat 50RTR/5APS throughout the studied irradiation doses. This is a consequence of higher content of SBR rubber in RTR used in Phase 3 leading to higher D values. In the event where higher NR content rubber was used, surely a distinct improvement will be observed in the chemical stability of the blends in the presence of radiation sensitizers.

6.9. Summary

RTR used in this phase was found to have higher content of SBR rubber which affected the thermal properties of the blends. However, mechanical, morphological and swelling properties were unaffected due to inferior properties of the RTR. Irradiated RTR in the presence of TMPTA and TPGDA showed improved mechanical, thermal and swelling properties.

However, originality and novelty of this study is reported based on the findings from this section of study. Simultaneous enhancement in tensile strength, elongation at break and other mechanical properties were observed in all the irradiated blends with radiation sensitizers. 50RTR/5APS/HVA2 showed the best properties, even though chain scissions were also presumed to prevail in the blend composition. Enhancements were inferred to be due to efficient co-crosslinking of EVA and RTR phase and restoration of RTR phase elasticity in the presence of radiation sensitizers. SEM micrographs showed RTR particles were heavily embedded in EVA matrix and displayed fracture characteristics.

Though degradation temperatures of the blends were not affected in the presence of radiation sensitizers, dynamic modulus was enhanced, especially in the presence of TMPTA. Swelling properties of the irradiated blends also improved in presence of HVA2 and TMPTA. However, presence of TPGDA increases the softness of the system, leading to deterioration of swelling properties of the blend.

CHAPTER 7. CONCLUSION

7.1. Introduction

This thesis has articulated the possibility of recycling waste tire rubber by blending with thermoplastic. An emphasis has been placed on the role of reclaimed waste tire rubber (RTR) in poly(ethylene-co-vinyl acetate) (EVA) matrix. To date, much of the existing literature has been devoted to studying the influence of ground tire rubber (GTR) on the mechanical properties of GTR/thermoplastic blends. However, the properties of GTR/thermoplastic blends suffered mainly due to lack of blend toughness and adhesion between GTR and thermoplastic matrix. This has dampened the effort of incorporating GTR into thermoplastic matrix. Substituting GTR with an alternative waste tire derivative such as RTR is a viable solution to diversify the recycling efforts of waste tires. This study was aimed at improving the inferior RTR properties by blending with EVA. This thesis also went a step forward by identifying the influence of compatibilization strategies and electron beam irradiation on the final properties of RTR/EVA blends.

7.2. Principal findings

Three different RTR/EVA blends with 30, 50 and 70 wt% RTR was compounded and characterized. Blends displayed intermediate processing, mechanical, thermal and swelling properties. In contrast to EVA and RTR, superior dynamic mechanical properties were observed in the blends. RTR and EVA exist as partially miscible blends with RTR being well dispersed in EVA matrix. The mere presence of RTR clearly decreased the crystallinity of EVA matrix. Blending RTR with EVA improves the inferior properties of RTR.

Three different compatibilization strategies; namely reactive, physical and combination strategies using APS, LR and MAEVA, respectively; were employed to enhance the properties of 50RTR blends. In addition to performing as reactive compatibilizer, APS was found to further reclaim the RTR phase, which improved the dispersion of smaller RTR phase in EVA matrix. Adhesion between RTR and EVA was enhanced, leading to superior mechanical properties. Enhancement was also noted in crystallinity, dynamic mechanical and swelling

properties of APS compatibilized blends. However, the ductility of the APS compatibilized blends decreased to a considerable extent. LR also effectively functioned as physical compatibilizer by encapsulating RTR, decreasing interfacial tension and improving the dispersion of RTR phase in EVA matrix. However, little to no influence of LR was observed on improving processing, mechanical and swelling properties of the 50RTR blend. Nevertheless, heterogeneity was slightly decreased in all compatibilized blends. MAEVA on the other hand, did not perform as a compatibilizing agent in this study.

Electron beam irradiation is an emerging technology that could help solve the problems faced with recycling of crosslinked polymeric waste. This study claims originality and novelty in addressing the third aim, which is to improve and enhance the properties of RTR and RTR/EVA blends through the use of electron beam irradiation. Electron beam irradiation on RTR revealed presence of radical stabilizing and scavenging additives, whereby chain scissions were predominant. This also prevailed in RTR/EVA blends. The blends required high irradiation dose to allow for consumption of the additives, which then allows for crosslinking process to take place in the blends. Hence, only marginal improvement was observed in mechanical, thermal and swelling properties of RTR and RTR/EVA blends. However, dynamic mechanical studies suggested replacement of S-S and S-C bonds with stronger and stiffer C-C bonds, resulting in retention of properties although chain scissions were predominant in RTR and RTR rich blends. This is further corroborated with swelling study whereby irradiated RTR was still sturdy and withstood the entire swelling study period while non-irradiated RTR broke to tiny powdery pieces within just hours of immersion in toluene.

Electron beam irradiation was also conducted on compatibilized blends. While irradiated LR and MAEVA compatibilized blends did not account for substantial improvement in mechanical properties compared to neat 50RTR blend; irradiated APS compatibilized blend displayed superior properties. Further reclaiming of RTR phase by APS allowed for crosslinking feasibility to be better, whereby APS was inferred to have interacted with the residual scavenging and stabilizing additives readily present in RTR. Irradiation improved the dynamic mechanical properties of compatibilized blends, in particular LR compatibilized blends. Crystallinity of APS and LR compatibilized blends decreased with increasing irradiation dose and recorded values lower than irradiated neat

50RTR blend upon 50 kGy irradiation dose. Oxidative degradation still prevails in compatibilized blends similar to neat 50RTR blend. Hence, no prominent improvement of swelling properties was recorded in irradiated APS, LR and MAEVA compatibilized blends.

Radiation sensitizers were used to aid in the final part of the study. Simultaneous enhancement in toughness and tensile strength was observed with irradiated RTR and 50RTR/5APS blends in the presence of radiation sensitizers. Even though TMPTA and TPGDA were found as the best radiation sensitizers for RTR and EVA system, respectively; 50RTR/5APS blend fared the best in the presence of HVA2. Radiation sensitizers were responsible in restoring elastic capacity of RTR component and mediate strong adhesion between RTR and EVA ensuring efficient stress transfer; leading to the observed simultaneous improvement in toughness and tensile strength. However, thermal and dynamic mechanical properties of irradiated 50RTR/5APS only recorded a small improvement. Swelling properties also improved in RTR and 50RTR/5APS blends in the presence of TMPTA or HVA2.

The findings of this study suggest the aims to enhance the properties of RTR by blending, compatibilization and electron beam irradiation have been achieved. It also leads to a new possibility to recycle waste tire rubber.

7.3. Limitations

This study, though profoundly contributes to the knowledge and feasibility of recycling waste tire rubber, it also gives rise to some limitations that could probably affect the commercialization of RTR/EVA blends. In most cases, the limitations are drawn from the lack of resources or the need for completion of project within the stipulated time. However, these limitations also serve as opportunities for future research.

Firstly, properties reported in this study were confined to processing, mechanical, thermal and swelling characterization. It is a known fact; this alone could not push the door to commercialization of recycled products. More studies addressing the fatigue, rheological, weathering and re-processability should be derived. Since the mechanical, dynamic mechanical and swelling properties have

been shown to excel through this study, the possibilities of the other properties being studied will increase.

The loadings of radiation sensitizers were fixed at 4phr in this study. However, to have a congruent comparison, the loading of the radiation sensitizers should be varied to be able to pick the precise loading of each radiation sensitizers with the optimal properties balance. The different blends loaded with the precise amount of radiation sensitizers should be compared instead.

Finally, in this study, both the RTR and EVA phases were crosslinked with the aid of electron beam irradiation. This would limit the possibility of the resulting compound to be recycled. Hence, a method of crosslinking only the RTR phase while keeping the crosslinking minimal in the EVA phase should be considered.

7.4. Recommendation for future studies

Recycling of waste tires by blending with polymers presents a sustainable route to polymeric waste management. Thermoplastics hold the biggest share of polymeric product market. Incorporating waste tire rubber in thermoplastics is a smart move to address the growing number of waste tires around the globe. However, negative implications of past studies on GTR/thermoplastics have stifled the move. It is important to re-formulate and re-direct studies on incorporation of waste tire derivatives into thermoplastics. This is important to ensure the torch to “recycling waste tires by incorporation into polymers” keeps burning.

There are two most uplifting findings from this study. First, is the ability of common aliphatic primary amine in reclaiming crosslinked rubber. Presence of silane group along with the amine ensured good interfacial formation in the blends. Second, radiation sensitizer such as multifunctional acrylates and bismaleimide; help in restoring the elastic capacity of the reclaimed rubber upon exposure to ionizing irradiation. The recommendations for future studies have been formulated based on these findings.

Most of the reclaimed tire rubber available in the market is produced from mechanochemical method. In this method, the crosslinked rubber is mechanically processed to break the macromolecular chain, forming

macromolecular radicals. These radicals are stabilized and scavenged by the chemicals. In most cases, excessive amount of chemicals are added during the reclaiming process. The extra un-reacted chemicals stay active in the rubber and affect the final property of the reclaimed rubber. Tailoring this chemical with an aliphatic primary amine equipped with side chain, such as APS, could be cost saving and also produces good quality reclaimed rubber that can be re-crosslinked again. Furthermore, it also helps in building a good interfacial adhesion with the thermoplastic matrix in the subsequent step.

Radiation sensitizers helped in restoring the elastic capacity of reclaimed rubber upon exposure to ionizing radiation. However, exposing the blends results in both the RTR and the thermoplastic matrix being crosslinked, which is not particularly necessary. The main contribution of the blend's mechanical properties comes from the thermoplastic matrix even before irradiation. Additionally, irradiation shuns out the re-processability and recyclability of the blends. Hence, incorporating the radiation sensitizers into the RTR before the blending with thermoplastics is proposed here. By doing this, the radiation sensitizers will be predominantly placed in the RTR phase and this will also increase the odds of crosslinking only at the interfacial regions of the blends. One can also go further; in synthesizing radiation sensitizers with functionalities and an amine group; to be incorporated in the reclaiming process. By doing this, the amine group will be responsible in reclaiming the rubber while the functional group will mediate crosslinking upon exposure to ionizing radiation later.

Lastly, influence of different ionizing radiation, microwave irradiation, ultraviolet irradiation and ultrasonic cavitation on reclaiming of waste tire rubber in the presence of amine should be studied. Though there are past studies on reclaiming rubber by the use of amine; none ventured into synergistic use of emerging new technologies in polymeric industries as suggested above.

BIBLIOGRAPHY

- ABOU ZEID, M. M., RABIE, S. T., NADA, A. A., KHALIL, A. M. & HILAL, R. H. 2008. Effect of gamma irradiation on ethylene propylene diene terpolymer rubber composites. *Nuclear Instruments and Methods in Physics Research Section B: Beam Interactions with Materials and Atoms*, 266, 111-116.
- ADHIKARI, B., DE, D. & MAITI, S. 2000. Reclamation and recycling of waste rubber. *Progress in Polymer Science*, 25, 909-948.
- AHMED, S., BASFAR, A. A. & ABDEL AZIZ, M. M. 2000. Comparison of thermal stability of sulfur, peroxide and radiation cured NBR and SBR vulcanizates. *Polymer Degradation and Stability*, 67, 319-323.
- AKIBA, M. & HASHIM, A. S. 1997. Vulcanization and crosslinking in elastomers. *Progress in Polymer Science*, 22, 475-521.
- AL-MALAIKA, S. 2012. *Reactive modifiers for polymers*, Springer Science & Business Media.
- AL-MALAIKA, S. & AMIR, E. J. 1989. Thermoplastic elastomers: Part III—Ageing and mechanical properties of natural rubber-reclaimed rubber/polypropylene systems and their role as solid phase dispersants in polypropylene/polyethylene blends. *Polymer Degradation and Stability*, 26, 31-41.
- AMARI, T., THEMELIS, N. J. & WERNICK, I. K. 1999. Resource recovery from used rubber tires. *Resources Policy*, 25, 179-188.
- AVILES, F., CAUICH-RODRIGUEZ, J. V., RODRIGUEZ-GONZALES, J. A. & MAY-PAT, A. 2011. Oxidation and silanization of MWCNTs for MWCNT/vinyl ester composites. *eXRESS Polymer Letters*, 5, 766-776.
- AWANG, M. & ISMAIL, H. 2008. Preparation and characterization of polypropylene/waste tyre dust blends with addition of DCP and HVA-2 (PP/WTDP-HVA2). *Polymer Testing*, 27, 321-329.
- AWANG, M., ISMAIL, H. & HAZIZAN, M. A. 2007. Polypropylene-based blends containing waste tire dust: Effects of trans-polyoctylene rubber (TOR) and dynamic vulcanization. *Polymer Testing*, 26, 779-787.
- AWANG, M., ISMAIL, H. & HAZIZAN, M. A. 2008. Processing and properties of polypropylene-latex modified waste tyre dust blends (PP/WTDMML). *Polymer Testing*, 27, 93-99.

- BALASUBRAMANIAN, M. 2009. Cure modeling and mechanical properties of counter rotating twin screw extruder devulcanized ground rubber tire—natural rubber blends. *Journal of Polymer Research*, 16, 133-141.
- BANDYOPADHYAY, A., THAKUR, V., PRADHAN, S. & BHOWMICK, A. K. 2010. Nanoclay distribution and its influence on the mechanical properties of rubber blends. *Journal of Applied Polymer Science*, 115, 1237-1246.
- BANIK, I., DUTTA, S. K., CHAKI, T. K. & BHOWMICK, A. K. 1999. Electron beam induced structural modification of a fluorocarbon elastomer in the presence of polyfunctional monomers. *Polymer*, 40, 447-458.
- BASFAR, A. A., ABDEL-AZIZ, M. M. & MOFTI, S. 2002. Influence of different curing systems on the physico-mechanical properties and stability of SBR and NR rubbers. *Radiation Physics and Chemistry*, 63, 81-87.
- BASFAR, A. A. & ALI, Z. I. 2011. Physico-chemical properties of low density polyethylene and ethylene vinyl acetate composites cross-linked by ionizing radiation. *Radiation Physics and Chemistry*, 80, 257-263.
- BENMESLI, S. & RIAHI, F. 2014. Dynamic mechanical and thermal properties of a chemically modified polypropylene/natural rubber thermoplastic elastomer blend. *Polymer Testing*, 36, 54-61.
- BOGUSKI, J., PRZYBYTNIAK, G. & ŁYCZKO, K. 2014. New monitoring by thermogravimetry for radiation degradation of EVA. *Radiation Physics and Chemistry*, 100, 49-53.
- BURILLO, G., GALICIA, M., CARREÓN, M. D. P., VÁZQUEZ, M. & ADEM, E. 2001. Crosslinking of recycled polyethylene by gamma irradiation in the presence of sensitizers. *Radiation Physics and Chemistry*, 60, 73-78.
- CANAVATE, J., CASAS, P., COLOM, X. & NOGUÉS, F. 2011. Formulations for thermoplastic vulcanizates based on high density polyethylene, ethylene-propylene-diene monomer, and ground tyre rubber. *Journal of Composite Materials*, 45, 1189-1200.
- CHAKRABORTY, S. K., SABHARWAL, S., DAS, P. K., SARMA, K. S. S. & MANJULA, A. K. 2011. Electron beam (EB) radiation curing—a unique technique to introduce mixed crosslinks in cured rubber matrix to improve quality and productivity. *Journal of Applied Polymer Science*, 122, 3227-3236.
- CHANG, Y.-W., MISHRA, J. K., KIM, S.-K. & KIM, D.-K. 2006. Effect of supramolecular hydrogen bonded network on the properties of maleated ethylene propylene diene rubber/maleated high density polyethylene blend based thermoplastic elastomer. *Materials Letters*, 60, 3118-3121.

- CHEN, F. & QIAN, J. 2003. Studies of the thermal degradation of waste rubber. *Waste Management*, 23, 463-467.
- COLOM, X., CAÑAVATE, J., CARRILLO, F. & SUÑOL, J. J. 2009. Effect of the particle size and acid pretreatments on compatibility and properties of recycled HDPE plastic bottles filled with ground tyre powder. *Journal of Applied Polymer Science*, 112, 1882-1890.
- COLOM, X., CAÑAVATE, J., CARRILLO, F., VELASCO, J. I., PAGÈS, P., MUJAL, R. & NOGUÉS, F. 2006. Structural and mechanical studies on modified reused tyres composites. *European Polymer Journal*, 42, 2369-2378.
- DA COSTA, H. M. & RAMOS, V. D. 2008. Analysis of thermal properties and rheological behavior of LLDPE/EPDM and LLDPE/EPDM/SRT mixtures. *Polymer Testing*, 27, 27-34.
- DA COSTA, H. M., RAMOS, V. D. & ROCHA, M. C. G. 2006. Analysis of thermal properties and impact strength of PP/SRT, PP/EPDM and PP/SRT/EPDM mixtures in single screw extruder. *Polymer Testing*, 25, 498-503.
- DAHLAN, H. M., KHAIRUL ZAMAN, M. D. & IBRAHIM, A. 2002a. The morphology and thermal properties of liquid natural rubber (LNR)-compatibilized 60/40 NR/LLDPE blends. *Polymer Testing*, 21, 905-911.
- DAHLAN, H. M., ZAMAN, M. D. K. & IBRAHIM, A. 2002b. Liquid natural rubber (LNR) as a compatibiliser in NR/LLDPE blends—II: the effects of electron-beam (EB) irradiation. *Radiation Physics and Chemistry*, 64, 429-436.
- DE, D., DE, D. & SINGHAROY, G. M. 2007. Reclaiming of ground rubber tire by a novel reclaiming agent. I. virgin natural rubber/reclaimed GRT vulcanizates. *Polymer Engineering & Science*, 47, 1091-1100.
- DE, D., MAITI, S. & ADHIKARI, B. 2000. Reclaiming of rubber by a renewable resource material (RRM). III. evaluation of properties of NR reclaim. *Journal of Applied Polymer Science*, 75, 1493-1502.
- DEMJÉN, Z., PUKÁNSZKY, B. & NAGY JR, J. 1999. Possible coupling reactions of functional silanes and polypropylene. *Polymer*, 40, 1763-1773.
- DIJKHUIS, K. 2008. Recycling of Vulcanized EPDM-Rubber, PhD Thesis, University of Twente. *Enschede, the Netherlands*.
- DIJKHUIS, K., DIERKES, W., SUTANTO, P., PICCHIONI, F., JANSSEN, L. & NOORDERMEER, J. Devulcanization of EPDM-Rubber Vulcanizates with Amine Devulcanization Agents. International Rubber Conference, Maastricht, the Netherlands, 2005.

- DONG, W., CHEN, G. & ZHANG, W. 2001. Radiation effects on the immiscible polymer blend of nylon1010 and high-impact strength polystyrene (II): mechanical properties and morphology. *Radiation Physics and Chemistry*, 60, 629-635.
- DONG, W., ZHANG, W., CHEN, G. & LIU, J. 2000. Radiation effects on the immiscible polymer blend of nylon1010 and high-impact polystyrene (HIPS) I: Gel/dose curves, mathematical expectation theorem and thermal behaviour. *Radiation Physics and Chemistry*, 57, 27-35.
- DU, M., GUO, B. & JIA, D. 2005. Effects of Thermal and UV-induced Grafting of Bismaleimide on Mechanical Performance of Reclaimed Rubber/Natural Rubber Blends. *Journal of Polymer Research*, 12, 473-482.
- DUBEY, K. A., BHARDWAJ, Y. K., CHAUDHARI, C. V., BHATTACHARYA, S., GUPTA, S. K. & SABHARWAL, S. 2006. Radiation effects on SBR-EPDM blends: A correlation with blend morphology. *Journal of Polymer Science Part B: Polymer Physics*, 44, 1676-1689.
- DUTTA, S. K., BHOWMICK, A. K. & CHAKI, T. K. 1996. Structure property relationship of ethylene vinyl acetate copolymer grafted with triallyl cyanurate by electron beam radiation. *Radiation Physics and Chemistry*, 47, 913-926.
- DUTTA, S. K., BHOWMICK, A. K., MUKUNDA, P. G. & CHAKI, T. K. 1995. Thermal degradation studies of electron beam cured ethylene-vinyl acetate copolymer. *Polymer Degradation and Stability*, 50, 75-82.
- EL-NEMR, K. F. 2011. Effect of different curing systems on the mechanical and physico-chemical properties of acrylonitrile butadiene rubber vulcanizates. *Materials & Design*, 32, 3361-3369.
- EPA, U. S. E. P. A. 1993. Scrap Tire Technology and Markets. In: CLARK, C., MEARDON, K. & RUSSELL, D. (eds.). United States of America: William Andrew Publishing/Noyes.
- ETRMA. 2013. *European Tyre & Rubber Manufacturers' Association: The annual report and statistic 2012* [Online]. Belgium. [Accessed 23rd January 2013].
- FANG, Y., ZHAN, M. & WANG, Y. 2001. The status of recycling of waste rubber. *Materials & Design*, 22, 123-128.
- FERRÃO, P., RIBEIRO, P. & SILVA, P. 2008. A management system for end-of-life tyres: A Portuguese case study. *Waste Management*, 28, 604-614.
- FERRER, G. 1997. The economics of tire remanufacturing. *Resources, Conservation and Recycling*, 19, 221-255.

- FIKSEL, J., BAKSHI, B., BARAL, A., GUERRA, E. & DEQUERVAIN, B. 2011. Comparative life cycle assessment of beneficial applications for scrap tires. *Clean Technologies and Environmental Policy*, 13, 19-35.
- FORMELA, K., KOROL, J. & SAEB, M. R. 2015. Interfacially modified LDPE/GTR composites with non-polar elastomers: From microstructure to macro-behavior. *Polymer Testing*, 42, 89-98.
- FUKUMORI, K., MATSUSHITA, M., OKAMOTO, H., SATO, N., SUZUKI, Y. & TAKEUCHI, K. 2002. Recycling technology of tire rubber. *JSAE Review*, 23, 259-264.
- GANESH, B. & UNNIKRISHNAN, G. 2006. Cure characteristics, morphology, mechanical properties, and aging characteristics of silicone rubber/ethylene vinyl acetate blends. *Journal of Applied Polymer Science*, 99, 1069-1082.
- GEORGE, S., NEELAKANTAN, N. R., VARUGHESE, K. T. & THOMAS, S. 1997. Dynamic mechanical properties of isotactic polypropylene/nitrile rubber blends: Effects of blend ratio, reactive compatibilization, and dynamic vulcanization. *Journal of Polymer Science Part B: Polymer Physics*, 35, 2309-2327.
- GEORGE, S., VARUGHESE, K. & THOMAS, S. 2000a. Thermal and crystallisation behaviour of isotactic polypropylene/nitrile rubber blends. *Polymer*, 41, 5485-5503.
- GEORGE, S. C., NINAN, K. N., GROENINCKX, G. & THOMAS, S. 2000b. Styrene-butadiene rubber/natural rubber blends: Morphology, transport behavior, and dynamic mechanical and mechanical properties. *Journal of Applied Polymer Science*, 78, 1280-1303.
- GHOSH, P., CHATTOPADHYAY, B. & SEN, A. K. 1996. Thermal and oxidative degradation of PE-EPDM blends vulcanized differently using sulfur accelerator systems. *European Polymer Journal*, 32, 1015-1021.
- GIRI, R., NASKAR, K. & NANDO, G. B. 2012. Effect of electron beam irradiation on dynamic mechanical, thermal and morphological properties of LLDPE and PDMS rubber blends. *Radiation Physics and Chemistry*, 81, 1930-1942.
- GRIGORYEVA, O., FAINLEIB, A., GRENET, J. & SAITER, J. M. 2008. Reactive compatibilization of recycled polyethylenes and scrap rubber in thermoplastic elastomer: Chemical and radiation-chemical approach. *Rubber Chemistry and Technology*, 81, 737-752.
- GRIGORYEVA, O., FAINLEIB, A., STAROSTENKO, O., TOLSTOV, A. & BROSTOW, W. 2004. Thermoplastic elastomers from rubber and recycled polyethylene:

- chemical reactions at interphases for property enhancement. *Polymer international*, 53, 1693-1703.
- GRIGORYEVA, O., FAINLEIB, A., TOLSTOV, A., PISSIS, P., SPANOUDAKI, A., VATALIS, A. & DELIDES, C. 2006. Thermal analysis of thermoplastic elastomers based on recycled polyethylenes and ground tyre rubber. *Journal of Thermal Analysis and Calorimetry*, 86, 229-233.
- GROBLER, J. H. A. & MCGILL, W. J. 1994. Effect of network heterogeneity on tensile and tear strengths of radiation, peroxide, efficient and conventional cured polyisoprene. *Journal of Polymer Science Part B: Polymer Physics*, 32, 287-295.
- HAN, D. H., SHIN, S.-H. & PETROV, S. 2004. Crosslinking and degradation of polypropylene by electron beam irradiation in the presence of trifunctional monomers. *Radiation Physics and Chemistry*, 69, 239-244.
- HAN, S.-C. & HAN, M.-H. 2002. Fracture behavior of NR and SBR vulcanizates filled with ground rubber having uniform particle size. *Journal of Applied Polymer Science*, 85, 2491-2500.
- HASSAN, M. M., ALY, R. O., ABDEL AAL, S. E., EL-MASRY, A. M. & FATHY, E. S. 2013a. Mechanochemical devulcanization and gamma irradiation of devulcanized waste rubber/high density polyethylene thermoplastic elastomer. *Journal of Industrial and Engineering Chemistry*, 19, 1722-1729.
- HASSAN, M. M., ALY, R. O., EL-GHANDOUR, A. & ABDELNABY, H. A. 2013b. Effect of gamma irradiation on some properties of reclaimed rubber/nitrile-butadiene rubber blend and its swelling in motor and brake oils. *Journal of Elastomers and Plastics*, 45, 77-94.
- HASSAN, M. M., BADWAY, N. A., ELNAGGAR, M. Y. & HEGAZY, E.-S. A. 2013c. Thermo-mechanical properties of devulcanized rubber/high crystalline polypropylene blends modified by ionizing radiation. *Journal of Industrial and Engineering Chemistry*, 19, 1241-1250.
- HASSAN, M. M., BADWAY, N. A., ELNAGGAR, M. Y. & HEGAZY, E.-S. A. 2014a. Effects of peroxide and gamma radiation on properties of devulcanized rubber/polypropylene/ethylene propylene diene monomer formulation. *Journal of Applied Polymer Science*, 131, n/a-n/a.
- HASSAN, M. M., BADWAY, N. A., ELNAGGAR, M. Y. & HEGAZY, E.-S. A. 2014b. Synergistic effect of gamma radiation and peroxide on dynamic vulcanization of thermoplastic vulcanizates based on (devulcanized rubber)/polypropylene. *Journal of Vinyl and Additive Technology*, 20, 168-176.

- HASSAN, M. M., BADWAY, N. A., ELNAGGAR, M. Y. & HEGAZY, E.-S. A. 2015. Physical properties of irradiated thermoplastic elastomeric olefins based on (devulcanized rubber)/(high crystalline polypropylene) formulations. *Journal of Vinyl and Additive Technology*, 21, 33-41.
- HASSAN, M. M., MAHMOUD, G. A., EL-NAHAS, H. H. & HEGAZY, E.-S. A. 2007. Reinforced material from reclaimed rubber/natural rubber, using electron beam and thermal treatment. *Journal of Applied Polymer Science*, 104, 2569-2578.
- HE, M., LI, Y., QIAO, B., MA, X., SONG, J. & WANG, M. 2014. Effect of dicumyl peroxide and phenolic resin as a mixed curing system on the mechanical properties and morphology of TPVs based on HDPE/ground tire rubber. *Polymer Composites*, n/a-n/a.
- HERNÁNDEZ, M., VALENTÍN, J. L., LÓPEZ-MANCHADO, M. A. & EZQUERRA, T. A. 2015. Influence of the vulcanization system on the dynamics and structure of natural rubber: Comparative study by means of broadband dielectric spectroscopy and solid-state NMR spectroscopy. *European Polymer Journal*, 68, 90-103.
- HONG, C. K. & ISAYEV, A. I. 2001. Plastic/Rubber Blends of Ultrasonically Devulcanized GRT with HDPE. *Journal of Elastomers and Plastics*, 33, 47-71.
- ISAYEV, A. 2011. Recycling of Rubbers. In: MARK, J. E., ERMAN, B. & EIRICH, F. R. (eds.) *Science and Technology of Rubber*. 3 ed. United State of America: Elsevier Academic Press.
- ISMAIL, H., AWANG, M. & HAZIZAN, M. 2006. Effect of waste tire dust (WTD) size on the mechanical and morphological properties of polypropylene/waste tire dust (PP/WTD) blends. *Polymer-Plastics Technology and Engineering*, 45, 463-468.
- ISMAIL, H. & SURYADIANSYAH 2002. Thermoplastic elastomers based on polypropylene/natural rubber and polypropylene/recycle rubber blends. *Polymer Testing*, 21, 389-395.
- JANA, R. N. & NANDO, G. B. 2003. Thermogravimetric analysis of blends of low-density polyethylene and poly(dimethyl siloxane) rubber: The effects of compatibilizers. *Journal of Applied Polymer Science*, 90, 635-642.
- JANG, J.-W., YOO, T.-S., OH, J.-H. & IWASAKI, I. 1998. Discarded tire recycling practices in the United States, Japan and Korea. *Resources, Conservation and Recycling*, 22, 1-14.

- JANSEN, P., GARCIA, F. G. & SOARES, B. G. 2003. Effect of mercapto-modified ethylene-vinyl acetate on the curing parameters and mechanical and dynamic mechanical properties of vulcanized nitrile rubber/ethylene-vinyl acetate blends. *Journal of Applied Polymer Science*, 90, 2391-2399.
- JOHN, B., VARUGHESE, K. T., OOMMEN, Z., PÖTSCHKE, P. & THOMAS, S. 2003. Dynamic mechanical behavior of high-density polyethylene/ethylene vinyl acetate copolymer blends: The effects of the blend ratio, reactive compatibilization, and dynamic vulcanization. *Journal of Applied Polymer Science*, 87, 2083-2099.
- JOSEPH, A., MATHAI, A. E. & THOMAS, S. 2003. Sorption and diffusion of methyl substituted benzenes through cross-linked nitrile rubber/poly(ethylene co-vinyl acetate) blend membranes. *Journal of Membrane Science*, 220, 13-30.
- JUNG, C.-H., LEE, D.-H., HWANG, I.-T., IM, D.-S., SHIN, J., KANG, P.-H. & CHOI, J.-H. 2013. Fabrication and characterization of radiation-resistant LDPE/MWCNT nanocomposites. *Journal of Nuclear Materials*, 438, 41-45.
- KARGER-KOCSIS, J. 2013. Waste tyre rubber - what to do next? *eXRESS Polymer Letters*, 7, 406.
- KARGER-KOCSIS, J., MÉSZÁROS, L. & BÁRÁNY, T. 2013. Ground tyre rubber (GTR) in thermoplastics, thermosets, and rubbers. *Journal of Materials Science*, 48, 1-38.
- KHONAKDAR, H., JAFARI, S., TAHERI, M., WAGENKNECHT, U., JEHNICHEN, D. & HÄUSSLER, L. 2006a. Thermal and wide angle X-ray analysis of chemically and radiation-crosslinked low and high density polyethylenes. *Journal of Applied Polymer Science*, 100, 3264-3271.
- KHONAKDAR, H. A., JAFARI, S. H., WAGENKNECHT, U. & JEHNICHEN, D. 2006b. Effect of electron-irradiation on cross-link density and crystalline structure of low- and high-density polyethylene. *Radiation Physics and Chemistry*, 75, 78-86.
- KIM, D. H., HWANG, S. H., PARK, T. S. & KIM, B. S. 2013. Effects of waste ground fluororubber vulcanizate powders on the properties of silicone rubber/fluororubber blends. *Journal of Applied Polymer Science*, 127, 561-569.
- KIM, J. I., RYU, S. H. & CHANG, Y. W. 2000. Mechanical and dynamic mechanical properties of waste rubber powder/HDPE composite. *Journal of Applied Polymer Science*, 77, 2595-2602.

- KIM, S.-J., SHIN, B.-S., HONG, J.-L., CHO, W.-J. & HA, C.-S. 2001. Reactive compatibilization of the PBT/EVA blend by maleic anhydride. *Polymer*, 42, 4073-4080.
- KUMNUANTIP, C. & SOMBATSOMPOP, N. 2003. Dynamic mechanical properties and swelling behaviour of NR/reclaimed rubber blends. *Materials Letters*, 57, 3167-3174.
- L'ABEE, R. M. A., VAN DUIN, M., SPOELSTRA, A. B. & GOOSSENS, J. G. P. 2010. The rubber particle size to control the properties-processing balance of thermoplastic/cross-linked elastomer blends. *Soft Matter*, 6, 1758-1768.
- LEE, S. H., BALASUBRAMANIAN, M. & KIM, J. K. 2007. Dynamic reaction inside co-rotating twin screw extruder. II. Waste ground rubber tire powder/polypropylene blends. *Journal of Applied Polymer Science*, 106, 3209-3219.
- LEE, S. H., ZHANG, Z. X., XU, D., CHUNG, D., OH, G. J. & KIM, J. K. 2009. Dynamic reaction involving surface modified waste ground rubber tire powder/polypropylene. *Polymer Engineering & Science*, 49, 168-176.
- LI, S., LAMMINMÄKI, J. & HANHI, K. 2005. Effect of ground rubber powder and devulcanizates on the properties of natural rubber compounds. *Journal of Applied Polymer Science*, 97, 208-217.
- LI, Y., ZHANG, Y. & ZHANG, Y. 2003a. Mechanical properties of high-density polyethylene/scrap rubber powder composites modified with ethylene-propylene-diene terpolymer, dicumyl peroxide, and silicone oil. *Journal of Applied Polymer Science*, 88, 2020-2027.
- LI, Y., ZHANG, Y. & ZHANG, Y. X. 2003b. Structure and mechanical properties of SRP/HDPE/POE (EPR or EPDM) composites. *Polymer Testing*, 22, 859-865.
- LI, Y., ZHAO, S. & WANG, Y. 2012a. Improvement of the properties of natural rubber/ground tire rubber composites through biological desulfurization of GTR. *Journal of Polymer Research*, 19, 1-7.
- LI, Y., ZHAO, S. & WANG, Y. 2012b. Microbial Desulfurization of Ground Tire Rubber by *Sphingomonas* sp.: A Novel Technology for Crumb Rubber Composites. *Journal of Polymers and the Environment*, 20, 372-380.
- LI, Z., NAMBIAR, S., ZHENG, W. & YEOW, J. T. W. 2013. PDMS/single-walled carbon nanotube composite for proton radiation shielding in space applications. *Materials Letters*, 108, 79-83.
- MAGIOLI, M., SIRQUEIRA, A. S. & SOARES, B. G. 2010. The effect of dynamic vulcanization on the mechanical, dynamic mechanical and fatigue properties

- of TPV based on polypropylene and ground tire rubber. *Polymer Testing*, 29, 840-848.
- MAKUUCHI, K. & CHENG, S. 2012a. Chain Scission and Oxidation. *Radiation Processing of Polymer Materials and its Industrial Applications*. John Wiley & Sons, Inc.
- MAKUUCHI, K. & CHENG, S. 2012b. Frontmatter. *Radiation Processing of Polymer Materials and its Industrial Applications*. John Wiley & Sons, Inc.
- MANGARAJ, D. 2005. *Chapter 7: Rubber recycling by blending with plastics*, United State of America, Taylor & Francis/CRC Press.
- MARKOVIĆ, G., MARINOVIĆ-CINCOVIĆ, M., JOVANOVIĆ, V., SAMARŽIJA-JOVANOVIĆ, S. & BUDINSKI-SIMENDIĆ, J. 2013. Characterization of composites based on chlorosulfonated polyethylene rubber/chlorinated natural rubber/waste rubber powder rubber blends. *Journal of Thermoplastic Composite Materials*.
- MARTÍNEZ-PARDO, M. E. & VERA-GRAZIANO, R. 1995. Gamma radiation induced crosslinking of polyethylene/ethylene—vinylacetate blends. *Radiation Physics and Chemistry*, 45, 93-102.
- MAZIAD, N. A. & HASSAN, M. M. 2007. Study of some properties of waste LDPE/waste butyl rubber blends using different compatibilizing agents and gamma irradiation. *Journal of Applied Polymer Science*, 106, 4157-4163.
- MÉSZÁROS, L., BÁRÁNY, T. & CZVIKOVSKY, T. 2012. EB-promoted recycling of waste tire rubber with polyolefins. *Radiation Physics and Chemistry*, 81, 1357-1360.
- MITRA, S., CHATTOPADHYAY, S., SABHARWAL, S. & BHOWMICK, A. K. 2010. Electron beam crosslinked gels—Preparation, characterization and their effect on the mechanical, dynamic mechanical and rheological properties of rubbers. *Radiation Physics and Chemistry*, 79, 289-296.
- MITTAL, V. 2012. *Functional polymer blends: synthesis, properties, and performance*, CRC Press.
- MOHAMAD, Z., ISMAIL, H. & RATNAM, C. T. 2006. Characterization of epoxidized natural rubber/ethylene vinyl acetate (ENR-50/EVA) blend: Effect of blend ratio. *Journal of Applied Polymer Science*, 99, 1504-1515.
- MOLY, K. A., BHAGAWAN, S. S., GROENINCKX, G. & THOMAS, S. 2006. Correlation between the morphology and dynamic mechanical properties of ethylene vinyl acetate/linear low-density polyethylene blends: Effects of the blend

- ratio and compatibilization. *Journal of Applied Polymer Science*, 100, 4526-4538.
- MUJAL-ROSAS, R., ORRIT-PRAT, J., RAMIS-JUAN, X., MARIN-GENESCA, M. & RAHHALI, A. 2011. Study on dielectric, thermal, and mechanical properties of the ethylene vinyl acetate reinforced with ground tire rubber. *Journal of Reinforced Plastics and Composites*, 30, 581-592.
- MUNUSAMY, Y., ISMAIL, H., MARIATTI, M. & RATNAM, C. T. 2009. Effect of electron beam irradiation on the properties of ethylene-(vinyl acetate) copolymer/natural rubber/organoclay nanocomposites. *Journal of Vinyl and Additive Technology*, 15, 39-46.
- MUNUSAMY, Y., ISMAIL, H. & RATNAM, C. T. 2012. Effect of organoclay loading on the crosslinking and degradation of irradiated ethylene(vinyl acetate) copolymer/natural rubber nanocomposites. *Journal of Reinforced Plastics and Composites*, 31, 946-958.
- MYHRE, M., SAIWARI, S., DIERKES, W. & NOORDERMEER, J. W. M. 2012. Rubber recycling: Chemistry, processing, and applications. *Rubber Chemistry and Technology*, 85, 408-449.
- NAKASON, C., NUANSOMSRI, K., KAESAMAN, A. & KIATKAMJORNWONG, S. 2006. Dynamic vulcanization of natural rubber/high-density polyethylene blends: Effect of compatibilization, blend ratio and curing system. *Polymer Testing*, 25, 782-796.
- NASKAR, A. K., BHOWMICK, A. K. & DE, S. K. 2001. Thermoplastic elastomeric composition based on ground rubber tire. *Polymer Engineering & Science*, 41, 1087-1098.
- NG, H.-M., BEE, S.-T., RATNAM, C. T., SIN, L. T., PHANG, Y.-Y., TEE, T.-T. & RAHMAT, A. R. 2014. Effectiveness of trimethylpropane trimethacrylate for the electron-beam-irradiation-induced cross-linking of polylactic acid. *Nuclear Instruments and Methods in Physics Research Section B: Beam Interactions with Materials and Atoms*, 319, 62-70.
- NORIMAN, N., ISMAIL, H., RATNAM, C. & RASHID, A. 2010. The effect of electron beam (EB) irradiation in presence of TMPTA on cure characteristics and mechanical properties of styrene butadiene rubber/recycled acrylonitrile-butadiene rubber (SBR/NBRr) blends. *Polymer-Plastics Technology and Engineering*, 49, 228-236.
- NORIMAN, N. Z., ISMAIL, H. & RASHID, A. A. 2012. Properties of styrene butadiene rubber/recycled acrylonitrile-butadiene rubber (SBR/NBRr)

- blends: Effect of the addition of trans-polyoctylene rubber. *Journal of Applied Polymer Science*, 126, E56-E63.
- PATACZ, C., COQUERET, X. & DECKER, C. 2001. Electron-beam initiated polymerization of acrylate compositions 3: compared reactivity of hexanediol and tripropyleneglycol diacrylates under UV or EB initiation. *Radiation Physics and Chemistry*, 62, 403-410.
- PECHURAI, W., NAKASON, C. & SAHAKARO, K. 2008. Thermoplastic natural rubber based on oil extended NR and HDPE blends: Blend compatibilizer, phase inversion composition and mechanical properties. *Polymer Testing*, 27, 621-631.
- PENG, P., CHENG, S. & HU, F. 1993. The sensitizing effect of acrylates on radiation vulcanization of natural rubber latex. *Radiation Physics and Chemistry*, 42, 121-124.
- PICHAIIYUT, S., NAKASON, C., KAESAMAN, A. & KIATKAMJORNWONG, S. 2008. Influences of blend compatibilizers on dynamic, mechanical, and morphological properties of dynamically cured maleated natural rubber and high-density polyethylene blends. *Polymer Testing*, 27, 566-580.
- PUKÁNSZKY, B. & DEMJÉN, Z. 1999. Silane treatment in polypropylene composites: Adsorption and coupling. *Macromolecular Symposia*, 139, 93-105.
- PUNNARAK, P., TANTAYANON, S. & TANGPASUTHADOL, V. 2006. Dynamic vulcanization of reclaimed tire rubber and high density polyethylene blends. *Polymer Degradation and Stability*, 91, 3456-3462.
- PURCELL, A. H. 1978. Tire recycling: Research trends and needs. *Conservation & Recycling*, 2, 137-143.
- QIN, J., DING, H., WANG, X., XIE, M. & YU, Z. 2008. Blending LLDPE and Ground Rubber Tires. *Polymer-Plastics Technology and Engineering*, 47, 199-202.
- RADHAKRISHNAN, C. K., KUMARI, P., SUJITH, A. & UNNIKRISHNAN, G. 2008. Dynamic mechanical properties of styrene butadiene rubber and poly (ethylene-co-vinyl acetate) blends. *Journal of Polymer Research*, 15, 161-171.
- RAJAN, A., UPADHYAYA, P., CHAND, N. & KUMAR, V. 2014. Effect of nanoclay on the thermal properties of compatibilized ethylene vinyl acetate copolymer/high-density polyethylene blends. *Journal of Thermoplastic Composite Materials*, 27, 650-662.

- RAJAN, V. V., DIERKES, W. K., JOSEPH, R. & NOORDERMEER, J. W. M. 2006. Science and technology of rubber reclamation with special attention to NR-based waste latex products. *Progress in Polymer Science*, 31, 811-834.
- RAMARAD, S., KHALID, M., RATNAM, C. T., CHUAH, A. L. & RASHMI, W. 2015a. Waste tire rubber in polymer blends: A review on the evolution, properties and future. *Progress in Materials Science*, 72, 100-140.
- RAMARAD, S., RATNAM, C. T., KHALID, M. & CHUAH, A. L. 2015b. Improving the properties of reclaimed waste tire rubber by blending with poly(ethylene-co-vinyl acetate) and electron beam irradiation. *Journal of Applied Polymer Science*, 132, n/a-n/a.
- RAMESH, V., BISWAL, M., MOHANTY, S. & NAYAK, S. K. 2014. Compatibilization effect of EVA-g-MAH on mechanical, morphological and rheological properties of recycled PC/ABS blend. *Materials Express*, 4, 499-507.
- RATNAM, C. & ZAMAN, K. 1999a. Enhancement of polyvinyl chloride (PVC)/epoxidised natural rubber (ENR) blend properties by electron beam irradiation: effect of antioxidants. *Polymer Degradation and Stability*, 65, 481-490.
- RATNAM, C. & ZAMAN, K. 1999b. Modification of PVC/ENR blend by electron beam irradiation: effect of crosslinking agents. *Nuclear Instruments and Methods in Physics Research Section B: Beam Interactions with Materials and Atoms*, 152, 335-342.
- RATNAM, C. T. 2001. Irradiation Crosslinking of PVC/ENR Blend: A Comparative Study with the Respective Homopolymers. *Macromolecular Materials and Engineering*, 286, 429-433.
- RATNAM, C. T., NASIR, M., BAHARIN, A. & ZAMAN, K. 2000. Electron beam irradiation of epoxidized natural rubber. *Nuclear Instruments and Methods in Physics Research Section B: Beam Interactions with Materials and Atoms*, 171, 455-464.
- RATNAM, C. T., NASIR, M., BAHARIN, A. & ZAMAN, K. 2001a. Effect of electron-beam irradiation on poly (vinyl chloride)/epoxidized natural rubber blend: dynamic mechanical analysis. *Polymer international*, 50, 503-508.
- RATNAM, C. T., NASIR, M., BAHARIN, A. & ZAMAN, K. 2001b. The effect of electron beam irradiation on the tensile and dynamic mechanical properties of epoxidized natural rubber. *European Polymer Journal*, 37, 1667-1676.

- RATNAM, C. T., NASIR, M., BAHARIN, A. & ZAMAN, K. 2001c. Electron-beam irradiation of poly(vinyl chloride)/epoxidized natural rubber blend in the presence of Irganox 1010. *Polymer Degradation and Stability*, 72, 147-155.
- RATNAM, C. T., NASIR, M., BAHARIN, A. & ZAMAN, K. 2001d. Electron-beam irradiation of poly (vinyl chloride)/epoxidized natural rubber blends in presence of trimethylolpropane triacrylate. *Journal of Applied Polymer Science*, 81, 1926-1935.
- RATNAM, C. T., RAMARAD, S., SIDDIQUI, M. K., ZAINAL ABIDIN, A. S. & CHUAH, L. T. 2014. Irradiation cross-linking of ethylene vinyl acetate/waste tire dust: Effect of multifunctional acrylates. *Journal of Thermoplastic Composite Materials*.
- REYES-LABARTA, J., OLAYA, M. & MARCILLA, A. 2006. DSC and TGA study of the transitions involved in the thermal treatment of binary mixtures of PE and EVA copolymer with a crosslinking agent. *Polymer*, 47, 8194-8202.
- ROCHE, N., ICHCHOU, M. N., SALVIA, M. & CHETTAH, A. 2011. Dynamic Damping Properties of Thermoplastic Elastomers Based on EVA and Recycled Ground Tire Rubber. *Journal of Elastomers and Plastics*, 43, 317-340.
- RODGERS, B. & WADDELL, W. 2011. Tire Engineering. In: MARK, J. E., ERMAN, B. & EIRICH, F. R. (eds.) *Science and Technology of Rubber*. 3 ed. United State of America: Elsevier Academic Press.
- ROOJ, S., BASAK, G. C., MAJI, P. K. & BHOWMIC, A. K. 2011. New route for devulcanization of natural rubber and the properties of devulcanized rubber. *Journal of Polymer Environment*, 19, 382-390.
- RYTLEWSKI, P., MALINOWSKI, R., MORACZEWSKI, K. & ŻENKIEWICZ, M. 2010. Influence of some crosslinking agents on thermal and mechanical properties of electron beam irradiated polylactide. *Radiation Physics and Chemistry*, 79, 1052-1057.
- SAKINAH, Z. A., RATNAM, C., CHUAH, A. L. & YAW, T. 2009. Effect of Mixing Conditions on the Tensile Properties of Ethylene Vinyl Acetate/Waste Tire Dust (EVA/WTD) Blend. *Polymer-Plastics Technology and Engineering*, 48, 1139-1142.
- SAKINAH, Z. A. A., RATNAM, C. T., CHUAH, A. L. & YAW, T. C. S. 2011. Performance of Irradiated and Crosslinked Ethylene Vinyl Acetate/Waste Tire Dust Blend. *Journal of Elastomers and Plastics*.
- SALEESUNG, T., SAEQUI, P. & SIRISINHA, C. 2010. Mechanical and thermal properties of thermoplastic elastomer based on low density polyethylene

- and ultra-fine fully-vulcanized acrylonitrile butadiene rubber powder (UFNBRP). *Polymer Testing*, 29, 977-983.
- ŞEN, M. & GÜVEN, O. 1995. A comparative study of thermal and mechanical stabilities of gamma irradiated ethylene-ethyl acrylate and ethylene-vinyl acetate copolymers. *Radiation Physics and Chemistry*, 46, 871-874.
- SENGUPTA, R., TIKKU, V. K., SOMANI, A. K., CHAKI, T. K. & BHOWMICK, A. K. 2005. Electron beam irradiated polyamide-6,6 films—I: characterization by wide angle X-ray scattering and infrared spectroscopy. *Radiation Physics and Chemistry*, 72, 625-633.
- SHAH, A. A., HASAN, F., SHAH, Z., KANWAL, N. & ZEB, S. 2013. Biodegradation of natural and synthetic rubbers: A review. *International Biodeterioration and Biodegradation*, 83, 145-157.
- SHANMUGHARAJ, A. M., KIM, J. K. & RYU, S. H. 2005. UV surface modification of waste tire powder: Characterization and its influence on the properties of polypropylene/waste powder composites. *Polymer Testing*, 24, 739-745.
- SHARIF, J., AZIZ, S. H. S. A. & HASHIM, K. 2000. Radiation effects on LDPE/EVA blends. *Radiation Physics and Chemistry*, 58, 191-195.
- SHASHIDHARA, G. M. & PRADEEPA, K. G. 2014. Isothermal crystallization of Polyamide 6/Liquid natural rubber blends at high under cooling. *Thermochimica Acta*, 578, 1-9.
- SHEN, J., WEN, S., DU, Y., LI, N., ZHANG, L., YANG, Y. & LIU, L. 2013. The network and properties of the NR/SBR vulcanizate modified by electron beam irradiation. *Radiation Physics and Chemistry*, 92, 99-104.
- SHI, J., JIANG, K., REN, D., ZOU, H., WANG, Y., LV, X. & ZHANG, L. 2013. Structure and performance of reclaimed rubber obtained by different methods. *Journal of Applied Polymer Science*, 129, 999-1007.
- SHI, J., JIANG, K., ZOU, H., DING, L., ZHANG, X., LI, X., ZHANG, L. & REN, D. 2014. Independent investigation on the influences of the processing conditions on the reclamation of crosslinked isoprene rubber after the impregnation of a reclaiming reagent. *Journal of Applied Polymer Science*, 131, n/a-n/a.
- SHIN, B. Y. & HAN, D. H. 2013. Compatibilization of immiscible poly(lactic acid)/poly(ϵ -caprolactone) blend through electron-beam irradiation with the addition of a compatibilizing agent. *Radiation Physics and Chemistry*, 83, 98-104.

- SHIRODKAR, B. D. & BURFORD, R. P. 2001. Interpenetrating polymer networks based on a thermoplastic elastomer, using radiation techniques. *Radiation Physics and Chemistry*, 62, 99-105.
- SHULMAN, V. L. 2011. Chapter 21 - Tyre Recycling. In: TREVOR, L. & DANIEL, V. (eds.) *Waste*. Boston: Academic Press.
- SIENKIEWICZ, M., KUCINSKA-LIPKA, J., JANIK, H. & BALAS, A. 2012. Progress in used tyres management in the European Union: A review. *Waste Management*, 32, 1742-1751.
- SIRCAR, A. K., GALASKA, M. L. & CHARTOFF, R. P. 1997. Compatibility of tire elastomers using derivative heat flow traces in the glass transition region. *Journal of thermal analysis*, 49, 407-415.
- SOARES, B. G., ALVES, F. F., OLIVEIRA, M. G. & MOREIRA, A. C. F. 2002. The effect of mercapto-modified ethylene-vinyl acetate (EVA) on curing parameters, mechanical properties, and thermal properties of vulcanized styrene-butadiene rubber (SBR)/EVA blends. *Journal of Applied Polymer Science*, 86, 239-249.
- SOMBATSOMPOP, N. & KUMNUANTIP, C. 2003. Rheology, cure characteristics, physical and mechanical properties of tire tread reclaimed rubber/natural rubber compounds. *Journal of Applied Polymer Science*, 87, 1723-1731.
- SONNIER, R., LEROY, E., CLERC, L., BERGERET, A. & LOPEZ-CUESTA, J. 2007. Polyethylene/ground tyre rubber blends: influence of particle morphology and oxidation on mechanical properties. *Polymer Testing*, 26, 274-281.
- SONNIER, R., LEROY, E., CLERC, L., BERGERET, A. & LOPEZ-CUESTA, J. M. 2006. Compatibilisation of polyethylene/ground tyre rubber blends by γ irradiation. *Polymer Degradation and Stability*, 91, 2375-2379.
- SONNIER, R., LEROY, E., CLERC, L., BERGERET, A., LOPEZ-CUESTA, J. M., BRETTELE, A. S. & IENNY, P. 2008. Compatibilizing thermoplastic/ground tyre rubber powder blends: Efficiency and limits. *Polymer Testing*, 27, 901-907.
- SUJIT, K., BHOWMICK, A., CHAKI, T., MAJALI, A. & DESPANDE, R. 1996. Electron beam initiated modification of ethylene vinyl acetate using TMPTA. *Polymer*, 37, 45-55.
- SUJITH, A., RADHAKRISHNAN, C. K., UNNIKRISHNAN, G. & THOMAS, S. 2003. Mass transfer characteristics of natural rubber/ethylene vinyl acetate blends. *Journal of Applied Polymer Science*, 90, 2691-2702.

- SUJITH, A., UNNIKRISHNAN, G., RADHAKRISHNAN, C. K. & PADMINI, M. 2007. Interaction of silica and carbon black fillers with natural rubber/poly(ethylene-co-vinyl acetate) matrix by swelling studies. *Polymer Composites*, 28, 705-712.
- SUNTHONPAGASIT, N. & DUFFEY, M. R. 2004. Scrap tires to crumb rubber: feasibility analysis for processing facilities. *Resources, Conservation and Recycling*, 40, 281-299.
- SUTANTO, P., LAKSMANA, F. L., PICCHIONI, F. & JANSSEN, L. P. B. M. 2006. Modeling on the kinetics of an EPDM devulcanization in an internal batch mixer using an amine as the devulcanizing agent. *Chemical Engineering Science*, 61, 6442-6453.
- SVOBODA, P., THERAVALAPPIL, R., SVOBODOVA, D., MOKREJS, P., KOLOMAZNIK, K., MORI, K., OUGIZAWA, T. & INOUE, T. 2010. Elastic properties of polypropylene/ethylene-octene copolymer blends. *Polymer Testing*, 29, 742-748.
- TADIELLO, L., D'ARIENZO, M., DI CREDICO, B., HANEL, T., MATEJKA, L., MAURI, M., MORAZZONI, F., SIMONUTTI, R., SPIRKOVA, M. & SCOTTI, R. 2015. The filler-rubber interface in styrene butadiene nanocomposites with anisotropic silica particles: morphology and dynamic properties. *Soft Matter*.
- TANTAYANON, S. & JUIKHAM, S. 2004. Enhanced toughening of poly(propylene) with reclaimed-tire rubber. *Journal of Applied Polymer Science*, 91, 510-515.
- TAO, G., HE, Q., XIA, Y., JIA, G., YANG, H. & MA, W. 2013. The effect of devulcanization level on mechanical properties of reclaimed rubber by thermal-mechanical shearing devulcanization. *Journal of Applied Polymer Science*, 129, 2598-2605.
- TAO, Y. & MAI, K. 2007. Non-isothermal crystallization and melting behavior of compatibilized polypropylene/recycled poly(ethylene terephthalate) blends. *European Polymer Journal*, 43, 3538-3549.
- VAN BEUKERING, P. J. H. & JANSSEN, M. A. 2001. Trade and recycling of used tyres in Western and Eastern Europe. *Resources, Conservation and Recycling*, 33, 235-265.
- VARGHESE, H., JOHNSON, T., BHAGAWAN, S. S., JOSEPH, S., THOMAS, S. & GROENINCKX, G. 2002. Dynamic mechanical behavior of acrylonitrile butadiene rubber/poly(ethylene-co-vinyl acetate) blends. *Journal of Polymer Science Part B: Polymer Physics*, 40, 1556-1570.

- VIJAYABASKAR, V., BHATTACHARYA, S., TIKKU, V. K. & BHOWMICK, A. K. 2004. Electron beam initiated modification of acrylic elastomer in presence of polyfunctional monomers. *Radiation Physics and Chemistry*, 71, 1045-1058.
- VIJAYABASKAR, V. & BHOWMICK, A. K. 2005. Electron-beam modification of nitrile rubber in the presence of polyfunctional monomers. *Journal of Applied Polymer Science*, 95, 435-447.
- VUKANTI, R., CRISSMAN, M., LEFF, L. G. & LEFF, A. A. 2009. Bacterial communities of tyre monofill sites: growth on tyre shreds and leachate. *Journal of Applied Microbiology*, 106, 1957-1966.
- WANG, H.-Z., XU, H. & XUAN, X.-J. 2009a. Review of Waste Tire Reuse & Recycling in China—current situation, problems and countermeasures. *Advances in Natural Science*, 2, 9.
- WANG, Q., WANG, F. & CHENG, K. 2009b. Effect of crosslink density on some properties of electron beam-irradiated styrene-butadiene rubber. *Radiation Physics and Chemistry*, 78, 1001-1005.
- WANG, Z., ZHANG, Y., DU, F. & WANG, X. 2012. Thermoplastic elastomer based on high impact polystyrene/ethylene-vinyl acetate copolymer/waste ground rubber tire powder composites compatibilized by styrene-butadiene-styrene block copolymer. *Materials Chemistry and Physics*, 136, 1124-1129.
- WU, C.-J., KUO, J.-F. & CHEN, C.-Y. 1993. Rubber toughened polyamide 6: The influences of compatibilizer on morphology and impact properties. *Polymer Engineering & Science*, 33, 1329-1335.
- XANTHOS, M. & DAGLI, S. S. 1991. Compatibilization of polymer blends by reactive processing. *Polymer Engineering & Science*, 31, 929-935.
- XIE, Y., HILL, C. A. S., XIAO, Z., MILITZ, H. & MAI, C. 2010. Silane coupling agents used for natural fiber/polymer composites: A review. *Composites Part A: Applied Science and Manufacturing*, 41, 806-819.
- XU, H., ZHANG, Y., YANG, J., YE, L., WU, Q., QU, B., WANG, Q. & WANG, Z. 2013. Simultaneous enhancements of toughness and tensile strength for thermoplastic/elastomer blends through interfacial photocrosslinking with UV radiation. *Polymer Chemistry*, 4, 3028-3038.
- YAMAUCHI, K., AKASAKA, S., HASEGAWA, H., KOIZUMI, S., DEEPRASERTKUL, C., LAOKIJCHAROEN, P., CHAMCHANG, J. & KORNDUANGKAEAO, A. 2005. Structural study of natural rubber thermoplastic elastomers and their composites with carbon black by small-angle neutron scattering and

- transmission electron microscopy. *Composites Part A: Applied Science and Manufacturing*, 36, 423-429.
- YANG, G. C. C. 1993. Recycling of discarded tires in Taiwan. *Resources, Conservation and Recycling*, 9, 191-199.
- YASIN, T., AHMED, S., YOSHII, F. & MAKUUCHI, K. 2002. Radiation vulcanization of acrylonitrile-butadiene rubber with polyfunctional monomers. *Reactive and Functional Polymers*, 53, 173-181.
- YASIN, T., KHAN, S., SHAFIQ, M. & GILL, R. 2015. Radiation crosslinking of styrene-butadiene rubber containing waste tire rubber and polyfunctional monomers. *Radiation Physics and Chemistry*, 106, 343-347.
- YIN, Y., LIU, M., ZHENG, X., SHEN, S. Z. & DENG, P. 2013. Improvement of compatibility of poly(ethylene terephthalate) and poly(ethylene octene) blends by γ -irradiation. *Journal of Applied Polymer Science*, 127, 200-207.
- YONG, M. K. 2007. *Preparation And Properties Of New Thermoplastic Elastomer Based On Ethylene Vinyl Acetate (EVA)/Natural Rubber Blends [TP1180. T5 Y55 2007 frb]*. Universiti Sains Malaysia.
- ZHANG, M. M., YAN, H. X., GONG, C. & LI, T. T. 2014. Hyperbranched polysiloxane functionalized graphene oxide for dicyclopentadiene bisphenol dicyanate ester nanocomposites with high performance. *eXRESS Polymer Letters*, 8, 413-424.
- ZHANG, S. L., XIN, Z. X., ZHANG, Z. X. & KIM, J. K. 2009. Characterization of the properties of thermoplastic elastomers containing waste rubber tire powder. *Waste Management*, 29, 1480-1485.
- ZHANG, S. L., ZHANG, Z. X., XIN, Z. X., PAL, K. & KIM, J. K. 2010. Prediction of mechanical properties of polypropylene/waste ground rubber tire powder treated by bitumen composites via uniform design and artificial neural networks. *Materials & Design*, 31, 1900-1905.
- ZHU, S. H. & TZOGANAKIS, C. 2010. Effect of interfacial strengthening in blends of reclaimed rubber and polypropylene. *Journal of Applied Polymer Science*, 118, 1051-1059.
- ZULKEPLI, N. N., ISMAIL, H. & RASHID, A. 2009. Effects of Different Particle Sizes of Recycled Acrylonitrile-butadiene Rubber and its Blend Ratios on Mechanical and Morphological Properties and Curing Characteristics of SBR/NBRr Blends. *Iranian Polymer Journal*, 18(2), 1-10.

ZURINA, M., ISMAIL, H. & RATNAM, C. T. 2008. The effect of HVA-2 on properties of irradiated epoxidized natural rubber (ENR-50), ethylene vinyl acetate (EVA), and ENR-50/EVA blend. *Polymer Testing*, 27, 480-490.

APPENDIX

A1. Determination of p_0/q_0 values using Charlesby-Pinner equation.

$$S + S^{1/2} = \frac{p_0}{q_0} + \frac{10}{q_0 D u_1} \quad \text{Equation 3.2}$$

Where S is the soluble fraction, u_1 the number averaged degree of polymerization, D is radiation dose (in kGy), p_0 and q_0 are fraction of ruptured and cross linked main-chain units per unit dose respectively. By regression analysis, plots of $S+S^{1/2}$ vs $1/D$ were drawn to determine the p_0/q_0 value which is the intercept of the plot's Y-axis. Do note that the soluble fraction used in this evaluation was derived from the absolute yield of gel fraction upon irradiation (gel content before irradiation subtracted by gel content after irradiation) as RTR contained a substantial amount of gel before irradiation

Plots of $S + S^{1/2}$ vs. $1/D$ were plotted as shown in Figure A1. The values of p_0/q_0 were determined from the intercept of $S + S^{1/2}$ axis.

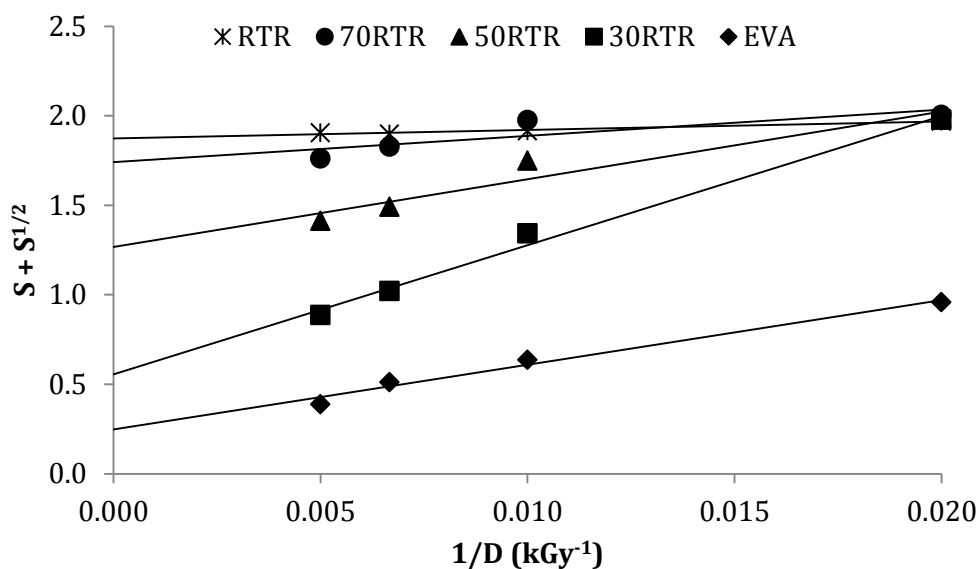


Figure A1.1 Charlesby-Pinner plot for RTR/EVA blends

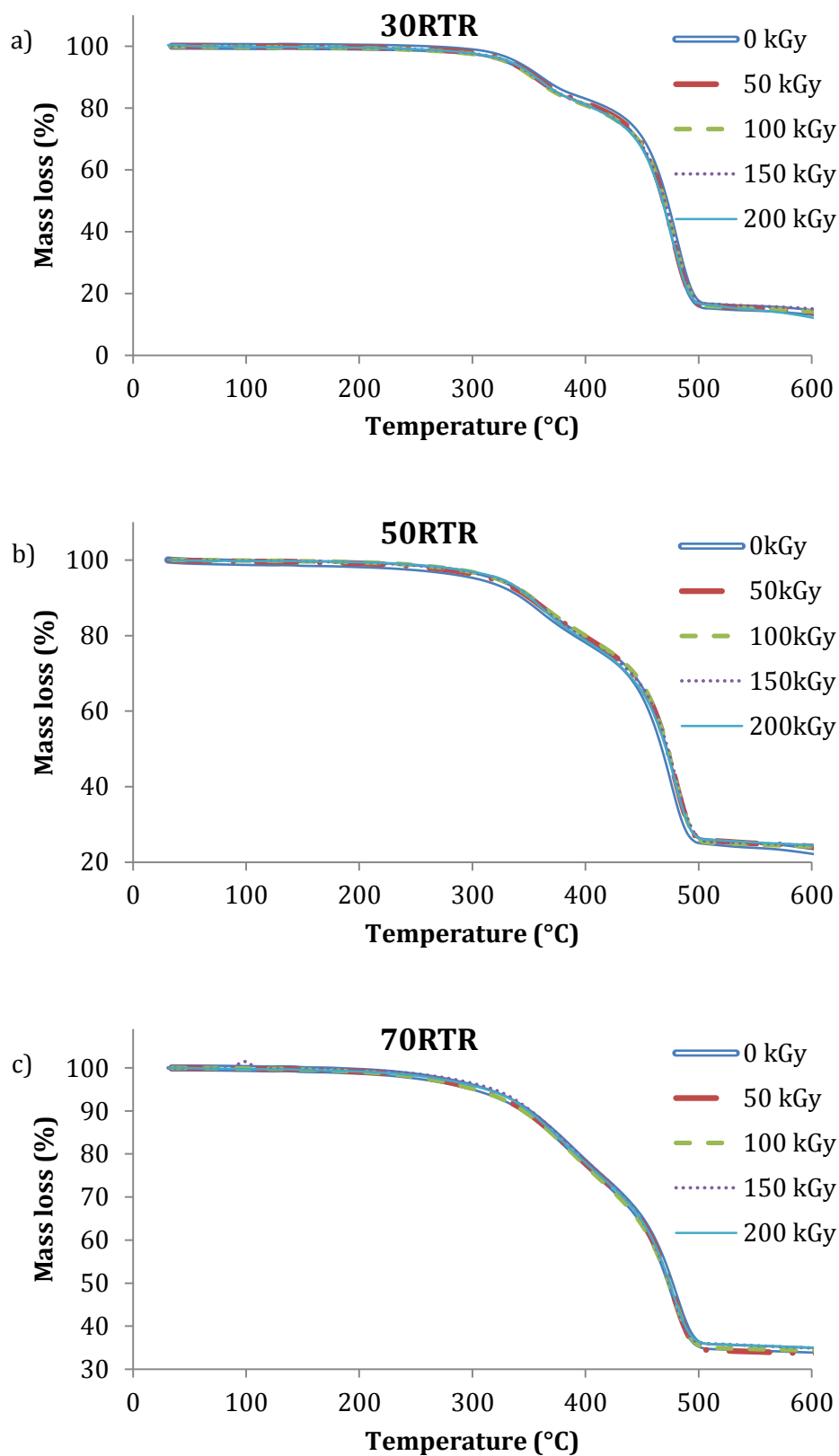
A2. Representation of TGA curves of irradiated blends.

Figure A2.1 Typical TGA curve of a) 30RTR b) 50RTR and b) 70RTR at different irradiation doses